THE UNIVERSITY
of EDINBURGH

Quantitative retinal traits and their association with cardiovascular disease and cardio-metabolic genetic variants in people with type 2 diabetes

Emmanuel Sandoval García

Doctor of Philosophy

The University of Edinburgh

2020

Declaration

I declare that this thesis is of my own composition. The work presented here has not been submitted for any other degree or professional qualification

I used the data collected of The Edinburgh Type 2 Diabetes Study, which provided the data for the large proportion of the content of the work presented here.

Signed:

Date: 22.01.2020

Abstract

Introduction: Type 2 diabetes (T2D) is one of the most prevalent non-communicable diseases in the world and its cardiovascular complications present a huge socio-economic burden. In 2015, in the UK alone, 3.8 million people have been diagnosed with T2D and cardiovascular disease accounts for almost 1.7 million episodes throughout the country. Early diagnosis of cardiovascular disease in people with T2D thus becomes critical.

The retina gives a unique opportunity to study the human microcirculation, which can then offer insights into the pathophysiology of cardiovascular disease. By using semi-automatic software, retinal images can provide quantitative traits derived from the microvasculature. Previous research has found that arteriolar and venular calibres are associated with cardiovascular outcomes such as hypertension and stroke. Moreover, retinal vascular tortuosity, a novel quantitative biomarker which measures the degree to which blood vessels visible in the retina twist and turn, has been associated with traditional cardiovascular risk factors in the general population. However, this area needs to be further explored, especially in the population with T2D and in prospective analyses.

Aims: To determine whether quantitative retinal traits such as vessel widths, vessel tortuosity and multifractal dimensions are associated with the subsequent development of major cardiovascular events such as ischaemic heart disease and stroke in people with T2D. Also, to use a genome-wide association approach to investigate if these quantitative retinal traits are associated with cardio-metabolic genetic variants, which could help identify novel biomarkers of cardiovascular disease for future research.

Methods: Analyses used the Edinburgh Type 2 Diabetes Study, a prospective cohort of 1066 men and women with T2D aged 60-75 years at baseline with eight years of follow-up for cardiovascular events. A total of 1028 retinal images from baseline were analysed using the semi-automatic retinal software VAMPIRE (Vascular Assessment and Measurement Platform for Images of the Retina). Cross-sectional analyses including ANOVA and Chi-square test were performed along with prospective analysis using Cox regression. Additionally, a genome-wide association study was performed to explore the association of 12 quantitative retinal traits with cardio-metabolic genetic variants. Imputation of variants included in the MetaboChip array was used.

Results: In an unadjusted model, there was a significant association between arteriolar tortuosity and incident stroke (Hazard Ratio (HR) 1.26; 95% CI 1.02, 1.57; *p*=0.03). This association remained significant after full adjustment for age, sex, cardiovascular risk factors (body mass index, HbA_{1c}, total cholesterol, duration of diabetes, renal dysfunction) and previous cardiovascular events (HR 1.26; 95% CI 1.01, 1.58; *p*=0.04). Multifractal dimensions, a novel retinal biomarker which provides an insight into vascular geometry, was inversely associated with incident stroke (unadjusted HR 0.73; 95% CI 0.57, 0.94; *p*=0.01). This association also remained significant after adjustment for age, sex, cardiovascular risk factors and previous cardiovascular event (HR 0.73; 95% CI 0.56, 0.94 *p*=0.02). Associations between other retinal traits and stroke, and between traits and ischaemic heart disease, tended not to be statistically significant, especially after multivariable adjustment.

The genome-wide association analysis of arteriovenous ratio (ratio of arteriolar to venular vessel width) revealed a genome wide significant locus, rs73198094 ($p = 5.27 \times 10^{-8}$), an intergenic variant located between *ASAH1* and *LOC101929066* genes in chromosome 8. The *ASAH1* gene has been associated with atrial fibrillation. Although no further single nucleotide

polymorphisms reached genome-wide significance, some additional promising findings emerged. Analysis for retinal arteriolar width revealed a genome-wide suggestive intronic locus, rs4944903 (p= 8.5x10^{-7}), of the gene *POLD3* in chromosome 11. Identified loci for minimum arteriolar tortuosity, rs7991332 (p=1.54 x 10^{-6}) and rs2172724 (p=2.46 x10^{-6}), are located in the *COL4A2* gene in chromosome 13 and another identified variant, rs7319323 (p=3.53 x 10^{-6}), is located in an intron of the neighbouring *COL4A1* gene. Previous studies showed the relevance of these genes including an association with stroke and intracerebral haemorrhage. These two genes encode collagen protein chains, which are major components of the vascular basement membrane. Another promising variant identified was the rs34013641 locus, associated with minimum venular tortuosity (p=2.81 x 10^{-6}), which is located in the *MYH11* gene in chromosome 2. This gene encodes smooth muscle myosin heavy chain protein, which is highly expressed in human arteries. Finally, identified loci for the multifractal dimension D0, rs10963694 (p=8.53 x 10^{-7}) and rs4977506 (p=4.95 x 10^{-6}), located on the *ADAMTSL-1* gene in chromosome 9, are also strong candidates in the pathophysiology of vascular disorders.

Conclusions: In older people with T2D, arteriolar tortuosity and multifractal dimensions were significantly and independently associated with incident stroke. GWAS findings for these and other quantitative retinal traits offer insight into pathophysiological changes of the vasculature, which may result in cardiovascular disease. These findings, in the context of further research, could potentially be used to reveal biological mechanisms related to major cardiovascular complications of T2D and to guide efforts on prevention and early interventions.

Lay Summary

Type 2 diabetes is a leading risk factor for morbidity and mortality in the UK and worldwide, and it has been shown to increase the risk of cardiovascular disease namely heart attacks and stroke. People who are overweight, often as a result of multiple environmental factors, are more likely to develop diabetes. This disease leads to the development of changes in the vessels which has been shown to increase risk of develop cardiovascular events particularly stroke. There is uncertainty around the main risk factors for these specific events in people with type 2 diabetes. The aim of this study was to find the association of the measurements of the retinal vessels with cardiovascular events namely heart attacks and stroke.

The Edinburgh Type 2 Diabetes study uses information collected over a period of eight years from a large group of men and women aged 60-75 years, with type 2 diabetes, living in Scotland. Cardiovascular events was measured using data records from the NHS Lothian that is linked to the medical history of the people recruited in the aforementioned dataset. Other medical information on lifestyle such as smoking, previous diseases such as heart attacks, and medications was also collected. A baseline photography of the eyes was taken for each person. After eight years, the number of people who developed cardiovascular events were recorded. By using a state-of-art software different parameters of the vessels of the retina were measured. In addition, using advanced statistical techniques, associations between retinal parameters and heart attacks and stroke were modelled as were the associations between the curvature (tortuosity) and multifractal dimensions with people who developed stroke.

This study found that the curvature of the vessels and the ‘decomplexification’ of the retinal vasculature were associated with incident events of cerebrovascular stroke. Further research using the findings of this study can help in developing strategies to prevent major cardiovascular complications in people with diabetes who are already at a higher risk than the general population.

Abbreviations

ABI	Ankle brachial index
ApoA	Apolipoprotein A
ApoB	Apolipoprotein B
ARIC	The Atherosclerosis Risk in Communities Study
AUC	Area Under the Curve
AVR	Arteriovenous ratio
BDES	Beaver Dam Eye Study
BMI	Body mass index
BMES	Blue Mountains Eye Study
BSTD	Standard deviation of the width in zone B
CHD	Coronary heart disease
CHS	Cardiovascular Health Study
CI	Confidence interval
CKD	Chronic kidney disease
CRAE	Central Retinal Arteriolar Equivalent
CRVE	Central Retinal Venular Equivalent
CRP	C-reactive protein
CVD	Cardiovascular disease
DPB	Diastolic blood pressure
DR	Diabetic Retinopathy
DTRS	Danish Twin Register Study
ECG	Electrocardiogram
eGFR	Estimated glomerular filtration rate

ET2DS	Edinburgh Type 2 Diabetes Study
ETDRS	Early Treatment Diabetic Retinopathy Study
GP	General Practitioner
GWAS	Genome-wide association study
HbA_{1C}	Glycated haemoglobin
HDL	High-density lipoprotein
HR	Hazard ratio
IHD	Ischaemic heart disease
IQR	Interquartile ranges
IVAN	Integrative Vessel Analysis
ISD	Information Services Division
LD	Linkage disequilibrium
LDL	Low-density lipoprotein
LDR	Lothian Diabetes Register
MABP	Mean arterial blood pressure
MAF	Minor allele frequency
MESA	Multi-Ethnic Study of Atherosclerosis
MI	Myocardial infarction
MRI	Magnetic resonance imaging
NHS	National Health Service
NICE	National Institute for Health and Care Excellence
OD	Optic disc
OR	Odds ratio
ORCADES	The Orkney Complex Disease Study
PAD	Peripheral arterial disease

SIVA	Singapore "I" Vessel Assessment
SMES	Singapore-Malay Eye Study
SNP	Single-nucleotide polymorphism
SBP	Systolic blood pressure
SIMD	Scottish index of multiple deprivation
T2D	Type 2 diabetes
TIA	Transient ischaemic attack
VAMPIRE	Vascular Assessment and Measurement Platform for Images of the Retina
VLDL	Very-low density lipoprotein
WHO	World Health Organisation

Acknowledgements

I would like to express my sincere gratitude to my supervisors Professor Jackie Price and Professor Jim Wilson for their support and guidance throughout the PhD. Without the thoughtful encouragement, careful supervision and patience of Professor Jackie Price, this thesis would not never have taken shape. Their advice was invaluable, and they were supportive supervisors.

I would also like to acknowledge all the staff and participants of The Edinburgh Type Diabetes Study. Without them, this thesis would not have been possible. Particular thanks also go to Dr Tom MacGillivray for his support in analysing the retinal images. Thanks to Professor Mark Strachan for his support and comments during national and international conferences.

I am so grateful to my PhD peers and academic colleagues in the Usher Institute. I much appreciate the camaraderie of all the current and former occupants of Room 666 at the Usher Institute, who were an absolute pleasure to collaborate with. I am deeply thankful to, former Usher member, Dr Marco Colombo for his support and insightful advice in statistical and genetics analyses. Thanks to Dr Stela McLachlan for her help with data analysis and data manipulation. I am so grateful to my peers Eduardo, Luciana, Evelyn, Daniel, Teodora and Reebus, who have been an invaluable source of support and example of tenacity. They provided me distractions in the most critical moments of this academic journey over the last four years. This thesis would not have been completed without the support of Genevie Fernandes, who has been one of the friendliest and kindest PhD peers in the Usher Institute. Thanks to my long-distance friends in Mexico and Spain, Elena, Juanito, Maria Victoria and Patricia for their moral support and encouragement.

I am kindly grateful to Dr Miguel Cruz and his team at *Instituto Mexicano del Seguro Social (IMSS)* for their encouragement and academic support to

continue my postgraduate training in the UK. This PhD project would not be possible without the support and funding from Consejo Nacional de Ciencia y Tecnologia (CONACyT).

Many thanks to the medical team in Forth Valley Royal hospital including Dr Santosh Salunke, Dr Catherine Labinjoh and Dr Daniel Beckett for their support and fellowship during the last 12 months, and for giving me the opportunity for being a member of this great medical team.

Finally, I wish to extend my deepest gratitude to my parents, Manuel Sandoval and Maria Consuelo Garcia, my sister Karla Sandoval and my niece Sofi, for being the greatest inspiration in my life. Their endless love, kindness and unwavering support at every good and not so good point in my career, has kept me motivated and grounded. This thesis would have never completed without them.

Contents

List of Tables

List of Figures

Chapter 1 Background: Type 2 diabetes, cardiovascular disease and quantitative retinal traits

1.1 Type 2 diabetes

The World Health Organisation (WHO) defines diabetes mellitus as a “metabolic disorder of multiple aetiology characterised by chronic hyperglycaemia with disturbances of carbohydrates, fat and protein metabolism resulting from defects in insulin secretion, insulin action or both” (World Health Organisation, 2014). The vast majority of cases of diabetes mellitus are classified as type 2 diabetes (T2D). This condition is characterised by insulin resistance, hyperinsulinaemia and pancreatic ß cell dysfunction. It negatively affects multiple organs including the liver, skeletal muscle, kidneys, brain, small intestine and adipose tissue. Importantly, the incretin effect changes in the colon and microbiome and immune dysregulation and inflammation have emerged as significant pathophysiological factors in T2D. Type 1 diabetes, commonly referred to as “insulin-dependent diabetes”, is mainly caused by autoimmune destruction of ß cells in the pancreas, leading to insulin deficiency. Although Type 1 diabetes is becoming more prevalent, it is still considerably less common than T2D.

Diabetes mellitus is one of the most prevalent non-communicable diseases in the world, and the number of people living with this condition has quadrupled in the past three decades (WHO, 2016). This rising prevalence indicates that the number of people with diabetes mellitus has increased dramatically from 108 million in 1980 to 422 million in 2014. Overall, about 1 in 11 adults aged 20-79 years (425 million) worldwide now have diabetes mellitus, 90% of whom have T2D (International Diabetes Federation, 2017). Asia is a major contributor to the rapidly emerging T2D global epidemic, including China and India. The estimate of affected people with T2D is projected to rise to 642 million by 2040, and the largest increases will come from regions undergoing economic transition (International Diabetes Federation, 2017). The rise of obesity (defined as a Body Mass Index or BMI ≥30 kg/m_2), a sedentary life-style, energy-dense diets and population aging are the main drivers of the global epidemic of T2D (Chatterjee et al, 2017). Evidence has shown that many cases of

T2D could be prevented by maintaining a healthy body weight (BMI ≤ 25 kg/m_2), following a restrictive calorie diet, exercise and avoiding smoking and excess alcohol consumption (Zheng et al, 2018).

Mortality and morbidity from the complications directly associated with diabetes mellitus, such as cardio-metabolic diseases and renal failure, accounted for approximately five million deaths globally in 2017 (International Diabetes Federation, 2017). The loss of quality of life in people with diabetes mellitus and further complications cause severe disability and despair. Global expenditure on T2D has also been increasing steeply. The International Diabetes Federation (2017) conservatively estimated that in 2015, 673 billion US dollars (nearly 12% of global health expenditure) was spent on treating diabetes mellitus and its complications. This expenditure is three times higher in people with diabetes mellitus than the general population without diabetes.

Clinically, the signs and symptoms of T2D include polyuria, polydipsia, polyphagia, weight loss, paraesthesia in the extremities, blurred vision or recurring infections. Severe cases may present acid-base electrolyte-metabolic disturbances including ketoacidosis (seen mainly in Type 1 diabetes) and hyperosmolar hyperglycaemic state. Confirmation of T2D involves fasting plasma glucose concentration greater than 7mmol/l (126mg/dL) (World Health Organisation, 2016). Glycated haemoglobin (HbA_{1c}) is also commonly used in clinical settings to help diagnose T2D. HbA_{1c} is an approximate measure of glucose control in the previous 6-8 weeks. The World Health Organization (WHO) recommends that an HbA_{1c} of 6.5% (7.7 mmol/l) or greater should be used as a diagnosis of T2D, although lower levels of HbA_{1c} do not exclude T2D in the presence of elevated blood glucose (World Health Organisation, 2016). The onset of diabetes mellitus frequently occurs years before the signs and symptoms of the disease develop. Globally, 45.8% of all diabetes mellitus cases in adults have been estimated to be undiagnosed (Beagley et al, 2014).

Management of T2D aims to relieve and reverse symptoms and minimise development and progression of microvascular and macrovascular complications. T2D is managed, in the vast majority of cases, with a combination of balanced diet, exercise and either oral antidiabetic medication (e.g. sulphonylureas or biguanides) or the addition of injected insulin, if necessary.

Impaired metabolic management leads to microvascular and macrovascular complications. The former includes retinopathy, nephropathy and neuropathy while the latter comprises cardiovascular complications such as acute coronary syndrome (myocardial infarction, angina) and ischaemic stroke. People with T2D require regular screening (urine test, eye examination, foot care) to detect early signs of potential complications and to self-monitor for symptoms. Despite increasing knowledge regarding risk factors for T2D, the predicted worldwide increase in the incidence and prevalence of T2D is likely to lead to severe complications, which require regular monitoring from health care providers. The burden of T2D in the UK and globally, therefore, poses one of the most challenging health problems of human history.

1.2 Cardiovascular disease

Cardiovascular disease (CVD) is a leading cause of morbidity and mortality worldwide and in the UK (Zheng et al, 2018). This burden is a major barrier to human development and the United Nations has formally recognised non-communicable diseases, including CVD, as a major concern for global health, and set up an ambitious plan to reduce the effect of these diseases in all regions (Roth et al, 2017). The cost of CVD to the UK economy (including premature death, disability and informal costs) is an estimated £19 billion each year according to the British Heart Foundation statistics (BHF analysis of European Cardiovascular Disease Statistics, 2017). Scotland (Glasgow) had the highest CVD death rate for men and women among the four nations in the UK. CVD accounted for almost 1.7 million episodes in the National Health Service (NHS) hospitals throughout the UK and this number has been increasing (Bhatnagar et al, 2016).

According to the WHO, CVD includes coronary heart disease (CHD) or ischaemic heart disease (IHD), cerebrovascular disease, and peripheral vascular disease (PVD). CHD is characterised by an impaired supply of the blood flow to the myocytes of the heart due to narrowing or blocking by fatty deposits (atheroma) of the inner walls of coronary arteries. This chronic process makes the arteries hard and swell, restricting oxygen and nutrients from the blood flow to the heart. This may lead to angina and eventually, if the coronary artery is completely blocked, then the myocyte

is starved of oxygen, which results in necrosis or myocardial infarction. Cerebrovascular disease encompasses two types of stroke - ischaemic and haemorrhagic. Ischaemic strokes include thrombotic strokes, embolic strokes, and hypoxic strokes, which may involve the development of symptoms with a duration of a few minutes (transient ischaemic stroke) without evidence of structural damage (e.g. infarcts). Haemorrhagic strokes include subarachnoid haemorrhages (e.g. ruptured aneurysm) and intracerebral haemorrhages (e.g. due to hypertension or anticoagulant medication). Finally, peripheral arterial disease (PAD) occurs when blood vessels develop atherosclerosis, which results in impaired blood supply (ischaemia) mainly in the lower limbs.

Individuals with T2D are twice as likely to develop CVD as those without T2D, independent of age, smoking status, BMI and systolic blood pressure (Rao Kondpally Seshasai et al, 2011; Emerging Risk Factors Collaboration, 2010) and despite considerable advances in the management of CVD, it remains the leading cause of death globally in people with T2D. The incidence and mortality of these cardiovascular complications are particularly high in specific groups of the diabetic population. For instance, this excess risk disproportionally affects women such that T2D eliminates or decreases the reduced risk of CVD that is generally seen in premenopausal women (Zhang et al, 2017).

1.3 Cardiovascular risk factors

1.3.1 Traditional cardiovascular risk factors

Traditional cardiovascular risk factors can be sub-categorised in two groups, non-modifiable and modifiable. The former includes age, sex and ethnicity and the latter includes hypertension, dyslipidaemia, high BMI, smoking, reduced physical activity and diabetes.

Age is a well-established contributor to risk of CVD, with the risk increasing as both sexes age. Among adults, men are approximately twice as likely to develop CVD as women; although this difference is reduced when women age, reaching menopause, leading to vascular changes (Bots el al, 2017). There are also ethnic differences in

the presentation of CVD, which extend to sub-populations with T2D. For example, Chinese individuals with T2D had lower rates of CHD than those from other countries, whereas individuals with an ethnic Indian subcontinent background who had T2D had double the risk of CHD deaths compared with those with white European ethnicity who had T2D, independent of traditional risk factors (Zhang et al, 2017).

Modifiable risk factors include cardiometabolic factors (e.g. high blood pressure and abnormal blood lipid) and lifestyle factors such as obesity, smoking, and physical inactivity. High blood pressure or hypertension is one of the biggest contributors to mortality from CVD across all age groups and in both sexes (Pazoki et al, 2018). The risk of developing CVD is on average between two and three times higher in people with hypertension (Nayor et al, 2018). Dyslipidaemia is also an important risk contributor to developing CVD. This disorder occurs when total cholesterol, low-density lipoprotein (LDL) cholesterol or triglycerides are elevated or when levels of high-density lipoprotein (HDL) cholesterol are reduced. Other lipids such as lipoprotein (a) and apolipoproteins A1 and B are also involved in developing CVD (Lacey et al, 2017). However, large epidemiological studies such as Framingham Heart Study have tended to focus on the analysis of the most commonly measured lipids (e.g. triglycerides, cholesterol and its subtypes).

There is a strong association between lifestyle factors and the risk of CVD. Obesity has increased dramatically over the last decade, doubling between 1980 and 2008, and reaching epidemic proportions globally (Piché et al, 2018). Obesity is linked to several cardiovascular risk factors and outcomes, including cardiac structure, hypertension, metabolic abnormalities, ischaemic heart disease, and atrial fibrillation (Parto et al, 2017). Moreover, previous studies have shown that obesity is an independent risk factor not only for CVD but also for other morbidities (e.g. cancer) (Avgerinos et al, 2019).

Smoking is another well-known risk factor for CVD, and over the last decade, compelling evidence has emerged that exposure to passive smoking is also associated with CHD, increasing the risk by 25% among non-smokers (Heindrich et al, 2007). Public policies have been instituted (e.g. increasing the price of cigarettes) to reduce this preventable cause of CVD. There is also a broad consensus that

regular physical activity improves cardiovascular health. In the 1960s, Morris investigated the association between physical activity and cardiovascular disease prevalence (Morris, 1961). Recently, in the UK, the EPIC Norfolk prospective study (Lachman et al, 2018) found an inverse association between physical activity and the risk of CVD in middle-aged and elderly adults. Among individuals aged over 65 years, hazard ratios for CVD were 0.86 (95% CI 0.78-0.96), 0.87 (95% CI 0.77-0.99) and 0.88 (95% CI 0.77-1.02) in moderately inactive, moderately active and active people, respectively compared with inactive people. The results of this association were similar among people aged 55-65 years and less than 55 years.

1.3.2 Cardiovascular risk factors in people with type 2 diabetes

In general, people with type 2 diabetes tend to present more detrimental levels of cardiovascular risk factors (WHO, 2016). There are also some 'diabetes-specific' risk factors associated with T2D. The duration of diabetes is a key determinant and risk factor for CVD in people with T2D. Individuals with T2D with a duration longer than 10 years can be considered at a higher risk of developing CVD (Einarson et al, 2018). In a prospective study, it was found that people with a mean duration of T2D of 16.7 years showed similar CHD risk as those with previous myocardial infarction (MI) without T2D (Bertoluci et al, 2017).

The increased risk of CVD in this population is due to the complex combination of various traditional and non-traditional risk factors that play an important role in the beginning and the evolution of atherosclerosis and an impaired endothelial function, which lead to CV events (Martin-Timon et al, 2014).

Non-traditional risk factors include insulin resistance, hyperinsulinaemia, postprandial hyperglycaemia, glucose variability, microalbuminuria, thrombogenic factors, elevated inflammation markers (e.g. C-reactive protein), visceral adiposity, and genetic factors.

Insulin resistance is characteristic of T2D and it develops in multiple organs involving the skeletal, liver, adipose tissue and the heart. In fact, elevated hyperglycaemia and diabetes are often preceded by several years of insulin resistance, which is influenced by the presence of visceral adiposity and accumulation of fat. Importantly,

hyperinsulinaemia as a consequence of insulin resistance precedes the onset of T2D and could be related to vascular disease.

Insulin resistance is measured by surrogate methods including the HOMA index, the intravenous glucose tolerance test, and the insulin suppression test. Insulin resistance is followed by compensatory hyperinsulinaemia. Molecular physiopathology of insulin resistance are yet poorly understood but includes the mechanism of insulin action on GLUT-4 translocation, glucose transport, and the activation of nitrous oxide (NO) synthase. These signalling pathways are implicated in the mitogenic, nonmetabolic, proinflammatory, and proliferative effects of insulin (Martin-Timon et al, 2014). Insulin resistance leads to decreased glucose uptake and impaired NO synthesis. Additionally, compensatory hyperinsulinemia stimulates in vascular smooth muscle and endothelial cells, an increased production of vasoconstrictors including endothelin, interleukins and an augmented surface expression of adhesion molecules. These mechanisms influence the blood vessels through the activation of endothelium-derived NO mainly mediated by insulin. This state of increased NO production leads to its anti-atherogenic effects and becomes pro-atherogenic.

Postprandial hyperglycaemia is associated with increased postprandial triglycerides levels, and these are related to increased oxidative stress, systemic inflammation and endothelial dysfunction, all of which are associated with atherosclerosis. A study conducted in 505 T2DM patients followed up for 14 years in a hospital in Turin, Italy (Cavalot et al, 2011), indicated that both postprandial blood glucose and HbA1c predict cardiovascular events and all-cause mortality, showing the independent predictive power of postprandial glycaemia on cardiovascular events after correction for HbA1c. Moreover, a meta-analysis of five randomized controlled trials showed that, in T2D subjects, intensive glycaemic control considerably decreases coronary events without an increased risk of death (Ray et al, 2009).

In people with diabetes, glycated haemoglobin (HbA_{1c}) is a biomarker to measure glucose levels over the previous two to three months. Cross-sectional and longitudinal studies have shown that higher levels of glycaemia have been associated with higher cardiovascular events rates and a recent meta-analysis (Cavero-Redondo et al, 2017) found HbA_{1c} to be a reliable risk factor for all-cause

cardiovascular mortality in both diabetic and non-diabetic individuals. This study also found optimal HbA_{1c} levels, for the lowest all-cause and cardiovascular mortality, ranging from 6% to 8% (7 mmol/l to 10.1mmol/l) in people with diabetes and from 5% to 6% (5.4 – 7.0 mmol/l) in those without diabetes.

Impaired renal function is an independent risk factor for CVD. Approximately 10% of deaths in people with T2D are attributable to renal failure (Zheng et al, 2017).There is evidence which shows that both decreased glomerular filtration rate and proteinuria independently increased cardiovascular risk (Bertoluci et al, 2017). Thus, targeting multiple biomarkers of CVD risk can, hopefully, offer a substantial chance of improving CVD events in this population.

The complex interaction of the risk factors in people with T2D make it necessary to apply a rounded approach in the management of this metabolic disorder. While diet and life style changes are key to the successful control of T2D, different types of medications help to regulate the glycaemic control in this population. Metformin (a type of Biguanide) was as effective as sulphonylurea or insulin in glucose control and reduction of microvascular risk in the UK Prospective Diabetic Study (UKPDS) (Holman et al, 2008).

Although glucose control is a high priority for the prevention of vascular complications, blood pressure control is also necessary to prevent progression of cardiovascular disease. Ideally, all patients should therefore aim to have their HbA1c levels < 8.6 mmol/l in order to reduce the risk of long-term microvascular complications. Additionally, blood pressure control is essential and this can be achieved using usually angiotensin-converting enzyme (ACE) inhibitors or angiotensin II receptor antagonists. A large systematic review found that lowering blood pressure was associated with improved mortality and clinical outcomes including stroke and heart failure (Emdin et al, 2015). Another recent systematic review, which included randomised controlled trials, showed that in adults with T2D and hypertension, lowering the blood pressure at 120-130/80 mmHg reduced risk of stroke (Aronow and Shamliyan, 2018).

Also, inhibitors of HMG-CoA reductase (Statins) have shown to improve endothelial dysfunction and microvascular dysfunction in people with T2D and dyslipaemia,

suggesting improvement of cardiovascular morbidity and mortality (Abdul-Ghani et al, 2017). This intervention has shown slow atherosclerosis.

1.4 The retina and its vasculature

The eye (Bulbus oculi) of an adult is an organ forming part of the central nervous system. It is made up of a number of complex structures, including the retina, the vasculature of which forms the topic of this thesis. Over the years, scientists have been searching for evidence for the concept of “the eyes as the window of the soul”. The retina is the only place where blood vessels can be directly visualised non-invasively *in vivo,* and several studies have confirmed the association of retinal vascular changes with systemic diseases and cardiovascular disorders (London et al, 2013; Flammer et al, 2013). This section discusses the details of the anatomy and physiology of the human retina, followed by details of its vasculature and links with cardiovascular disease.

1.4.1 Anatomy and physiology of the retina

The embryological development of the retina and optic nerve extended from diencephalon and hence both are considered part of the central nervous system. These new vessels initially form a flat plexus that subsequently develops into the retina forming a deeper plexus. Retinal vasculature development is closely associated to the retinal astrocytes. These are part of the glial cells, which provide the foundation for retinal angiogenesis (London et al, 2013). Furthermore, immature retinal astrocytes start emerging from the optic disc into the retina as extended spindle cells filling the nerve fibre layer, and they migrate to the inner limiting membrane, which is rich in extracellular matrix proteins (Selvam et al, 2018). These proteins serve as an adhesive substance and contain instructive signals and growing factors such as glycosaminoglycans and proteoglycans, which play an important role in the neural network structure. Hence, the retinal vessels tightly interact with the astrocytes and as a consequence, vascular growing factors (e.g. vascular endothelial growth factor) express and stimulate blood vessel growth.

Anatomically, the retina consists of layers composed of neurones, which intercommunicate through synapses (Selvam et al 2018; London et al, 2013).

Physiologically, the capture of light is made by the photoreceptor cells in the outermost layer of the retina, which results in a cascade of neuronal signs and biochemical processes reaching the retinal ganglion cells (Country et al, 2017). These axons, which are part of the optic nerve, extend to the lateral and geniculate nucleus in the thalamus and the superior colliculus in the midbrain. In this region, information is further transmitted to the visual processing centres that enables us to perceive an image of the world. As a part of the central nervous system, the eye – particularly the retina – must preserve the regulated interaction with the immune and vascular systems (De Boever et al, 2014). In fact, the eye consists of unique structures such as an array of blood-ocular barriers that share structures, characteristics and mechanisms with the central nervous system gating system (Pournaras et al, 2008).

1.4.2 Retinal vascular system

The microcirculation (including the retinal microvasculature) makes up a large part of the circulatory system and plays a crucial role in maintaining cardiovascular health (De Boever et al, 2014). Over the last few years, the retinal vasculature has been widely studied because it is easily accessible by non-invasive technical methods, extending its study into several fields in medicine. The retina has a complex vascular supply, which, as described above, functions to maintain the physiological and metabolic homeostasis of the inner part of the retina via a laminar network that permeates the neural tissue. Conversely, the outer retina (the region with photoreceptors) is avascular, and receives its nutrients from the choroidal vasculature.

Blood flow in the brain and therefore in the retina is essential because the brain is energetically costly and accounts for 20% of total energy consumption in resting humans, despite weighing 2% of total mass (Country et al, 2017). Retinal vascular alterations occur in response to metabolites (such as glucose and oxygen) in order to match tissue demand and to drain waste products and carbon dioxide (De Boever et al, 2014). The retinal circulation is an end-arterial system, which does not contain anastomoses at outer layers. The central retinal artery emerges at the optic disc, dividing into two major branches, which further split into arterioles, each supplying

one quadrant of the retina (Kur et al, 2012). In general, retinal arteries divide by dichotomous and side-arm branching. The venous system presents some similarity with the arteriolar arrangement, with the central retinal vein leaving the eye through the optic nerve to drain venous blood into the cavernous sinuous.

Retinal arteries differ from arteries of the same size in other organs in several respects. The rheological properties of the retinal microvasculature differ from larger arteries in its unusually developed smooth muscle layer and lack of an internal elastic lamina (Selvam et al, 2018). The smooth muscle cells are oriented both circularly and longitudinally, each of them surrounded by a basal lamina that contains a considerable amount of collagen toward the cellular adventitia. Innervation of the retinal vessels is also complex compared to other vascular regions of the human body (e.g. coronary vessels). For instance, the distal retinal vessels to the central retinal artery are not innervated. However, α and β adrenergic and angiotensin II receptors have been found along the optic nerve head and within the retina, (Pournaras et al, 2008; Senanayake et al, 2007).

Several extracellular structures interact with the retinal vessels including extracellular matrix and blood retinal barriers. The former assembles numerous components (e.g. integrins) that are secreted in a cell type specific manner. Both major barrier tissues, epithelium and vascular endothelium of the retinal vessels, produce a specialized extracellular matrix scaffold, namely basal lamina which provides elasticity and tensile strength to the vessels. These extracellular structures are synthesised mainly in the endothelium of the retinal vessels (Xu et al, 2014; Lee et al, 2012). The blood retinal barriers include structures such as the pericytes and the glial cells (e.g. astrocytes). Moreover, the endothelium plays an important role in the regulation of the blood flow in the retina (Selvam et al, 2018). The blood flow and vessel tone in the retina are controlled by a myogenic as well as a metabolic mechanism. The endothelium releases a number of metabolic factors such as oxide nitric, endothelins, and metabolites of the arachidonic acid, and these regulate the tone of the vessels (Eelen et al, 2015).

1.4.3 Retinal vessel system and cardiovascular disease

The retinal microvasculature consists of a regulated mechanical system that maintains the internal pressure due to blood flow and variations in axial stretch as a result of tethering to other tissues. The vascular network has a branching pattern that can be considered as a fractal structure (Causin et al, 2016). Many factors influence retinal haemodynamics and tissue oxygenation, including blood pressure, blood rheology, oxygen arterial permeability and tissue metabolic demand. Alterations in the retinal circulation, including ischaemic conditions, are associated with many local and systemic pathologies. For instance, reduced retinal blood flow and retinal tissue hypoxia have been associated with diabetic retinopathy (Causin et al, 2016). However, whilst the scientific community has been investigating the relationship between haemodynamic alterations, ischaemic conditions and retinal and systematic disorders, the main mechanisms governing these relationships remain poorly understood (Causin et al, 2016).

The cerebral microcirculation and therefore the retinal microvasculature is regulated by the general physiological principles of the small vessels system. The arterioles are very small vessels, and even when they are relaxed, the site offers most of the flow resistance (Hill et al, 2015). This is because there are many smooth muscle cells in their walls, and active reduction of the diameter of the vessel can have a significant effect on the resistance. Previous studies have found that contraction of the third of the original diameter of an arteriole may increase the flow resistance up to 81-fold (Vanzetta et al, 2005; Dobrin et al, 1988). Therefore, it is evident that the microvasculature (including the retinal microcirculation), but not necessarily the conduit arteries, can have a significant effect on the distribution of blood flow.

Changes in the retinal microvasculature have been associated with multiple cardiovascular complications in healthy individuals and in individuals with type 2 diabetes, such as hypertension and diabetic retinopathy. Retinal microvascular changes have also been associated with major cardiovascular outcomes including ischaemic heart disease (discussed on the following chapter) and stroke. Epidemiological studies have provided accumulating evidence that cerebrovascular disease occurs in the context of a much broader vasculopathy that affects target regions in multiple organs, including the retina, heart and kidney. Recent studies

have found associations between retinal vascular abnormalities and cerebral white matter lesions. These are biomarkers for small vessel disease and indeed, these are surrogates of cardiovascular dysfunction (Kwa and Lopez, 2010).

In the context of retinal vessel abnormalities, it is particularly relevant to study cerebrovascular disease as the retina and the brain share similar anatomic, physiologic and embryologic features (e.g mesenchymal cells).

A study found a correlation between the loss of branching complexity of the retinal vessels (decreased multifractal dimensions) and cerebral lacunar strokes (Doubal et al, 2010). Furthermore, an association was found between loss of branching complexity and increasing age. This suggests that changes occur in the retinal vasculature with increasing age. Measures of complexity derived from the field of nonlinear dynamics (fractals theory) may help to assess age-related anatomic and physiologic changes and possibly predict pathology (Lipsitz and Golderberg, 1992).

Microvascular dysfunction of the heart may share underlying pathophysiological mechanisms with that of the brain, including endothelial dysfunction, thrombosis, vascular remodelling and capillary rarefaction (Mejia-Renteria et al, 2018). The coronary microcirculation is constituted by arterioles, capillaries and venules and vessels of size less than 300 micrometres represents a major vascular contributor to the heart's density. This microcirculation plays an essential role in resistance of heart circulation through modulation of the vascular tone of the arterioles (Mejia-Renteria et al, 2018). Capillaries are abundant in the heart and their highest density is in the myocardium, accounting for 90% of the intramyocardial blood volume.

Endothelial cells play a key role in both the coronary and cerebral microcirculation. These mediate vasodilation and vasoconstriction from different triggers, including nitrous oxide and other factors such as metabolic, neurohumoral, shear stress and adaptative responses to changes in blood pressure. Cerebral microcirculation features include the presence of the blood-brain barrier, the absence of energy reserves and the influence of astrocytes and neurovascular nerves of the cerebral blood flow self-regulation (Mejia-Renteria et al, 2018).

There has also been an interest in the relationship of the renal microcirculation with the retinal vasculature. Chronic kidney disease is associated with low-grade

inflammation, endothelial dysfunction and platelet activation. These characteristics have been also found in the pathogenesis of impaired coronary and cerebral microcirculation. Progression of renal dysfunction may also be associated with retinal vessel constriction (Nagaoka and Yoshida, 2013). Recent clinical studies have reported that the calibre of retinal arterioles and venules decreased progressively with each CKD stage of renal failure (Yau et al, 2011), suggesting that progression of renal dysfunction might be associated with retinal vessel abnormalities. Although these studies did not include patients with diabetes, the findings seemed to support the finding that vessel diameter and blood flow in the retinal arterioles were significantly lower in patients with stage 3 CKD compared with those without CKD in patients with type 2 diabetes and no or minimal retinopathy (Ooi et al, 2011).

1.5 Measurement of retinal vessels

The first direct ophthalmoscope, named “Augenspiegel” or “the mirror of the eye,” was developed by the German doctor Hermann von Helmholtz in 1851. It allowed for the first time, the examination of the fundus of the eye through the pupil (McGinnity et al, 2019). Since then, there has been a great interest to analyse and measure the components of the retina, including the microvasculature. Retinal vasculature analysis is important for the early diagnostics of the various eye and systemic diseases. Characteristics of the retinal vasculature make potentially useful novel biomarkers (MacGillivray et al, 2014). Both qualitative and quantitative assessment have been widely used in numerous studies using state-of-the-art computerised methods (McGrory et al, 2018). These semi-automatic computerised methods use retinal photographs.

Methodologically, the retina is photographed directly through the dilated pupil using a specialised fundus camera illuminating the fundus of the eye. An external source of light is captured in the retinal surface, which in consequence, is reflected back to the camera, capturing the image of the retinal surface. This two-dimensional image of the retinal surface is called a retinal fundus image. A typical fundus camera is located between 30-50 degrees of the retinal surface, and it is magnified 2.5 times (Panwar et al, 2016).

Fundus images can be focused on different retinal features, depending on the medical purpose. The most common sites analysed are: the optic disc (e.g. glaucoma), macula (e.g. macular degeneration) and characteristics between the optic disc and the macula (e.g. diabetic retinopathy) (Trucco et al, 2013). The vast majority of epidemiological studies describing the association of retinal vessel with different disorders have used images centred around the optic disc or between optic disc and the macula (Fraz et al 2015; Bankhead et al, 2012). These regions provide detailed traits of the retinal microvasculature as they capture the areas where the vessels enter and leave the retina. These features of the retinal vasculature can be analysed by using a highly specialised computer software and could possibly be used as imaging biomarkers. This is because there is a considerable heterogeneity in cardiovascular risk in people with T2D and there exists a need for additional risk predictors to explain the CVD risk. In this context, there has been a significant interest in the potential utility of imaging biomarkers as possible clinical tools that might facilitate risk prediction and could inform therapeutic and preventative decision-making in cardiovascular disease (Selleck et al, 2017).

Traditional CVD biomarkers should possess certain key features to be used optimally in clinical practice/settings. First, there needs to be a robust association between the imaging biomarker and the clinical outcome. Importantly, although it is essential, such association does not in and of itself ensure that measurement of the imaging biomarker can improve risk prediction, which is a second critical feature that must be present. Third, there are practical considerations to consider, including the availability of a reliable method or technique for measurement of the imaging biomarker and the cost-effectiveness to support its application in clinical practice. In the natural history of the development of a new imaging biomarker, these three features are typically addressed in turn, with the practical considerations representing the final steps before clinical uptake.

1.5.1 Software to detect and measure retinal images

Measuring retinal microvasculature manually is time consuming, laborious, prevents the assessment of a large number of individuals, and impedes the detection of small differences. Over the last few years, engineers, scientists and doctors have together

developed computerised approaches to analyse retinal images on a larger scale. Several institutions have different computerised approaches to analyse the retinal traits. Retinal microvascular parameters have been measured from digitalised images using, for example, custom written programs running such as MATLAB® programming environments on a personal computer. These include software such as **S**ingapore "**I**" **V**essel **A**ssessment (SIVA), and **V**ascular **A**ssessment and **M**easurement **P**latform for **I**mages of the **Re**tina (VAMPIRE). Both are available commercially and publicly, respectively. Several studies have used these platforms and validation of such software applications has been carried out (McGrory et al, 2018).

SIVA is a software developed by the National University of Singapore. This platform can automatically compute a spectrum of retinal vascular parameters including retinal vascular calibres, tortuosity, branching angle, fractal dimension and junction exponent deviation from retinal fundus photographs to quantify the retinal vasculature. Other automation of SIVA includes retinal vasculature tracing, vessel type classification (venule or arteriole) and optic disc detection.

VAMPIRE is a software application for semi-automatic quantification of the retinal vessel properties with large collections of fundus camera images (Perez-Rovira et al, 2011). This software has been developed and validated by an international collaboration of the University of Edinburgh and clinical centres of Europe, Asia and the UK. VAMPIRE aims to provide efficient and reliable detection of the retinal traits including the optic disc, the retinal zones, fovea, macula and the vasculature. It computes quantitative retinal traits including arteriovenous ratio, arteriolar and venular calibres, arteriolar tortuosity (mean, minimum and maximum), venular tortuosity (mean, minimum, maximum) multifractal dimensions (D0, D1, D2) and Monofractal. Additionally, this software automatically detects, vasculature tracing, vessel classification, and optic disc detection.

Traditional computational methods for retinal vascular analyses have also measured branching angle, branching coefficient, and monofractal dimensions. These measurements have shown association with several systemic pathologies. Other methods to quantify the vasculature include ocular coherence tomography and smartphone-based platforms (Panwar et al, 2016), which are novel techniques to

quantify the retinal vasculature. However, they can be costly and demand further resources and devices to analyse the retinal vessels.

1.6 Quantitative retinal vessel traits and their investigation in major epidemiological studies

Numerous retinal vessel traits have now been measured in a range of clinical and epidemiological studies. This section describes the quantitative retinal traits related to vessel widths (arteriolar, venular and the ratio of these), tortuosity (arteriolar and venular) and multifractal dimensions, including their measurement in major epidemiological studies where they have been associated with traditional cardiovascular risk factors, systemic diseases and cardiovascular outcomes (table 1.1).

Each retinal trait may be associated with specific anthropometric, or characteristics of the population. For instance, narrower arterioles –an indicative sign of lower CRAE and decreased AVR- has been associated with increasing age, male gender, high blood pressure and chronic kidney disease. Further details of these associations are found in table 1.1

Moreover, venular dilation – a sign of higher CRVE and increased AVR – has been associated with increased blood pressure, inflammatory markers (e.g. CRP, fibrinogen, interleukin 6), obesity and dyslipidaemia. As for tortuosity, decreased arteriolar tortuosity has been associated with increased aging (Cheung et al, 2011), higher blood pressure (Taarnhoj et al, 2008) higher BMI (Cheung et al, 2008;Taarnhoj et al 2009) and increased $Hb1_{Ac}$ (Sasongko et al, 2013). Moreover, increased venular tortuosity is associated with higher blood pressure and lower HDL cholesterol levels.

Finally, lower retinal monofractal dimensions have been associated with increasing age and with high blood pressure (Doubal et al, 2010). Detailed description of the association of these retinal traits with cardiovascular outcomes (rather than CV risk factors) is given in subsequent sections.

Study (ref)	Sample Size	Study/analysis types	Quantitative traits	Main findings
Atherosclerotic Risk in Communities Study (ARIC) (Klein et al 2000, Wong et al, 2002, Seidelmann et al 2016)	~10000	Cross-sectional and longitudinal	Arteriolar and venular diameters, AVR, focal narrowing	Association of narrower arterioles, wider venules and reduced AVR with CHD risk (especially in women) and with stroke
Blue Mountain Eye Study (BMES) (Kawasaki et al 2011, Wang et al 2006, Liew G et al 2011)	~3500	Cross-sectional and longitudinal	Vessel widths (CRAE, CRVE, AVR), fractal dimensions	Association of narrower arterioles, wider venules and reduced AVR with fatal CHD. Some evidence for association of 'suboptimal' fractal dimensions (i.e. highest and lowest values) with fatal CHD and for reduced fractal dimensions with stroke
Beaver Dam Eye Study (BDES) (Wang et al 2007, Wong et al 2003, Witt el al 2005)	~8000	Nested case control	Retinopathy, vessel widths (including CRAE, CRVE), tortuosity	Association of retinopathy and narrower arterioles with CV mortality. Association of reduced arteriolar tortuosity with fatal CHD. In analysis combined with BMES, association of narrower arterioles and wider venules with both CHD and stroke mortality.
Cardiovascular Health Study (CHS) (Wong et al 2003)	~6000	Cross-sectional and longitudinal	Retinopathy, arteriolar and venular diameters, AVR	Association of retinopathy with CHD and subclinical atherosclerosis. Wider venules associated with incident CHD and stroke. Narrower arterioles associated with incident CHD.
Wisconsin Epidemiological Study of Diabetic Retinopathy (WESDR) (Wong et al, 2003)	~1000	Longitudinal	Vessel widths (CRAE and CRVE)	Associations of narrower arterioles and wider venules with stroke mortality (but not CHD mortality).
Rotterdam Study (Ikram et al, 2006)	~8000	Longitudinal, cross-sectional	Arteriolar and venular diameters	Narrower arterioles associated with increased risk of BP
Singapore-Malay Eye Study (SMES) (Cheung et al 2011)	~3300	Longitudinal, cross-sectional	Vessel widths (CRAE, CRVE and AVR), tortuosity	Greater venular tortuosity associated with younger age, female gender, higher BP and lower HDL cholesterol
Multi-Ethnic Study of Atherosclerosis (MESA) (Wong et al 2006)	~5000	Cross-sectional	Arteriolar and venular diameters (CRAE and CRVE)	Some evidence for association of CRAE with physiological cardiac blood flow
Danish Twin Register Study (DTRS) (Taarnhøj et al, 2006)	~100	Twin study	Arteriolar and venular diameters	Narrower arterioles associated with increasing BP

Table 1.1 Major epidemiological studies where quantitative retinal traits have been measured. Central Retinal Arteriolar Equivalent (CRAE); Central Retinal Venular Equivalent (CRVE); Arteriovenous ratio (AVR)

1.6.1 Vessel widths

Retinal vessel calibres have been analysed in relation to subclinical cardiovascular disease, metabolic outcomes, and vascular events such as stroke and ischaemic heart disease (Flammer et al, 2013). The associations of retinal arteriolar and venular narrowing with cardiovascular disorders such as hypertension and increased macrovascular stiffness have often shown opposing results, so these traits are considered separately in this section. Initially, calibre measurements included the width of the streaming column of reflective erythrocytes (red blood cells). However, this measurement did not include the vessel wall and the plasma volume, which are transparent in fundus photography. In some studies, it was not clear whether computer-assisted methods actually measured the outer vessel diameter (vessel wall and lumen), central red blood column or even the overall lumen (Pakter et al, 2011).

The arteriolar diameter is often expressed in terms of CRAE (Central Retinal Arteriolar Equivalent), which summarises the mean diameter of six arterioles. Similarly, the venular diameter is frequently presented as CRVE (Central Retinal Venular Equivalent), which summarises the mean of the diameter of six venules. The arteriovenous ratio (AVR) is the ratio of the diameter of the arterioles to that of the venules. This is a dimensionless retinal parameter, which means that a smaller AVR signals a relatively smaller arteriolar diameter and wider venular diameter. As such, this retinal biomarker has limitations, as arterioles and venules can have different responses to different cardio-metabolic pathology.

Many studies have described a decreased arteriolar diameter as a lower value of AVR. For example, Wong et al (2002) quantified retinal arteriolar narrowing to examine the association between this biomarker and incident coronary heart disease in The Atherosclerosis Risk Communities Study. After full adjustment, it was found that in women, each decrease of standard deviation of AVR was associated with an increased risk of incident coronary heart disease and acute myocardial infarction. AVR was unrelated to any incident coronary heart disease events in men. Further studies using AVR have found contradictory findings including the Cardiovascular Health Study, which showed no consistent association between the smaller AVR and large artery atherosclerosis (Wong et al, 2003).

Several epidemiological studies have associated narrower arterioles with increasing age including ARIC (Hubbard et al, 1999), DTRS (Taarnhøj et al, 2006), BMES (Sherry et al, 2002) and BDES (Wong et al, 2003). Additionally, cardiovascular disorders such as hypertension have been explored in studies. The Multi-Ethnic Study Atherosclerosis (MESA) found hypertension associated with narrower retinal arteriolar diameter and wider venular diameter (Wong et al, 2006). A large study from the US, the Atherosclerosis Risk in Community (ARIC) which included nearly 11,000 participants, found that any degree of generalised arteriolar had statistically mean arterial blood pressure approximately 8 mmHg higher than those without (Hubbard et al, 1999). Moreover, the Blue Mountain Eye Study (BMES) from Australia, found that after adjusting for age, sex, BMI, smoking, glucose and total cholesterol, retinal arteriolar narrowing at baseline was associated with increased risk of severe hypertension (OR 2.6; 95%CI, 1.7, 3.9) when comparing the narrowest versus the widest quintile (Smith et al, 2004).

Chronic kidney disease and impaired renal function in people with cardiovascular risk factors represents a major public health problem associated with adverse renal and cardiovascular complications and premature deaths. Impaired renal function has been widely explored in the aforementioned datasets. The Singapore-Malay Eye Study using a multivariable analysis and follow-up period of 6 years, found that smaller retinal arterioles (HR 1.34; 95%CI 1.00, 1.78), larger retinal venules (HR 2.35; 95%CI 1.12, 5.94) and the presence of retinopathy (HR 2.54; 95% CI 1.48, 4.36) were associated with chronic kidney disease (Yip et al, 2017). However, an Irish study with data from 1233 participants, did not find any association between retinal arteriolar and venular parameters and chronic kidney disease (McGowan et al, 2015).

In terms of major cardiovascular outcomes such as stroke, an association between the narrower arterioles and increased risk of stroke has been described in several cross-sectional and cohort studies and smaller studies (Kawasaki et al, 2012; Kwa et al, 2002; Wong et al, 2001). In the ARIC study, ischaemic stroke was associated with narrower arterioles (but wider venules). However, other studies have not shown any association between decreased arteriolar diameter and stroke (MacGeechan et al,

2009). Overall, there is no conclusive evidence in the association between arteriolar diameter with either haemorrhagic or ischaemic stroke.

Several studies have also shown that retinal venules are associated with traditional cardiovascular risk factors, subclinical CVD, and major cardiovascular outcomes. For instance, larger venular calibre but not arteriolar calibre, was related to anthropometric measurements of obesity (higher BMI and waist-hip ratio) and dyslipidaemia (higher levels of LDL and triglyceride and lower HDL cholesterol) in the Rotterdam study (Ikram et al, 2004). Moreover, prospective analysis from the Blue Mountains Eye Study further indicated that a larger retinal venular calibre may predict the incidence of obesity (Wang et al, 2006). Data from the Dutch Hoorn study showed that retinal venular dilatation was associated with increased subclinical atherosclerosis such as intima-media thickness. Likewise, larger venular calibre has been associated with peripheral vascular disease such as lower ankle-arm index (Ikram et al, 2004).

Results from several population-based studies have showed a significant association between larger retinal venular calibre and inflammatory markers including C-reactive protein (Ikram et al, 2004) and similar findings were found in a Singaporean cohort (Yim-Lui et al, 2010). In the Beaver Dam Study eye, increased venular calibre was associated with biomarkers related to endothelial dysfunction including soluble intercellular adhesion molecule-1 and serum-E selectin (Klein et al, 2006). Increased dilatation of retinal venules may be the outcome of increased production of nitric oxide secondary to release of pro-inflammatory mediators.

Importantly, retinal venular calibre has been associated with stroke. In The Rotterdam Study, larger venular calibre was associated with 12% higher risk of stroke and a 15% higher risk of cerebral infarction (Ikram et al, 2006). The association of wider retinal venular calibre with an increased risk of stroke has also been confirmed in a meta-analysis (McGeechan et al, 2009)

1.6.2 Vessel Tortuosity

Normal retinal blood vessels are straight or gently curved, but they tend to dilate and start to become tortuous with age and with a number of retinal and systemic

disorders (Cheung et al, 2011). Tortuosity can be defined as full of turns and twists. However, this is not quite accurate when it comes to describing the tortuosity of the retinal vasculature. Bearing in mind that the retinal vasculature is spread in a spherical structure, these vessels are naturally slightly curved and twisted. Qualitatively, there is no established agreement among graders on abnormal tortuosity of the retinal vasculature or on the general levels of vessel tortuosity. Commonly, image graders or ophthalmologists describe the retinal vasculature based on their experience. This is done by identifying characteristics such as differences from normal healthy vessels, length, width, location, type and numbers of twists. Currently, the tortuosity of the retinal vasculature can be quantitatively examined with improved image processing software and algorithm implementation, and more consistent results can be obtained to prevent misclassification.

The tortuosity of the retinal vasculature may be attributed to build-up of the natural capabilities to avoid or adapt to physiological changes including aging, hemodynamic factors or systemic disorders. Vessel tortuosity may result from the ability of the blood vessel to dilate, gain more length and become more curvy and twisty to an abnormal state. Severe vessel tortuosity has been associated with aging and it rarely occurs in children (Han et al, 2012). In terms of mechanical changes that occur in the tortuous vasculature, experimental and physiological studies have shown strong associations between tortuous vessels and mechanical factors such as blood pressure, blood flow, axial tension and structural vessel wall changes (Ciuricā et al, 2019). Retinal arteries and venules are subject to mechanical stress generated by lumen blood flow, pressure and surrounding tissue tethering (Han et al, 2013). These mechanical characteristics are influenced by many physical and mechanical factors such as exercise and gravity. Previous studies have documented that these mechanical factors play an important role in regulating the vascular endothelium (Hartnett et al, 2008). These factors may restrict, partially or completely, the blood flow, which as a result may lead to stroke, transient ischaemic attack, or hindrance of arteriogenesis and tissue regeneration. Moreover, thrombosis (the formation of a blood clot or thrombus within a blood vessel), which has been observed in tortuous blood vessels may lead to vessel occlusion with subsequent myocardial infarction or stroke (Owens and Mackman, 2010).

Extensive clinical studies have shown that vessel tortuosity is associated with cardiovascular conditions, including atherosclerosis, abdominal aortic aneurysms, hypertension, diabetic retinopathy, and arterial tortuosity syndrome (Chessnut et al, 2011). Indeed, tortuosity of the retinal vasculature has been identified as one of the earliest developing biomarkers for a number of systemic vascular disorders (Han et al, 2011), and, interestingly, there is an association of retinal tortuosity with tortuosity of major vessels such as the abdominal aorta (Beyons et al, 2016). Hence, it may be important to detect retinal vessel tortuosity early to potentially help identify systemic vascular disorders in their early stages and reduce further complications.

Tortuous retinal arterioles are a fairly common finding, and while mild tortuosity is asymptomatic, severe tortuosity can lead to serious clinical symptoms or ischaemic damage (Han et al, 2012). Arteries may take a more tortuous path due to abnormal development or vascular disease. Retinal arteriolar tortuosity has been associated with increased age (Cheung et al, 2011) and with arterial hypertension, diabetic retinopathy, cerebral vessel disease, stroke and familiar arteriolar tortuosity (Chessnut et al, 2011; Ciuricā et al, 2019). Interestingly though, Taarnhøj et al (2008) found hypertension to be associated with decreased retinal arteriolar tortuosity, while higher BMI was associated with reduced tortuosity.

Tortuosity, specifically of the retinal venules, has been investigated in several epidemiological studies. The Singapore-Malay cohort (Cheung et al, 2011) found retinal venules to be significantly more tortuous than retinal arterioles, and greater venular tortuosity was independently associated with younger age, female gender, higher blood pressure and lower HDL cholesterol level. This study also showed that non-diabetic subjects with retinopathy signs had significantly more tortuous venules than those without retinopathy, although venular tortuosity was not significantly associated with diabetes. However, findings from Sasongko and colleagues showed that individuals with diabetes had more tortuous retinal arterioles and venules (Sasongko et al, 2011) and that retinal venular tortuosity was associated with any grade of diabetic retinopathy compared with individuals without diabetic retinopathy. Recently, in a study carried out in the Norfolk (UK) found that increased venular tortuosity was associated with higher BMI, HbA_{1c}, and prevalent type 2 diabetes. These associations persisted after full adjustment. Interestingly, arteriolar tortuosity

but not venular tortuosity, increased with those with prevalent stroke. No associations were seen with prevalent myocardial infarction (Owen et al, 2019).

In the cross-sectional Multi-Centre Retinal Stroke study, Singaporean individuals were recruited and it was found that after full adjustment, increased venular tortuosity and increased arteriolar tortuosity were associated with stroke (Ong et al, 2013). Lastly, in a recent study which included individuals from Orkney Scotland (ORCADES study) and data from the isolated population Korčula Croatia, larger venular tortuosity was found to be associated with longer cardiac QT interval and that arteriolar tortuosity was associated with carotid intima media thickness (Kirin et al, 2017).

1.6.3 Multifractal dimensions

In recent years, fractal analysis has attracted much interest as a novel biomarker from the biomedical imaging communities, and has been used in several cohorts to analyse the retinal vasculature. Fractal dimensions is the link between fractal theory and practical applications to cardiovascular medicine. This is a unitless number that measures nontrivial, self-similar scaling (Captur et al, 2017). A phenomenon is self-similar if the whole resembles its scaled parts, and its self-similarity is non-trivial if, in essence, the design detail and repetitive arrangement creates a pattern too 'irregular' to be defined by Euclidean geometry (Captur et al, 2017). Fractal dimensions measures a phenomenon's complexity, which is the logarithmic ratio of the change in detail to the change in scale. The retinal vasculature typically shows fractal properties or self-similarity at multiples scales and over the last decade, there has been increasing interest in using fractal dimensions to quantify the "state" of the human retinal vasculature (considered as a geometrical object).

Fractal dimensions include measurements such as mono-fractal (D_f) and multifractal dimensions. Fractal dimension (monofractal) describes how much space is filled, but does not indicate how the space is filled by the fractal structure. An object (e.g. retinal vasculature) is considered multifractal when its different regions have different fractal properties. In fact, Costa and Nogueira (2015) observed that not only the entire retinal vasculature, but also several regions of the retina follow a multifractal

behaviour. Multifractal dimensions detects the multifractal scaling using the box counting technique, which takes into account the distribution of pixel values in a digital image. This methods gathers information about the distribution of pixel values which leads to calculation of multiple scaling rules.

One value of the generalized multifractal dimension D0 (Q=0) is equal to what is called the "capacity dimension", which can be understood as the box counting dimension. Multifractal dimension D1 (Q=1) is equal to what is called the "information dimension", and multifractal D2 (Q=2) to the "correlation dimension" (Stosić et al, 2006). These traits are measured with VAMPIRE software.

Previously, it was stated that the vascular network of retinal regions presents multifractality and not only the vascular network of the whole retina, but its regions, can also be considered a superposition of monofractal structures (Costa and Nogueira, 2015).

Fractal dimension (D_f) has been studied widely in different cohorts. In a prospective cohort of adults, participants with suboptimal D_f (lowest and highest quartiles) had 50% higher 14-year ischaemic heart disease mortality than those with optimal D_f after full adjustment (Liew et al, 2011). In a cross-sectional study performed in an Asian population, the history of hypertension was significantly associated with D_f, as was age (Zhu et al 2014). Indeed, in this study, blood pressure exhibited a stronger association with D_f than with central retinal arteriolar equivalent. In a recent study (Wang et al, 2018), D_f was lower in women, decreased with increasing age and was significantly associated with coronary artery disease vessel score. These results showed that a sparser retinal microvasculature (smaller D_f) was not only associated with older age and female gender but also with more diffuse and severe coronary artery disease.

There is great interest in the association of retinal fractal dimensions with cerebral small vessel disease and cerebrovascular disease. Higher retinal fractal dimension (highest vs lowest quartile and per standard deviation increase) has been independently and positively associated with lacunar stroke (OR 4.27; 95% CI 1.49-12.7 and OR 1.85; 95% CI 1.20-2.84, respectively) (Cheung et al, 2010). Conversely, in the Blue Mountains Eye Study, each standard deviation decrease in

baseline fractal dimension was associated with 40% greater risk of stroke events (OR 1.39, 95% CI 1.06 -1.83). Individuals in the smallest quartile of fractal dimensions were twice as likely to have a subsequent stroke than those in the largest quartile (OR 2.30, 95% CI 1.06 - 4.97) (Kawasaki et al, 2011). This study may suggest that reduced complexity in the branching pattern of the retinal microvasculature indicated by reduced fractal dimensions affects perfusion, which might increase vulnerability to hypoxia. Consistent with the BMES study findings, a cross-sectional analysis found that decreased mono-fractal and multifractal traits were associated with increasing age and lacunar stroke after correcting for hypertension, diabetes, stroke severity and white matter hyperintensity scores (Doubal et al, 2010).

These findings are likely to be related to focal manifestation of a widespread non-atheromatous small vessel vasculopathy, perhaps resulting from an increased blood–brain barrier permeability associated with endothelial dysfunction. This mechanism results in decreased diametre of the retinal vessels causing decreased branching complexity, and therefore, reduced multifractal dimensions (Doubal et al, 2010).

1.7 Genetics of retinal microvasculature

The identification of genetic variants in complex diseases such as cardiovascular and metabolic disorders has been studied widely. The identification of novel susceptibility genetic variants offers new insights into pathophysiological pathways and may help to better understand the physiopathology and factors, which contribute to the rapid development of the disease. These findings may also help to enrich genetic risk profiling alongside traditional cardiovascular risk factors.

The genome-wide association study (GWAS) is an experimental design used to detect associations between genetic variants (also called single nucleotide polymorphisms, SNPs) and traits in samples from populations (Visscher et al, 2017). The main goal of these studies is to better understand the biology of disease under the assumption that this will help to prevent and better treat the disorder. GWAS have been successful in exploring the relative role of genes in a disorder and

interaction with the environment, assisting in risk prediction (personalised medicine) and investigating differences among the populations (Visscher et al, 2017). GWAS have also driven the discovery of over 10,000 robust associations with complex diseases and disorders, quantitative traits and genomic traits (Visscher et al, 2017). The retinal vasculature is an important area to identify novel variants as the retinal microvasculature shares structural and physiological characteristics with the cerebral and coronary circulation (Mejía-Renteria et al, 2018).

Few studies have investigated the contribution of genetic variants to retinal microvasculature traits. Heritability of the retinal microvasculature has been studied, showing that retinal traits have different percentages of heritability. Lee et al (2004) performed the first study to report on family aggregation of quantitative retinal vessel traits. This study found a high correlation of the arteriolar and venular calibre (CRAE and CRVE, respectively) and AVR among relatives (more highly correlated than between unrelated individuals). Twin studies have shown different proportions of heritability among the quantitative retinal vessel traits. Taarnhøj et al (2006) analysed 55 monozygotic and 50 dizygotic same-sex healthy twin pairs. Heritability was found to be 70% for CRAE and 83% for CRVE. This study also concluded that retinal vessel calibres are involved in risk of vascular disease due primarily to genetic characteristics. However, a range of heritabilities have since been demonstrated for the retinal traits. In a cohort in the UK, Fahy et al (2011) found heritability estimates for CRAE and CRVE of 66% and 72% respectively using a bivariate model, while Kirin et al (2017) showed heritabilities of 35.9% for CRAE, 39.6% for CRVE, 30.2% for AVR, 50% for arteriolar tortuosity, 22.9% for venular tortuosity and just 21.1% for multifractal dimensions. A summary of heritability is shown in table 1.2

Quantitative retinal trait	Taarnhoj et al 2006	Fahy et al, 2011	Liu et al, 2013	Kirin et al, 2017
AVR	45%	--	27%	30.2%
CRAE	70%	66%	21%	35.9%
CRVE	83%	72%	34%	39.6%
Arteriolar tortuosity	82%	--	--	55%
Venular tortuosity	--	--	--	22.9%
Multifractal dimensions	--	--	--	21.2%

Table 1.2 Summary of the genetic heritability of quantitative retinal traits in different datasets. Although, there is variation among the results in these cohorts, the direction of the quantitative vessels width indicates a higher proportion of heritability in venular calibre than in arteriolar cal bre. Additionally, heritability of monofractal dimensions in Danish twin study was 79% (Vergmann, et al 2017)

A small number of genome-wide linkages studies have been performed to analyse quantitative retinal vessel traits. Xing et al (2006) conducted a genome-wide linkage scan on retinal vessel calibres using data from the Beaver Dam Eye Study in the Netherlands. In this dataset, it was found that the regions 3q28, 5q35, 7q21, 7q32, 11q14, 11q24 and 17q11 showed linkage signals at the multipoint significance level for either unadjusted or adjusted models for CRAE. Regions on chromosomes 1p36, 6p25, 6q14, 8q21, 11p15, 13q34 and 14q21 showed linkage signals at the significance level in either unadjusted or adjusted models for CRVE. These results indicate genetic contributions that remain significant even after adjusting for hypertension and other covariates. In a genome-wide linkage analysis study conducted in Brisbane Australia (Sun et al, 2009), two multipoint peaks detected on chromosomes 3p12.3 and 8p23.1 for CRAE had suggestive linkage with the highest multipoint on chromosome 8p23.1 (p = 7.0 x10^{-4}). Two suggestive regions for CRVE were identified on chromosomes 2p14 and 9q21.13. The most significant association was found on chromosome 2p14 (p = 2.0 x 10^{-4}). Hence, in this twin population study, genetic factors appeared to play a significant role in the variation of retinal vessel calibres.

Other studies have assessed whether genetic background may contribute to differences in retinal vessel diameters between different ethnic groups. Cheng et al

(2010) scanned 1737 African Americans searching for genomic regions where individuals have narrower retinal arteriolar calibre or wider retinal venular calibre. The percentage of African ancestry was positively correlated with retinal venular calibre, particularly in hypertensive individuals. They showed that the association was found on chromosome 6p21.1 especially in individuals with hypertension. The 6p21.1 region contains genes that are biologically relevant in the development and modulation of the retinal vessels. One of these genes in this region includes the vascular endothelial growth factor gene. These genes plays a critical role for retinal vessels, as an endothelial-cell selective mitogen intimately associated with vasculogenesis, angiogenesis and vascular permeability.

Larger scale GWAS and meta-analyses have been performed over the last few years. These studies have reported on genetic associations mainly for retinal arteriolar and venular calibres. Sim et al (2013) found one loci significantly associated with CRAE on chromosome 5. The SNP rs2194025 on chromosome 5q14 near the myocyte enhancer factor 2C *MEF2C* gene was associated in the discovery cohorts with *p*-value $<5x10^{-8}$. This variant in combined meta-analysis and replication cohorts showed that rs2194025 reached a *p*-value=$2.11x10^{-12}$. In a large meta-analysis, Ikram et al (2010) reported that four loci were associated with CRVE in cohorts from North America, Europe, Asia and Australia. The top SNPs were rs2287921 on chromosome 19q13 ($p = 1.61 \times 10^{-25}$) within the *RASIP1* locus and rs225717 on chromosome 6q24 ($p = 1.25 \times 10^{-16}$). This SNP is located adjacent to the *VTA1* and *NMBR* loci. Moreover, the SNPs rs10774625 on chromosome 12q24 ($p = 2.15 \times 10^{-13}$) located in the region *ATXN2*, *SH2B3* and *PTPN11* loci and rs17421627 on chromosome 5q14 ($p = 7.32 \times 10^{-16}$) next to *MEFC2C* locus. Further, replication in two independent samples showed that locus 12q24 was also associated with ischaemic heart disease and hypertension. Another large-scale genome-wide association study carried out by Jensen et al (2016) with 24 000 individuals reported 4 new loci associated with CRVE. The rs7926971 in *TEAD1* gene ($p = 3.1 \times 10^{-11}$), rs201259422 in *TSPAN10* ($p = 4.4x10^{-9}$), rs5442 in *GNB3* ($p = 7.0 \times 10^{10}$) and rs1800407 in *OCA2* ($p = 3.4 \times 10^{-8}$).

The latter SNP, rs1800407 was also associated with CRAE. Further analyses in the dataset, showed that rs201255422 was also associated with cardiovascular parameters including systolic (p=0.001) and diastolic blood pressure (p=8.3 x 10^{-4}).

Literature on the associations of retinal vascular traits with ischaemic heart disease including angina, myocardial infarction and coronary ischaemia are presented in the next chapter.

Chapter 2 Literature Review: Association of retinal vascular traits with ischaemic heart disease in people with diabetes

Whilst examining the epidemiological literature on associations between retinal traits and cardiovascular disease, it became apparent that the association of retinal traits with ischaemic heart disease in people with diabetes was not well covered by the major epidemiological studies discussed in chapter 1. I chose this association as the topic of a detailed and comprehensive review using a systematic literature search, to better understand the current state of knowledge on this area and to inform my own subsequent analyses for this thesis. I present the methods and findings of this literature review in this chapter.

2.1 Objectives

The objectives of this review were to:

- Systematically identify the relevant epidemiological literature on the association between quantitative retinal traits and ischaemic heart disease in people with diabetes
- Describe the associations between quantitative retinal traits and ischaemic heart disease in the identified literature
- Consider the quantity and quality of the evidence found and therefore the need for further research in this area

2.2 Methods

2.2.1 Inclusion criteria

2.2.1.1 Types of studies

I included longitudinal cohort studies, cross-sectional studies and case-control studies in this analysis. I analysed articles in English and Spanish language as it was not feasible to find translators for articles in other languages for the purposes of my

PhD. I decided to include studies performed from 1970 onwards because the technology to assess the retinal vasculature started to be used in the mid-1970s. I reviewed full text articles to ensure good quality information.

2.2.1.2 Participants

Participants were adults with diabetes (either type 1 or type 2), including male and female, from any population in the world. I excluded studies on individuals with infections or other inflammatory medical conditions (liver disease, malignancy) or with other retinal conditions (such as age-related maculopathy, retinal artery/vein occlusion). Although, for the purposes of this review I included only adults with diabetes, I also retrieved studies on the general population in order to identify relevant literature for other sections of my thesis.

2.2.1.3 Retinal traits

I considered assessment of any quantitative retinal microvascular trait. This included characteristics associated with retinopathy (e.g. microaneurysms, hemorrhages) as well as quantitative retinal vascular traits such as arteriovenous ratio (AVR), central retinal arteriolar equivalent (CRAE), central retinal venular equivalent (CRVE), tortuosity and fractal dimensions.

2.2.1.4 Outcomes measures

The main cardiovascular outcome of interest was ischaemic heart disease (IHD). This included coronary artery disease, ischemic heart disease and myocardial infarction (fatal and/or non-fatal).

2.2.2 Exclusion criteria

I excluded any articles, which were systematic reviews, notes, conference abstracts and editorials, from this review.

2.2.2.1 Search strategy

I identified articles using a sensitive search strategy across two major medical databases to gather potentially relevant literature. I used free-text terms and indexed keywords (MeSH for MEDLINE; EMTREE for EMBASE) in Medline and EMBASE electronic databases. I developed a comprehensive list of different free-text terms to

identify as much as possible of the relevant literature. I also conducted an analysis of the references of the relevant articles and reviews to find other potential papers.The full search strategy is included in appendix 1. I screened the titles and abstracts of potentially relevant articles and then obtained the full text of these articles. This systematic review search was carried out on December 2, 2017. Although the Cochrane guidelines for systematic reviews (Higgins and Green, 2011) suggest that two reviewers should carry out this process, this was not practical for my PhD project.

2.3 Results

2.3.1 Study selection

The search strategy conducted in MEDLINE and EMBASE databases retrieved a total of 1421 potentially relevant articles. The PRISMA flow diagram, describing the study identification process, is shown in Figure 2.1.

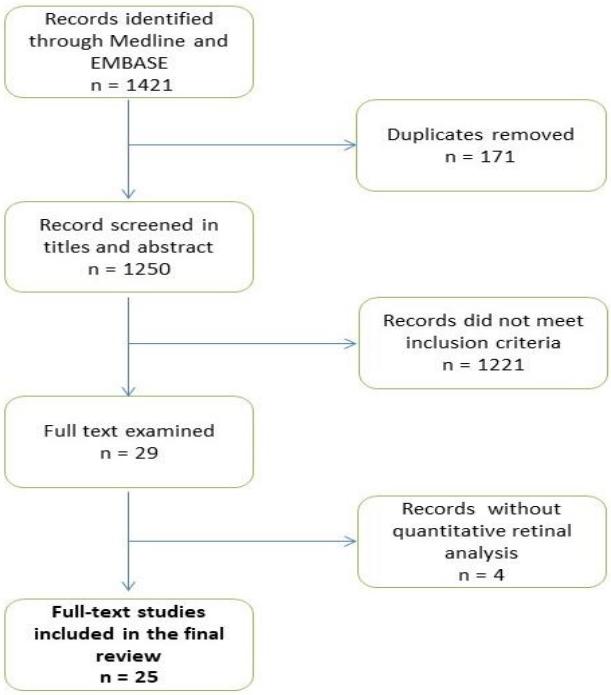

Figure 2.1. Prisma Flow diagram

I exported 1421 articles returned by the search, to Endnote. A total of 171 duplicate papers were identified using Endnote and removed, leaving 1250 articles to be screened. These 1250 papers were screened by the title and abstract and 1221 records were removed at this stage, as they were irrelevant and did not meet the

criteria. This resulted in 29 articles remaining for a full-text assessment against the eligibility criteria.

After an examination of the full text articles, 25 studies remained of which eight included populations with diabetes. The findings from these eight papers are discussed in detail below, and information from the other 17 studies (on the general population) was incorporated into other sections of the thesis (a table summarizing these studies is given in (appendix 2).

2.3.2 Study findings

2.3.2.1 Studies on individuals with type 2 diabetes

Five studies on individuals with type 2 diabetes were identified (table 2.1). Klein et al (2007) analysed a subset of the study population in the Wisconsin Epidemiologic Study of Diabetic Retinopathy cohort. This was a prospective study with a follow-up of 22 years, which included incident diabetic complications such as nephropathy, neuropathy, and lower extremities amputations as well as all-cause mortality and mortality from ischaemic heart disease (IHD) and stroke, although non-fatal incident cardiovascular events were not analysed separately. The main results showed significant independent associations of the narrower retinal arteriolar calibre (lower CRAE) with lower extremity amputations and all-cause mortality and stroke mortality (HR, 1.47; 95% CI, 1.04-2.07; $p = 0.03$) in the multivariate model, adjusted for age, sex, HbA_{1c}, hypertension, proteinuria and previous cardiovascular history. However, no association was seen with IHD mortality. Wider venular calibres (higher CRVE) were independently associated with incidence of nephropathy and stroke mortality (HR 1.71; 95% CI, 1.20-2.44; $p = 0.003$), but not with IHD mortality. It is important to highlight that the quantitative retinal measurements were classified into quartiles in this study. The reference group for CRAE included the second, third and fourth quartiles while the reference group for CRVE included the first, second and third quartiles. A more powerful and informative analysis may have resulted from keeping the traits as continuous variables, but no information on such an analysis was reported.

Phan et al (2016) analysed and compared individuals with and without type 2 diabetes in a cross-sectional study of 1677 individuals in which both retinal arteriolar and venular calibres were measured. Associations with coronary heart disease were investigated using Gensini and Extent scores from findings on coronary angiograms. Three different scores were used, including the vessel score of obstruction (stenosis, IV grade), the Gensini scores (severity score) and the Extent score (for the detection of atheroma). In a model adjusted for age, sex, BMI, hypertension, smoking status and eGFR, individuals with undiagnosed (newly diagnosed in this study) and diagnosed diabetes versus those with no diabetes had increased odds of being in the highest quartile of Gensini scores odds ratio (OR)= 7.02 (95% CI, 2.04-24.1) and (OR) =2.76 (95% CI, 1.67-4.55), respectively. Similarly, using a model with the abovementioned covariates, recruited individuals with newly diagnosed and diagnosed diabetes versus those with no diabetes also had increased odds of being in the highest quartile of Extent scores, OR =7.63 (95% CI, 2.15 -27.10) and OR = 3.72 (95% CI, 2.22-6.27), respectively. The results showed no significant differences in the association of any of the angiograms scores and the retinal arteriolar and venular calibres with undiagnosed versus diagnosed diabetes in the unadjusted and fully adjusted models.

Drobnjak et al (2016) carried out a prospective analysis in individuals from Copenhagen, Denmark, with type 2 diabetes diagnosed by the oral glucose tolerance test, known diabetes mellitus, or impaired glucose tolerance, aged 30 years or older, and with a mean follow-up of 15 years. In this study, 908 individuals were recruited, CRAE and CRVE were measured and the end points included mortality from ischaemic heart disease (IHD defined as bypass, recanalization, reconstruction of coronary arteries), as well as stroke mortality and non-cardiovascular mortality. This study found narrower CRAE to be associated with higher systolic blood pressure but with higher HDL cholesterol and lower smoking levels, while wider CRVE was associated with higher smoking levels and lower HDL cholesterol. In age-adjusted models and using linear regression model, an association between wider CRVE and risk of IHD was found ($p < 0.001$), but no significant association was reported between CRAE and IHD. Although, wider CRVE was associated with all-cause mortality (HR=2.02, (95% CI, 1.0 – 3.8); p=0.03) in a basic model, the association was attenuated in a model which was fully adjusted for

age, sex, blood pressure and smoking. It is important to highlight that these results were obtained when the third tertile of CRVE was compared to the first tertile of CRVE. This study confirmed an association of retinal arteriolar and venular calibres with traditional cardiovascular risk factors as well as reporting on associations between the traits and IHD as a disease outcome.

Guo et al (2016) recruited 229 individuals (79 with cardiovascular disease and 150 controls who were free from cardiovascular disease) from the urban area of Hong Kong. Participants were aged 18 years and older. In this study, several quantitative retinal parameters were measured including CRAE, CRVE, AVR, arteriolar and venular standard deviation of the vessel width (BSTD), fractal dimensions, tortuosity, branching angles, branching coefficient, asymmetry factor, junctional exponent, angular asymmetry, length to-diameter ratio and diabetic retinopathy. In this cross-sectional analysis, individuals with stroke, transient ischaemic stroke and CHD were defined as cases (n=79). Three models were created. The first model included traditional cardiovascular risk factors such as diabetes duration, hypertension and HDL cholesterol, of which only diabetes duration was associated with CVD (OR 1.09; 95%CI 1.04-1.14 p <0.001). In the second model, only retinal traits were analysed, including AVR, diabetic retinopathy and junctional exponent (a novel quantitative retinal trait that describes the deviation from optimality at a bifurcation). The results in this second model showed an association of the junctional exponent with cardiovascular events (OR 0.19; 95%CI, 0.06-0.62; p=0.006). In the third model, both the traditional cardiovascular risk factors and the retinal traits were included. Interestingly, the results showed that diabetes duration (OR 1.08; 95%CI 1.03-1.14; p=0.001), HbA_{1c} (OR 1.29; 95%CI 1.02-1.61; p =0.03) and junctional exponent (OR 0.03; 95%CI 0.003-0.33; p=0.004) were associated with cardiovascular events.

Phan et al (2018) carried out another analysis in The Australian Heart Eye Study. They recruited 748 individuals, which included 96 with impaired fasting glucose and 189 with diabetes mellitus. Associations with coronary heart disease were investigated using Gensini and Extent scores from findings on coronary angiograms. Two scores were used, including the Gensini scores (severity score) and the Extent score (for the detection of atheroma). No association was found between CRAE and individuals with impaired fasting glucose or diabetes. In an analysis stratified by

gender, males with the second and third tertiles were associated with diabetes in a model adjusted for age, BMI, alcohol, smoker, hypertension, history of diabetes, cholesterol total, HDL, use of statin, and CRAE, OR 2.45 (95% CI, 1.31 – 4.5) p = 0.005 and OR 2.76 (95% CI, 1.46-5.21) p = 0.002, respectively. CRVE was associated with the first tertile Gensini Score in a model adjusted for age and sex in people with diabetes OR 1.56 (95% CI, 1.04 – 2.34). Moreover, this association was also seen in participants below the median Extent score (i.e. less diffuse coronary artery disease) OR 1.67 p = 0.008). However, in both the models, the associations were attenuated in a multivariate adjustment. Conversely, there were no associations between CRVE and diabetes in women. No associations were found in the group with impaired fasting glucose.

Title	Reference	Study Population	Recruitment method	Study Type / Model	Number of people included in the analysis	Duration of follow-up (years)	Retinal Vasculature Exam	End Points	Events	Results
Severity of coronary artery disease and retinal microvascular signs in patients with diagnosed versus undiagnosed diabetes: cross-sectional study	Phan et al, 2016	Stratifying participants with previously diagnosed diabetes, undiagnosed diabetes and no diabetes	Individuals from the Australian Heart Eye Study. Greater Western Sydney area	Cross-sectional / Logistic	1677	Cross-sectional	1-Retinal arteriolar calibre 2-Retinal venular calibre. Digitised photographs of the right eye was used mainly, if not available, left eye. Knudtson-Hubbard formula.	Coronary heart disease assessed by angiograms 1-Vessel score of obstruction (stenosis, IV grades) 2-Gensini scores (severity score) 3-Extent score (proposed by Sullivan) detection of atheroma	Angiogram scores available for all recruited individuals. 1- DM n=489 2- undiagnosed diabetes n=76 3- healthy n=1112	No significant differences in the association of any of the angiograms scores and the retinal arteriolar and venular calibres with undiagnosed versus diagnosed diabetes in the unadjusted and fully adjusted models.
Associations between retinal arteriolar and venular calibre with the prevalence of impaired fasting glucose and diabetes mellitus: A cross-sectional study	Phan et al, 2018	Stratifying participants with impaired fasting glucose (IFG) and diabetes mellitus	Individuals from the Australian Heart Eye Study. Greater Western Sydney area	Cross-sectional / Logistic	1033	Cross-sectional	1-CRAE 2-CRVE Digitalised images, right eye was used mainly, if not available, left eye. Knudtson-Hubbard formula.	Gensini Score and Extent Scores similar to the paper above	Subjects with 1- IFG n= 96 2- DM n=189 3- Healthy n=748	CRVE was associated with the first tertile Gensini Score in a model adjusted for age and sex in people with diabetes OR 1.56 (95% CI, 1.04 , 2.34). Association was also seen in participants below the median Extent score [OR 1.67; *p*=0.008)].

Title	Reference	Study Population	Recruitment method	Study Type / Model	Number of people included in the analysis	Duration of follow-up (years)	Retinal Vasculature Exam	End Points	Events	Results
Retinal Information is Independently Associated with Cardiovascular Disease in Patients with Type 2 diabetes	Guo et al, 2016	Type 2 diabetes	Subjects recruited from Ma On Shan Family Medicine Center. Hong Kong	Cross-sectional / Logistic	229	Cross-sectional	1-Vessel widths: CRAE, CRVE, AVR, BSTD (standard deviation of the vessel width 2-Branching: fractal dimensions, tortuosity, branching angle, branching coefficient 3-Other: Asymmetry factor, junctional exponent, angular asymmetry, Length to-diameter ratio. 4-Qualitative: DR Randomly selected eye image. Knudtson-Parr-Hubbard formula	1-Stroke or TIA 2-Coronary heart disease	1-79 CVD cases (non-specified what type of event occurred) and 2- 150 non CVD controls	Association of the junctional exponent with cardiovascular events (OR 0.19; 95%CI, 0.06, 0.62; p=0.006). In fully adjusted model, the results showed that diabetes duration (OR 1.08; 95%CI 1.03, 1.14; p=0.001), HbA_{1c} (OR 1.29; 95%CI 1.02, 1.61; p =0.03) and junctional exponent (OR 0.03; 95%CI 0.003, 0.33; p=0.004) were associated with cardiovascular events.

Title	Reference	Study Population	Recruitment method	Study Type / Model	Number of people included in the analysis	Duration of follow-up (years)	Retinal Vasculature Exam	End Points	Events	Results
Retinal vessel caliber and microvascular and macrovascular disease in type 2 diabetes: XXI: the Wisconsin Epidemiologic Study of Diabetic Retinopathy	Klein et al 2007	Type 2 diabetes	Wisconsin Epidemiologic Study of Diabetic Retinopathy	Prospective / Logistic and Cox regression	962	22	1-CRAE 2-CRVE 3-Retinal focal arteriolar narrowing (Present or Absent) 4-Arteriovenous nicking 5-Diabetic Retinopathy (ETDRS) Both images were digitised (scanned) Knudtson-Parr-Hubbard formula	1- Nephropathy 2- Neuropathy 3-Lower extremity amputation 4-IHD mortality 5-Stroke mortality 6-All cause mortality	1-Ischaemic heart disease mortality (n=548) 2- Stroke mortality (n=204)	Narrower CRAE was associated with lower extremity amputations and all-cause mortality and stroke mortality (HR, 1.47; 95% CI, 1.04, 2.07; *p* = 0.03) in fully adjusted model. Wider venular calibres were associated with incidence of nephropathy and stroke mortality (HR 1.71; 95% CI, 1.20, 2.44; *p*=0.003)
Retinal Vessel Diameters and Their Relationship with Cardiovascular Risk and All-Cause Mortality in the Inter99 Eye Study: A 15-Year Follow-Up	Drobnjak et al, 2016	Type 2 diabetes and impaired glucose tolerance	Inter Eye Study individuals from Copenhagen.	Prospective / Linear and Cox regression	908	10	1-CRAE 2-CRVE Right eye Knudtson-Parr-Hubbard formula	1- IHD 2- Stroke 3 All cause mortality	1- IHD n=8 2- Stroke n=5 3- All cause mortality n =49	In age-adjusted models an association between high CRVE and risk of IHD was found (*p* < 0.001). Wider, CRVE was associated with all-cause mortality (HR=2.02, (95% CI, 1.0, 3.8); *p*=0.03) in a basic model.

Table 2.1 Results of studies including people with type 2 diabetes

Title	Reference	Study Population	Recruitment method	Study type / Model	Number of people recruited	Duration of follow-up (years)	Retinal Vasculature Exam	End Points	Events	Results
Relationship of Retinal Vessel Caliber to Cardiovascular Disease and Mortality in African Americans With Type 1 Diabetes Mellitus	Roy et al, 2012	Type 1 diabetes	Africans American from New Jersey University Hospital	Prospective / Logistic	468	6	1-CRAE 2-CRVE Measurements in both eyes. On average 7 to 14 arterioles and an equal number of venules were combined into summary indices	1-Foot or leg amputation for a circulatory problem 2-Myocardial infarction 3-Stroke 4-Hypertension 5-Mortality	1 - Any CVD n=460 2 - MI or Stroke n=427 3 – Lower extremity arterial disease n=438 4- Hypertension n=281	Narrower CRAE predicted incident any CVD (HR 1.60, 95% CI 1.14, 2.26) and amputation (HR 1.94, 95% CI 1.10, 3.42). Larger CRAE predicted incident HTN (HR 1.41, 95% CI 1.03, 1.94).
Retinal Vessel Diameter and the Incidence of Coronary Artery Disease in Type 1 Diabetes	Miller et al, 2009	Type 1 diabetes	Children (< 18 years old at baseline) from Children Hospital Pittsburgh	Prospective / Cox regression	448	18	1) CRAE 2) CRVE Photographs were digitised. Knudtson-Parr-Hubbard formula	1 -Coronary Artery Disease defined as CAD death, MI and or Q waves, stenosis >50% revascularisation ischaemic ECG or Angina	1- Coronary artery disease cases n=80 2- no CVD n=368	Decreased CRAE was significantly associated with CAD (HR 1.42; 95% CI 1.04, 1.96, *p*=0.03).
Cardiovascular Disease, Mortality, and Retinal Microvascular Characteristics in Type 1 Diabetes	Klein et al 2004	Type 1 diabetes	Wisconsin Epidemiologic Study of Diabetic Retinopathy	Prospective / Cox regression	996 (871 with retinal data)	20	1-CRAE 2-CRVE 3-AVR 4-Diabetic retinopathy Images were digitised (Scanned). Mean value of two eyes. Parr-Hubbard formula	1-Angina 2-MI 3-Stroke 4- Mortality CVD	1- Angina n=180 2- MI n=147 3- Stroke n=59. 4- Mortality of CVD n=176 (273 total deaths from which 176 involved heart disease)	Severe DR and fourth AVR quartile were associated with mortality from heart disease HR 1.3 (95%CI 1.1, 1.5) and HR 0.8, (95%CI 0.6, 0.9),respectively.

Table 2.2 Results of studies including people with type 1 diabetes

2.3.2.2 Studies in type 1 diabetes

Three studies on individuals with type 1 diabetes were identified (table 2.2). Klein et al (2004) recruited 996 individuals with type 1 diabetes. In this study, it was found that the severity of diabetic retinopathy was associated with an increased odds of angina (OR 1.2, 95% CI 1.0-1.5) and stroke (OR 1.6, 95% CI 1.1-2.3). In a model including diabetic retinopathy and AVR, the AVR quartile was associated with myocardial infarction (MI) (OR 0.8, 95%CI 0.6-0.9,). Whereas in a multivariable analysis adjusted for age, sex, diastolic blood pressure, neuropathy, pulse pressure, smoking and history of CVD, severe diabetic retinopathy was associated with mortality from heart disease (e.g. angina and myocardial infarction) (HR 1.3, 95%CI 1.1-1.5) and the AVR fourth quartile (HR 0.8, 95%CI 0.6-0.9). CRAE and CRVE were not included in the multivariable analysis of this study, and it is likely that there was no association. Furthermore, when nephropathy was considered in the model in addition to retinopathy, the results showed that nephropathy was significantly associated with the cardiovascular outcome and retinopathy was no longer significantly associated.

Miller et al (2009) studied 468 African American children with type 1 diabetes, measuring retinal CRAE and CRVE. In this prospective study, it was found that after full adjustment for diabetes duration, gender, hypertension, serum lipids, and smoking status, smaller arteriolar calibre was significantly associated with coronary artery disease (HR 1.42; 95% CI 1.04- 1.96, p=0.03). There was no association between coronary artery disease and venular calibre. There was a statistically significant vessel diameter-gender interaction (p= 0.006) and in an analysis stratified by gender, smaller arteriolar calibre was significantly associated with incidence of coronary artery disease in females (HR 1.92, 95% CI 1.24 - 3.16) in a full adjusted model (*p*= 0.004) but not in males. Retinal venular calibre was not associated with coronary artery disease in either gender. These results showed that for each standard deviation decrease in retinal arteriolar calibre, there was a 42% increased risk of coronary artery disease after adjustment for other risk factors. Interestingly, alternate models assessing the risk for more strictly

defined coronary artery disease (e.g. coronary artery disease death, MI, revascularization or stenosis >50%) incident events (n=47) showed a somewhat weaker association with smaller arteriolar (HR 1.48, 95% CI 1.05, 2.09; *p* = 0.02) than previously described models that included ischemic ECG and Angina. However, this association remained attenuated after full adjustment.

Roy et al (2012) measured CRAE and CRVE in individuals with type 1 diabetes living in New Jersey. In this study, CRAE and CRVE were measured in 468 African American persons. Cardiovascular disease was defined as foot or leg amputation for a circulatory problem, myocardial infarction, stroke, hypertension and mortality. After full adjustment, narrower CRAE (lowest quartile) at baseline, significantly and independently predicted 6- year incidence of any cardiovascular disease (HR 1.60, 95% CI 1.14 – 2.26) and amputation (HR 1.94, 95% CI 1.10 -3.42) whereas larger retinal venular diameter (highest quartile) at baseline, significantly and independently predicted 6-year incidence of hypertension (HR 1.41, 95% CI (1.03 – 1.94). Proteinuria and diabetic retinopathy (ETDRS) were stronger predictors of mortality than retinal arteriolar and venular calibres. This study did not present results separately for ischaemic heart disease.

2.4 Discussion

This literature review found a small number of studies, with generally inconsistent results, on the association of quantitative retinal traits with ischaemic heart disease in people with type 2 diabetes.

Although the study carried out by Klein et al (2007) was performed prospectively and the results showed significant independent associations of smaller values of CRAE with lower extremity amputations, all-cause of mortality and stroke mortality, there was no association with ischaemic heart disease in this population with type 2 diabetes. The ability of this study to detect associations may have been impaired by the use of trait quartiles

rather than using the traits as continuous variables. Similarly, in the cross-sectional analysis by Phan et al (2016), no association was found between retinal venular calibres and coronary disease measured by angiograms. As angiograms have been used as a gold standard measure of stable anatomical coronary disease (Kochar et al, 2013), it could usefully be considered as an outcome in future studies analysing the association of quantitative retinal traits with coronary disease in prospective studies. In the final study on people with type 2 diabetes, Drobnjak et al (2016) found a statistically significant association between wider CRVE and risk of ischaemic heart disease. However, after multivariable adjustment, this association was attenuated and all-cause mortality and cardiovascular mortality were no longer associated with retinal arteriolar and venular calibres.

Interestingly, in people with type 1 diabetes, the results were more promising. For instance, AVR and signs of diabetic retinopathy were significantly associated with myocardial infarction in the study carried out by Klein et al (2004); although the results were attenuated after adjustment for nephropathy. In the cohort of children with type 1 diabetes analysed by Miller et al (2009), smaller calibre arterioles (lower CRAE) were associated with incident coronary artery disease, and this association remained significant in multivariable analysis in females. This latter finding supports further investigation into the use of CRAE as an early quantitative retinal trait biomarker in female populations. The presentation and diagnosis of ischaemic heart disease are different in women from men, which make women prone to under-treatment for these diseases, stressing the need for more gender-based research and interventions on risk factors for ischaemic heart disease.

The studies included in the population with type 1 diabetes were more homogenous. All these studies were designed prospectively and also were carried out for a significant amount of time (e.g. 6, 18 and 20 years of follow-up). Additionally, in these studies CRAE and CRVE were measured. The results in this subgroup showed consistency and this should be considered

when comparing to the studies included in the subgroup with type 2 diabetes individuals.

Overall, in terms of the retinal traits, which have been most extensively investigated, there is some evidence that calibres of arterioles (CRAE) and venules (CRVE) and the dimensionless parameter AVR may be predictive of risk of coronary heart disease in relatively young adult diabetic populations, especially in women and in type 1 diabetes. The results in such populations are in the same direction as those found in the general population (Appendix 2), as discussed further elsewhere in this thesis.

2.5 Conclusion

To date, traditional cardiovascular risk factors such as age, sex, blood pressure, hypercholesterolaemia, smoking and even qualitative retinal characteristics (such as diabetic retinopathy) have been used as cardiovascular risk predictors. More recently, studies are beginning to explore a number of quantitative retinal traits (such as CRAE, CRVE, AVR, tortuosity and fractal dimensions) as additions to such models, but studies on such traits are scarce, especially in diabetes. This suggests that there is a gap in cardiovascular research for further investigation of the retinal microcirculation.

Further research must consider key methodological issues. First, prospective studies will be more informative than cross-sectional studies, and, since sample size plays a key role in obtaining valid results, such studies should include an appropriately large number of incident cardiovascular events. Second, it might be particularly productive to analyse whether the quantitative retinal traits are useful predictors of ischaemic heart disease especially in younger adults free of cardiovascular disease and in women with type 2 diabetes. It will be necessary to carry out these explorations in large datasets in populations with type 2 diabetes. Finally, a key finding from this literature review was the need to harmonise the technical aspects of

measurement of quantitative retinal traits. For instance, in some studies the retinal images were scanned whereas in more recent studies digitised images were used (directly from the ophthalmoscope). Differences in such technical approaches may interfere with the comparability of the measurements and cause bias, especially when measuring the calibres of the arterioles and venules.

This literature review has thus identified a paucity of high quality, prospective studies on a range of retinal vascular traits as potential risk factors for cardiovascular disease in type 2 diabetes, especially ischaemic heart disease. A previous review of the literature on retinal traits and stroke (Doubal et al, 2009) also failed to identify many studies concentrating on retinal traits as predictors of stoke in people with diabetes. These findings therefore support my rationale for undertaking further analysis on the association of retinal vascular traits with coronary artery disease and stroke outcomes in people with type 2 diabetes, as well as highlighting key methodological issues to consider in my own study.

Chapter 3 Aims and objectives

3.1 Aims

The main aim of this thesis was to explore the association of quantitative retinal traits with major cardiovascular outcomes such as stroke and ischaemic heart disease and with cardio-metabolic genetic variants in people with type 2 diabetes.

Specific objectives were to:

(i) Determine whether the measured quantitative retinal traits are associated with a cross-sectional analysis with traditional cardiovascular risk factors and with cardiovascular outcomes including ischaemic heart disease and stroke. To achieve this, prevalent events from the ET2DS were used, followed by detailed data analysis.

(ii) Determine the association prospectively of the measured quantitative retinal traits with cardiovascular outcomes using Cox regression analysis. To achieve this, incident cardiovascular events were identified using the record linkage in an established prospective cohort, namely ET2DS.

(iii) Determine the association of the measured quantitative retinal traits with cardio-metabolic genetic variants included in the MetaboChip array and its imputed genetic data using genome-wide association methodology. To achieve this, the genetic variants included in the MetaboChip were imputed to the 1000 Genomes data. All the data were harmonised and analysed statistically.

3.2 Thesis outline

Background information on traditional risk factors for cardiovascular disease in people with type 2 diabetes, cardiovascular disease, retinal microvasculature and information of the analysis of the retinal traits has been summarised in Chapter 1. Chapter 2 presents a review of the literature on quantitative retinal traits and its association with ischaemic heart disease. This literature review not only pointed out to the paucity of studies in this area; it also helped me refine my research aims and objectives (outlined in this current chapter) and formulate the models for statistical analyses for this study.

In chapter 4, I describe the methods employed for data collection and analysis, including details of the software used to collect the quantitative retinal traits, the design of the epidemiological models used cross-sectionally and prospectively in the ET2DS and the statistical modelling of the GWAS.

I describe the results of this study in three chapters. The first section of the results (in chapter 5) presents relevant descriptive statistics from the ET2DS. The second section of the results (in chapter 6), describes the findings of the cross-sectional analyses. Furthermore, the prospective results of the association of the quantitative retinal traits with cardiovascular outcomes are described here. The third section of the results chapter (in chapter 7) presents the results of the genome-wide association analyses and the statistically associated SNPs with the quantitative retinal traits using the aforementioned method.

Finally, this thesis ends with a discussion (Chapter 8) summarising the key findings of this research and discussing the strengths and the limitations of this study. Additionally, recommendations for future research are provided at the end of this chapter.

Chapter 4 Methods

In this chapter, I describe the methods of data collection and analyses performed in this study. First, I describe the design and follow-up of the Edinburgh Type 2 Diabetes Study (ET2DS) on which my own research is based. I then summarise the data collection for baseline variables (including demographic and cardiovascular risk factor data, genetic data and retinal images) and the eight-year follow-up for cardiovascular events. These data were collected by current and former ET2DS team members and the methods have been published in detail previously (Price et al, 2008). I describe the methods that I used to measure quantitative retinal traits by means of the stored retinal images taken at baseline. Finally, I describe the details of the statistical analyses, which I undertook. While, in the literature, the term ‘arterial’ has been used to refer to the arteries found in the retinal microcirculation, for the purpose of this thesis, I use the concept ‘arteriolar’ to refer to the same.

4.1 Recruitment of the Edinburgh Type 2 Diabetes Study population

The ET2DS is a population-based prospective study of 1066 individuals aged between 60 and 75 years at baseline (2006-2007) with an established diagnosis of type 2 diabetes, living in the Lothian region in Scotland. Details of the study protocol have been published previously (Price et al, 2008). The overarching aim of the ET2DS was to investigate the role of risk factors in the development of microvascular and macrovascular complications of diabetes, including cognitive impairment, diabetic retinopathy, renal impairment, ischaemic heart disease, and cerebrovascular disease. The ET2DS dataset comprises biochemical, clinical and genetic data from both baseline and follow-up phases of the study, including the eight-year follow-up for cardiovascular events.

Although epidemiological studies may be carried out cross-sectionally, prospective analysis provides a clear and consistent definition of predictors and outcomes. These studies can assess multiples exposures and outcomes and they provide the ability to control for multiple cofounders (Thiese et al, 2014). The ET2DS, therefore, constituted an ideal study population for my research aimed at investigating the predictive role of retinal vessel traits.

Potentially eligible participants for the ET2DS were identified from the Lothian Diabetes Register (LDR). This is a large automated dataset containing clinical data on 20,000 individuals who have been diagnosed in primary or secondary care with type 2 diabetes, living in the Lothian region of Scotland. The diagnosis of type 2 diabetes was confirmed, based on the WHO criteria for type 2 diabetes, using the following criteria:

- Individuals taking oral anti-hyperglycaemic medication and/or insulin
- Glycated haemoglobin (HbA_{1c}) measure >6.5% (7.8mmol/l) at baseline if the individual was controlled with dietary modification only

Those individuals with HbA_{1C} below 6.5% (7.8 mmol/l) and not using medication or insulin were reviewed by a consultant diabetologist to confirm the diagnosis. Additionally, those individuals using insulin within one year of diagnosis of diabetes, those who reported pancreatic disease at the clinic and those who were treated with insulin and aged under 35 years at diagnosis, were assessed by the consultant diabetologist.

Exclusion criteria used in the ET2DS included non-English speakers and individuals with poor eyesight (defined as corrected visual acuity worse than 6/36 for distance vision or unable to read large print text), since these are pre-requisites for accurate completion of cognitive function tests. Also excluded were individuals who were unable to provide signed consent and those who were physically unable to complete all assessment elements.

The aim of the study was to recruit at least 1000 subjects to provide 90% power at the two-sided 5% significance level to ascertain a Pearson

correlation coefficient of ≥0.10 between a continuous outcome and a continuous predictor variable. The sample size was also calculated for detection of any risk factor that contributed 1% or more to the variance in the outcome for observed associations, both at baseline and during follow-up analysis.

A flow diagram illustrating recruitment of the ET2DS participants is presented below in figure 4.1.

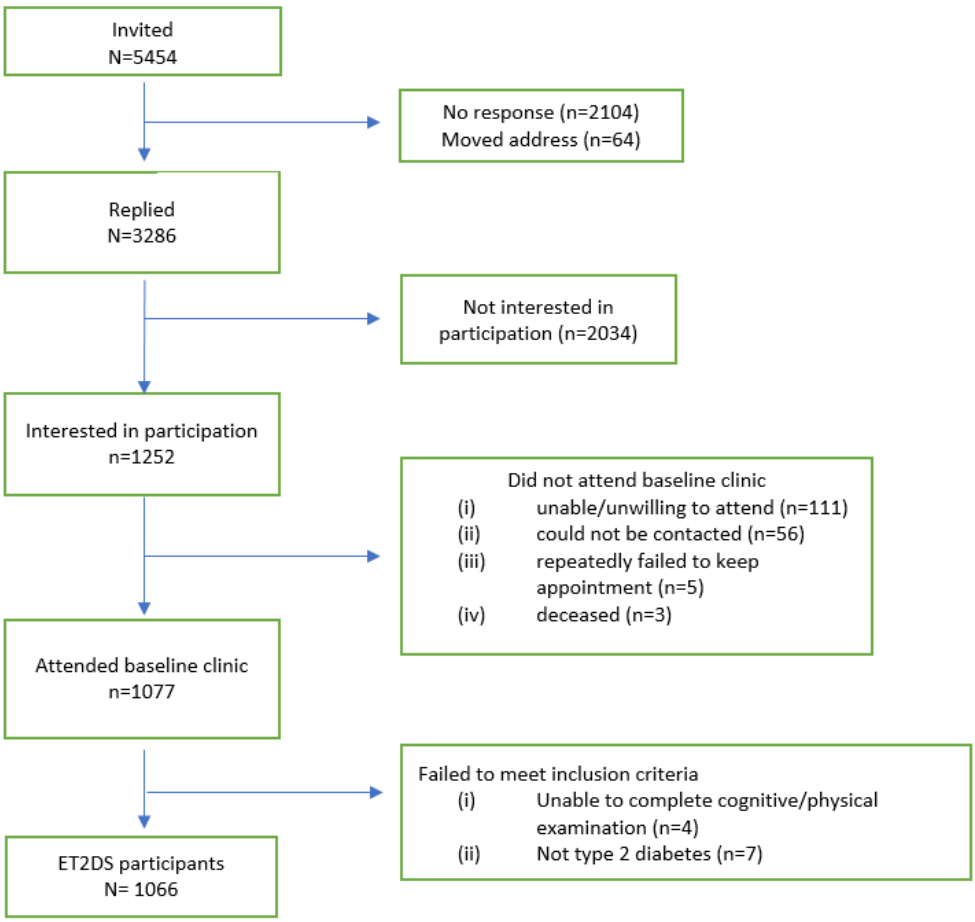

Figure 4.1 ET2DS Recruitment (Adapted from Price et al, 2008)

All ET2DS participants provided written, informed consent prior to recruitment into the study and the start of data collection. Ethical approval was granted by the Lothian Medical Research Ethics Committee, including approval for

Information Services Division (ISD) record linkage performed at baseline and during follow-up.

4.2 Baseline data and retinal image collection in the ET2DS

Data was primarily collected in four phases in the ET2DS: a baseline clinic (2006-2007), a liver sub-study clinic after one year, and four and eight year follow-up phases. A summary of these data collection points is given in table 4.1. Data used in this thesis came primarily from the baseline data collection phase (plus incident cardiovascular event data). Baseline data collection, including the collection of retinal images and genetic data, is described in this section.

Data collected	Baseline	Year 1 clinic	Year four follow-up	Year eight follow-up
General questionnaire	✓	✓	✓	
Cardiovascular questionnaire	✓		✓	
Physical examination	✓	✓	✓	
Retinal imaging (graded for diabetic retinopathy)	✓			
Fasting venous blood sample (for biochemistry and baseline genotyping)	✓	✓	✓	
Electrocardiogram	✓		✓	
Data linkage (for cardiovascular events)	✓		✓	✓

Table 4.1. Summary of the data collected in the Edinburgh Type 2 Diabetes Study

4.2.1 Physical examination

Physical examination at baseline was carried out at the Wellcome Trust Clinical Research Facility, Western General Hospital, Edinburgh, UK. Patients were invited to attend the clinic and transportation was arranged if required, travel expenses were offered and flexibility in the date and time of

appointments or rescheduling was offered to encourage participation. Participants underwent an overnight fast before attending the clinic; then blood samples were obtained through venepuncture. In addition, urine samples were collected and a 12 lead electrocardiogram was taken. All examinations were carried out by trained nurses and qualified technicians who were following standard operating protocols and procedures, ensuring consistency in the evaluations. In order to obtain body mass index (BMI), height in metres (International system units), was measured without shoes using a wall-mounted vertical ruler and weight (in kilograms) was measured without outdoor clothing using calibrated electronic scales. BMI was defined as weight/height$_2$ (kg/m$_2$). Blood pressure (systolic and diastolic) was measured in the right arm (± 2 mmHg), with the participants in the supine position with their arm extended and resting using a standard stethoscope and sphygmomanometer cuff (Acceson TM, AC Cossor & Son (Surgical) Ltd, Harlow, UK).

4.2.2 Self-completion questionnaire and ISD record linkage

Participants completed baseline self-completion questionnaires including questions on demographic characteristics, diabetes history, cardiovascular disease (CVD), smoking, and medications. This included age (date of birth), sex, duration of diabetes (date of diagnosis of diabetes), ethnicity and social class. Answers to questions on diabetes treatment were used to define three groups, (i) diet controlled only, (ii) oral anti-diabetic medication only (this included medication such as Metformin, Sulphonylureas and Thiazolidinediones), and (iii) insulin (with or without additional oral anti-diabetic medication). Data on smoking were collected using a standard smoking questionnaire, which has been used widely in epidemiological studies. Participants were asked whether they currently smoked, and if so, how many cigarettes, cigars or tobacco they usually smoked per week. Participants who reported having quit smoking in the previous six months

were considered to be current smokers for the purposes of this thesis as in previous ET2DS analyses (Marioni et al, 2010).

Data linkage to the Scottish Morbidity Records scheme was performed at baseline (and repeated at 8-year follow-up) by the ISD of the National Health Service (NHS) Scotland to locate information on medical and surgical hospital discharges. Answers to questions on past medical history and current medications in the self-completion questionnaire were used in combination with this ISD hospital discharge data and with electrocardiogram (ECG) findings to identify and confirm diagnoses of cardiovascular disease.

4.2.3 Blood sampling, genotyping and imputation

Fasting blood samples taken at the research clinic were used to measure fasting glucose, total cholesterol, high-density lipoprotein (HDL) cholesterol and glycated haemoglobin (HbA_1c). Total cholesterol, HDL cholesterol, HbA_1c and eGFR were all determined using Vitros Fusion Chemistry System (Ortho Clinical Diagnostics, Bucks, UK) at the Western General Hospital, Edinburgh UK.

Furthermore, at baseline, blood samples for DNA extraction were taken for subsequent genotyping. Genomic DNA was isolated from whole blood following standard procedures at the Wellcome Trust Clinical Research Facility Genetics Core, Western General Hospital, Edinburgh, UK. Genotyping using the Illumina MetaboChip was undertaken at Kbiosciences.

The Illumina Metabochip is a custom genotyping array. This array provides coverage for over 200,000 tag single nucleotide polymorphisms (SNPs) of the human genome. The array was designed from SNPs based on genome-wide association study (GWAS) meta-analyses of 23 cardiometabolic traits. SNPs were selected from the catalogues of the HapMap Project and 1000 Genomes Project, allowing the inclusion of SNPs across a wide range of allele frequency spectrum.

Genotyping procedures and quality control in the ET2DS have been described in detail previously (McLachlan et al, 2016, Shah et al, 2013). In summary, all samples were assessed for consistency. Quality control consisted of exclusion of SNPs or samples with Illumina GenCall score <0.15, sample and SNP rates <0.95, Hardy Weinberg Equilibrium *p* value ≤ 0.001, replicate discordance, discrepancy in sex, ethnicity and relatedness checks or against previous genotype data. No minor allele frequency (MAF) cut-off was applied at this stage.

Data used for this thesis included imputed genotype data. Imputation was used to increase the number of genome-wide SNPs. This method has been used in many previous studies and is a statistical technique for predicting unobserved genotypes in the population studied, based on the correlation of observed study haplotypes and guided by the reference haplotypes of the same genetic population (Howie et al, 2009). Imputation was carried out by Dr. Stela McLachlan (ET2DS data manager) for the purposes of a previous genetic analysis. Metabochip variants were imputed using as reference panel the 1000 Genomes (Phase 1, CEU haplotype set). Imputation was carried out on cleaned genotypes in three phases – chunking, phasing and imputing - using MACH1 and Minimac software (McLachlan et al 2016). The final file contained ~4.5 million autosomal SNPs (R_2 > 0.3, MAF > 0.001). The data were collated and stored in the University of Edinburgh secure data servers ready for use by the R package snpStats.

4.2.4 Retinal Images

Retinal images were collected at baseline between 2006 and 2007. People recruited into the study at the Wellcome Trust Clinical Research Facility research clinic were given a second appointment for an ‘eye’ clinic, held in the major ophthalmology department for NHS Lothian. Retinal photographs were taken between 9.30 am and 3.00 pm from Monday to Friday and by a single specially trained medical photographer. Caution should be taken when

analysing data from individuals with poor vision because anatomico-physiological factors may influence the measurement of retinal vasculature. Moreover, cataract develops earlier in people with T2D than in the general population. Refractive errors are common findings in people with poor vision and these include near sightedness (myopia), farsightedness (hypermetropia) or blurry vision (astigmatism). Lim et al (2011) found that myopic refractive errors and longer axial length are associated with narrower retinal arterioles and venules, less tortuous arterioles, and increased branching coefficients in the vessels.

During the assessment, digital retinal images were stored electronically. Subjects had 1% tropocamide drops instilled into both eyes to allow pupillary dilatation before having the image captured. Inspection of the pupils was carried out. If dilatation was insufficient, a further 1% tropocamide dose was given. Retinal images were taken using a high-resolution digital retinal camera (TOPCON TRC-50FX, Topcon Optical Company, Tokyo, Japan). All the individuals provided standard 7-field non-stereoscopic retinal colour photographs. An example of the 7-field non-stereoscopic retinal colour photographs is seen in Figure 4.2. The seven standard photographic fields were stored as JPEG or TIFF format files on a laptop attached to the retinal camera. Specially trained optometrists working in the Scottish Diabetes Retinal Screening programme used these images for grading of diabetic retinopathy.

Evaluation of stages of diabetic retinopathy was performed following ETDRS protocols. According to the NICE guidelines, full laser scatter treatment is indicated for retinal new vessels (e.g. new vessels in the disc and new vessels elsewhere). Importantly, treatment should be considered in people with only eye (e.g. first eye lost due to proliferative diabetic retinopathy), and in people with poor clinical attendance. In the ET2DS, there were a small number (1.4% of total population) of individuals with proliferative diabetic retinopathy (n=15).

Images were backed up onto an external drive and subsequently transferred to a local server at the University of Edinburgh for long-term backup and storage.

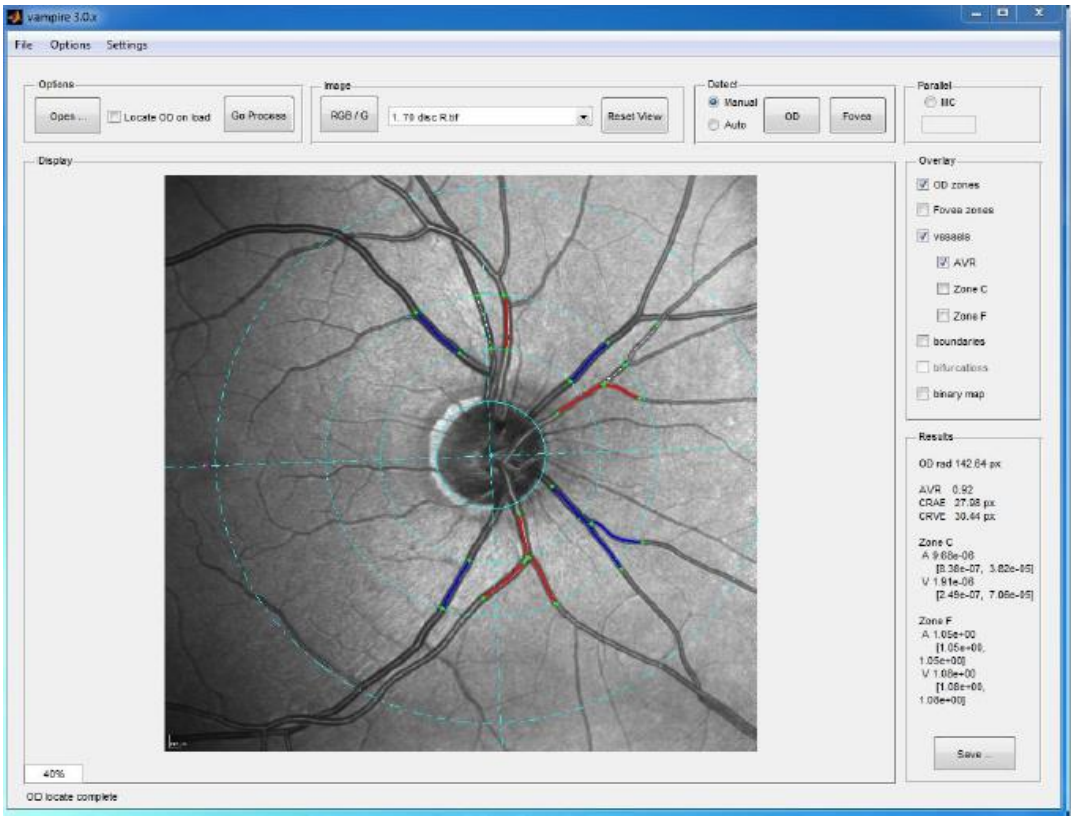

Figure 4.2. Screenshot of VAMPIRE software. The vessels are highlighted (red for arteries and blue for veins). On the right side, the measurements taken are displayed. *With permission from Dr T MacGillivray*

4.3 Retinal image analysis

Whereas the data described previously in this chapter were collected by other members of the ET2DS team, I conducted all the analyses of retinal images described here, to collect data on retinal vessels traits. I obtained the retinal images from the server where they were stored and I chose the central field image to perform the analysis.

Retinal images for analyses were taken from the central field. This central image has two important eye structures, the optic disc and the fovea (Figure 4.3). The former is the optic nerve head and is the entry point for the major

blood vessels that supply the retina and also is the exit point for the ganglion cell axons leaving the eye. This is small blind spot in each eye. The latter, *fovea centralis,* is located in the centre of the macula lutea, a small flat spot located exactly in the centre of the posterior portion of the retina. Fovea is responsible for high-acuity vision and is densely saturated with cone photoreceptors. Blood supply is not provided by central retinal arteries or any of its branches, instead is supplied by choroid.

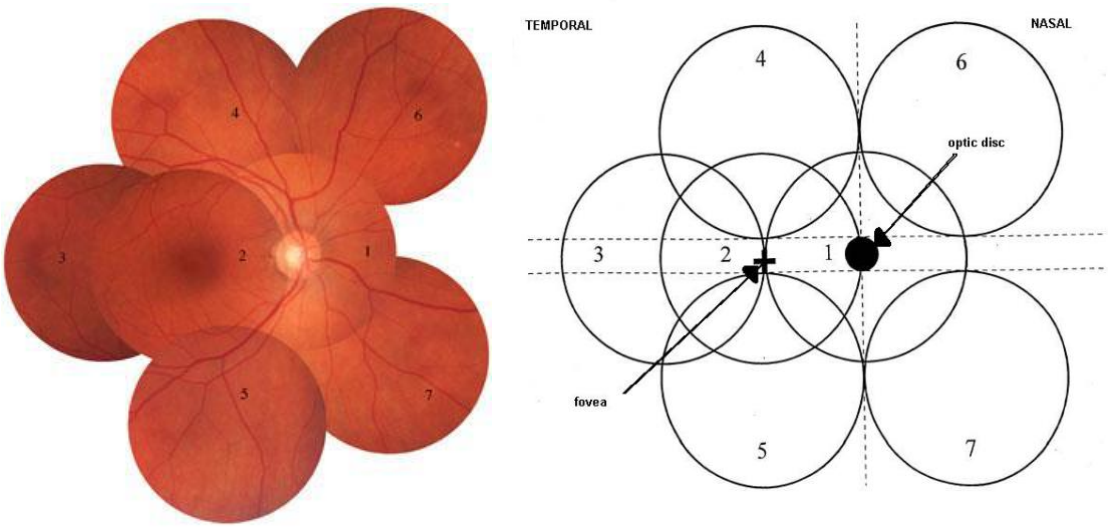

Figure 4.3. Retinal diagrams showing 7-field definition in right eye. Field 1 (Left) is centred on the optic disc, field 2 on the macular. Field 3 is temporal to the macula. Fields 4 to 7 are tangential to horizontal lines passing through the upper and lower poles of the disc and to a vertical line passing through its centre *Taken from Diabetic retinopathy grading protocol for ET2DS, 2007).*

Initially, I only analysed one image (mainly the right eye) of the field 1 (figure 4.3) from each subject using the semi-automated (VAMPIRE) software described below, if the quality was good enough to run the analysis with the software (e.g. no blurry image). After completing the analyses, if the image had good quality but the software proved unable to determine the required traits successfully, the image from the opposite eye was analysed. This was carried out to achieve the highest number of analysed images possible. All the images included in the analysis (n=1028) were verified manually by

myself. This was carried out to ensure that vessels (e.g. arterioles and venules) were correctly selected by the semi-automated software.

Correlations of the measurements made from the right eye versus the left eye, together with results of an inter and intra-observer reliability study (both performed on small subgroups of the total study population), are described below. Importantly, qualitative findings used for grading diabetic retinopathy should be careful interpreted as the presence of abnormalities (e.g. microaneurysms) in one eye may not represent systemic diseases and these traits may not be present in the opposite eye. As stated above, the diabetic retinopathy grading was performed according to protocols in the ET2DS.

4.3.1 Correlations of retinal images

In the early stages of retinal image analysis, an exploration of the correlation of the quantitative retinal traits between the right and left eyes was undertaken. A randomly selected subgroup of 50 individuals with images from both the right and left eyes was analysed. This was carried out to inform my decision on which eye to use for measurement of the retinal traits.

Results are shown in the table 4.2 For AVR, there was a moderate correlation of 0.47 between right and left eye. The correlations for CRAE and CRVE were both 0.42. Correlations for arteriolar tortuosity were slightly higher (0.53 for minimum arteriolar tortuosity and 0.48 for maximum arteriolar tortuosity), with the highest correlation seen for mean arteriolar tortuosity (0.64). Correlations for venular tortuosity traits were generally lower (mean venular tortuosity was moderately correlated 0.43), with lowest values for minimum venular tortuosity (0.10) and maximum venular tortuosity (0.21). Multifractal dimensions D0, D1 and D2 were moderately correlated showing a correlation of 0.40, 0.38 and 0.38 between right and left eye, respectively.

Quantitative retinal traits	Correlation	*p*-value
AVR	0.47	**<0.001**
CRAE	0.42	**<0.01**
CRVE	0.42	**<0.001**
Arteriolar tortuosity		
Mean	0.64	**<0.001**
Minimum	0.53	**<0.001**
Maximum	0.48	**<0.001**
Venular tortuosity		
Mean	0.43	**<0.01**
Minimum	0.10	0.49
Maximum	0.21	0.12
Multifractal dimensions		
D1	0.40	**<0.01**
D2	0.38	**<0.01**
D3	0.38	**<0.01**

Table 4.2. Pearson correlation between right and left eye of 50 individuals.

High correlation between both eyes is expected as they share same environmental factors and genes. Several studies have reported high correlation in quantitative retinal traits (Leung *et al* 2013 and Ikram *et al*, 2016). In such studies other software has been used (e.g. Singapore "I" Vessel Assessment, SIVA,) which may influence the results of the correlation analyses. Physiological factors may also influence the measurement of quantitative traits in the retinal images. This is important to consider as the images from both sides were taken independently. Such factors may influence differences between right and left sides and include cardiac cycle variations, arterial and venular dilatation, refractive error and axial length. Technical factors such as photographic distance may also have an influence

as the area analysed with the software is dependent on the area of the retina photographed by the camera (this area is different in each eye).

As previously decsribed, one image was ultimately selected to be included in the analysis, rather than selecting either both eyes or always the right or left eye. This was done because it was not feasible to measure the traits in both eyes within a realistic timeframe for my PhD and since a majority of other large longitudinal studies have also adopted this approach. This also means that higher quality measurements (from higher quality images) could be expected on average.

Analyses using intra-class correlation coefficients were carried out to assess the reliability and repeatability of all retinal quantitative traits within the same grader (myself) at two different time points and between different graders (myself and one other grader). A randomly selected subgroup of 50 individuals was selected for these analyses. The analyses were necessary to determine the reliability of the measurements, as the software (VAMPIRE) used is a semi-automated software and human input accounts for a significant part of the measurement process. Analyses were carried out to determine inter-grader and intra-grader reliability (correlation of the quantitative retinal traits results with one operator and correlation of the results between two different operators using the same VAMPIRE 3.1 software).

The purpose of intra-class correlation is to determine the proportion of variation in the measurements that affects a particular group. The technique is performed firstly by carrying out two-ways analysis of the variance and then, the results of the mean sum squares (between graders) are compared. If there is no significant difference in the residual error, then concordance is achieved.

Previous cross-sectional and longitudinal studies have reported from moderate to strong reliability of the quantitative retinal traits. In my study, high repeatability values were consistently reported as well as high reliability

for tortuosity and multifractal dimensions. A summary of the results are presented in the table 4.3.

Quantitative retinal traits	Intra-class correlation coefficient	
	Intra-grader repeatability	Inter-grader repeatability
AVR	0.91	0.85
CRAE	0.98	0.90
CRVE	0.95	0.90
Arteriolar tortuosity		
Mean	0.98	0.95
Minimum*	0.83	0.96
Maximum	0.99	0.92
Venular tortuosity		
Mean	0.97	0.84
Minimum	0.90	0.97
Maximum	0.96	0.83
Multifractal dimensions		
D0	0.83	0.83
D1	0.83	0.80
D2	0.82	0.81

Table 4.3 Results of intra-grader and inter-grader repeatability. Logarithm transformation (log-10) was used for all arteriolar tortuosity and venular tortuosity traits. Multifractal dimensions were rank transformed to achieve the normal distribution. * The results for minimum arteriolar tortuosity were repeated in 60 individuals achieving an inter-grader repeatability of 0.92.

4.3.2 Software to analyse retinal images (VAMPIRE 3.1)

VAMPIRE (version 3.1) is a software developed by a consortium from the Universities of Edinburgh and Dundee, UK. It is a semi-automated software which quantifies retinal blood vessel parameters, and was used in this study, to measure the retinal vessel traits used in my analyses – vessel widths (arteriovenous ratio (AVR)), central retinal arteriolar equivalent (CRAE), central retinal venous equivalent (CRVE), arteriolar tortuosity (mean, minimum and maximum of several readings in a single subject), venular tortuosity (mean, minimum and maximum) and multifractal dimensions (three traits D0, D1 and D2 depending on the precise retinal area from which readings are taken).

Analyses of the images is a computationally demanding task. Initially, the software was installed, and the images were analysed, on a Windows desktop PC (Intel M5, 1.3 GHz, 6 Gb RAM). However, analysis of the images took more time than expected as the average pre-processing time (visualisation and selection of the vessels for each image) was around 12 to 15 minutes. Therefore, the software was subsequently installed on a MacBook (Intel Core i7, with 4 cores, 2.2GHz, 16Gb RAM). Processing images with this processor proved much faster and the analysis was completed using this computer.

The correct procedure for operating the software has been described in detail previously (MacGillivray *et al*, 2015). First, the boundaries of the optic disc (OD) in a retinal image were detected and a conventional OD-centred circular measurement zone was established (see figure 5.3 for the zones detected and labelled in VAMPIRE software). Second, the software attempted to detect the retinal blood vessels present in the image and locate bifurcations. If the software was able to detect the vasculature within the measurement zone the image was classified as processable; otherwise it was classified as non-processable. For processable images, the operator (myself) was asked

to identify, visually, the six thickest arteries and the six thickest venules in the measurement zone.

The software then calculated the mean of the arteriolar and venular diameters (CRAE and CRVE, respectively) and the median for each set of arteriolar and venular tortuosity measurements in order to summarise arteriolar and venular parameters for each image. Successful completion of the measurement protocol categorised the image as analysable, i.e. there was sufficient detection of retinal vessels in the image to enable the measurement of the target parameters; otherwise the image was recorded as non-analysable (MacGillivray et al, 2015).

4.3.3 Vessel widths (CRAE and CRVE) and arteriovenous ratio (AVR)

To measure vessel widths, vessels were selected from zone B in an area 0.5 and 1 disc diameters from the optic disc (see figure 4.3). Measurements of the widths of the six largest arteries and the six largest venules that crossed zone B were taken and used by the software to calculate CRAE and CRVE respectively.

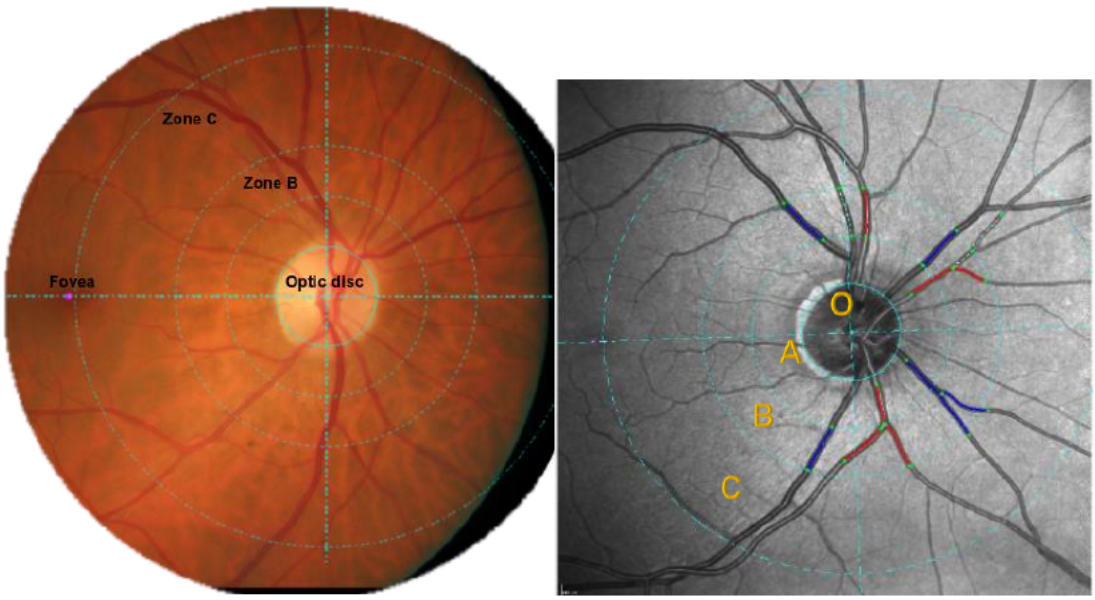

Figure 4.3. Retinal photograph including the fovea and the optic disc, illustrating zone B and zone C used in the measurement of the retinal vascular traits. At the centre, it is located the optic disc (OD). CRAE and CRVE are measured from zone B. The adjacent area, zone C, is where arteriolar and venular tortuosity are measured. In the photograph on the right, the arterioles are highlighted in red and the venules are highlighted in blue. *Original images taken from ET2DS using VAMPIRE software.*

The measurement of the width of the arterioles and venules has been described elsewhere (Lupaşcu et al, 2013). In summary, this measurement consists in a cross-sectional width at regular intervals down the length of a vessel segment in zone B (Figure 4.4). The arteriovenous ratio (AVR) describes the ratio of the CRAE to the CRVE.

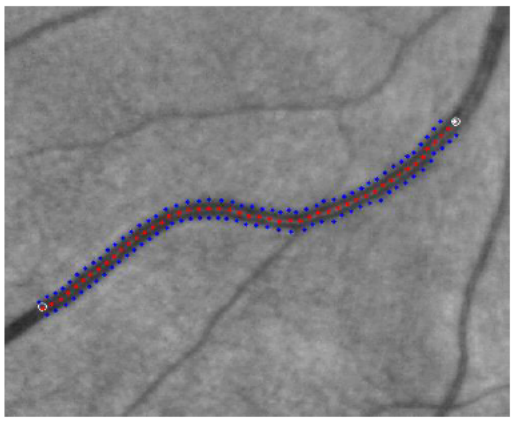

Figure 4.4 Example of tracking width in a segment of the vessel to obtain vessel diameters. *With permission from Dr Tom MacGillivray*

4.3.4 Vessel tortuosity

Tortuosity was calculated by the software using the six widest arteries and venules crossing zone C (see figure 4.3). VAMPIRE implements a tortuosity measure integrating axis curvature, length and thickness of the vessel for both the arteriolar and venular tortuosity. The outcome of these measurements included the median of vessels tortuosity, the median of the minimum values of vessels tortuosity and the median of the maximum vessels tortuosity. A summary of the algorithm has been described elsewhere (Patton et al, 2006; Azegrouz et al, 2006).

4.3.5 Multifractal dimension

Multifractal dimension is a novel retinal biomarker, which is characterised by complex, repeated geometrical patterns at different spatial scales. Multifractal dimensions measure the degree of branching complexity of the vascular tree (including arteries and venules) in two dimensions. An example of the visualisation of multifractal dimension is showed in figure 4.5. The measurement of multifractal dimensions was performed by using the generalised sand-box method. This method measures a random set of pixels and counts the vessel pixels in square regions centred at the selected pixels with an increasing linear dimension (Patton et al, 2006; Stošić et al, 2006).

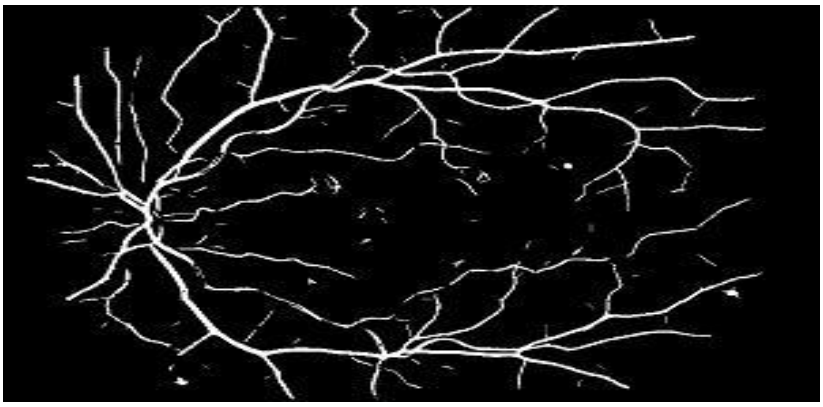

Figure 4.5 Visual representation of multifractal dimensions using VAMPIRE software. This represent the entire vasculature of the retinal fundus image. *With permission from Dr Tom MacGillivray.*

4.3.6 Manual input for the semi-automated VAMPIRE 3.1 software

After the processing of the images, manual input is required to double-check that the arteries and venules have been correctly selected by the software. This process requires visualisation of the fundus images to differentiate between arteries and veins by taking into account several features. In general, arteries appear brighter and thinner than venules. Importantly, the central reflex is usually wider in arteries and conversely, smaller in venules. Nevertheless, there are other factors, which can influence the appearance of the retinal vessels. For instance, patient ethnicity, age, lesions and images quality. These factors were considered in the selection of the vessels.

4.4 Identification of cardiovascular events

To meet one of the primary aims of this thesis, I planned to associate retinal vessel traits measured on baseline retinal images with cardiovascular events occurring during follow-up. The current section describes the data collection and event definitions for both prevalent and incident cardiovascular events in the ET2DS.

4.4.1 Prevalent events

Several sources were used to identify prevalent cardiovascular events at baseline. This included participants' self-reported medical diagnoses and or treatment (medical and/or surgical) for angina, myocardial infarction, stroke and peripheral arterial disease, as well as the WHO chest pain questionnaire, a 12-lead electrocardiogram coded using the Minnesota coding system and data linkage to hospital discharge data from ISD. Additionally, when necessary, clinical notes from general practices and hospitals were obtained to confirm or refute a possible cardiovascular event. The specific criteria used to define a prevalent cardiovascular event are given in Appendix 5.

4.4.2 Incident events

Incident and recurrent cardiovascular events were recorded at the four-year follow-up phase of the ET2DS and again after eight years. At year four, events were identified using self-reported questionnaires completed in the research clinic, questionnaires from general practitioners, ECGs and record linkage from ISD (Morling et al, 2015). If necessary, clinical notes from the hospital were searched to confirm clinical information. Also, senior clinicians and researchers were contacted to discuss cases with uncertain diagnoses or with unclear clinical information. After eight years from baseline, repeat record linkage at ISD was undertaken to identify further cardiovascular events. The specific criteria used to define an incident cardiovascular event during the total eight years of follow-up are given in Appendix 6.

4.5 Data processing and analysis

4.5.1 Data entry and cleaning for ET2DS master database

ET2DS data from baseline, year four and year eight follow-up were coded and transcribed into a master database (Microsoft Access 2003/2010; Microsoft Corporation, Washington USA). When data entry was carried out, double data entry was undertaken by members of the ET2DS team for quality control purposes. All data were double entered at baseline. At year four, a 10% random sample of data was double entered - error rates were found to be very low and no systematic sources of error were identified, so no further double data entry was undertaken. All input errors were checked against the original data source and changed to the correct value. Further quality assessment using descriptive analysis of the data was carried out after completing data entry to inspect for missing values and outliers. Those values, which were extremely high or low and could not be explained were removed from the dataset if not biologically possible and retained if simply

high or low true values. Missing data was also scrutinised, and, wherever possible, data were retrieved from alternative sources (for example from the Lothian Diabetes Register rather than the original research clinic) to ensure a minimum amount of missing data in the master ET2DS dataset.

All the variables in this thesis apart from the retinal variables came from this master database file, and were provided to me by Dr. McLachlan, the ET2DS data manager. All individuals in the ET2DS are assigned a study ID number (a unique five-digit number) and these were used to match the retinal image data with all the other variables used in this thesis.

4.5.2 Data analysis

I developed a statistical analysis plan in discussion with my supervisors and experts in relevant analysis techniques. I carried out the statistical analysis using SPSS v21 (StataCorp, College Station, TX, USA) and R, a free widely available software (R: A language and environment for statistical computing, Vienna Austria). For the non-genetic analyses, a *p* value of less than 0.05 was taken as statistically significant, as is standard in most scientific and epidemiological studies. All variables were examined for outliers/extreme values and missing values prior to undertaking any statistical analyses.

All the continuous variables used in this thesis were assessed visually for normality using histograms. Those variables that were not normally distributed included duration of diabetes, mean arteriolar tortuosity, minimum arteriolar tortuosity, maximum arteriolar tortuosity, mean venular tortuosity, minimum venular tortuosity and multifractal dimensions D0, D1 and D2. Logarithmic natural transformation was used to normalise the distribution of diabetes duration, mean arteriolar tortuosity, minimum arteriolar tortuosity, maximum arteriolar tortuosity, mean venular tortuosity, minimum venular tortuosity and maximum venular tortuosity. Rank transformation was used to normalise the distribution of multifractal dimensions. Histograms after transformation were visualised to confirm that normal transformation had

been achieved. For normally distributed variables, means and standard deviations (SD) were quoted and for skewed variables, medians and interquartile ranges (IQR) were described.

4.5.3 Bivariate statistical analysis

Unadjusted associations between two continuous variables were analysed using Pearson correlation coefficients if the general assumptions were achieved (normal distribution, no significant outliers). The r value and the *p* value were reported to determine the direction, strength and statistical significance of the relationship. Adjusted Pearson correlation (partial correlation) was used to analyse the association between two continuous variables adjusted for categorical variables (e.g. sex and age). The corresponding r partial association and p values were reported. For categorical variables, unadjusted and age-sex adjusted associations with continuous variables were assessed using ANOVA (mean values and p values were reported). Chi squared tests were used to explore relationships between two categorical variables (chi square and *p*-value reported). The Mann-Whitney U Test or Kruskal-Wallis test was applied to assess the differences in median levels of non-normally distributed quantitative retinal traits and incident cardiovascular events.

4.5.4 Prospective statistical analysis (association of quantitative retinal traits with incident cardiovascular events)

Cox regression analyses were used to examine the association of the retinal traits with incident cardiovascular events. Variables were selected as possible cofounders to build different models and assess the strength and independence of the association of the quantitative retinal traits with incidental cardiovascular outcomes. Co-variables were selected according to the significant univariate association results and also to reflect traditional risk

factors described previously in the literature. In people with diabetes, the traditional risk factors associated with cardiovascular disease include hyperglycaemia, duration of diabetes, high levels of HbA_{1c}, high levels of total cholesterol and lower levels of high-density cholesterol. These variables are also included in the UKPDS risk score and were selected as co-variates for my models because they specifically take into account diabetes status.

Analyses were fitted in five different models for all the quantitative retinal data, presented below:

(i) Model 1: Unadjusted model.

(ii) Model 2: Adjusted for sex and age.

(iii) Model 3: Adjusted for sex, age, duration of diabetes, HbA_{1c}, total cholesterol, systolic blood pressure, and smoking.

(iv) Model 4: Adjusted for sex, age, duration of diabetes, HbA_{1c}, total cholesterol, systolic blood pressure, smoking and eGFR.

(v) Model 5: Adjusted for sex, age, duration of diabetes, HbA_{1c}, total cholesterol, systolic blood pressure, smoking, eGFR and prevalent cardiovascular disease.

The association between baseline events and future cardiovascular events was assessed using Cox Hazard regression. Hazard ratios with their respective 95% confidence intervals and the statistical significance represented by p-values were reported. Time to event was calculated from the baseline until the eight-year follow-up according to the number of weeks during this period of time. All variables used met the proportional hazards assumptions for each outcome event. This type of analysis is richer than cross-sectional analyses and helps elucidate the prospective association of the predictor variable with the outcome. After completing the analyses of the Cox Regression models, assessment of any improvement on addition of the retinal variables was examined for the model which showed significance by

determining the area under the curve (AUC). For each model, predicted individual risk (X Beta) was calculated and plotted.

Finally, little work has been done for multiple testing is descriptive statistics. Examples of multiple comparisons tests include the Bonferroni correction and false discovery rate . Bonferroni correction is the most popular family wise error rate control: for fixed level α of probability of type I error, it consists in doing m hypothesis tests controlling the significance level per test at α*=α/m. This approach is extremely conservative whenever the number of tests is large (Catelan et al, 2010). Those approachs should be considered as complementary procedures to point estimates and confidence intervals in data analysis and genomics data analysis.

4.5.5 Genetic analysis (association of retinal traits with genetic variants)

The associations between genotyped and imputed SNPs and retinal traits were tested by linear regression using an additive genetic model. Further adjustment was made for age and sex. Analyses for all retinal traits were carried out using R package snpStats. Imputed data were analysed with SNPstats. SNPstats carries out the association analysis by using a linear regression model with a quantitative phenotype. This software performs the regression analysis in a fast and memory efficient way as it deals with millions of SNPs. SNPstats provides a set of results for the analysis, including descriptive statistics such as (for quantitative phenotypes), the absolute frequencies, means, standard errors, mean differences with respect to the reference category and 95% CI of the differences. For each SNP, it describes the allele and genotype frequencies and Hardy–Weinberg equilibrium is calculated.

For all retinal traits, genomic-control inflation factors (λGC) were calculated and used to correct test statistics for each retinal trait. Genome-wide association significance threshold was set at *p*-value < 5×10^{-8} and a

suggestive significance threshold was set at *p*-value < 5×10^{-6}. Also, the SNPs with MAF frequency <0.005 were filtered out.

After these analyses, taking into account the sample simple, the SNPs reaching the suggestive significance threshold were analysed further. Given the high number of the variants surpassing this suggestive threshold, I decided to filter out variants using a cut off of MAF ≥ 0.05 and *p*-value <1×10^{-6}. This was used as the SNPs with low MAF are rare, hence, power may be lacking for detecting SNP-phenotype associations and these SNPs are also more prone to genotyping errors (Marees et al, 2018). The MAF also depends strongly on the sample size and for this reason; it was decided to have a MAF greater or equal to 0.05. The SNPs showed in the results chapter followed this stringent approach.

I performed a locus analysis using Locus Zoom for the suggestive locus. Locus Zoom is an internet-based tool where loci can be plotted and visualised to assess relevant independence with other nearby SNPs. The locus zoom was defined as all SNPs below the threshold with SNPs located less than 500 Kb apart. Locus Zoom (Pruim et al, 2010) was used to display results, using 1000 Genomes Phase 1 CEU haplotype set for linkage disequilibrium (LD) calculation. The positions of SNPs are given based on human genome build 19.

4.5.6 Analysis of linkage disequilibrium

Linkage disequilibrium (LD) is a term used in population genetics to determine the non-random association of alleles at two or more loci (SNPs). The term was firstly used by Lewontin and Kojima in 1960 (Lewontin and Kojima, 1960). The concept of LD is useful to determine gene mapping, to understand past evolutionary and demographic events and the joint evolution of linked sets of genes. The LD was calculated with the purpose of determining the independence of the SNPs, which showed association with quantitative retinal traits at the suggestive statistical threshold. The coefficient

of LD and related quantities are descriptive statistics. Their magnitude does not indicate whether or not there is a statistically significant association among the loci (SNPs) in the haplotypes. For the purposes of this thesis, the correlation coefficient, r squared results are presented to test the independent significance of the SNPs.

Chapter 5 Results I: Descriptive analysis

In this chapter, I describe the baseline characteristics and representativeness of the ET2DS study population. I also describe the incident cardiovascular events which occurred during follow-up are also described and present the descriptive statistics for the quantitative retinal traits. Lastly, I present an assessment of missing data.

5.1 Baseline demographics characteristics

The baseline demographic characteristics of the ET2DS population are summarised in table 5.1. The baseline cohort included 1066 individuals recruited from the Lothian region of Scotland, UK. A total of 547 (51.31%) participants were male and the mean age was 67.9 years. Baseline numbers (prevalence) of participants with prior myocardial infarction (MI), angina, stroke, transient ischaemic attack (TIA), and coronary intervention were 150 (14.1%), 298 (28.0%), 62 (5.8%), 31 (2.9%) and 110 (10.3%), respectively. The prevalence of diabetic retinopathy at baseline was 31.8%; mild non-proliferative diabetic retinopathy (n=292, 27.4%), moderate non-proliferative diabetic retinopathy (n=21, 2%), severe non-proliferative diabetic retinopathy (n=11, 1%) and proliferative diabetic retinopathy (n=15, 1.4%). A summary of cardiovascular events and diabetic retinopathy at baseline is shown in table 5.2.

Variable	Mean (SD) or n (%)
Age - years	67.9 (4.2)
Gender (% men)	547 (51.3)
Body mass index (kg/m2)	31.4 (5.6)
Blood pressure	
systolic (mmHg)	133.3 (16.4)
diastolic (mmHg)	69.1 (9.01)
Plasma glucose (mmol/L)	7.56 (2.0)
Total cholesterol (mmol/L)	4.31 (0.9)
Plasma HbA1c (mmol)	9.2 (1.3)
High density lipoprotein cholesterol (mmol/L)	1.29 (0.3)
Duration of diabetes (years)	6.0 (8.04)
Current diabetes treatment	
diet only	200 (18.8)
tablets	675 (63.4)
insulin ± tablets	190 (17.8)
Anti-hypertensive medication	872 (81.8)
Lipid-lowering medication	912 (85.6)
Smoking	
current smoker	153 (14.4)
ex-smoker	499 (46.8)
never smoker	414 (38.8)
Estimated glomerular filtration rate (ml/min/1.73m2)	78.27 (23.1)

Table 5.1. Baseline characteristics of the ET2DS population (maximum n=1066). Data are presented as means (SD) or n (%)

Variable	n (%)
Cardiovascular event†	
Myocardial infarction	150 (14.1%)
Angina	298 (27.5%)
Stroke	62 (5.8%)
Transient ischaemic attack	31 (2.9%)
Coronary intervention	110 (10.3%)
Diabetic retinopathy	
Mild non proliferative DR	292 (27.4%)
Moderate non proliferative DR	21 (2%)
Severe non proliferative DR	11 (1%)
Proliferative DR	15 (1.4%)

Table 5.2. Prevalence of cardiovascular events and diabetic retinopathy at baseline in the ET2DS (max n=1066). Data are presented as n (%). †Note that there is overlap between these event subgroups. DR, diabetic retinopathy

5.2 Representativeness

At baseline, members of the ET2DS research team assessed the representativeness of the ET2DS population. Table 3 compares the key demographic and clinical characteristics of the people recruited into the study (participants n=1066) against the people invited from the Lothian Diabetes Register (LDR), but who did not participate in the final study (non-responders= 4386). No statistically significant differences were found between the ET2DS population and non-responders for age, duration of diabetes, glycated haemoglobin (HbA_{1c}) and treatment by insulin (Marioni et al, 2010). A summary of these results is presented in table 5.3.

	ET2DS population (max n = 1066)	**Non-responders** (max n = 4386)
Age (years)	67.9 ± 4.2	67.9 ± 4.4
Male Sex	547 (51.3)	1839 (41.9)
Duration of diabetes		
up to 5 years	516 (48.4)	2135 (48.7)
≥ 5 years	550 (51.6)	2251(51.3)
Glycated haemoglobin (mmol/l)	9.2 (1.3)	9.2 (1.6)
Insulin treatment	185 (17.4)	704 (16.1)
Systolic blood pressure (mmHg)	133.3 ± 16.4	137.2 ± 18.2
Total cholesterol (mmol/l)	4.3 (0.90)	4.2 (0.96)

Table 5.3. Characteristics of the ET2DS study population and the non-responder population. Data are means (SD) or n (%). [taken from Marioni et al 2010]

5.3 Incident cardiovascular events

For the purposes of this thesis, incident cardiovascular events were defined as the first fatal or non-fatal major cardiovascular event that an individual experienced during the eight-year follow-up period. Thus, the events could be true incident events, if the individual had not experienced a cardiovascular event before baseline, or could be a recurrent event, if the individual had already experienced a previous cardiovascular event prior to baseline. During the eight-year follow-up period, 208 participants had an incident cardiovascular event (19.5% of the ET2DS population). A detailed summary of these events is presented in table 5.4 and table 5.5.

Outcome	No. events	Sample %
Myocardial infarction	61	29.3
Angina	38	18.2
Stroke	53	25.4
Transient Ischaemic Accident	12	5.7
Coronary Intervention	26	12.5
Fatal Ischaemic Heart Disease	18	8.6
Total	208	100

Table 5.4. Incident cardiovascular events in the period between baseline (2006) and follow up (2016) in the ET2DS. The sample % is calculated from the total number of incident events.

Composite event outcomes	No. events	%
Any cardiovascular disease	208	19.5
Ischaemic heart disease (non-fatal)	125	11.7
Cerebrovascular Accident (fatal/non-fatal)	65	6.1
Fatal ischaemic heart disease	18	1.6

Table 5.5. Composite cardiovascular outcomes for participants in the ET2DS. The % is calculated from the total number of individuals in the dataset (n=1066).

5.4 Descriptive statistics for quantitative retinal traits

Descriptive statistics for the baseline quantitative retinal traits are presented in table 5.6. The values for the median, minimal and maximal arteriolar and venular tortuosity were right skewed. These values were converted by logarithmic transformation (natural logarithm) for use in subsequent statistical analysis. The distributions for multifractal dimensions D0, multifractal dimensions D1 and multifractal dimensions D2 were left skewed. Both logarithmic transformation (commonly used because it is a strong transformation with a major effect on distribution shape) and square transformation (often applied to left skewness) were attempted, and although square transformation had a moderate effect on the distribution, left skewness remained and a rank transformation was finally used to normalise these traits (table 5.7). A summary of the normal distribution of the quantitative retinal traits is shown in table 5.8 and figure 5.1.

Quantitative retinal traits	Mean (SD) or median (IQR)	Mean (SD) after transformation
Arteriovenous ratio (px)	0.74 (0.08)	0.74 (0.08)
Central retinal arteriolar equivalent (px)	33.00 (3.87)	33.02 (3.87)
Central retinal venular equivalent (px)	44.70 (5.01)	44.67 (5.01)
arteriolar tortuosity	0.00003 (0.00001, 0.00009)	-10.07 (1.14)
Minimum arteriolar tortuosity	0.000004 (0.000001, 0.00001)	-12.32 (1.14)
Maximum arteriolar tortuosity	0.0001 (0.00009, 0.0004)	-8.51 (1.11)
Venular tortuosity	0.00004 (0.00002, 0.00008)	-9.95 (0.89)
Minimum venular tortuosity	0.000007 (0.000002, 0.00001)	-11.92 (1.26)
Maximum venular tortuosity	0.0002 (0.0001, 0.0003)	-8.47 (1.00)
Multifractal dimensions D0	1.75 (1.71, 1.80)	1.75 (0.06)
Multifractal dimensions D1	1.74 (1.70, 1.78)	1.73 (0.06)
Multifractal dimensions D2	1.73 (1.69, 1.78)	1.72 (0.06)

Table 5.6. Descriptive statistics of quantitative retinal traits. Px, pixels. Natural logarithmic transformation was used for all traits apart from multifractal dimensions (rank transformation). Data are presented as means (SD) or median (lower IQR, upper IQR)

Trait	Distribution of data and normalisation method			
	N	Normal	Logarithmic transformation	Rank transformation
Arteriovenous ratio	1028	**Yes**	-	-
Central retinal arteriolar equivalent	1028	**Yes**	-	-
Central retinal venular equivalent	1028	**Yes**	-	-
Arteriolar tortuosity	1028	No	**Yes**	-
Minimum arteriolar tortuosity	1028	No	**Yes**	-
Maximum arteriolar tortuosity	1028	No	**Yes**	-
Venular tortuosity	1028	No	**Yes**	-
Minimum venular tortuosity	1028	No	**Yes**	-
Maximum venular tortuosity	1028	No	**Yes**	-
Multifractal dimensions D0	1015	No	No (still left skewed)	**Yes**
Multifractal dimensions D1	1015	No	No (still left skewed)	**Yes**
Multifractal dimensions D2	1015	No	No (still left skewed)	**Yes**

Table 5.7. Summary of method used to normalise the distr bution of the quantitative retinal traits.

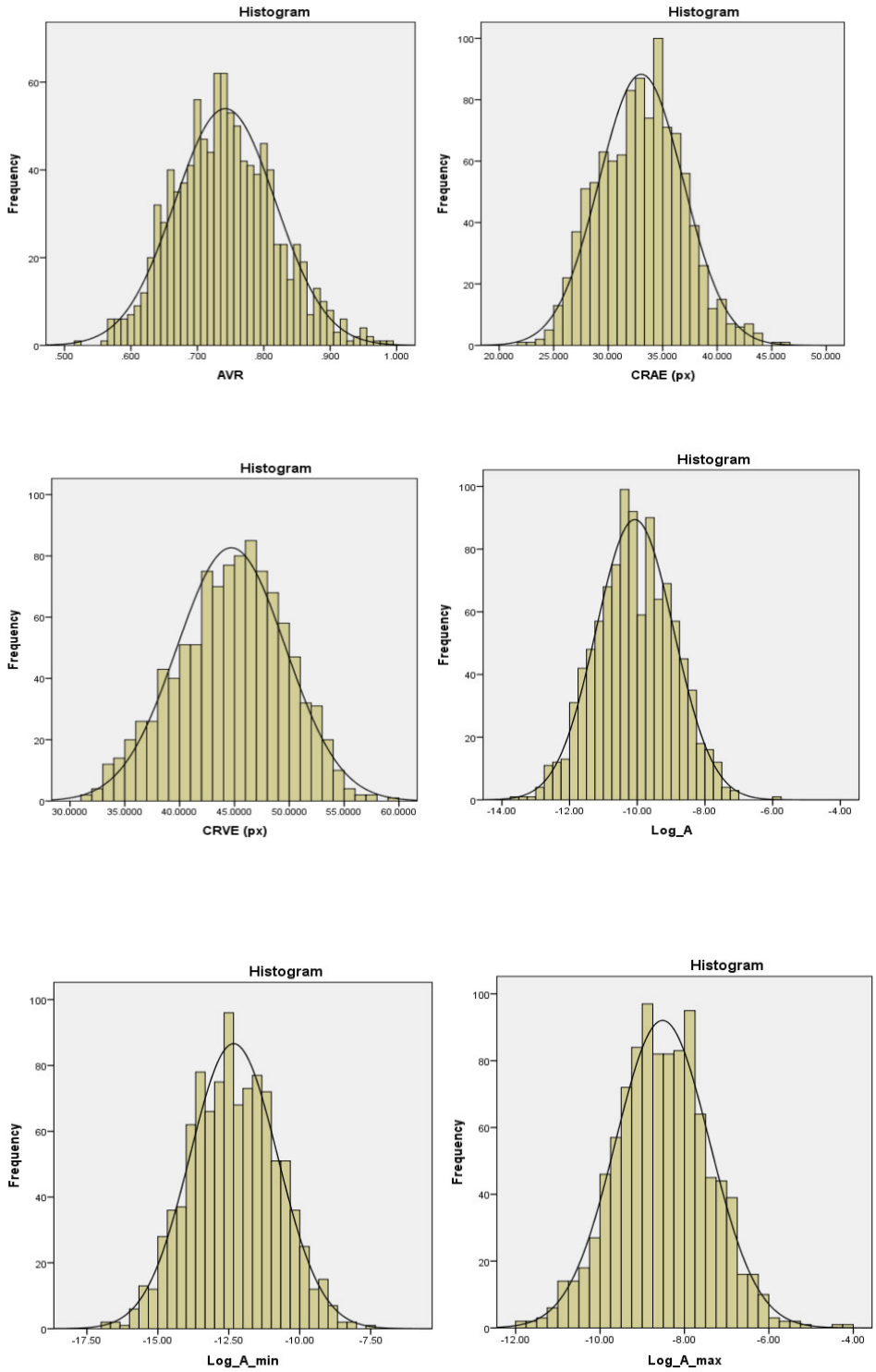

Figure 5.1. Graphs of the distr bution of the quantitative retinal traits, either untransformed, or following transformation where data initially skewed. Arteriovenous ratio, AVR; central retinal arteriolar equivalent, CRAE; central retinal venular equivalent, CRVE; Arteriolar tortuosity, Log_A; Minimum arteriolar tortuosity, Log_A_min; Maximum arteriolar tortuosity, Log_A_max.

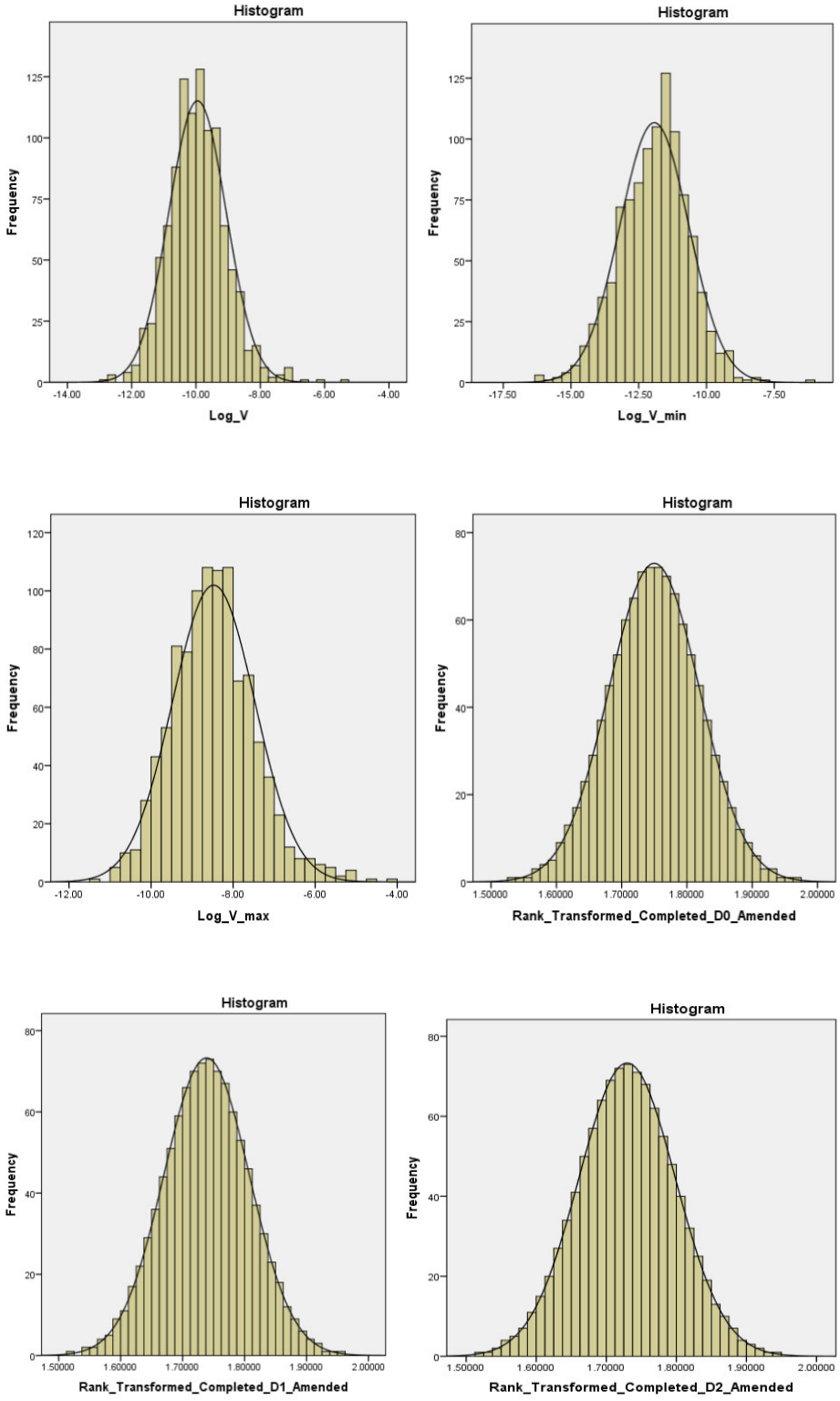

Figure 5.1 (cont.) Graphs of the distr bution of the quantitative retinal traits. Venular tortuosity, Log_V; Minimum venular tortuosity, Log_V_min; Maximum venular tortuosity Log_V_max; Multifractal dimensions D0, rank_tranforsformed_completed_amended_D0; Multifractal dimensions D1, rank_tranforsformed_completed_amended_D0; Multifractal dimensions D2, rank_tranforsformed_completed_amended_D2

5.5 Inter-relationship between quantitative retinal traits

This section describes the association between all the quantitative retinal traits (table 5.8).

Arteriovenous ratio (AVR) was highly and inversely correlated with arteriolar tortuosity (r = -0.081, $p < 0.001$) and minimum arteriolar tortuosity (r = -0.088, $p < 0.001$). Central retinal arteriolar equivalent (CRAE) was highly correlated with central retinal venous equivalent (CRVE) (r = 0.58, $p < 0.001$) and multifractal dimensions D0, D1 and D2 (all r = 0.42, $p < 0.001$). Similarly, CRVE was highly correlated with multifractal dimension traits (all r = 0.48, $p < 0.001$). As expected, log transformed arteriolar tortuosity was highly correlated with log transformed minimum arteriolar tortuosity (r = 0.68, $p < 0.001$) and log transformed maximum arteriolar tortuosity (r = 0.75, $p < 0.001$). Although log transformed arteriolar tortuosity was inversely correlated with CRAE (r = -0.13, $p < 0.001$) and multifractal dimension traits (all r = -0.11, $p < 0.001$), these correlations were weaker. Log transformed minimum arteriolar tortuosity was highly correlated with log transformed arteriolar tortuosity and log transformed maximum arteriolar tortuosity (r = 0.67, $p < 0.001$ and r = 0.51, $p < 0.001$ respectively). Log transformed minimum arteriolar tortuosity was inversely correlated with CRAE (r = -0.15, $p < 0.001$) and multifractal dimension traits (all r = -0.11, $p < 0.001$). Log transformed maximum arteriolar tortuosity was highly correlated with log transformed arteriolar tortuosity (0.75, $p < 0.001$). There were inverse correlations between log transformed maximum arteriolar tortuosity and both CRAE (r = -0.11, $p < 0.001$) and multifractal dimension traits (all r = -0.12, $p < 0.001$).

Log transformed venular tortuosity was correlated with log transformed minimum venular tortuosity and log transformed maximum venular tortuosity (r = 0.59, $p < 0.001$ and r = 0.68, $p < 0.001$ respectively). As for other tortuosity traits, log transformed venular tortuosity was negatively correlated with multifractal dimension traits (all r = -0.15, $p < 0.001$). Not surprisingly, log transformed minimum venular tortuosity was highly correlated with log

transformed venular tortuosity (r = 0.59, $p < 0.001$) and log transformed maximum venular tortuosity (r = 0.40, $p < 0.001$) and there was an inverse correlation with multifractal dimension traits (all r = -0.11, $p < 0.001$).

Multifractal dimension traits were highly inter-correlated (r = 0.99, $p < 0.001$). The other strongest correlations for these traits were with CRAE (r = 0.42, $p < 0.001$) and CRVE (r = 0.48, $p <0.001$). The remaining retinal traits were negatively correlated with multifractal dimensions and only AVR did not show a statistically significant correlation.

	AVR	CRAE	CRVE	Arteriolar Tort	Min Arteriolar Tort	Max Arteriolar Tort	Venular Tort	Min Venular Tort	Max Venular Tort	Multifractal Dimensions D0	Multifractal Dimensions D1	Multifractal Dimensions D2
AVR	1	0.47**	-0.43**	-0.081**	-0.088**	-0.043**	-0.021	-0.019	-0.026	-0.05	-0.04	-0.04
CRAE	0.47**	1	0.58**	-0.13**	-0.15**	-0.11**	0.13**	-0.10**	-0.13**	0.42**	0.42**	0.42 **
CRVE	-0.43**	0.58**	1	-0.05	-0.07*	-0.06	-0.11**	-0.08**	-0.11**	0.48**	0.47**	0.47**
Arteriolar Tortuosity	-0.08**	-0.13**	-0.05	1	0.68**	0.75**	0.24**	0.18**	0.2**	-0.11**	-0.11**	-0.11**
Min Arteriolar Tort	-0.09**	-0.15**	-0.07*	0.67**	1	0.51**	0.19**	0.15**	0.20**	-0.11**	-0.10**	-0.10**
Max Arteriolar Tort	-0.04	-0.11	-0.06	0.75**	0.51**	1	0.23**	0.16**	0.22**	-0.12**	-0.12**	-0.12**
Venular Tortuosity	-0.02	-0.13**	-0.11**	0.24**	0.19**	0.23**	1	0.59**	0.68**	-0.15**	-0.15**	-0.15**
Min Venular Tort	-0.019	-0.10**	-0.08**	0.18**	0.15**	0.16**	0.59**	1	0.40**	-0.11**	-0.11**	0.11**
Max Venular Tort	-0.03	-0.13**	-0.11**	0.20**	0.20**	0.22**	0.68**	0.40**	1	-0.12**	-0.12**	-0.12**
Multifractal Dimensions D0	-0.05	0.42**	0.48**	-0.11**	-0.11**	-0.12**	-0.15**	-0.11**	-0.12**	1	0.99**	0.99**
Multifractal Dimensions D1	-0.04	0.42**	0.47**	-0.11**	-0.10**	-0.12**	-0.15**	-0.11**	-0.12**	0.99**	1	0.99**
Multifractal Dimensions D2	-0.04	0.42**	0.47**	-0.11**	-0.10**	-0.12**	-0.15**	-0.11**	-0.12**	0.99**	0.99**	1

Table 5.8. Pearson correlation coefficients for correlations between all quantitative retinal traits. AVR, arteriovenous ratio; CRAE, central retinal arteriolar equivalent; CRVE, central retinal venular equivalent; min, minimum; max, maximum; tort, tortuosity. All arteriolar and venular tortuosity traits are log transformed. All multifractal dimensions values are rank transformed.*$p<0.05$, **$p<0.01$.

5.6 Missing data

The missing data for baseline demographic and risk factor variables used in subsequent analyses in this thesis are summarised in table 5.9.

Variable	Total baseline	*n* missing	% missing
Age and sex	1066	0	0%
Body mass index	1064	2	0.2%
Systolic blood pressure	1064	2	0.2%
Diastolic blood pressure	1064	2	0.2%
Plasma glucose	1049	17	1.6%
Total cholesterol	1057	9	0.9%
HbA1c	1028	38	3.6%
High density lipoprotein cholesterol	1057	9	0.8%
Duration of diabetes	1066	0	0%
Current diabetes treatment			
diet only	939	127	12%
tablets	1055	11	1%
insulin ± tablets	1041	25	2.3%
Anti-hypertensive medication	1056	10	1%
Lipid-lowering medication	1062	4	0.4%
Smoking	1066		0%
Estimated glomerular filtration rate	1057	9	0.9%
Diabetic retinopathy	1044	22	2.1%

Table 5.9. Missing demographic and risk factor data in the ET2DS at baseline

A flow diagram for inclusion of participants in my analyses on the ET2DS study population (participants with retinal images from which data on retinal traits could be extracted) is presented in figure 5.2. I undertook the retrieval and assessment of the retinal images, stored since baseline within the ET2DS datasets. Only retinal images with high quality could be used for the analysis of traits using VAMPIRE software. Most individuals had retinal images available from both the right and left eyes. In some cases, images were available but the software was not able to analyse the images due to technical issues or incompatibility of the format of the file. When quantitative

retinal data could not be extracted from the initially selected image, the image from the opposite eye was selected; but adequate quality could not be assured. Therefore, an important cause of missing data in the quantitative retinal traits was the original quality of the images taken at baseline in the ET2DS.

In total, data were available from 1028 images for measurement of quantitative retinal traits including AVR, CRAE, CRVE, arteriolar tortuosity, minimum arteriolar tortuosity, maximum arteriolar tortuosity, venular tortuosity, minimum venular tortuosity and maximum venular tortuosity. Due to technical issues, data from 13 of the 1028 images were unavailable for multifractal dimensions D0, multifractal dimensions D1 and multifractal dimensions D2.

A summary of the missing data for each of the individual quantitative retinal traits is presented in table 5.10. Overall, the loss of retinal data due to missing data was less than 5% for the traits used in this thesis. This suggests a small risk of bias due to missing data affecting association estimates or reducing statistical power.

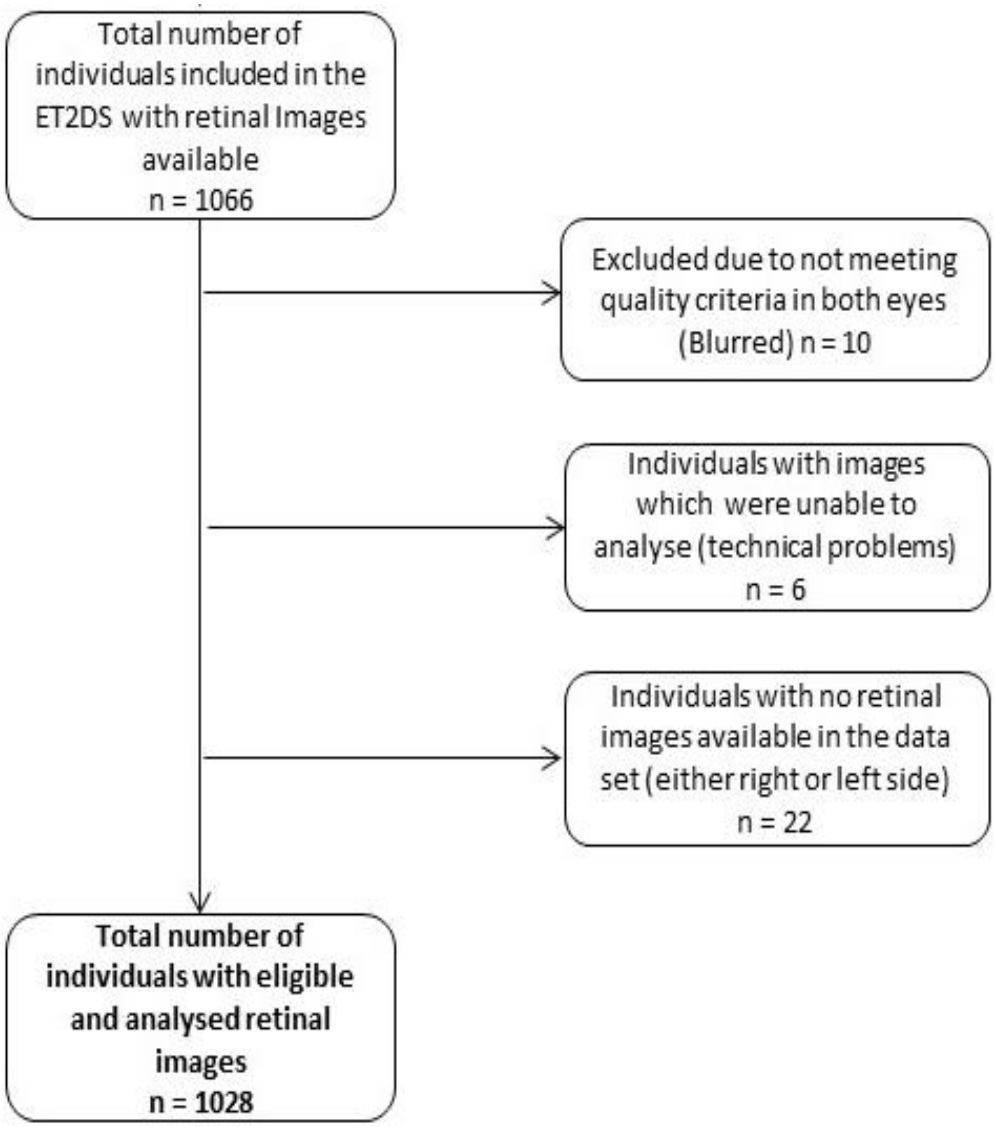

Figure 5.2. Flow diagram for missing retinal images and retinal trait data in the ET2DS. The total number of individuals in the retinal ET2DS dataset at baseline included 1066 individuals. A total of 22 ET2DS subjects had no retinal images available from baseline.

Quantitative retinal trait	Total measurements	Missing measurements (n)	Missing measurements (%)
Arteriovenous ratio	1028	38	3.6%
Central retinal arteriolar equivalent	1028	38	3.6%
Central retinal venular equivalent	1028	38	3.6%
Arteriolar tortuosity	1028	38	3.6%
Minimum arteriolar tortuosity	1028	38	3.6%
Maximal arteriolar tortuosity	1028	38	3.6%
Venular tortuosity	1028	38	3.6%
Minimum venular tortuosity	1028	38	3.6%
Maximal arteriolar tortuosity	1028	38	3.6%
Multifractal dimensions D0	1015	51	4.8%
Multifractal dimensions D1	1015	51	4.8%
Multifractal dimensions D2	1015	51	4.8%

Table 5.10. Missing data for the quantitative retinal traits measured on baseline retinal images in the ET2DS

Chapter 6 Results II - Cross sectional and prospective association between quantitative retinal traits and cardiovascular disease

In this chapter, I present the results of the cross-sectional and prospective analyses of the association of quantitative retinal traits with cardiovascular events and diabetic retinopathy. First, I describe the associations of retinal traits with cardiovascular events, retinopathy and traditional cardiovascular risk factors at baseline (including risk factors used in the UKPDS risk score), and, then present the association of baseline quantitative retinal traits with incident major cardiovascular events occurring during follow up.

6.1 Association of quantitative retinal traits with traditional cardiovascular risk factors, cardiovascular events and diabetic retinopathy at baseline

The unadjusted and adjusted (for age and sex) Pearson correlation coefficients for associations of quantitative retinal traits with continuous cardiovascular risk factors, together with ANOVA parameter estimate coefficients for associations with categorical risk factors, cardiovascular events and diabetic retinopathy at baseline, are shown in tables 6.1 to 6.6. The ANOVA statistic quoted quantifies the difference in the mean value of the variable between the test group and the reference category.

First, I present the results on vessel diameter and the arteriovenous ratio, followed by the results on arteriolar and venular tortuosity. Lastly, I describe the results for multifractal.

6.1.1 Association of vessel diameters and arteriovenous ratio with traditional cardiovascular risk factors, prevalent cardiovascular events and diabetic retinopathy

In cross-sectional analyses of baseline data, a number of demographic factors, cardiovascular risk factors and disease variables were significantly associated with the quantitative retinal traits reflecting vessel widths; central retinal arteriolar equivalent (CRAE), central retinal venular equivalent (CRVE) and the arteriovenous ratio (AVR) (table 6.1). Increasing age was associated with a lower CRVE (r=-0.076, *p* =0.01) and a correspondingly higher AVR (r=0.068, p=0.02). Men had significantly lower mean AVR (ANOVA 0.01, *p*=0.04), CRAE (ANOVA 1.05, p<0.0001) and CRVE (ANOVA 0.73, *p*=0.02) than women.

In terms of associations with cardiovascular risk factors, CRVE was positively associated with BMI (r= 0.080, *p*=0.01), although this association was not statistically significant after adjustment for age and sex. Participants using tablets for diabetes treatment had a higher AVR compared with those who were diet controlled (ANOVA 0.01, *p*=0.03), and higher AVR was also associated with lower total cholesterol (r=-0.099, *p*=0.002). Both associations remained statistically significant after age and sex adjustment, whereas an association between higher AVR and lower diastolic blood pressure (r=-0.069, *p*=0.02) was not significant in the adjusted model. CRAE (r=-0.07, *p*<0.05) and CRVE (r=-0.07, *p*<0.05) were both negatively associated with plasma glucose (r=-0.068, *p* =0.03 and r=-0.063, *p*=0.04 respectively) in both unadjusted and adjusted models.

There were few statistically significant associations between retinal traits and either cardiovascular events or diabetic retinopathy. After adjustment for age and sex, individuals with prevalent cardiovascular disease (e.g. one or more of MI, angina, stroke and TIA) were found to have significantly higher CRAE than those without prevalent cardiovascular disease (ANOVA 0.43, *p*=0.01), and a similar result was found for individuals who had angina alone versus those without angina (ANOVA 0.60, *p*=0.02). Individuals with prevalent diabetic retinopathy had higher CRVE than those without prevalent diabetic retinopathy (ANOVA 0.74, *p*=0.02).

	Arteriovenous ratio		CRAE (pixels)		CRVE (pixels)	
	Pearson correlation	**ANOVA**	**Pearson correlation**	**ANOVA**	**Pearson correlation**	**ANOVA**
Age (years)	**0.068***		-0.022		**-0.076***	
Sex (male)		**-0.01***		**-1.05*****		**-0.73***
Body mass index (kg/m2)	-0.049		0.034		**0.080***	
Diabetes treatment						
Tablets		**0.01***		0.13		-0.55
Insulin ± Tablets		-0.0004		0.15		0.21
Anti-hypertensive meds		-0.009		0.11		0.60
Lipid-lowering meds		0.0001		0.40		0.50
Smoking status						
Current smoker		-0.0008		0.44		0.62
Ex-smoker		0.006		0.41		0.08
Systolic BP (mmHg)	-0.025		-0.035		-0.018	
Diastolic BP (mmHg)	**-0.069***		-0.029		0.032	
Plasma glucose (mmol/l)	-0.005		**-0.068***		**-0.063***	
HbA1C (mmol/l)	0.005		-0.015		-0.011	
Cholesterol (mmol/l)	**-0.099****		-0.035		0.055	
HDL Cholesterol (mmol/l)	0.011		0.015		0.04	
Duration diabetes (years)	0.027		0.042		0.010	
eGFR	0.024		-0.035		-0.061	
Cardiovascular event		0.007		0.43		0.16
Myocardial Infarction		0.007		0.20		-0.22
Angina		0.008		**0.60***		0.30
Stroke		-0.005		-0.30		0.12
TIA		0.03		0.70		0.20
Diabetic retinopathy		-0.005		0.32		**0.74***
Mild NP		0.004		-0.47		-0.89
Moderate NP		-0.002		0.47		0.85
Severe NP		0.03		-0.02		-2.18
Proliferative		0.01		1.35		1.21

Table 6.1. Associations of AVR, CRAE and CRVE with demographic, cardiovascular risk factor and disease variables at baseline (unadjusted). Data are Pearson correlation coefficient (*p* values) for continuous variables. For categorical variables, the ANOVA statistic quantifies the difference in mean of AVR, CRAE and CRVE for the given categorical variable compared with the reference level (reference levels are female sex, diet alone for diabetes treatment, no lipid lowering medication, no anti-hypertensive medication, never smoker). CRAE, central retinal arteriolar equivalent; CRVE, central retinal venular equivalent; HDL, high density lipoprotein; eGFR, estimated glomerular filtration rate; TIA transient ischaemic attack; NP, non-proliferative. *$p<0.05$, **$p<0.01$, ***$p<0.001$

	Arteriovenous ratio		CRAE (pixels)		CRVE (pixels)	
	Pearson correlation	**ANOVA**	**Pearson correlation**	**ANOVA**	**Pearson correlation**	**ANOVA**
BMI (kg/m2)	-0.051		0.005		0.055	
Diabetes treatment						
Tablets		**0.01***		0.13		-0.55
Insulin ± tablets		-0.0004		0.15		0.21
Anti-hypertensive meds		-0.009		0.11		0.60
Lipid-lowering meds		0.0001		0.40		0.50
Smoking status						
Current smoker		-0.0008		0.44		0.62
Ex-smoker		0.006		0.41		0.08
Systolic BP (mmHg)	-0.029		-0.033		-0.012	
Diastolic BP (mmHg)	-0.050		-0.010		0.034	
Plasma glucose (mmol/l)	-0.0003		**-0.064**		**-0.063***	
HbA1C (mmol/l)	0.007		-0.022		-0.019	
Cholesterol (mmol/l)	**-0.109****		-0.061		0.040	
HDL Cholesterol (mmol/l)	0.009		-0.015		-0.007	
Duration diabetes (years)	0.025		0.047		0.016	
eGFR	0.046		-0.032		-0.032	
Cardiovascular event		0.007		**0.43***		0.16
Myocardial Infarction		0.007		0.20		-0.22
Angina		0.008		**0.60***		0.30
Stroke		-0.005		-0.30		0.12
TIA		0.03		0.70		0.20
Diabetic retinopathy		-0.005		0.32		**0.74***
Mild NP		0.004		-0.47		-0.89
Moderate NP		-0.002		0.47		0.85
Severe NP		0.03		-0.02		-2.18
Proliferative		0.01		1.35		1.21

Table 6.2. Associations of AVR, CRAE and CRVE with demographic, cardiovascular risk factor and disease variables at baseline (adjusted for age and sex). Data are Pearson correlation coefficient (*p* values) for continuous variables. For categorical variables, the ANOVA statistic quantifies the difference in mean of AVR, CRAE and CRVE for the given categorical variable compared with the reference level (reference levels are female sex, diet alone for diabetes treatment, no lipid lowering medication, no anti-hypertensive medication, never smoker). CRAE, central retinal arteriolar equivalent; CRVE, central retinal venular equivalent; HDL, high density lipoprotein; eGFR, estimated glomerular filtration rate; TIA transient ischaemic attack; NP, non proliferative. *$p<0.05$, **$p<0.01$, ***$p<0.001$

6.1.2 Association of arteriolar and venular tortuosity with traditional cardiovascular risk factors, prevalent cardiovascular events and diabetic retinopathy

Associations of arteriolar and venular tortuosity with traditional cardiovascular risk factors, prevalent cardiovascular events and diabetic retinopathy are shown in tables 6.3 to 6.6. All analyses were cross-sectional and the models used were unadjusted (tables 6.3 and 6.5) or adjusted for sex and age (tables 6.4 and 6.6). Values for arteriolar and venular tortuosity were normalised using logarithmic transformation. Logarithmic transformations follow the same direction as the original values and hence these ease the interpretation of the results.

6.1.2.1 Association of arteriolar tortuosity with traditional cardiovascular risk factors, prevalent cardiovascular events and diabetic retinopathy

Increasing age was associated with lower mean arteriolar tortuosity (r=-0.072, *p*=0.02) and men had significantly higher mean arteriolar tortuosity than women (ANOVA 0.013, *p*=0.0002).

There were very few statistically significant associations between any of the measures of arteriolar tortuosity and either the cardiovascular risk factor or disease variables, although raised diastolic blood pressure was associated with higher mean arteriolar tortuosity (r=0.090, *p*=0.004). This association remained significant after adjusting for sex and age (r=0.063, *p*=0.04). Total cholesterol showed a positive association with maximum arteriolar tortuosity) in both the unadjusted (r=0.062, *p* =0.04) and adjusted models (r=0.070, *p*=0.03). No further significant associations were found between arteriolar tortuosity and either prevalent cardiovascular events or diabetic retinopathy.

6.1.2.2 Association of venular tortuosity with traditional cardiovascular risk factors, prevalent cardiovascular events and diabetic retinopathy.

Results of association with venular tortuosity are presented in table 6.5 (unadjusted) and table 6.6 (adjusted for age and sex). A number of statistically significant associations were found between mean venular tortuosity and cardiovascular risk factors. Body mass index was positively associated with mean venular tortuosity (r=0.105, *p*=0.001) and maximum venular tortuosity (r=0.085, *p*=0.007). These

associations remained significant in the adjusted model for both venular traits (r=0.115, *p*=0.0002 and r=0.086, *p*=0.006). Systolic blood pressure was also significant associated with mean venular tortuosity (r=0.081, *p*=0.009) in the unadjusted model and this statistical significance persisted after adjustment for age and sex (r=0.083, *p*=0.008). Although duration of diabetes did not show a statistically significant association with venular tortuosity traits, it is important to notice that it followed a consistent negative trend with all venular tortuosity traits.

Individuals with prevalent cardiovascular disease had higher mean venular tortuosity than those without prevalent cardiovascular disease (ANOVA *p*-value) in both the unadjusted and adjusted models (ANOVA 0.15, *p*=0.01 and *p*=0.02 respectively). In the sub classification of these prevalent events, individuals with stroke had higher mean venular tortuosity than those without stroke (ANOVA 0.30, *p*=0.01 and *p*=0.03 for unadjusted and age/sex adjusted models respectively). No further statistically significant associations were found between other venular tortuosity traits and any of the individual cardiovascular events or diabetic retinopathy.

	Mean arteriolar tortuosity		Minimum arteriolar tortuosity		Maximum arteriolar tortuosity	
	Pearson correlation	**ANOVA**	**Pearson correlation**	**ANOVA**	**Pearson correlation**	**ANOVA**
Age (years)	**-0.072***		-0.048		-0.050	
Sex (male)		**0.01*****		0.002		0.003
BMI (kg/m2)	0.031		-0.039		0.015	
Diabetes treatment						
Tablets		0.008		-0.03		0.01
Insulin ± tablets		0.001		-0.14		-0.05
Anti-hypertensive meds		0.08		0.20		0.07
Lipid-lowering meds		0.07		-0.04		0.02
Smoking status						
Current smoker		0.12		-0.02		0.004
Ex-smoker		0.08		0.02		0.02
Systolic BP (mmHg)	0.014		0.011		-0.002	
Diastolic BP (mmHg)	**0.090****		0.052		0.058	
Plasma glucose (mmol/l)	0.011		0.015		0.040	
HbA1C (mmol/l)	-0.003		-0.027		0.051	
Cholesterol (mmol/l)	0.039		0.053		**0.062***	
HDL Cholesterol (mmol/l)	-0.046		-0.021		-0.010	
Duration diabetes (years)	-0.021		-0.032		0.010	
eGFR	0.025		0.026		0.012	
Cardiovascular event		-0.01		-0.16		-0.04
MI		-0.04		-0.13		-0.03
Angina		-0.02		-0.16		-0.08
Stroke		0.12		0.31		0.08
TIA		-0.08		0.16		0.30
Diabetic retinopathy		0.14		0.17		0.10
Mild NP		-0.13		-0.16		-0.10
Moderate NP		-0.23		-0.033		-0.18
Severe NP		-0.15		0.09		-0.012
Proliferative		-0.16		-0.58		0.019

Table 6.3. Associations of mean, minimum and maximum arteriolar tortuosity with demographic, cardiovascular risk factor and disease variables at baseline (unadjusted). Data are Pearson correlation coefficient (p values) for continuous variables. For categorical variables, the ANOVA statistic quantifies the difference in mean tortuosity trait for the given categorical variable compared with the reference level (reference levels are female sex, diet alone for diabetes treatment, no lipid lowering medication, no anti-hypertensive medication, never smoker). HDL, high-density lipoprotein; eGFR, estimated glomerular filtration rate; TIA transient ischaemic attack; NP, non-proliferative. *p<0.05, **p<0.01, ***p<0.001

	Mean arteriolar tortuosity		Minimum arteriolar tortuosity		Maximum arteriolar tortuosity	
	Pearson correlation	**ANOVA**	**Pearson correlation**	**ANOVA**	**Pearson correlation**	**ANOVA**
BMI (kg/m2)	0.042		-0.041		0.018	
Diabetes treatment						
Tablets		0.008		-0.03		0.01
Insulin ± tablets		0.001		-0.14		-0.05
Anti-hypertensive meds		0.08		0.20		0.07
Lipid-lowering meds		0.07		-0.04		0.02
Smoking status						
Current smoker		0.12		-0.02		0.004
Ex-smoker		0.08		0.02		0.02
Systolic BP (mmHg)	0.018		0.014		0.001	
Diastolic BP (mmHg)	**0.063****		0.040		0.043	
Plasma glucose (mmol/l)	0.004		0.012		0.036	
HbA1C (mmol/l)	-0.002		-0.028		0.051	
Cholesterol (mmol/l)	0.056		0.058		**0.070***	
HDL Cholesterol (mmol/l)	-0.014		-0.008		0.008	
Duration diabetes (years)	-0.200		-0.030		-0.009	
eGFR	0.002		0.011		-0.005	
Cardiovascular event		-0.01		-0.16		-0.04
MI		-0.04		-0.13		-0.03
Angina		-0.02		-0.16		-0.08
Stroke		0.12		0.31		0.08
TIA		-0.08		0.16		0.30
Diabetic retinopathy		0.14		0.17		0.10
Mild NP		-0.13		-0.16		-0.10
Moderate NP		-0.23		-0.03		-0.18
Severe NP		-0.15		0.09		-0.01
Proliferative		-0.16		-0.58		0.02

Table 6.4. Associations of mean, minimum and maximum arteriolar tortuosity with demographic, cardiovascular risk factor and disease variables at baseline (adjusted for age and sex). Data are Pearson correlation coefficient (*p* values) for continuous variables. For categorical variables, the ANOVA statistic quantifies the difference in mean tortuosity trait for the given categorical variable compared with the reference level (reference levels are female sex, diet alone for diabetes treatment, no lipid lowering medication, no anti-hypertensive medication, never smoker). HDL, high-density lipoprotein; eGFR, estimated glomerular filtration rate; TIA transient ischaemic attack; NP, non-proliferative. *p<0.05, **p<0.01, ***p<0.001

	Mean venular tortuosity		Minimum venular tortuosity		Maximum venular tortuosity	
	Pearson correlation	ANOVA	Pearson correlation	ANOVA	Pearson correlation	ANOVA
Age (years)	-0.028		-0.009		-0.037	
Sex (male)		0.002		-0.001		-0.001
BMI (kg/m2)	**0.105****		0.057		**0.085****	
Diabetes treatment						
Tablets		0.11		0.10		0.13
Insulin ± tablets		0.01		-0.16		0.02
Anti-hypertensive meds		0.06		0.10		0.03
Lipid-lowering meds		0.08		0.03		0.005
Smoking status						
Current smoker		0.10		0.12		0.08
Ex-smoker		0.15		0.15		0.19
Systolic BP (mmHg)	**0.081****		0.054		0.051	
Diastolic BP (mmHg)	0.045		0.002		-0.003	
Plasma glucose (mmol/l)	0.021		-0.020		0.038	
HbA1C (mmol/l)	0.040		-0.013		0.040	
Cholesterol (mmol/l)	-0.020		0.010		-0.020	
HDL Cholesterol (mmol/l)	-0.031		0.033		-0.039	
Duration diabetes (years)	-0.026		-0.019		-0.028	
eGFR	-0.011		0.008		-0.025	
Cardiovascular event		**0.15***		-0.14		0.06
MI		0.04		0.001		0.04
Angina		0.09		0.17		0.02
Stroke		**0.30***		0.26		0.22
TIA		0.11		-0.07		-0.08
Diabetic retinopathy		0.08		0.08		0.09
Mild NP		-0.07		-0.11		-0.08
Moderate NP		0.11		0.34		0.23
Severe NP		-0.41		0.02		-0.59
Proliferative		-0.23		-0.12		-0.39

Table 6.5. Associations of mean, minimum and maximum venular tortuosity with demographic, cardiovascular risk factor and disease variables at baseline (unadjusted). Data are Pearson correlation coefficient (*p* values) for continuous variables. For categorical variables, the ANOVA statistic quantifies the difference in mean tortuosity trait for the given categorical variable compared with the reference level (reference levels are female sex, diet alone for diabetes treatment, no lipid lowering medication, no anti-hypertensive medication, never smoker). HDL, high density lipoprotein; eGFR, estimated glomerular filtration rate; TIA transient ischaemic attack; NP, non proliferative. *p<0.05, **p<0.01, ***p<0.001

	Mean venular tortuosity		Minimum venular tortuosity		Maximum venular tortuosity	
	Pearson correlation	**ANOVA**	**Pearson correlation**	**ANOVA**	**Pearson correlation**	**ANOVA**
BMI (kg/m2)	**0.115****		0.059		**0.086****	
Diabetes treatment						
Tablets		0.11		0.10		0.13
Insulin ± tablets		0.01		-0.16		0.02
Anti-hypertensive meds		0.06		0.10		0.03
Lipid-lowering meds		0.08		0.03		0.005
Smoking status						
Current smoker		0.10		0.12		0.08
Ex-smoker		0.15		0.15		0.19
Systolic BP (mmHg)	**0.083****		0.055		0.054	
Diastolic BP (mmHg)	0.034		0.001		-0.013	
Plasma glucose (mmol/l)	0.018		-0.020		0.036	
HbA1C (mmol/l)	0.040		-0.013		0.038	
Cholesterol (mmol/l)	-0.014		0.012		-0.020	
HDL Cholesterol (mmol/l)	-0.019		0.036		-0.033	
Duration diabetes (years)	-0.026		-0.019		-0.026	
eGFR	-0.022		0.008		-0.037	
Cardiovascular events		**0.15***		-0.14		0.06
MI		0.04		0.001		0.04
Angina		0.09		0.17		0.02
Stroke		**0.30***		0.26		0.22
TIA		0.11		-0.07		-0.08
Diabetic retinopathy		0.08		0.08		0.09
Mild NP		-0.07		-0.11		-0.081
Moderate NP		0.11		0.34		0.23
Severe NP		-0.41		0.02		-0.59
Proliferative		-0.23		-0.12		-0.39

Table 6.6. Associations of mean, minimum and maximum venous tortuosity with demographic, cardiovascular risk factor and disease variables at baseline (adjusted for age and sex). Data are Pearson correlation coefficient (p values) for continuous variables. For categorical variables, the ANOVA statistic quantifies the difference in mean tortuosity trait for the given categorical variable compared with the reference level (reference levels are female sex, diet alone for diabetes treatment, no lipid lowering medication, no anti-hypertensive medication, never smoker). HDL, high-density lipoprotein; eGFR, estimated glomerular filtration rate; TIA transient ischaemic attack; NP, non-proliferative. *p<0.05, **p<0.01, ***p<0.001

6.1.3 Association of multifractal dimensions with traditional cardiovascular risk factors, prevalent cardiovascular events and diabetic retinopathy

Results of the association of multifractal dimensions D0, D1 and D2 with cardiovascular risk factors and with disease variables are presented in table 6.7 and table 6.8. All multifractal dimensions traits were left-skewed and distributions were normalised using rank transformation prior to analysis. There were high levels of correlation between the multifractal-dimensions traits D0, D1, D2 (described above), such that the results presented in this section proved very similar or identical across these traits.

Overall, analyses did not show statistically significant associations for multifractal-dimensions with risk factor or disease variables, in either the unadjusted or adjusted models. Despite this, it is important to highlight the direction of the correlations. This is because multifractal dimension is a novel biomarker, which is poorly understood. Thus, there was a trend for multifractal-dimensions D0, D1 and D2 to be negatively correlated with age, systolic blood pressure, plasma glucose, total cholesterol and renal function (eGFR).

	Multifractal dimensions D0		Multifractal dimensions D1		Multifractal dimensions D2	
	Pearson correlation	ANOVA	Pearson correlation	ANOVA	Pearson correlation	ANOVA
Age (years)	-0.035		-0.035		-0.035	
Sex (male)		0.002		0.002		0.002
BMI (kg/m2)	0.015		0.017		0.017	
Diabetes treatment						
Tablets		-0.003		-0.003		-0.003
Insulin ± tablets		0.002		0.002		0.001
Anti-hypertensive meds		-0.002		-0.001		-0.001
Lipid-lowering meds		0.002		0.002		0.002
Smoking status						
Current smoker		0.01		0.01		0.01
Ex-smoker		0.01		0.01		0.01
Systolic BP (mmHg)	-0.027		-0.026		-0.024	
Diastolic BP (mmHg)	0.021		0.025		0.025	
Plasma glucose (mmol/l)	-0.017		-0.020		-0.020	
HbA1C (mmol/l)	0.005		0.003		0.003	
Cholesterol (mmol/l)	-0.022		-0.021		-0.021	
HDL Cholesterol (mmol/l)	0.050		0.051		0.052	
Duration diabetes (years)	0.049		0.049		0.050	
eGFR	-0.019		-0.020		-0.021	
Cardiovascular event		0.003		0.003		0.003
MI		0.003		0.003		0.003
Angina		0.003		0.004		0.004
Stroke		-0.004		-0.005		-0.005
TIA		-0.01		-0.01		-0.01
Diabetic retinopathy		-0.0002		-0.0001		-0.0001
Mild NP		-0.001		-0.001		-0.001
Moderate NP		0.009		0.009		0.008
Severe NP		0.005		0.004		0.004
Proliferative		0.01		0.01		0.01

Table 6.7. Associations of multifractal dimensions DO, D1 and D2 with demographic, cardiovascular risk factor and disease variables at baseline (unadjusted). Data are Pearson correlation coefficient (*p* values) for continuous variables. For categorical variables, the ANOVA statistic quantifies the difference in mean multifractal dimension trait for the given categorical variable compared with the reference level (reference levels are female sex, diet alone for diabetes treatment, no lipid lowering medication, no anti-hypertensive medication, never smoker). HDL, high-density lipoprotein; eGFR, estimated glomerular filtration rate; TIA transient ischaemic attack; NP, non-proliferative. **p*<0.05, ***p*<0.01, ****p*<0.001

	Multifractal dimensions D0		Multifractal dimensions D1		Multifractal dimensions D2	
	Pearson correlation	ANOVA	Pearson correlation	ANOVA	Pearson correlation	ANOVA
BMI (kg/m2)	0.001		0.003		0.004	
Diabetes treatment						
Tablets		-0.003		-0.003		-0.003
Insulin ± tablets		0.002		0.002		0.001
Anti-hypertensive meds		-0.002		-0.001		-0.001
Lipid-lowering meds		0.002		0.002		0.002
Smoking status						
Current smoker		0.01		0.01		0.01
Ex-smoker		0.01		0.01		0.01
Systolic BP (mmHg)	-0.023		-0.022		-0.021	
Diastolic BP (mmHg)	0.024		0.027		0.027	
Plasma glucose (mmol/l)	-0.017		-0.019		-0.019	
HbA1C (mmol/l)	0.0004		-0.001		-0.001	
Cholesterol (mmol/l)	-0.033		-0.032		-0.032	
HDL Cholesterol (mmol/l)	0.042		0.044		0.045	
Duration diabetes (years)	0.052		0.053		0.053	
eGFR	-0.025		-0.026		-0.027	
Cardiovascular event		0.003		0.003		0.003
MI		0.003		0.003		0.003
Angina		0.003		0.004		0.004
Stroke		-0.004		-0.005		-0.005
TIA		-0.01		-0.01		-0.01
Diabetic retinopathy		-0.0002		-0.0001		-0.0001
Mild NP		-0.001		-0.001		-0.001
Moderate NP		0.009		0.009		0.008
Severe NP		0.005		0.004		0.004
Proliferative		0.01		0.01		0.01

Table 6.8 Associations of multifractal dimensions D0, D1 and D2 with demographic, cardiovascular risk factor and disease variables at baseline (adjusted for age and sex). Data are Pearson correlation coefficient (*p* values) for continuous variables. For categorical variables, the ANOVA statistic quantifies the difference in mean multifractal dimension trait for the given categorical variable compared with the reference level (reference levels are female sex, diet alone for diabetes treatment, no lipid lowering medication, no anti-hypertensive medication, never smoker). HDL, high-density lipoprotein; eGFR, estimated glomerular filtration rate; TIA transient ischaemic attack; NP, non-proliferative. *p<0.05, **p<0.01, ***p<0.001

6.2 Prospective analysis of quantitative retinal traits with incident cardiovascular events

In this section, I present the results of the longitudinal analyses of the relationship between quantitative retinal traits and incident cardiovascular events. I describe the incident event rates as well as the traditional cardiovascular risk factor profile of those who presented with an incident event. I then present the results of survival analyses exploring the relationship between quantitative retinal traits and incident cardiovascular events.

6.2.1 Incident cardiovascular events in the ET2DS

During the eight-year period of follow-up in the ET2DS, there were 200 incident cardiovascular events in a total of 1028 individuals with quantitative retinal trait measurements (event rate 19.5%). An incident cardiovascular event was defined as the first fatal or non-fatal myocardial infarction (MI), diagnosis of angina, fatal or non-fatal stroke, transient ischaemic attack (TIA), coronary intervention or other fatal ischaemic heart disease (IHD) event experienced by a participant after baseline. These incident events were used to explore the prospective relationship of baseline variables with incident cardiovascular disease (all cardiovascular events), incident coronary disease (fatal and non-fatal) and cerebrovascular disease (fatal and non-fatal ischaemic or haemorrhagic stroke), before and after adjustment for sex and age and traditional cardiovascular risk factors.

In the initial part of my analysis, I focused on the combined outcome of ‘all cardiovascular events’ because the number of individuals with incident events in the subcategories was relatively small and so event-specific analyses lacked power. In the second part, associations which proved to be statistically significant were explored further by breaking the analyses down by component cardiovascular events.

6.2.2 Demographics, cardiovascular risk factors, diabetic retinopathy and incident cardiovascular events

Demographic variables and traditional cardiovascular risk factors were compared in those individuals with quantitative retinal traits measured (n = 1028) who had an incident cardiovascular event and those who did not (Table 6.9).

Individuals who had an incident event were older (p<0.01) and were more likely to be male (p<0.001). Individuals with an incident cardiovascular event had a poorer metabolic profile than those with no event, with a significantly longer median duration of diabetes (p<0.01), significant higher HbA_{1c} (p<0.01) and higher percentage of individuals using insulin ± hypoglycaemics (p<0.0001). When traditional cardiovascular risk factors were compared between the groups, there was no statistically significant difference in either systolic or diastolic blood pressure, but it is important to highlight that there were more individuals using antihypertensive medication in participants who presented with an incident event (p<0.05) which could explain why blood pressure did not differ. There were no statistically significant differences in plasma glucose or total cholesterol between the two groups, however, HDL cholesterol was significantly lower in subjects with incident events (p<0.001). There was also a higher percentage of individuals using lipid-lowering medication in the group that did not have an incident event but this result did not reach statistical significance. In terms of renal function, estimated glomerular filtration rate was significantly lower in those who experienced an incident event (p<0.0001). There was no significant difference in the percentage of current, ex or never smokers between the groups and BMI was also found not to be significantly different.

The relationship of prevalent cardiovascular events and diabetic retinopathy with incident cardiovascular event was also analysed. Those individuals who had incident events were more likely to have experienced a previous cardiovascular event (p < 0.0001). There was a significantly higher percentage of individuals without diabetic retinopathy in the group that did not go on to have a cardiovascular event (p<0.0001). In general, those individuals with presence of diabetic retinopathy at any grade were more likely to experience incident events. For instance, those individuals with mild non-proliferative diabetic retinopathy were more likely to have an incident event (p<0.05). Likewise, individuals who had moderate non-proliferative diabetic

retinopathy were more likely to experience an incident cardiovascular events (p<0.001). Although individuals with more severe non-proliferative grade of diabetic retinopathy appeared more likely to develop an incident event, this difference was not statistically significant, which may be due to the small sample size in this group.

Variable	No incident event (max n=828)	Incident event (max n=200)	p value
Sex (male)	49.7 (410)	59.0 (118)	**<0.01**
Age (years)	67.7 (4.2)	68.9 (4.2)	**<0.001**
BMI (kg/m2)	31.3 (5.7)	31.9 (5.6)	0.23
Oral diabetes medication	73.6 (607)	74.0 (142)	0.49
Insulin ± tablets	15.9 (128)	28.9 (57)	**<0.0001**
Anti-hypertensive medication	18.8 (154)	13.0 (26)	**<0.05**
Lipid-lowering medication	14.8 (122)	10.6 (21)	0.75
Smoking status			
Current smoker	14.3 (118)	14.0 (28)	0.78
Ex-smoker	46.5 (385)	50.0 (100)	0.35
Never smoker	39.3 (325)	36.0 (72)	0.64
Duration of diabetes (years)	7.8 (6.3)	9.3 (6.8)	**<0.01**
HbA1c (mmol/l)	9.0 (1.3)	9.5 (1.6)	**<0.01**
Systolic BP (mmHg)	132.8 (15.6)	134.9 (19.1)	0.10
Diastolic BP (mmHg)	69.0 (8.8)	69.1 (9.8)	0.92
Plasma glucose (mmol/l)	7.5 (1.9)	7.8 (2.6)	0.13
Total cholesterol (mmol/l)	4.3 (0.9)	4.4 (1.0)	0.061
HDL cholesterol (mmol/l)	1.3 (0.4)	1.2 (0.3)	**<0.0001**
eGFR (ml/min/1.73m2)	80.0 (22.6)	70.4 (23.9)	**<0.0001**
CVD at baseline	30.0 (248)	58.0 (116)	**<0.0001**
Diabetic retinopathy			
None	70.0 (579)	57.0 (114)	**<0.0001**
Mild non-proliferative	27.1 (224)	32.0 (64)	<0.05
Moderate non-proliferative	1.3 (11)	5.0 (10)	**<0.001**
Severe non-proliferative	0.8 (7)	2.0 (4)	0.09
Proliferative	0.7 (6)	4.0 (8)	**<0.001**

Table 6.9. Baseline characteristics of individuals with incident cardiovascular events and no events (maximum n = 1028 with retinal trait data). BMI, body mass index; HDL, high density lipoprotein; HbA_{1c}, glycated haemoglobin; eGFR, estimated glomerular filtration rate; CVD, cardiovascular disease. Values are mean (SD), median (IQR) or % (n)

6.2.3 Quantitative retinal traits and incident cardiovascular events

To examine the association of the quantitative retinal traits with incident events, unadjusted analyses were first undertaken and mean or median values of traits in those individuals experiencing an incident event and those not having an event were compared.

Tortuosity and multifractal dimensions traits which were not normally distributed were first analysed using non-parametric tests (e.g. Kruskal-Wallis). Subsequently, all quantitative retinal traits were analysed using parametric tests such as t-test following normalisation of skewed distributions where required. Assumptions for using this test include normal distribution of the data and adequacy of sample size.

Table 6.10 compares the median values of the quantitative retinal traits with non-normal distributions (all tortuosity measurements and the multifractal dimensions measurements) between the event and no event groups. In this analysis, there were no statistically significant differences between the two groups. In general, individuals who experienced an incident event had lower values for all multifractal dimension traits, but differences were not statistically significant.

Table 6.11 compares means of all quantitative retinal traits (following logarithmic transformation or rank transformation for those variables not normally distributed) between the incident event group and no incident event group. Although the diameter of the arteries and veins represented as CRAE and CRVE, respectively, tended to be lower in the group with incident events, these differences were not statistically significant. There were no further significant differences detected.

Retinal trait	Incident event (Max n=200)	No incident event (Max n=828)	p value
Arteriolar tortuosity†			
mean	4.0 (0.2, 600)	4.0 (1.0, 0.300)	0.21
minimum	0.4 (0.0, 0.20)	0.4 (0.0, 0.60)	0.77
maximum	20 (0.8, 500)	20 (0.7, 2000)	0.62
Venular tortuosity†			
mean	5.0 (0.3, 200)	5.0 (0.3, 400)	0.70
minimum	0.7 (0.01, 40)	0.7 (0.0, 200)	0.49
maximum	20 (1.0, 600)	20 (2.0, 1000)	0.58
Multifractal dimensions			
D0	1.75 (1.55, 1.87)	1.77 (1.48, 1.87)	0.05
D1	1.75 (1.54, 1.86)	1.76 (1.48, 1.87)	0.06
D2	1.74 (1.53, 1.85)	1.75 (1.47, 1.85)	0.06

Table 6.10. Median (IQR) retinal trait values in ET2DS participants with and without an incident cardiovascular event during follow up. Traits presented are those which were non-normally distributed. †Values multiplied x 10_{-5}. Data are median (lower IQR, upper IQR). P values calculated using Kruskal-Wallis test.

Retinal trait	Incident event (max n=200)	No incident event (max n=828)	p value
Arteriovenous ratio	0.74 (0.7)	0.74 (0.8)	0.34
Central retinal arteriolar equivalent	32.67 (3.7)	33.11 (3.9)	0.14
Central retinal venular equivalent	44.46 (4.9)	44.72 (5.0)	0.50
Arteriolar tortuosity			
Mean	-10.01 (1.2)	-10.09 (1.1)	0.40
Minimum	-12.31 (1.6)	-12.32 (1.5)	0.92
Maximum	-8.47(1.2)	-8.52 (1.1)	0.55
Venular tortuosity			
Mean	-9.92 (1.0)	-9.97 (0.9)	0.55
Minimum	-11.98(1.3)	-11.9(1.3)	0.47
Maximum	-8.48 (1.1)	-8.47(0.9)	0.96
Multifractal dimensions			
D0	1.74 (0.06)	1.75 (0.07)	0.08
D1	1.73 (0.06)	1.74 (0.07)	0.09
D2	1.72 (0.06)	1.73 (0.07)	0.09

Table 6.11. Mean (SD) retinal trait values in ET2DS participants with and without an incident cardiovascular event during follow up. Data are mean (SD). Values for arteriolar and venular tortuosity were normalised using logarithmic transformation. Rank transformation was used to normalise the data of the multifractal dimension variables.

6.2.4 Multivariable relationship between retinal traits and incident cardiovascular events - cox regression analyses

In order to explore further the relationship between quantitative retinal traits and incident cardiovascular events after adjusting for a range of traditional cardiovascular risk factors, a series of cox proportional hazards models was used. Three main models were created:

Model A: unadjusted,

Model B: adjusted for age sex,

Model C: adjusted for sex, age and traditional cardiovascular risk factors including systolic BP, duration of diabetes, $Hb1_{Ac}$, total cholesterol and smoking status.

If in any of these model a statistically significance association was found, two additional models were used to further the analysis. These models were:

Model D: adjusted for all variables included in Model C plus estimated glomerular filtration rate as a measure of renal function

Model E: adjusted for all variables included in Model D plus prevalent cardiovascular events

By adjusting for these risk factors, it is possible to comment on the potential to use quantitative retinal traits over and above these risk factors in cardiovascular risk prediction. The cox models were used to explore associations of the baseline retinal traits with 'any' cardiovascular events and with incident coronary disease (fatal and non-fatal) and cerebrovascular disease (fatal and non-fatal ischaemic or haemorrhagic stroke) separately. Fatal events were not analysed separately as the number of such events was small.

Results of the cox regression analyses are presented from table 6.12 to table 6.16. None of the models using all incident cardiovascular events as an outcome showed any statistically significant results for any of the retinal traits. The same was found for models using coronary artery disease as the outcome. However, when cerebrovascular disease was considered as a separate outcome, mean arteriolar

tortuosity and minimum arteriolar tortuosity were found to be predictive. In unadjusted models, for 1 SD increase in the mean arteriolar tortuosity there was a 1.26 fold increase in cerebrovascular disease, while for 1 SD increase in the minimum arteriolar tortuosity there was a 1.18 fold increase in cerebrovascular disease.

Adjustment for sex and age resulted in the association between cerebrovascular events and mean arteriolar tortuosity maintaining statistical significance. This association also survived further adjustment for traditional cardiovascular risk factors (Model C, HR; 1.26, 95% CI 1.01, 1.58) and for renal function (model D, HR; 1.26, 95% CI 1.01, 1.58), as well as full adjustment including prevalent cardiovascular disease in the final model (Model E, HR; 1.26, 95% CI 1.01, 1.58). The association of minimum arteriolar tortuosity with cerebrovascular events survived adjustment for age and sex (Model B, HR; 1.18, 95% CI 1.00, 1.40) and only just lost statistical significance after further adjustment for traditional cardiovascular risk factors (Model C, HR; 1.18, 95% CI 0.99, 1.40), renal function (model D, HR; 1.18 95% CI 0.99, 1.40) and prevalent cardiovascular disease (Model E, HR; 1.18, 95% CI 0.99, 1.39). No significant results were seen for the association between cerebrovascular events and maximum arteriolar tortuosity.

Based on further recommendations, significant models were analysed adding diabetic retinopathy. Fully adjusted model included additional binary covariate of diabetic retinopathy (e.g. absence/present diabetic retinopathy). The results for mean arteriolar tortuosity remained significant (HR 1.26; 95% CI 1.003, 1.58; p=0.047). In this model, using the binary model for diabetic retinopathy, the presence of diabetic retinopathy increased 12% risk of cerebrovascular event (HR 1.12; 95% CI 0.64, 1.96; p=0.68)

Multifractal dimensions also showed interesting results in the unadjusted and adjusted models when cerebrovascular disease was considered as a separate outcome. The results presented in table 6.15 were obtained from the rank transformed multifractal dimensions D0, D1 and D2. In the unadjusted model, for 1 SD increase in multifractal dimensions D0, there was a 0.01 fold decrease in cerebrovascular disease (HR 0.01; 95% CI 0.0001, 0.39; p= 0.01). This survived further adjustments. Full adjustment (Model E) resulted in a (HR 0.01; 95% CI

0.0002; *p*=0.49). Unsurprisingly, given the high correlation among the multifractal dimensions traits, the results obtained for multifractal dimensions D1 and multifractal dimensions D2 were very similar.

In regression analysis, different units and different scales are often used. This may cause difficulty in interpreting the results and comparison across findings, particularly for traits such as multifractal dimensions, a novel biomarker which is poorly understood and for which results from previous studies are contradictory (Liew, 2011). The results of standardised analyses are therefore presented in table 6.16 for this trait. In the unadjusted model, for 1 SD increase in multifractal dimensions D0, there was a 0.73 fold decrease in cerebrovascular disease (HR 0.73; 95%CI 0.57, 0.94; *p*<0.05). This survived further adjustments and full adjustment (model E) resulted in a (HR 0.73; 95% CI 0.56, 0.9., *p*<0.05). Again, corresponding significant results were seen in all models for multifractal dimensions D1 and D2, consistent with the high correlation among the multifractal dimensions traits.

Further analyses shown that the presence of absence of diabetic retinopathy did not modify the results for standarised multifractal dimensions D0 which remained significant in the fully adjusted model (HR 0.73; 95% CI 0.56, 0.94; *p*=0.017). In this model, the presence of diabetic retinopathy increased 16% risk of cerebrovascular event (HR 1.16; 95% CI 0.66, 2.03; *p*=0.60).

These results should be considered with caution. This is because a larger number of early progression (e.g. mild non-proliferative diabetic retinopathy) cases of diabetic retinopathy were available in the dataset and thus were included as covariate. As mentioned previously, in the ET2DS, there were few severe cases with non-proliferative DR and proliferative DR and this may lead to a bias in the results shown.

		Arteriovenous ratio			CRAE			CRVE		
	Max events	HR	95%CI	p-value	HR	95%CI	p-value	HR	95%CI	p-value
Any CV event	200									
Model A		0.39	0.07-2.32	0.30	0.97	0.94-1.01	0.15	0.99	0.96-1.01	0.56
Model B		0.38	0.07-2.22	0.29	0.98	0.94-1.01	0.34	0.99	0.97-1.02	0.92
Model C		0.57	0.10-3.34	0.54	0.98	0.94-1.01	0.32	0.99	0.96-1.02	0.56
Coronary events	139									
Model A		0.42	0.05-3.59	0.43	0.97	0.93-1.02	0.32	0.99	0.96-1.02	0.68
Model B		0.41	0.05-3.33	0.41	0.98	0.94-1.03	0.53	1.00	0.96-1.03	0.99
Model C		0.73	0.08-5.81	0.74	0.98	0.94-1.02	0.45	0.98	0.95-1.02	0.50
Cerebrovascular events	61									
Model A		0.32	0.01-8.19	0.492	0.96	0.90-1.03	0.28	0.98	0.94-1.03	0.67
Model B		0.33	0.01-8.11	0.501	0.97	0.91-1.04	0.42	0.99	0.94-1.04	0.88
Model C		0.34	0.14-8.83	0.522	0.97	0.91-1.04	0.49	0.99	0.95-1.05	0.95

Table 6.12 Association of arteriovenous ratio, CRAE and CRVE with incident cardiovascular events in Cox regression analysis. CRAE, central retinal arteriolar equivalent; CRVE, central retinal venular equivalent. Model A: unadjusted. Model B: adjusted for sex and age. Model C: adjusted for sex, age, duration of diabetes, systolic blood pressure, glycated haemoglobin, total cholesterol, high-density lipoprotein cholesterol and smoking.

		Mean arteriolar tortuosity			Minimum arteriolar tortuosity			Maximum arteriolar tortuosity		
	Max events	HR	95%CI	p-value	HR	95%CI	p-value	HR	95%CI	p-value
Any CV event	200									
Model A		1.05	0.93-1.18	0.42	0.99	0.91-1.09	0.96	1.03	0.91-1.17	0.54
Model B		1.05	0.93-1.19	0.39	1.00	0.91-1.09	0.99	1.04	0.92-1.18	0.46
Model C		1.05	0.92-1.19	0.44	0.99	0.90-1.09	0.94	1.05	0.92-1.19	0.45
Coronary events	139									
Model A		0.96	0.83-1.12	0.67	0.92	0.83-1.03	0.16	0.97	0.83-1.12	0.71
Model B		0.97	0.83-1.12	0.71	0.92	0.83-1.03	0.18	0.98	0.84-1.14	0.79
Model C		0.96	0.83-1.12	0.67	0.92	0.82-1.03	0.17	0.97	0.83-1.11	0.75
Cerebrovascular events	61									
Model A		1.26	1.02-1.57	**0.03**	1.18	1.00-1.39	**0.04**	1.20	0.97-1.50	0.10
Model B		1.27	1.02-1.58	**0.03**	1.18	1.00-1.40	**0.04**	1.21	0.97-1.51	0.09
Model C		1.26	1.01-1.58	**0.04**	1.18	0.99-1.40	0.05	1.23	0.98-1.56	0.07
Model D		1.26	1.01-1.58	**0.04**	1.18	0.99-1.40	0.05	1.22	0.97-1.54	0.08
Model E		1.26	1.01-1.58	**0.04**	1.18	0.99-1.39	0.05	1.22	0.98-1.54	0.07

Table 6.13. Association of arteriolar tortuosity traits with incident cardiovascular events in Cox regression analysis. All the tortuosity variables presented are log transformed. Model A: unadjusted. Model B: adjusted for sex and age. Model C: Adjusted for sex, age, duration of diabetes, systolic blood pressure, glycated haemoglobin, total cholesterol, high-density lipoprotein cholesterol and smoking. Model D: Model C plus estimated glomerular filtration rate. Model E: Model D plus prevalent cardiovascular disease at baseline.

		Mean venular tortuosity			Minimum venular tortuosity			Maximum venular tortuosity		
	Max events	HR	95%CI	p-value	HR	95%CI	p-value	HR	95%CI	p-value
Any CV event	200									
Model A		1.05	0.89-1.23	0.53	0.96	0.86-1.07	0.52	0.99	0.86-1.14	0.96
Model B		1.04	0.89-1.22	0.55	0.96	0.86-1.07	0.52	1.00	086-1.15	0.98
Model C		1.03	0.87-1.21	0.69	0.97	0.86-1.09	0.62	1.02	0.88-1.17	0.78
Coronary events	139									
Model A		0.96	0.79-1.16	0.72	0.97	0.85-1.11	0.69	0.98	0.82-1.16	0.81
Model B		0.96	0.79-1.16	0.71	0.97	0.85-1.11	0.70	0.98	0.83-1.16	0.85
Model C		0.94	0.77-1.15	0.57	0.97	0.85-1.12	0.73	1.00	0.83-1.19	0.99
Cerebrovascular events	61									
Model A		1.26	0.96-1.66	0.09	0.94	0.77-1.15	0.57	1.03	0.80-1.33	0.78
Model B		1.25	0.95-1.65	0.10	0.94	0.77-1.15	0.57	1.03	0.80-1.34	0.76
Model C		1.23	0.93-1.63	0.13	0.96	0.78-1.17	0.70	1.05	0.82-1.36	0.65

Table 6.14 Association of venous tortuosity traits with incident cardiovascular events in Cox regression analysis. All the tortuosity variables presented are log transformed. Model A: unadjusted. Model B: adjusted for sex and age. Model C: Adjusted for sex, age, duration of diabetes, systolic blood pressure, glycated haemoglobin, total cholesterol, high-density lipoprotein cholesterol and smoking.

		Multifractal dimension D0			Multifractal dimension D1			Multifractal dimension D2		
	Max events	HR	95%CI	p-value	HR	95%CI	p-value	HR	95%CI	p-value
Any CV event	198									
Model A		0.18	0.02-1.33	0.09	0.19	0.02-1.4	0.10	0.19	0.02-1.41	0.10
Model B		0.22	0.03-1.65	0.14	0.23	0.03-1.74	0.15	0.23	0.03-1.74	0.15
Model C		0.28	0.36-2.23	0.28	0.30	0.03-2.41	0.26	0.30	0.03-2.41	0.26
Coronary events	137									
Model A		0.66	0.06-7.14	0.73	0.68	0.06-7.41	0.75	0.68	0.06-7.41	0.75
Model B		0.82	0.07-8.88	0.87	0.84	0.07-9.22	0.88	0.84	0.07-9.22	0.88
Model C		0.97	0.08-11.87	0.98	1.02	0.08-12.65	0.98	1.02	0.08-12.65	0.98
Cerebrovascular events	61									
Model A		0.01	0.0001 -0.39	**0.01**	0.01	0.0001 - 0.44	**0.02**	0.01	0.0001 –0.46	**0.01**
Model B		0.01	0.0001 - 0.48	**0.02**	0.01	0.0001 - 0.54	**0.02**	0.01	0.0001 –0.56	**0.02**
Model C		0.02	0.0001- 0.82	**0.04**	0.02	0.0001- 0.92	**0.04**	0.02	0.0001-0.95	**0.05**
Model D		0.01	0.001 - 0.54	**0.02**	0.01	0.0001 - 0.60	**0.03**	0.01	0.0001 -0.63	**0.03**
Model E		0.01	0.0002- 0.44	**0.02**	0.01	0.0002- 0.49	**0.02**	0.01	0.0002- 0.51	**0.02**

Table 6.15. Association of multifractal dimension traits with incident cardiovascular events in Cox regression analysis. All the multifractal dimensions variables are rank transformed. Model A: unadjusted. Model B: adjusted for sex and age. Model C: Adjusted for sex, age, duration of diabetes, systolic blood pressure, glycated haemoglobin, total cholesterol, high-density lipoprotein cholesterol and smoking. Model D: Model C plus estimated glomerular filtration rate). Model E: Model D plus prevalent cardiovascular disease at baseline.

		Multifractal dimension D0			Multifractal dimension D1			Multifractal dimension D2		
	Max Events	HR	95%CI	p-value	HR	95%CI	p-value	HR	95%CI	p-value
Any CV event	198									
Model A		0.89	0.77-1.02	0.10	0.89	0.77-1.02	0.11	0.89	0.77-1.02	0.11
Model B		0.90	0.78-1.03	0.15	0.90	0.79-1.04	0.16	0.90	0.79-1.04	0.16
Model C		0.91	0.19-1.05	0.24	0.92	0.79-1.06	0.26	0.92	0.79-1.06	0.26
Coronary events (Coronary+ Fatal)	137									
Model A		0.97	0.82-1.14	0.73	0.97	0.82-1.14	0.75	0.97	0.82-1.14	0.74
Model B		0.98	0.83-1.16	0.87	0.98	0.83-1.16	0.88	0.98	0.83-1.16	0.87
Model C		0.99	0.83-1.18	0.98	1.00	0.84-1.19	0.98	1.00	0.84-1.19	0.99
Cerebrovascular events	61									
Model A		0.73	0.57-0.94	**0.01**	0.73	0.57-0.94	**0.01**	0.74	0.57-0.95	**0.01**
Model B		0.74	0.57-0.95	**0.02**	0.74	0.58-0.96	**0.02**	0.75	0.58-0.96	**0.02**
Model C		0.76	0.59-0.98	**0.04**	0.77	0.60-0.99	**0.04**	0.77	0.60-0.99	**0.04**
Model D		0.74	0.57-0.95	**0.02**	0.74	0.58-0.96	**0.02**	0.75	0.58-0.96	**0.02**
Model E		0.73	0.56-0.94	**0.02**	0.73	0.56-0.95	**0.02**	0.73	0.57-0.95	**0.02**

Table 6.16. Association of multifractal dimension traits with incident cardiovascular events in Cox regression analysis with standardised coefficients. Model A: unadjusted. Model B: adjusted for sex and age. Model C: Adjusted for sex, age, duration of diabetes, systolic blood pressure, glycated haemoglobin, total cholesterol, high-density lipoprotein cholesterol and smoking. Model D: Model C plus estimated glomerular filtration rate). Model E: Model D plus prevalent cardiovascular disease at baseline

6.3 ROC curve analysis

The association of mean arteriolar tortuosity and multifractal dimensions D0, D1 and D2 with incident cerebrovascular events survived adjustment for traditional cardiovascular risk factors and prevalent cardiovascular disease. The results of further survival analyses for both of these traits is described in this section. The Cox regression analysis provided predicted risk (X beta) values which are necessary to create ROC curves. Area under the curve (AUC) was compared for the model containing traditional risk factors alone and the model containing both traditional risk factors (sex, age, duration of diabetes, Hb1Ac, total cholesterol, HDL and smoking) and the mean arteriolar tortuosity (Figure 6.1). The area under the curve for the model containing only traditional risk factors was found to be 0.661 (95%CI 0.592, 0.730). Adding the mean of arteriolar tortuosity to the model, there was a small improvement in AUC to 0.677 (95% 0.608, 0.746) (table 6.17). This suggests that the mean arteriolar tortuosity may contribute additional, although modest, information to current risk classifications models of cerebrovascular disease.

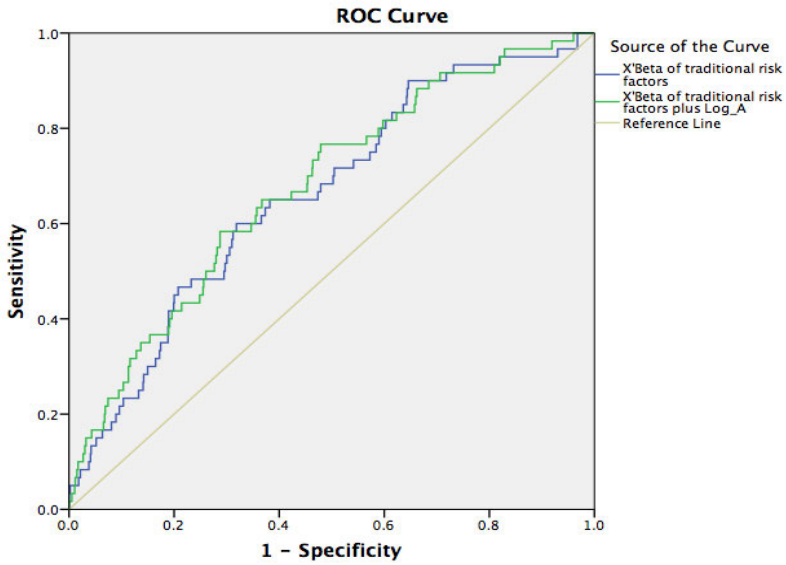

Figure 6.1 ROC curves of predicted risk of cerebrovascular events in a model containing traditional cardiovascular risk factors and model containing the mean arteriolar tortuosity and traditional risk factors. Mean arteriolar tortuosity was log transformed.

	Area Under the Curve	95% Confidence Interval
Model 1: Traditional risk factors	0.661	0.592-0.730
Model 2: Traditional risk factors + arteriolar tortuosity	0.677	0.608-0.746

Table 6.17 Area under the curve models containing traditional risk factors (model 1) and the mean of arteriolar tortuosity and traditional risk factors (model 2). Mean arteriolar tortuosity was log transformed.

For multifractal dimensions, cox regression analysis was again used to provide predicted risk (X beta) values. Area under the curve (AUC) was compared for the model containing traditional cardiovascular risk factors alone and the model containing both traditional risk factors and multifractal dimension D0 (Figure 6.2). The area under the curve for the model containing only traditional risk factors was found to be 0.662 (95%CI 0.592, 0.731). Adding multifractal dimensions D0 to the model, there was a small improvement in AUC to 0.684 (95% 0.618, 0.750) (table 6.18). This suggests that multifractal dimension D0 may contribute additional, albeit modest, information to current risk classifications models of cerebrovascular disease.

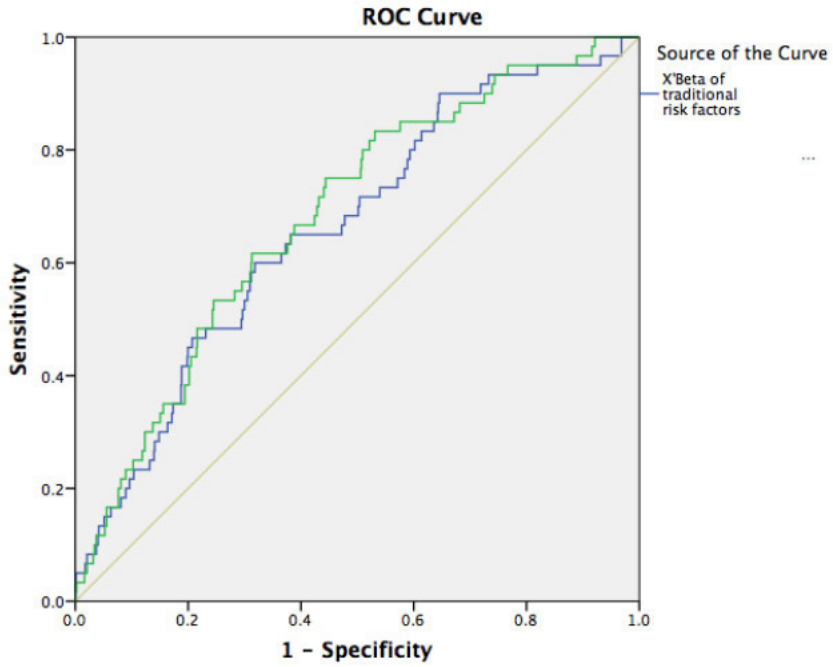

Figure 6.2 ROC curves of predicted risk of cerebrovascular events in a model containing traditional cardiovascular risk factors and model containing multifractal dimensions and traditional risk factors.

	Area Under the Curve	95% Confidence Interval
Model 1: Traditional risk factors	0.662	0.592-0.731
Model 2 Traditional risk factors + multifractal dimensions	0.684	0.618-0.750

Table 6.18 Area under the curve models containing traditional risk factors (model 1) and traditional risk factors plus standardised multifractal dimensions (model 2).

6.4 Chapter Summary

This chapter explored the relationship between quantitative retinal traits and incident cardiovascular disease in older adults with type 2 diabetes. Incident cardiovascular events in this study population were associated with male sex, increased age, longer duration of diabetes, increased HbA_{1c}, lower HDL cholesterol and reduced eGFR. Furthermore, there were associations with insulin ± hypoglycaemic usage, use of anti-hypertensives, previous history of cardiovascular disease and history of diabetic retinopathy.

In unadjusted and fully adjusted Cox regression models for cardiovascular disease, mean arteriolar tortuosity and minimum arteriolar tortuosity were associated with incident cerebrovascular events. Associations with these quantitative retinal traits survived adjustment for traditional cardiovascular risk factors and full adjustment. These retinal traits were not predictive for 'all' cardiovascular disease or for coronary events.

Finally, multifractal dimensions D0, D1 and D2 were associated with incident cerebrovascular events in unadjusted and fully adjusted models. This shows that the changes in the retinal vasculature branching (sparser branching pattern) may play a role in predicting and/or developing cerebrovascular disease. Further research into the role of these microvasculature findings in maintaining healthy vascular systems may provide novel understating of cerebrovascular pathophysiology, which is explored in the following chapter.

Chapter 7 Results III: Genome wide association of quantitative retinal traits

7.1 Introduction

Genome wide association studies (GWAS) are experimental designs to identify associations between genetic variants (loci) and traits (e.g. hypertension, diabetes, cholesterol) in populations. Visscher et al (2017) write that the main purpose of these studies is to better understand the biology of disease, under the assumption that this improved understanding will lead to prevention or better medical management. However, results obtained from GWAS must be interpreted with caution, because the pathway from the results of GWAS to biology may not be a straightforward association between a single genetic variant at a given genomic locus, and a trait is not directly informative with respect to the target gene (Visscher et al, 2017)

The following considerations were taken into account when interpreting the results presented in this chapter, (a) how many variants affecting the trait segregated in the ET2DS population, (b) the joint distribution of effect size and allele frequency at those variants (sometimes called genetic architecture), (c) the sample size analysed, (d) the number of genome-wide variants that were used in the experiment, and (e) how heterogeneous the trait or disease being studied was. The last consideration relates to both the biology of the trait and the ability to diagnose or measure it with precision, relevant to quantitative traits such as the retinal traits under investigation (Visscher et al, 2017).

Previous GWAS of quantitative retinal traits have focused mainly on arteriolar and venular widths including the dimensionless arteriovenous ratio. In this chapter, I describe the results of genome-wide associations for twelve quantitative retinal traits. Directly genotyped data as well as imputed data

were analysed for each retinal trait, with traits transformed to better approximate normal distributions using the methods described in the previous chapter.

7.2 Results

None of the GWAS analyses using the MetaboChip® array showed either significant or suggestive results. A total of 1022 individuals from ET2DS with the aforenmentioned quantitative retinal traits, were included in the GWAS with imputed data. In this chapter, results using the genome-wide imputed data and QQ plots are presented.

Q-Q (quantile-quantile) plots were obtained for each quantitative retinal trait. The Q-Q plot is a graphical representation of the deviation of the observed *P* values from the null hypothesis: this means that the observed *P* values for each SNP are sorted from largest to smallest and plotted against expected values from theoretical X_2 distribution. Ideally, observed values would correspond to the expected values, all points are on or near the middle line between the x-axis and the y-axis. If the results show an early deviation of the line of the expected and the observed values, this means that many moderately significant *P* values are more significant than expected under the null hypothesis (Ehret et al, 2010). In these analyses, the results are likely to be associated to population stratification (e.g. differences of allele frequencies in subpopulations).

7.2.1 GWAS of arteriovenous ratio

The GWAS of arteriovenous ratio (AVR) was performed using the ratio of central arteriolar retinal equivalent to central venular retinal equivalent obtained from measurements in Zone B of the retina. A summary of the most significant SNPs identified is presented in table 7.1. The Manhattan plot for AVR is presented in figure 7.1, the quantile-quantile (Q-Q) plot is presented in the appendix 6, only a modest genomic inflation factor ($\lambda = 0.99$) was observed for AVR. Regional plots are shown in figures 7.2a and 7.2b.

The GWAS of AVR identified several variants, which passed the suggestive significance threshold. This retinal trait showed the greatest number of variants which passed the threshold, had a MAF ≥ 0.05 and were in acceptable linkage disequilibrium (r_2) (table 1). Many of these variants were located at intergenic regions or regulatory regions between the genes.

The most significant variant was rs73198094 (*p* value = 5.27_{-8}), an intergenic variant located at the intergenic region of *ASAH1* and *LOC101929066* genes. The *ASAH1* gene has been associated with atrial fibrillation (*p* value = 5.16 x 10_{-10}) (Christophersen et al, 2017). Additionally, functional analysis on ASAH1 protein located in the lisosomes has shown oxidative stress generates sphingolipid death mediators in retinal cells and that induction of ASAH1 could rescue retinal cells from oxidative stress by hydrolyzing excess ceramides (Sugano et al, 2019). This plays an important role in the development of macular degeneration. Furthermore, rs7841239 (*p* value = $1.50x10_{-07}$) is a variant located in the intronic region *LOC101929066* gene. Although this gene has not been characterised, it plays an important role in the *trans* regulation of RNA.

Another identified intergenic variant, rs58774739, is located between the genes *LOC101929066* and *NAT1*. *NAT1* is involved in the transformation of drugs and environmental toxins. The enzyme encoded by this gene transfers the acetyl group from acetyl-coenzyme A to an amino group to aromatic amines and hydrazine compounds. There are a number of SNPs reported in *NAT1*, which lead to slow, and rapid acetylator phenotypes (Montazeri et al, 2016). The acetylation status of an individual might determine how they respond to xenobiotic exposures, therefore presenting the 2 genes as candidates for gene-environment interaction studies (Potts et al, 2012).

The unique variant, rs7318262, located in an intergenic region of chromosome 7 of the genes *LOC101928257* and *LOC107986796* also passed the suggestive threshold. Although functional characterisation of

these genes has not been performed, their activity remains mainly in RNA translation.

One variant in chromosome 15 passed the GWAS suggestive threshold. The variant, rs11071164, is located in the intronic region of the gene *OTUD7A.* The protein encoded by this gene is a deubiquitinizing enzyme and possible tumour suppressor. In a study carried out by Morrison (Morrison et al 2010) an association of this gene with mortality from heart failure in Europeans was found (*p* value = 1.37×10^{-6}). This gene may play a role in heart failure progression and survival by contributing to inadequate degradation of ubiquitin-protein conjugates resulting in autophagic myocyte death (Morrison et al, 2010).

Finally, 15 of the significant variants identified were located at the intron region of the *ATP11A* gene. The most significant variant was rs1625475. The gene *ATP11A* located at chromosome 13 has been associated in a previous GWAS with red cell distribution width (*p* value = 2.4×10^{-9}) (Pilling et al, 2017). Importantly, this gene has also been associated with the cardiometabolic trait, glycated haemoglobin (Wheeler et al, 2017). In this study, one variant located at the *ATP11A* gene was associated at genome-wide significance (*p* value = 1.70×10^{-12}). The *ATP11A* gene plays an important role in membrane transportation including related pathways such as transportation of glucose, organic acids and ion channel transport.

SNPs	chr	Position	Genomic location	r_2	Gene(s) nearby	Distance	Associated traits	A1/A2	MAF	β (SE)	*p*-value
rs73198094	8	17955528	intergenic variant	0.32	*ASAH1* *LOC101929066*	13Kb 2.0Kb	Atrial f brillation	T/A	0.05	0.064 (0.011)	5.27E-08
rs67164521	8	17962827	Intergenic variant	0.32	*ASAH1* *LOC101929066*	20Kb 10Kb	Atrial f brillation	T/C	0.06	0.055 (0.010)	1.79E-07
rs73200265	8	17969414	Intergenic variant	0.32	*ASAH1* *LOC101929066*	20Kb 9Kb	Atrial f brillation	G/A	0.05	0.055 (0.0107)	2.04E-07
rs7844251	8	17964559	Intergenic variant	0.32	*ASAH1* *LOC101929066*	13Kb 2.0Kb	Atrial f brillation	G/A	0.05	0.056 (0.011)	2.78E-07
rs73200259	8	17961874	Regulatory region variant	0.32	*ASAH1* *LOC101929066*	20Kb 9Kb	Atrial f brillation	A/G	0.06	0.054 (0.010)	2.88E-07
rs6999324	8	17961354	Regulatory region variant	0.32	*ASAH1* *LOC101929066*	19Kb 8Kb	Atrial f brillation	G/C	0.05	0.055 (0.010)	3.38E-07
rs56946363	8	17995722	Regulatory region variant	0.32	*ASAH1 NAT1* *LOC101929066*	42Kb 32Kb	Atrial f brillation	C/A	0.05	0.058 (0.011)	3.92E-07
rs7825369	8	17958628	Downstream gene variant 3'	0.32	*ASAH1* *LOC101929066*	16Kb 5Kb	Atrial f brillation	A/G	0.06	0.055 (0.010)	3.99E-07
rs58336491	8	17968887	Intergenic variant	0.32	*ASAH1* *LOC101929066*	27Kb 16Kb	Atrial f brillation	A/G	0.05	0.054 (0.010)	4.08E-07
rs112427012	8	17959845	Intergenic variant	0.32	*ASAH1* *LOC101929066*	18Kb 6Kb	Atrial f brillation	A/G	0.05	0.056 (0.011)	4.59E-07
rs76981859	8	17960062	Intergenic variant	0.32	*ASAH1* *LOC101929066*	18Kb 7Kb	Atrial f brillation	T/C	0.05	0.058 (0.012)	2.17E-06
rs7841239	8	17950857	Intron variant	0.36	*LOC101929066*	No, variant is within gene	Unknown	C/T	0.05	0.064 (0.012)	1.50E-07
rs11986482	8	17951763	intron variant	0.36	*LOC101929066*	-	Unknown	A/G	0.06	0.065 (0.012)	1.61E-0.7
rs58774739	8	17973053	Intergenic variant (forward strand)	0.36	*LOC101929066* *NAT1*	19Kb 55Kb	Drug metabolism	G/C	0.05	0.054 (0.010)	2.51E-07

Table 7.1. Results of GWAS of arteriovenous ratio. Results shown for p-values ≤1.00 x 10^{-6} and MAF ≥0.05. SNP, single nucleotide polymorphism; chr, chromosome; bp, position; r_2; A1, reference allele; A2, effect allele; MAF, minor allele frequency; SE, standard error. r2 is the linkage disequilibrium between the SNPs in the first column such that the first SNP relates to the second SNP and so on, in ascending order.

SNPs	chr	Position	Genomic location	r_2	Gene(s) nearby	Distance	Associated traits	A1/A2	MAF	β(SE)	*p*-value
rs2517335	8	17961752	Intergenic variant	0.36	*LOC101929066 ASAH1*	2kb 4Kb	Atrial f brillation	C/G	0.06	0.054 (0.010)	2.85E-07
rs17126214	8	17948804	Intron variant	0.36	*LOC101929066*	-	Unknown	A/G	0.06	0.060 (0.012)	2.26E-06
rs56688207	8	17973059	Intergenic variant	0.42	*LOC101929066 ASAH1*	17 Kb 31 Kb	Atrial f brillation	T/G	0.05	0.054 (0.010)	2.51E-07
rs1625475	13	113527111	Intron variant	0.61	*ATP11A*	-	HbA_{1c}/Red cell distribution width	G/T	0.40	-0.018 (0.003)	1.35E-06
rs4907549	13	113520668	Intron variant	0.61	*ATP11A*	-	HbA_{1c} /Red cell distribution width	C/T	0.34	-0.021 (0.004)	4.27E-06
rs945976	13	113523118	Intron variant	0.62	*ATP11A*	-	HbA_{1c} /Red cell distribution width	G/C	0.37	-0.016 (0.003)	4.49E-06
rs1933202	13	113523123	Intron variant	0.62	*ATP11A*	-	HbA_{1c} /Red cell distribution width	A/G	0.38	-0.016 (0.003)	4.49E-06
rs1320525	13	113527967	Synonymous variant	0.64	*ATP11A*	No changes	HbA_{1c} /Red cell distribution width	G/A	0.38	-0.017 (0.003)	2.06E-06
rs9549595	13	113531357	Intron variant	0.64	*ATP11A*	-	HbA_{1c} /Red cell distribution width	A/G	0.38	-0.017 (0.004)	2.38E-06
rs7319456	13	113525619	Intron variant	0.64	*ATP11A*	-	HbA_{1c} /Red cell distribution width	T/C	0.39	-0.017 (0.003)	3.05E-06
rs73118262	7	52667755	Intergenic variant	No, unique variant	*LOC101928257*	170Kb	Unknown	A/G	0.37	0.023 (0.005)	2.84E-06
rs11071164	15	31822531	Intron variant	No, unique variant	*OTUD7A*	-	Heart failure	G/A	0.42	0.020 (0.004)	4.03E-06
rs4907464	13	113525495	Intron variant	0.64	*ATP11A*	-	HbA_{1c} /Red cell distribution width	C/G	0.38	-0.016 (0.003)	3.99E-06
rs869372	13	113525200	Intron variant	0.64	*ATP11A*	-	HbA_{1c} /Red cell distribution width	G/A	0.36	-0.017 (0.003)	4.18E-06

Table 7.1 (cont.) Results of GWAS of arteriovenous ratio. Results shown for p-values ≤1.00 x 10^{-6} and MAF ≥0.05. SNP, single nucleotide polymorphism; chr, chromosome; bp, position; r2; A1, reference allele; A2, effect allele; MAF, minor allele frequency; SE, standard error. r2 is the linkage disequilibrium between the SNPs in the first column such that the first SNP relates to the second SNP and so on, in ascending order.

SNPs	chr	Position	Genomic location	r_2	Gene(s) nearby	Distance	Associated traits	A1/A2	MAF	β (SE)	*p*-value
rs9549593	13	113528499	Intron variant	0.66	*ATP11A*	-	HbA_{1c} /Red cell distribution width	A/C	0.38	-0.017 (0.003)	1.56E-06
rs9549594	13	113528501	Intron variant	0.66	*ATP11A*	-	HbA_{1c} /Red cell distribution width	C/G	0.37	-0.018 (0.003)	1.67E-06
rs4907550	13	113522369	Intron variant	0.66	*ATP11A*	-	HbA_{1c} /Red cell distribution width	G/A	0.37	-0.017 (0.003)	2.33E-06
rs945971	13	113522676	Intron variant	0.66	*ATP11A*	-	HbA_{1c} /Red cell distribution width	G/A	0.37	-0.017 (0.003)	2.34E-06
rs945972	13	113522717	Intron variant	0.66	*ATP11A*	-	HbA_{1c} /Red cell distribution width	C/T	0.38	-0.017 (0.004)	2.34E-06
rs945973	13	113522745	Intron variant	0.66	*ATP11A*	-	HbA_{1c} /Red cell distribution width	G/A	0.37	-0.017 (0.004)	2.34E-06
rs945974	13	113522752	Intron variant	0.66	*ATP11A*	-	HbA_{1c} /Red cell distribution width	G/A	0.38	-0.017 (0.003)	2.34E-06
rs1933201	13	113523066	Intron variant	0.66	*ATP11A*	-	HbA_{1c} /Red cell distribution width	C/T	0.37	-0.016 (0.003)	3.22E-06
rs7321764	13	113520820	Intron variant	0.66	*ATP11A*	-	HbA_{1c} /Red cell distribution width	C/T	0.37	-0.017 (0.003)	3.62E-06
rs7318323	13	113523843	Intron variant	0.66	*ATP11A*	-	HbA_{1c} /Red cell distribution width	C/A	0.37	-0.016 (0.003)	4.49E-06
rs871388	13	113524550	Intron variant	0.66	*ATP11A*	-	HbA_{1c} /Red cell distribution width	A/G	0.38	-0.016 (0.003)	4.74E-06
rs945977	13	113524554	Intron variant	0.69	*ATP11A*	-	HbA_{1c} /Red cell distribution width	T/C	0.38	-0.016 (0.003)	4.77E-06
rs4907552	13	113523990	Intron variant	0.69	*ATP11A*	-	HbA_{1c} /Red cell distribution width	T/C	0.38	-0.016 (0.003)	4.57E-06

Table 7.1 (cont.) Results of GWAS of arteriovenous ratio. Results shown for p-values ≤1.00 x 10_{-6} and MAF ≥0.05. SNP, single nucleotide polymorphism; chr, chromosome; bp, position; r2; A1, reference allele; A2, effect allele; MAF, minor allele frequency; SE, standard error. r2 is the linkage disequilibrium between the SNPs in the first column such that the first SNP relates to the second SNP and so on, in ascending order.

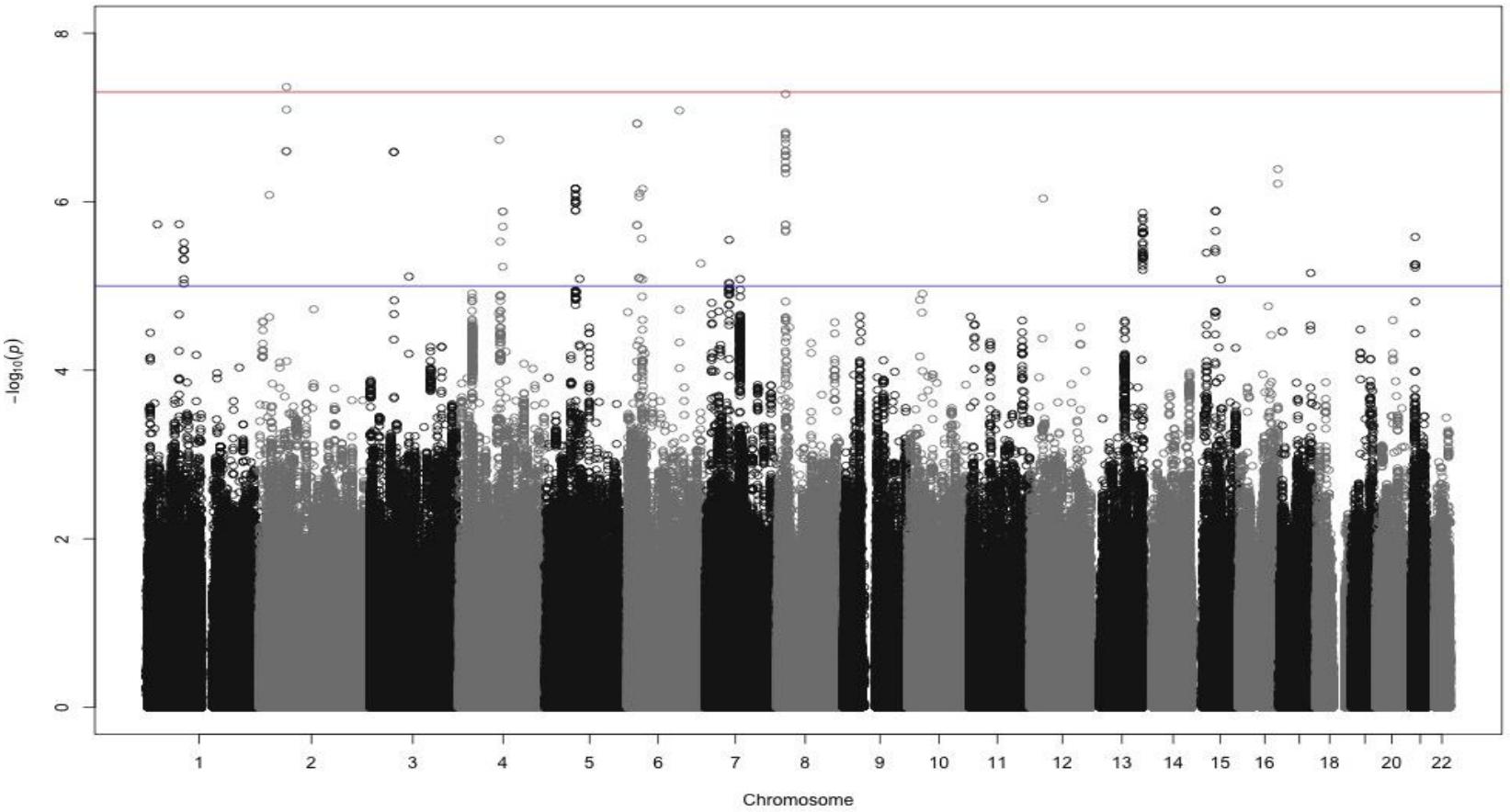

Figure 7.1. Manhattan plot of genome-wide association of arteriovenous ratio (AVR). The plot shows -$\log_{10}$ p values. The blue line corresponds to the suggestive threshold and the red line corresponds to significant GWAS threshold.

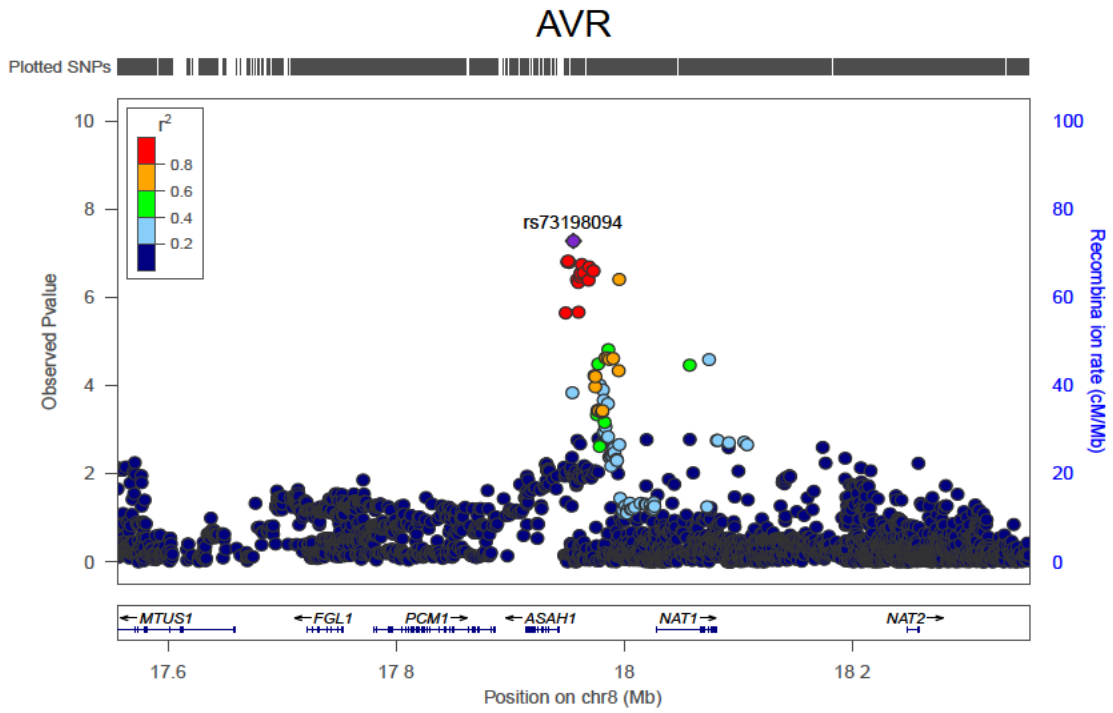

Figure 7.2a. Regional association plot for arteriovenous ratio (AVR). The colour coding of the LD between the SNP ranges from dark blue for r2 = 0-0.2 to red for r2 = 0.8-1.

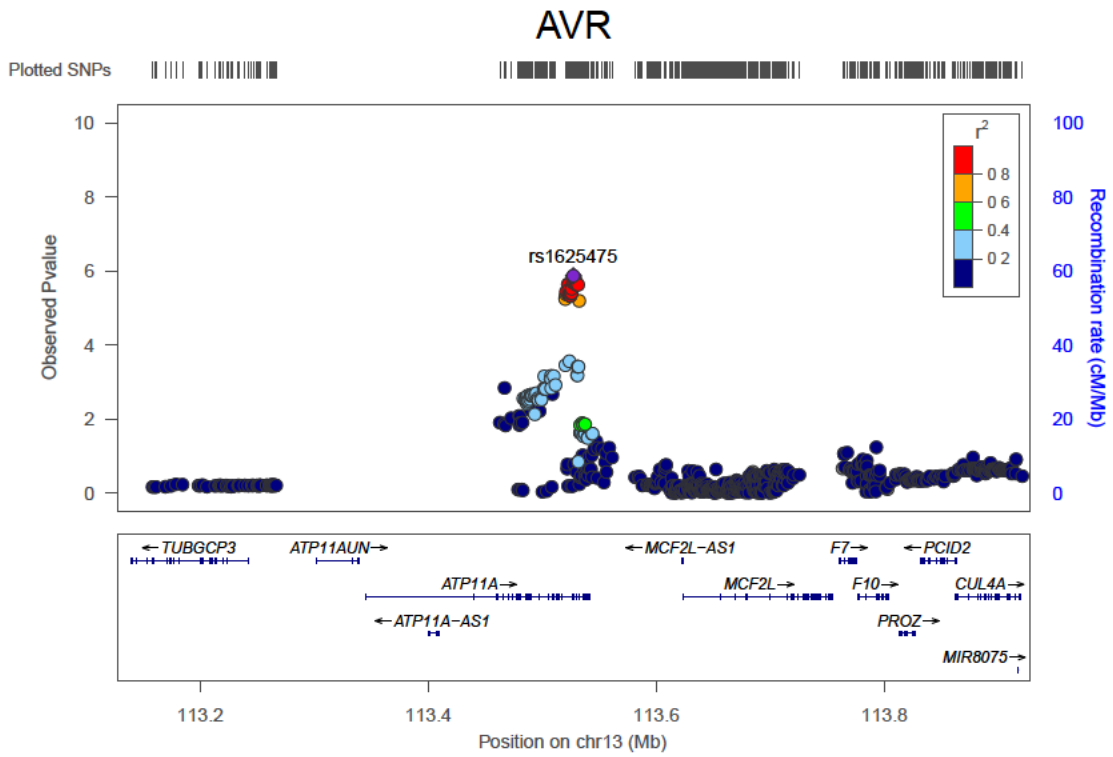

Figure 7.2b. Regional association plot for arteriovenous ratio (AVR). The colour coding of the LD between the SNP ranges from dark blue for r2 =0-0.2 to red for r2 = 0.8-1.

7.2.2 GWAS of Central Retinal Arteriolar Equivalent

I present the results of the GWAS of central retinal arteriolar equivalent (CRAE) in this section. A summary of the most significant SNPs for CRAE is presented in table 7.2 and the Manhattan plot is shown in figure 7.3. A Q-Q plot revealed a genomic inflation factor of 0.99 (QQ plot presented in the Appendix 6). Regional plots are shown in figures 7.4a and 7.4b.

Although none of the SNPs reached a genome-wide level of significance, 14 SNPs reached the suggestive threshold, including nine SNPs at chromosome 11q13.4. The most significant variant, rs4944903 (p = 8.51x10^{-7}) is an intronic variant in the *POLD3* gene. This gene encodes a DNA polymerase delta 3 accessory subunit. Mutations in this gene have been associated with muscular fitness (Willems *et al*, 2017) at genome-wide significance (p = 3.7 x10^{-12}). The remaining eight variants at chromosome 11q13.4 were also located within the intronic region of this gene. These included rs35500564 (p = 1.01 x 10^{-6}), rs35778922 (p = 1.02 x 10^{-6}), rs35167458 (p = 1.14x10^{-6}), rs34450669 (p = 1.73 x 10^{-6}), rs71465929 (p = 1.74 x 10^{-6}), rs67575589 (p = 1.85 x 10^{-6}), rs12807883 (p = 1.95 x 10^{-6}). These eight variants were all in moderate to high linkage disequilibrium (r^2=0.70).

Two variants in chromosome 2 were also identified: rs7579754 and rs7577561. These variants are located in the intergenic region between *LOC101927285*, long intergenic non-protein coding RNA *LINC01122* and *LOC105374754* genes. These SNPs are in weak LD (r^2=0.41) and have previously been associated with body mass index, obesity and adiposity (Zhang *et al*, 2017).

Two additional variants located in chromosome 5q31.1 were identified. These SNPs, rs10061726 (p = 1.76 x 10^{-6}) and rs76882062 (p = 2.42 x 10^{-6}), are located in the intronic region of RNA, long non-coding C5orf66 antisense RNA 2, *C5orf66-AS2* gene. This gene has been associated with intracranial

ruptured aneurysms in expression levels of RNA sequencing (p = 8.4 x 10^{-04}) (Kleinloog et al, 2016).

One variant located at chromosome 6p12.3-p12.2 was also identified. The SNP rs1268651 is an intronic variant in the fibrocystin – polyductin *PKHD1* gene. This gene encodes a transmembrane protein highly expressed in the kidneys. Rare variants in this gene cause autosomal recessive polycystic kidney disease while common variants have been associated with diastolic hypertension at genome-wide significance (p = 7.0 x 10^{-10}) (Warren et al, 2017).

SNP	Chr	bp	Genic location	r_2	Gene(s) nearby	Distance	Associated traits	A1/A2	MAF	ß (SE)	*p*-value
rs7579754	2	59375612	Intergenic	0.41	*LOC101927285 LINC01122*	75Kb 90Kb	Body mass index Obesity Adiposity	A/G	0.39	-0.877 (0.188)	3.43E-06
rs7577561	2	59370001	Intergenic	0.41	*LOC101927285 LINC01122*	75Kb 85kb	Body mass index Obesity Adiposity	A/G	0.38	-0.846 (0.184)	4.66E-06
rs76882062 (rs7709093)	5	*134574307*	Intron	Not available	*C5orf66 AS2*	-	Ruptured aneurysm	G/A	0.24	1.300 (0.275)	2.42E-06
rs10061726	5	*134580808*	Intron	Not available	*C5orf66 AS2*	-	Ruptured aneurysm	A/C	0.19	1.378 (0.2883)	1.76E-06
rs1268651	6	*51784341*	Intron	Unique SNP	*PKHD1*	-	Polycystic kidney disease Diastolic blood pressure	A/C	0.25	1.510 (0.321)	2.67E-06
rs4944903	11	74280336	Intron	0.55	*POLD3*	-	Muscular fitness	C/T	0.05	-2.006 (0.407)	8.51E-07
rs34601749	11	74312788	Intron	0.55	*POLD3*	-	Muscular fitness	C/T	0.05	-2.045 (0.418)	1.03E-06
rs35500564	11	74299279	Intron	0.70	*POLD3*	-	Muscular fitness	G/A	0.05	-2.050 (0.4194)	1.01E-06
rs35778922	11	74308571	Intron	0.70	*POLD3*	-	Muscular fitness	T/G	0.05	-2.056 (0.420)	1.02E-06
rs35167458	11	74296999	Intron	0.70	*POLD3*	-	Muscular fitness	A/C	0.05	-2.044 (0.4202)	1.14E-06
rs34450669	11	74329028	Intron	0.70	*POLD3*	-	Muscular fitness	C/T	0.05	-1.989 (0.4159)	1.73E-06
rs71465929	11	74341712	Intron	0.70	*POLD3*	-	Muscular fitness	G/C	0.05	-1.989 (0.416)	1.74E-06
rs67575589	11	74308218	Intron	0.70	*POLD3*	-	Muscular fitness	C/T	0.05	-2.012 (0.421)	1.85E-06
rs12807883	11	74327992	Intron	0.70	*POLD3*	-	Muscular fitness	A/G	0.05	-1.978 (0.4158)	1.95E-06

Table 7.2. Results of GWAS of central retinal arteriolar equivalent. Results are shown for *p* values ≤ 1.00 x 10^{-6} and MAF ≥ 0.05. Single nucleotide polymorphism (SNP); chromosome (chr); position (bp); correlation coefficients (R_2); reference allele (A1); effect allele (A2); minor allele frequency (MAF); standard error (SE). r2 is the linkage disequil brium between the SNPs in the first column such that the first SNP relates to the second SNP and so on, in ascending order.

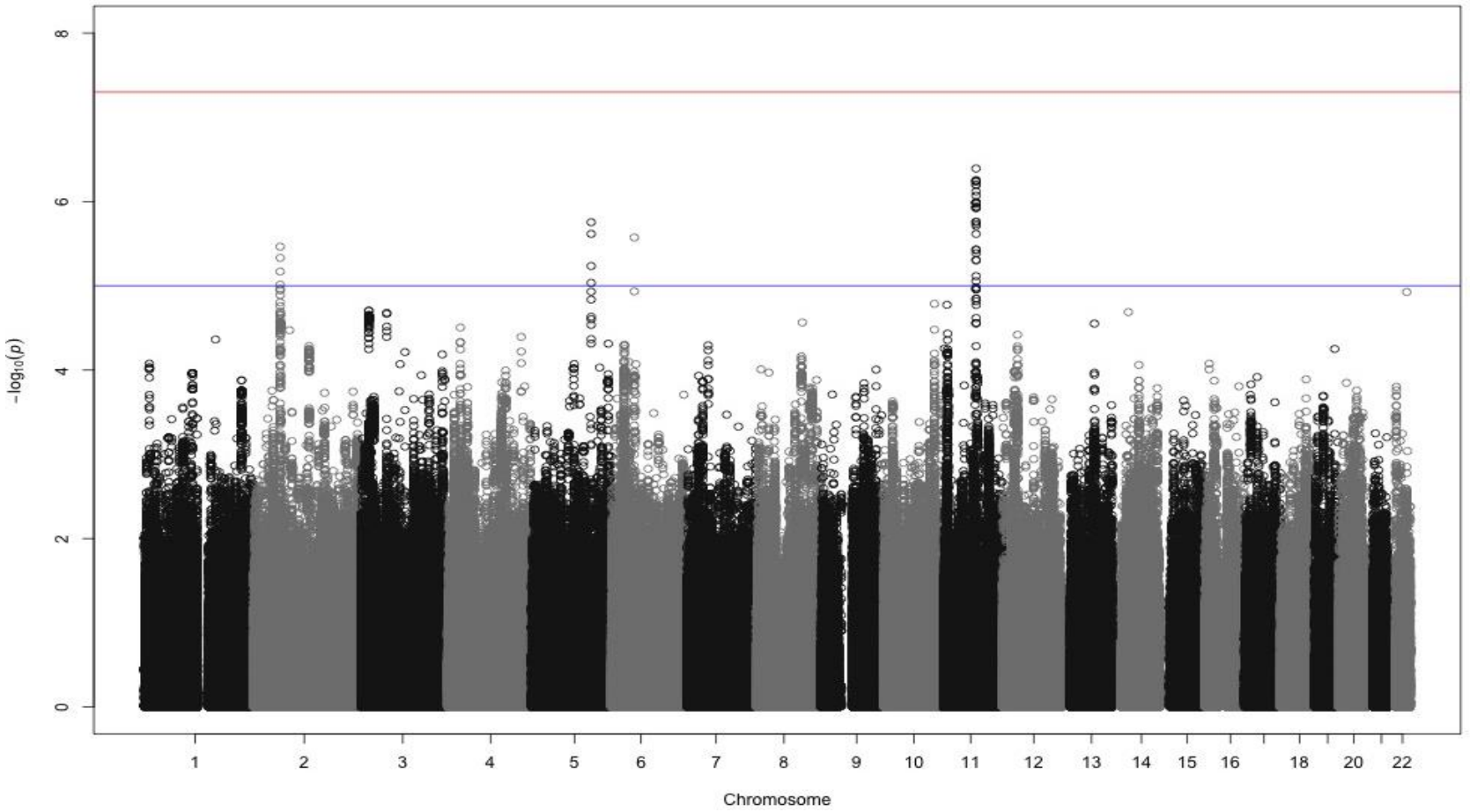

Figure 7.3. Manhattan plot of genome-wide association of central retinal arteriolar equivalent (CRAE). The plot shows -$\log_{10}$ p values. The blue line corresponds to the suggestive threshold and the red line corresponds to significant GWAS threshold.

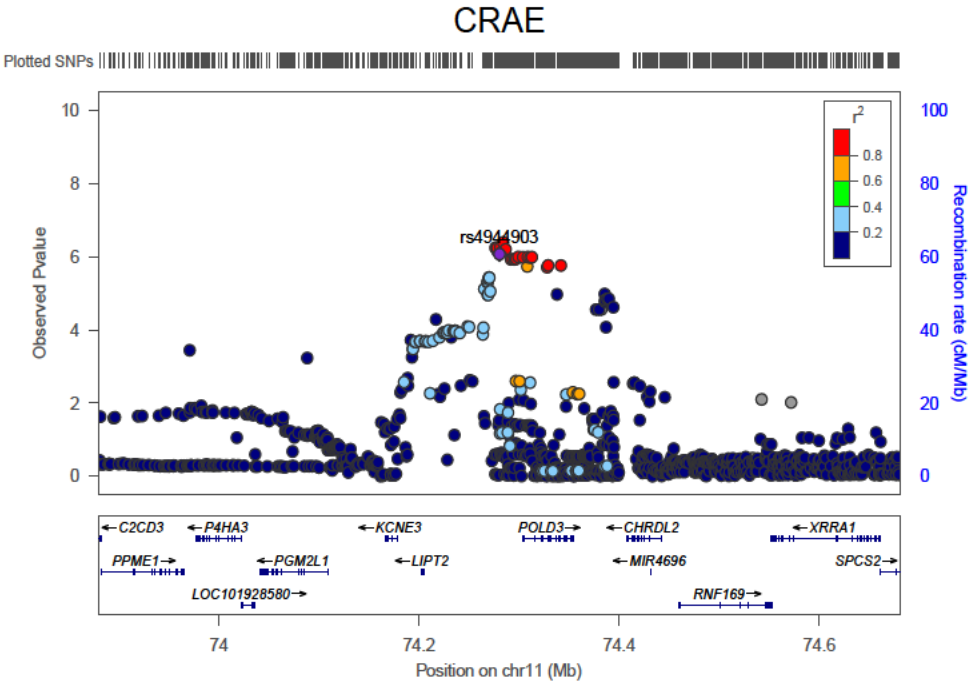

Figure 7.4a. Regional association plot for central retinal arteriolar equivalent (CRAE). The colour coding of LD between the SNP ranges from dark blue (r_2 = 0-0.2) to red (r_2 = 0.8-1).

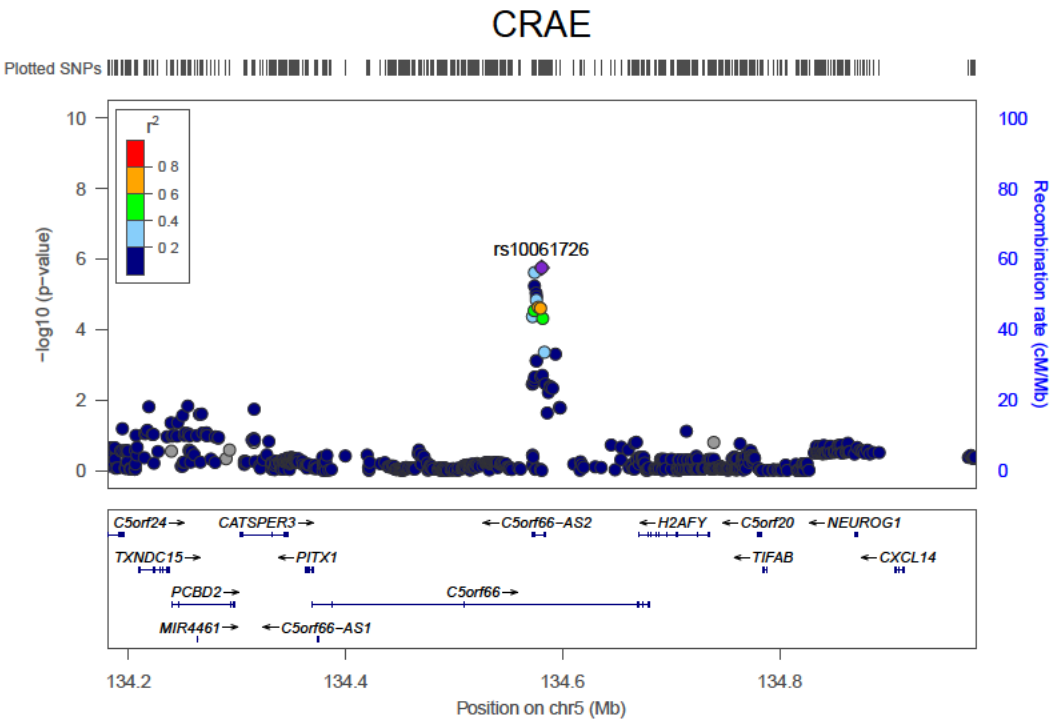

Figure 7.4b. Regional association plot for central retinal arteriolar equivalent (CRAE). The colour coding of the LD between the SNP ranges from dark blue for r_2 = 0-0.2 to red for r_2 = 0.8-1.

7.2.3 GWAS of Central Retinal Venular Equivalent

The Manhattan plot for CRVE is presented in figure 7.5. The genomic inflation factor was modest at 1.02 and the Q-Q plot is presented in the appendix 6. Only one variant reached the suggestive threshold (table 7.3). This variant is located in an intergenic region in chromosome 4. The variant, rs7685417 (p = 2.74 x 10^{-6}) is near to the *LOC105374520*, *GBA3* and *GPR125* genes (Figure 7. 6). The *GB3* gene has been associated with biomarkers related to human metabolism (p = 1.83x10^{-39}) in a recent meta-analysis (Shin et al, 2014).

7.2.4 GWAS of Mean Arteriolar Tortuosity

A summary of the most significant SNPs identified for arteriolar tortuosity is presented in table 7.3, with the Manhattan plot in figure 7.7. A quantile-quantile plot of -log10 (p values) from the GWAS showed a genomic inflation factor of only 0.99. The quantile-quantile plot is presented in the appendix 7.

Nine SNPs showed significant results at the suggestive threshold. These variants are located at 2q36.1. The most significant variant, rs77448408 (p = 1.33 x 10^{-06}) is intergenic between *SLC16A7* (600 Kb downstream) and *FAM19A2* (840 Kb upstream). The latter gene has been associated with insulin sensitivity (p = 1.9 x 10^{-8}) in a study performed in individuals with white ancestry in the United States and Europe (Walford et al, 2016). These genes encode the solute carrier family16 member 7 transporter and the family with sequence similarity 19 member A2, respectively. The locus zoom plot is presented in figure 7.8.

The remaining eight variants were located within the intronic region and the downstream 3' region (Figure 7.9). These included rs62178618 (p = 2.76 x 10^{-6}), rs13386128 (p = 2.78 x 10^{-6}), rs13385757 (p = 3.63 x 10^{-6}), rs17370971 (p = 3.67 x 10^{-6}), rs134333079 (p = 3.72 x 10^{-6}), rs104981110 (p = 3.75 x 10^{-6}), rs16862630 (p = 3.77 x 10^{-6}) and rs4674595 (p = 4.20 x 10^{-6}). These

SNPs are located within the *EPHA4* gene. This gene encodes the ephrin receptor, tyrosine kinase receptor, highly expressed in neurons. There is an association between mutations in *EPHA4* and familial dementia with Lewy bodies as demonstrated in a familial mapping analysis in Belgium (Meeus et al, 2010).

Central Retinal Venular Equivalent

SNPs	Chr	Position	Genomic location	r_2	Gene(s) nearby	Distance	Associated traits	A1/A2	MAF	ß (SE)	*p*-value
rs7685417	4	22603258	Intergenic variant	-	*LOC105374520* *GBA3* *GPR125 (ADGRA3)*	35Kb 90Kb 85Kb	Human metabolites and white matter lesion	G/A	0.07	-3.139 (0.669)	2.74E-06
Mean Arteriolar Tortuosity											
SNPs	**Chr**	**Position**	**Genomic location**	**r_2**	**Gene(s) or nearby**	**Distance**	**Associated traits**	**A1/A2**	**MAF**	**ß (SE)**	***p*-value**
rs62178618	2	222285450	Intron variant	0.81	*EPHA4*	-	Familial dementia	G/A	0.15	-0.547 (0.116)	2.76E-06
rs13386128	2	222285365	Intron variant	0.81	*EPHA4*	-	Familial dementia	G/C	0.15	-0.547 (0.116)	2.78E-06
rs13385757	2	222284992	Intron variant	0.81	*EPHA4*	-	Familial dementia	G/C	0.15	-0.541 (0.116)	3.63E-06
rs17370971	2	222284277	Intron variant	0.81	*EPHA4*	-	Familial dementia	C/T	0.15	-0.542 (0.117)	3.67E-06
rs13433079	2	222284034	Intron variant	0.81	*EPHA4*	-	Familial dementia	G/C	0.15	-0.525 (0.113)	3.72E-06
rs10498110	2	222287869	Intron variant	0.81	*EPHA4*	-	Familial dementia	T/C	0.15	-0.542 (0.117)	3.75E-06
rs16862630	2	222285699	Intron variant	0.81	*EPHA4*	-	Familial dementia	C/T	0.15	-0.542 (0.117)	3.77E-06
rs4674595	2	222280706	Downstream gene variant 3'	0.81	*EPHA4*	-	Familial dementia	C/T	0.15	-0.541 (0.117)	4.20E-06
rs77448408	12	61133476	Intergenic variant	-	*SLC16A7* *FAM19A2*	>100Kb	Insulin sensitivity	C/G	0.07	0.838 (0.173)	1.33E-06

Table 7.3. Results of GWAS of central retinal venular equivalent (CRVE) and mean arteriolar tortuosity. Results are shown for p values ≤ 1.00×10^{-6} and MAF ≥ 0.05. Single nucleotide polymorphism (SNP); chromosome (chr); position (bp); r_2; reference allele (A1); effect allele (A2); minor allele frequency (MAF); standard error (SE). r2 is the linkage disequilibrium between the SNPs in the first column such that the first SNP relates to the second SNP and so on, in ascending order.

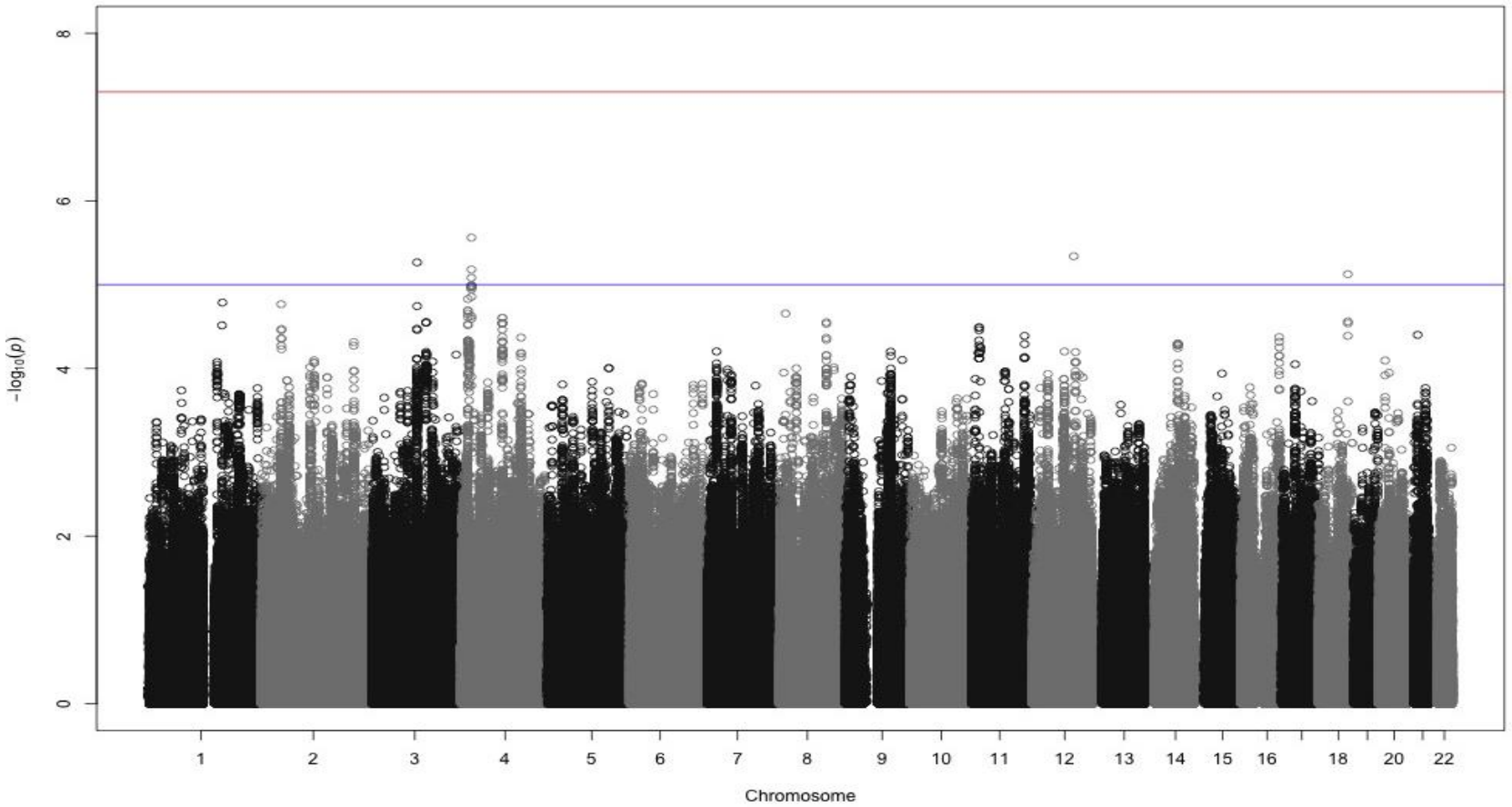

Figure 7.5. Manhattan plot of genome-wide association of central retinal venular equivalent (CRVE). The plot shows -$\log_{10}$ p values. The blue line corresponds to the suggestive threshold and the red line corresponds to significant GWAS threshold.

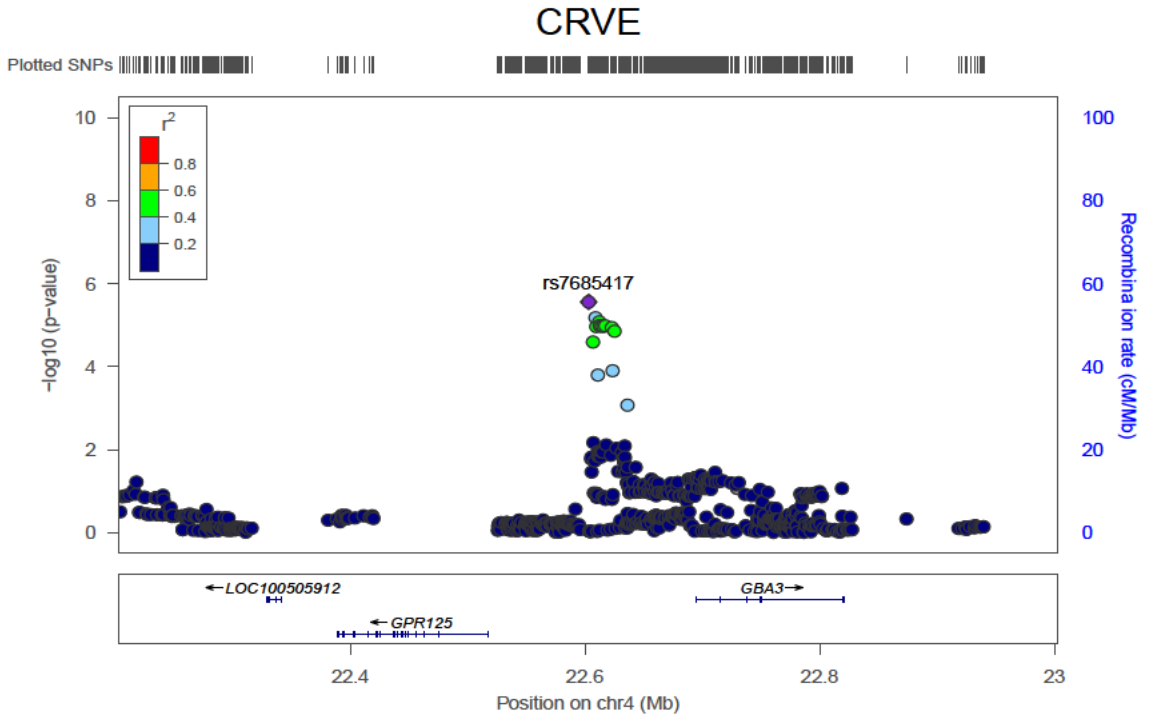

Figure 7.6. Regional association plot for central retinal venular equivalent (CRVE). The colour coding of the LD between the SNP ranges from dark blue for r_2 = 0-0.2 to red for r_2 = 0.8-1.

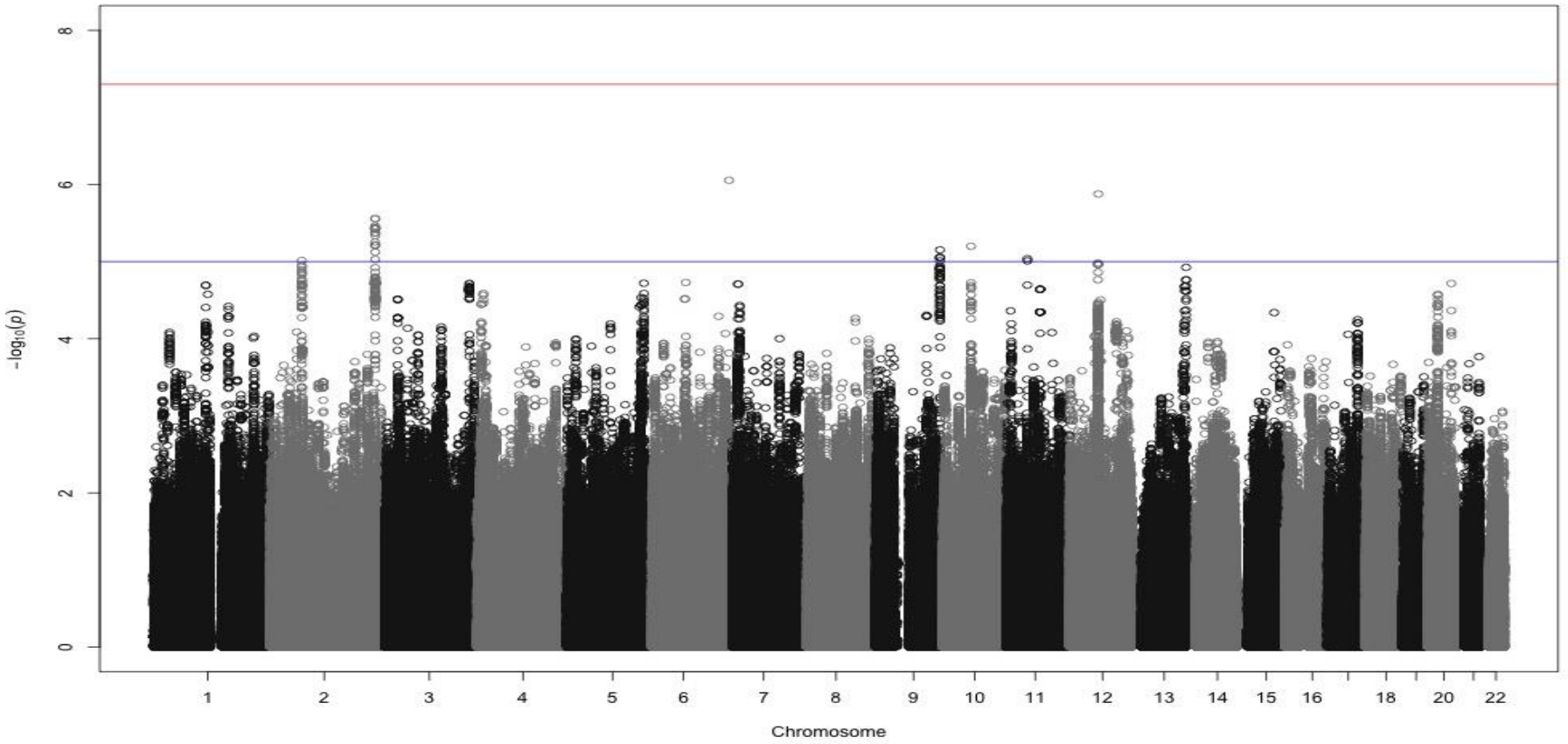

Figure 7.7. Manhattan plot of genome-wide association of mean arteriolar tortuosity. The plot shows -$\log_{10}$ p values. The blue line corresponds to the suggestive threshold and the red line corresponds to significant GWAS threshold.

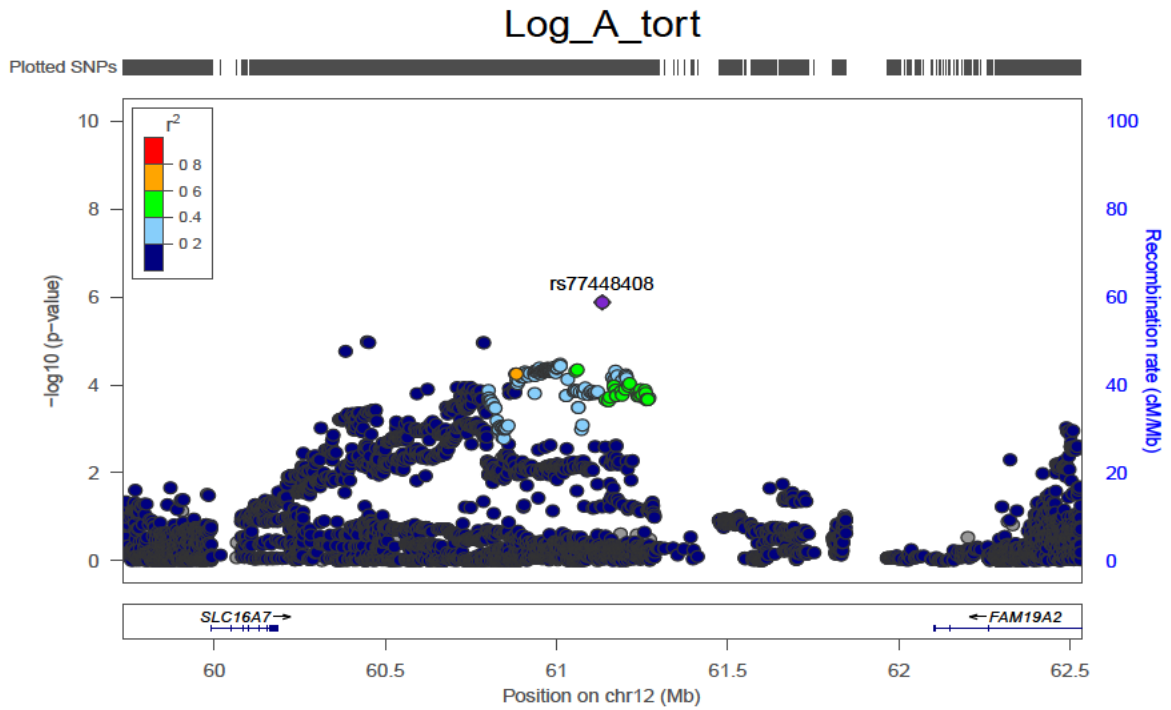

Figure 7.8. Regional association plot for mean arteriolar tortuosity. The colour coding of the LD between the SNP ranges from dark blue for r_2 = 0-0.2 to red for r_2 = 0.8-1.

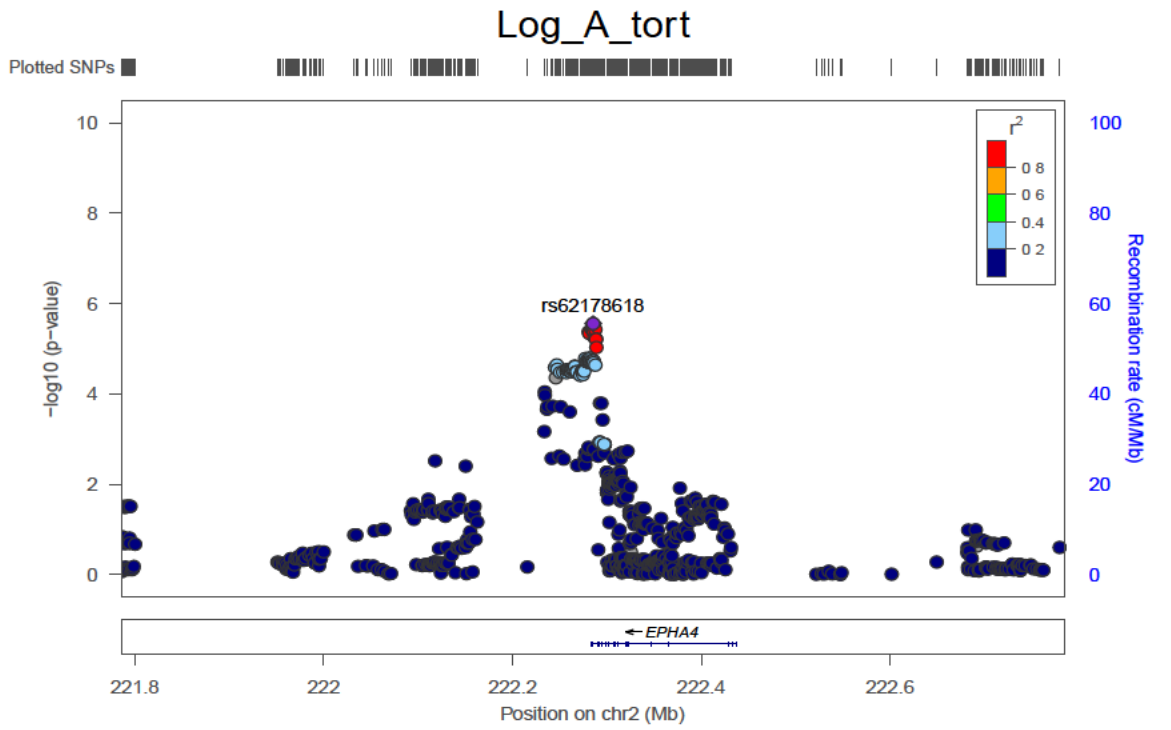

Figure 7.9. Regional association plot for mean arteriolar tortuosity. The colour coding of the LD between the SNP ranges from dark blue for r_2 = 0-0.2 to red for r_2 = 0.8-1.

7.2.5 GWAS of Minimum Arteriolar Tortuosity

A summary of the most significant SNPs in the GWAS of minimum arteriolar tortuosity is presented in table 7.4. The Manhattan plot is shown in figure 7.10. The quantile-quantile plot of from this GWAS revealed a genomic inflation factor of 0.99 (plot presented in appendix 6).

Two different regions, on chromosomes 13q34 and 20p12.3 showed suggestive significance. Three SNPs were located on chromosome 13: rs7991332 (p = 1.54 x 10^{-6}), rs2172724 (p = 2.46 x 10^{-6}) and rs7319323 (p = 3.53 x 10^{-6}). These SNPs showed weak LD (r_2=0.41) and are located in the 5'UTR region (rs7991332) and intron region (rs2172724 and rs7319323) of collagen type IV alpha-2, *COL4A2.* The regional plot for these SNPs is shown in figure 7.11. The *COL4A2* gene has been associated with familial retinal arteriolar tortuosity (Zenteno *et al*, 2014) and lacunar ischaemic stroke at the genome-wide significance level (p = 6.62 x 10^{-8}) (Rannikmäe et al*,* 2017). Another variant, rs7319323, is close to this region located within *COL4A1* gene. This gene has been associated with stroke and small vessel disease (p = 6.9 x 10^{-9}) (Traylor et al, 2016).

The remaining variants were located on chromosome 20 (figure 7.12): 20 SNPs were suggestively significant. Three SNPs were intergenic: rs6053561 (p = 8.87 x 10^{-7}), rs6139776 (p = 2.72 x 10^{-6}) and rs6139777 (p = 2.84 x 10^{-6}). These SNPs showed weak LD (r_2=0.33) and are located between glycerophosphocholine phosphodiesterase 1 (*GPCPD1,* 24Kb upstream) and chromosome 20 open reading frame 196 (*C20orf196,* 66Kb downstream).

The remaining variants were located in the intergenic region between *GPCPD1* and *C20orf196.* These included rs6085232, rsrs665426270, rs6038219, rs6133240 and rs13039871. These SNPs showed LD between r_2=0.54 and r_2=0.58. These SNPs are located within the 5′UTR of *GPCPD1* gene. This gene encodes glycerophosphocholine phosphodiesterase GDE1,

which in humans is highly expressed in the occipital cortex (p = 6.5 x 10^{-09}) (Bakken et al, 2012).

A further eight SNPs reached suggestive significance. Of these, two SNPs were located in the regulatory region: rs2102486 (p = 1.53 x 10^{-6}) and rs2423115 (p = 2.59 x 10^{-6}). These SNPs showed LD (r^2=0.58) and are located between glycerophosphocholine phosphodiesterase 1 (*GPCPD1,* 24 Kb upstream) and chromosome 20 open reading frame 196 (*C20orf196*, 66 Kb downstream).

SNPs	chr	Position	Genomic location	r_2	Gene(s) nearby	Distance	Associated traits	A1/A2	MAF	ß (SE)	*p*-value
rs7991332	13	110959717	5' UTR variant	0.41	*COL4A2*	-	Familial tortuosity, stroke	T/C	0.30	0.372 (0.077)	1.54E-06
rs7319323	13	110955187	Intron variant	0.41	*COL4A1*	-	Stroke, arterial stiffness	T/C	0.29	0.354 (0.076)	3.53E-06
rs2172724	13	110961409	Intron variant	0.45	*COL4A2*	-	Familial tortuosity, stroke	A/G	0.31	0.356 (0.075)	2.46E-06
rs6053561	20	5624890	Intergenic variant	0.33	*GPCPD1* *C20orf196*	24Kb 66Kb	Visual cortical surface	C/T	0.47	0.459 (0.093)	8.87E-07
rs6139776	20	5597276	Intergenic variant	0.33	*GPCPD1*	12Kb	Visual cortical surface	C/A	0.39	0.453 (0.096)	2.72E-06
rs6139777	20	5597386	Intergenic variant	0.33	*GPCPD1*	6Kb	Visual cortical surface	G/A	0.39	0.452 (0.096)	2.84E-06
rs6085227	20	5601882	Intergenic variant	0.43	*GPCPD1*	10Kb	Visual cortical surface	C/T	0.41	0.407 (0.087)	2.88E-06
rs2136583	20	5598672	Intergenic variant	0.44	*GPCPD1*	7Kb	Visual cortical surface	T/A	0.41	0.434 (0.092)	2.40E-06
rs2064715	20	5608955	Intergenic variant	0.47	*GPCPD1*	17Kb	Visual cortical surface	T/C	0.42	0.376 (0.078)	1.75E-06
rs6085231	20	5608428	Intergenic variant	0.47	*GPCPD1*	25Kb	Visual cortical surface	T/C	0.42	0.388 (0.081)	1.92E-06
rs73075632	20	5606311	Intergenic variant	0.47	*GPCPD1*	15Kb	Visual cortical surface	G/A	0.42	0.386 (0.081)	2.22E-06
rs6085230	20	5607325	Intergenic variant	0.47	*GPCPD1*	16Kb	Visual cortical surface	T/C	0.42	0.385 (0.081)	2.30E-06
rs925300	20	5624244	Regulatory region variant	0.48	*GPCPD1*	32Kb	Visual cortical surface	G/C	0.48	0.380 (0.077)	8.11E-07
rs4619684	20	5609830	Intergenic variant	0.51	*GPCPD1*	19Kb	Visual cortical surface	C/T	0.45	0.341 (0.074)	4.49E-06
rs6053549	20	5618582	Intergenic variant	0.52	*GPCPD1*	29Kb	Visual cortical surface	C/A	0.47	0.328 (0.071)	3.95E-06

Table 7.4. Results of the genome-wide association analysis of minimum arteriolar tortuosity. Results shown for *p* values ≤ 1.00×10^{-6} and MAF ≥ 0.05. Single nucleotide polymorphism (SNP); chromosome (chr); position (bp); (r_2); reference allele (A1); effect allele (A2); minor allele frequency (MAF). r2 is the linkage disequil brium between the SNPs in the first column such that the first SNP relates to the second SNP and so on, in ascending order.

SNPs	chr	Position	Genomic location	r_2	Gene(s) nearby	Distance	Associated traits	A1/A2	MAF	ß (SE)	*p*-value
rs2102486	20	5611886	Regulatory region variant	0.53	*GPCPD1*	40Kb	Visual cortical surface	T/C	0.43	0.364 (0.075)	1.51E-06
rs6085232	20	5611026	Intergenic variant	0.53	*GPCPD1*	19Kb	Visual cortical surface	T/C	0.43	0.369 (0.077)	1.72E-06
rs66542670	20	5614071	Intergenic variant	0.54	*GPCPD1*	22Kb	Visual cortical surface	C/T	0.47	0.330 (0.071)	4.14E-06
rs6038219	20	5610737	Intergenic variant	0.56	*GPCPD1*	19Kb	Visual cortical surface	G/A	0.47	0.335 (0.072)	3.59E-06
rs6133240	20	5615836	Intergenic variant	0.58	*GPCPD1*	24Kb	Visual cortical surface	G/A	0.43	0.366 (0.076)	1.50E-06
rs13039871	20	5617706	Intergenic variant	0.58	*GPCPD1*	28Kb	Visual cortical surface	G/A	0.43	0.364 (0.076)	1.60E-06
rs2423115	20	5621007	Regulatory region variant	0.58	*GPCPD1*	29Kb	Visual cortical surface	T/C	0.43	0.364 (0.077)	2.59E-06
rs66542670	20	5614071	Intergenic variant	0.59	*GPCPD1*	22Kb	Visual cortical surface	C/T	0.47	0.330 (0.071)	4.14E-06

Table 7.4 (cont.) Results of the genome-wide association analysis of minimum arteriolar tortuosity. Results shown for *p* values ≤ 1.00×10^{-6} and MAF ≥ 0.05. Single nucleotide polymorphism (SNP); chromosome (chr); position (bp); (r_2); reference allele (A1); effect allele (A2); minor allele frequency (MAF). r2 is the linkage disequilibrium between the SNPs in the first column such that the first SNP relates to the second SNP and so on, in ascending order.

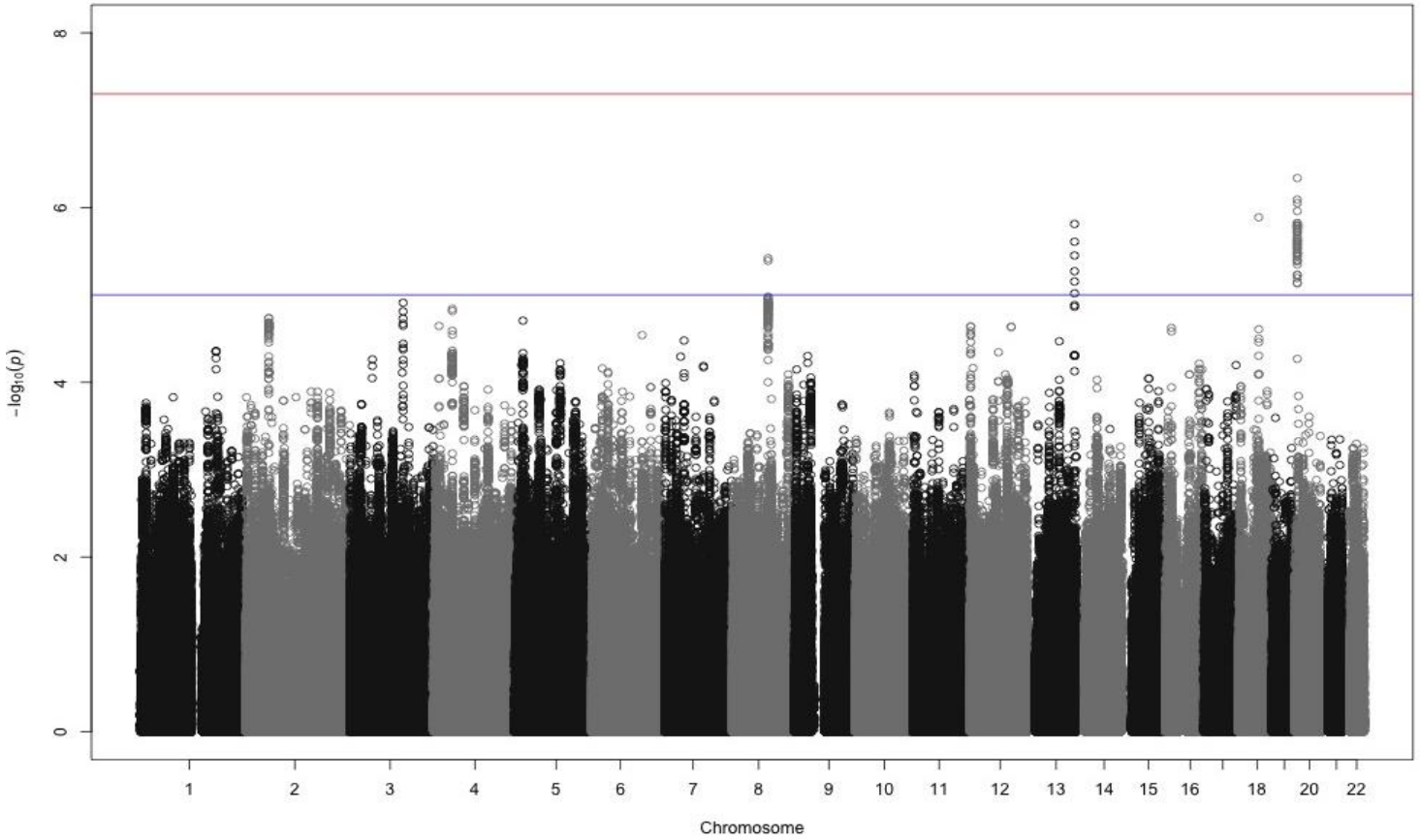

Figure 7.10. Manhattan plot of genome-wide association of minimum arteriolar tortuosity. The plot shows -$\log_{10}$ p values. The blue line corresponds to the suggestive threshold and the red line corresponds to significant GWAS threshold.

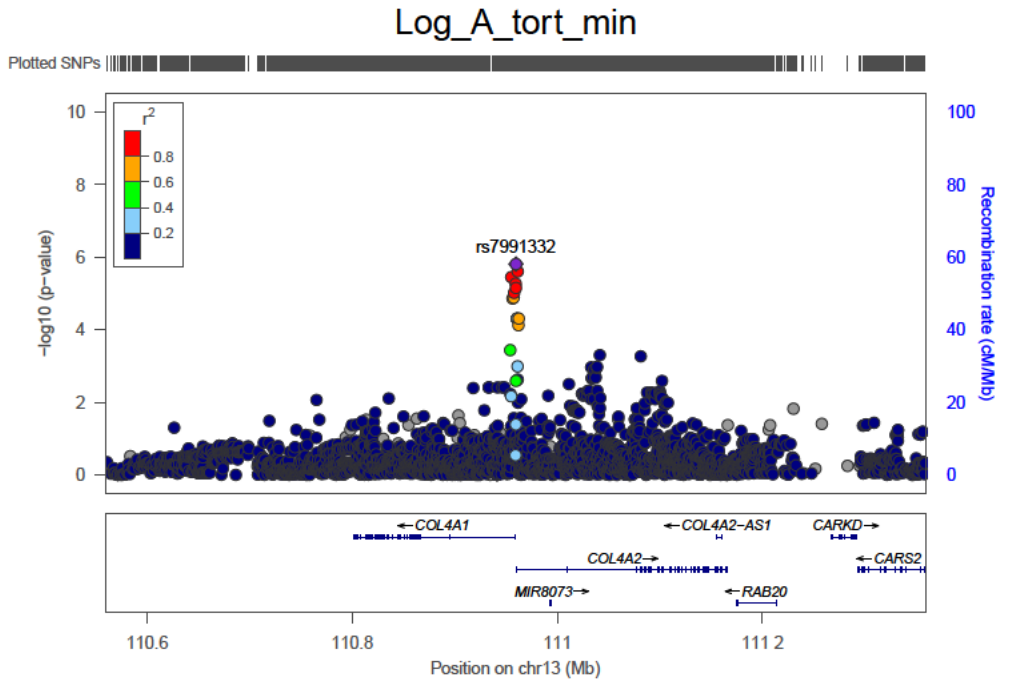

Figure 7.11. Regional plot for most significant SNP for minimum arteriolar tortuosity. The colour coding of the LD between the SNP ranges from dark blue for r_2 = 0-0.2 to red for r_2 = 0.8-1.

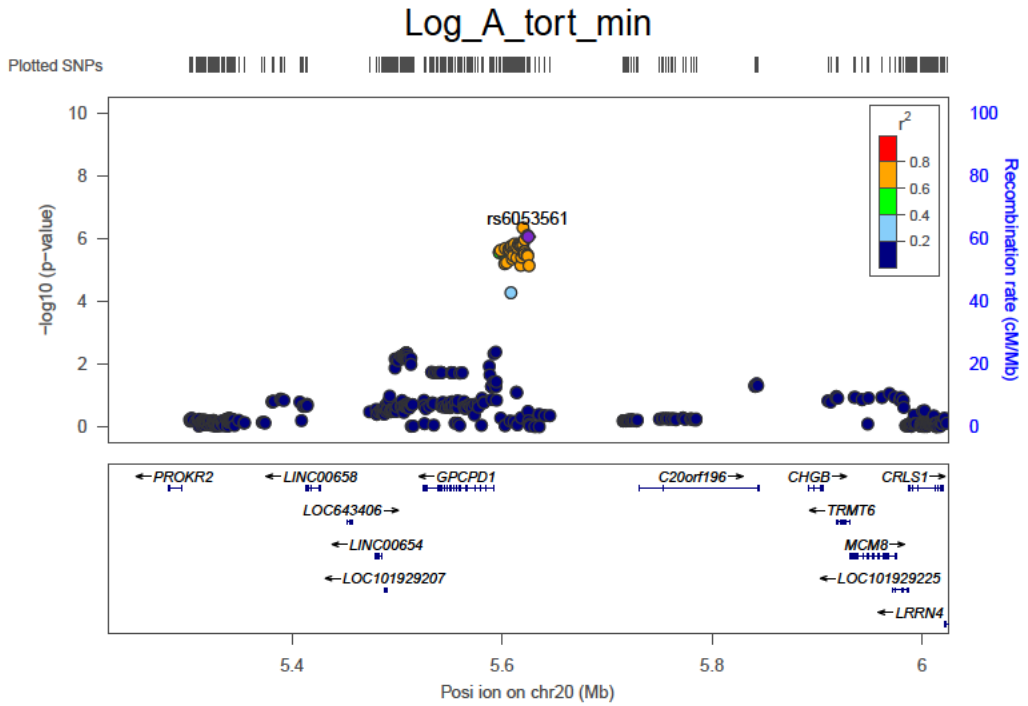

Figure 7.12. Regional plot for minimum arteriolar tortuosity. The colour coding of the LD between the SNP ranges from dark blue for r_2 = 0-0.2 to red for r_2 = 0.8-1.

7.2.6 GWAS of Maximum Arteriolar Tortuosity

No SNPs reached the suggestive threshold in GWAS of maximum arteriolar tortuosity. The Manhattan plot is shown in figure 7.13 and the quantile-quantile plot shown genomic inflation factor of 1.004. This result is shown in the appendix 6.

7.2.7 GWAS of Mean Venular Tortuosity

A summary of the most significant SNPs in the GWAS of mean venular tortuosity is presented in table 7.5. The Manhattan plot is shown in figure 7.14. A quantile-quantile plot of revealed a genomic inflation factor of 1.01. The quantile-quantile plot is presented in the appendix 7.

There were 16 SNPs located on chromosome 16, which reached the suggestive threshold. The most significant result was for rs6497451 (p = 7.33 x 10^{-7}). The regional association plot for this region is shown in figure 7.15.

This variant is in the downstream 3' region of *SNRPEP3*, a gene which encodes nuclear ribonucleoprotein polypeptide E pseudogene 3. This gene is located on chromosome 16p12.3. Another SNP, rs4474693 (p = 7.51 x 10^{-7}), is also located in this region. Four SNPs are located in the upstream 5' region. These included rs12598578 (p = 7.62 x 10^{-7}), rs11074446 (p = 7.62 x 10^{-7}), rs4238585 (p = 7.62 x 10^{-7}) and rs10852238 (p = 8.07 x 10^{-7}). The regional plot of such variants is shown in figure 7.16. The gene has been correlated with raised body mass index (Zhang et al, 2017).

Several SNPs located in the intergenic region of 16p12.3 showed suggestive significance. These included rs7193901 (p = 1.11 x 10^{-6}) and rs7203219 (p = 7.62 x 10^{-7}). The LD between them was weak (r_2 = 0.32) and they may be treated as independent loci. This chromosomal region harbours *GP2*, a gene encoding an integral membrane protein that is secreted from intracellular zymogen granules and associates with the plasma membrane via

glycosylphosphatidylinositol linkage (Locke et al, 2015). The nearby *UMOD* gene is expressed in the cells of the thick ascending loop of Henle in the kidney and has been associated with chronic kidney disease in diabetes (p = 4.4 x 10^{-12}) and hypertension (van Zuydam et al, 2018).

Several SNPs located in the 16p12.3. region also showed suggestive significance. These included rs8045740 (p = 7.62 x 10^{-7}) and rs4432271 (p = 7.62 x 10^{-7}). The LD between them was moderate (r_2 =0.46) and they might be treated as independent loci, but conditional analysis would be required to assess this properly.

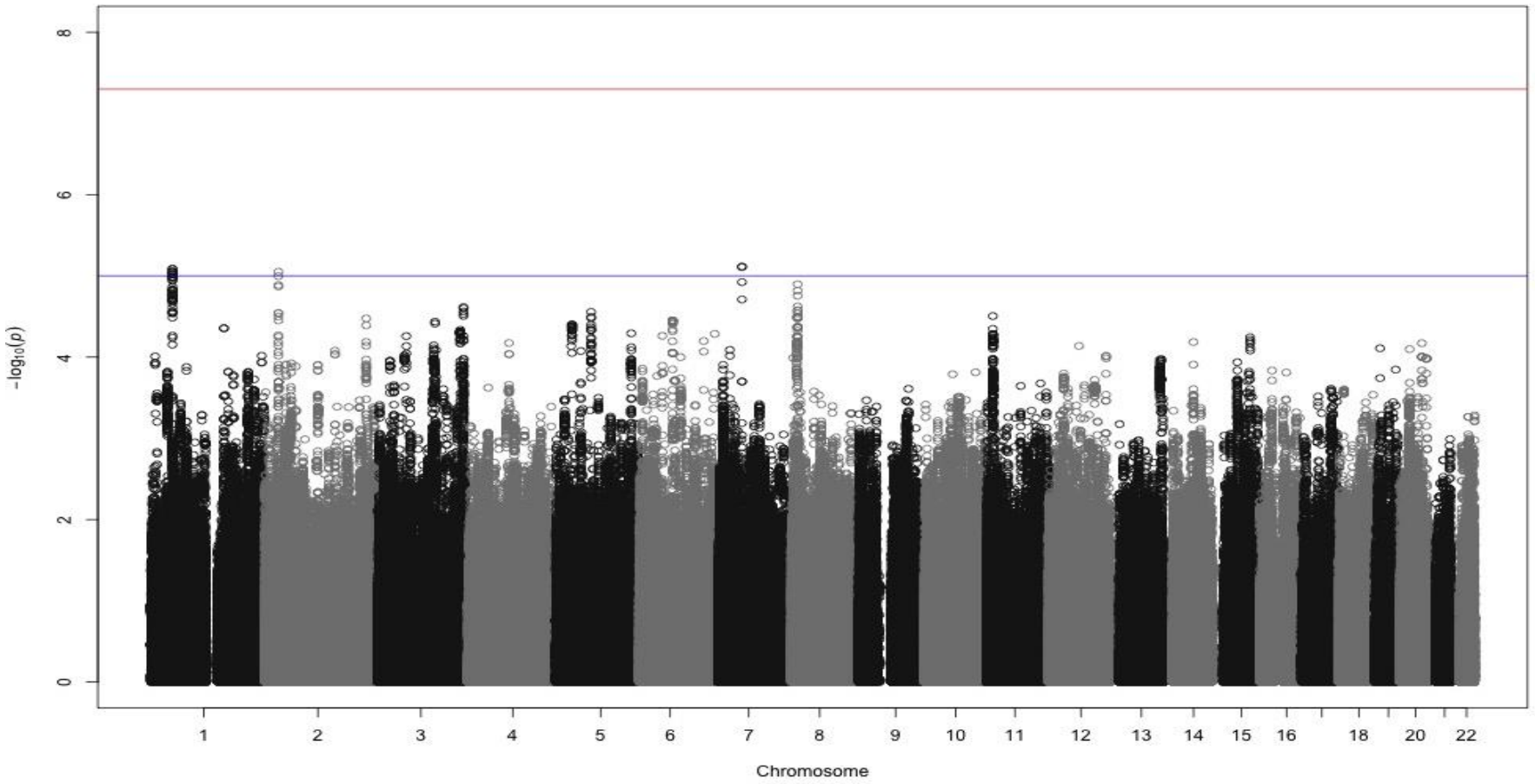

Figure 7.13. Manhattan plot of genome-wide association for maximum arteriolar tortuosity. The plot shows -$\log_{10}$ p values. The blue line corresponds to the suggestive threshold and the red line corresponds to significant GWAS threshold

SNPs	chr	Position	Genic	R2	Distance	Gene(s) nearby	Associated traits	A1/A2	MAF	ß (SE)	*p*-value
rs10852238	16	20253374	Upstream of gene	0.32	-	*SNRPEP3*	BMI	A/T	0.24	0.324 (0.065)	8.07E-07
rs7193901	16	20263764	Intergenic	0.32	15KB	*SNRPEP3*	BMI	T/C	0.16	0.280 (0.057)	1.11E-06
rs7203219	16	20261402	Intergenic	0.35	10Kb	*SNRPEP3*	BMI	T/C	0.13	0.286 (0.057)	7.62E-07
rs12598578	16	20254476	Upstream of gene	0.42	-	*SNRPEP3*	BMI	G/C	0.13	0.286 (0.057)	7.62E-07
rs11074446	16	20255123	Upstream of gene	0.42	-	*GP2*	BMI	T/C	0.13	0.286 (0.057)	7.62E-07
rs9935994	16	20255596	Intergenic	0.42	4.5 Kb	*GP2*	BMI	C/G	0.13	0.286 (0.057)	7.62E-07
rs13339519	16	20256892	Intergenic	0.42	5.2Kb	*GP2*	BMI	A/T	0.13	0.286 (0.057)	7.62E-07
rs28432726	16	20257440	Intergenic	0.42	7 Kb	*GP2*	BMI	G/A	0.13	0.286 (0.057)	7.62E-07
rs8057825	16	20257709	Intergenic	0.42	14Kb	*GP2*	BMI	G/A	0.13	0.286 (0.057)	7.62E-07
rs8063747	16	20258270	Intergenic	0.42	15Kb	*GP2*	BMI	T/C	0.13	0.286 (0.057)	7.62E-07
rs7188545	16	20259204	Intergenic	0.42	9 Kb	*GP2*	BMI	C/T	0.13	0.286 (0.057)	7.62E-07
rs8045740	16	20262776	Intergenic	0.42	12 Kb	*GP2*	BMI	G/T	0.13	0.286 (0.057)	7.62E-07
rs4432271	16	20245283	Intergenic	0.46	1.5Kb 4.7Kb	*LOC102723396 GP2*	BMI	T/C	0.13	0.294 (0.059)	7.42E-07
rs4474693	16	20246313	Downstream of gene	0.46	-	*SNRPEP3*	BMI	A/G	0.13	0.293 (0.059)	7.51E-07
rs6497451	16	20248466	Downstream of gene	0.46	-	*SNRPEP3*	BMI	T/G	0.13	0.292 (0.058)	7.33E-07
rs4238585	16	20255097	Upstream of gene	0.46	-	*SNRPEP3*	BMI	T/C	0.13	0.286 (0.057)	7.62E-07

Table 7.5. Results of the genome-wide association analysis of venular tortuosity. Results shown for *p* values ≤ 1.00 x 10_{-8} and MAF ≥ 0.05. Single nucleotide polymorphism (SNP); chromosome (chr); position (bp); (r2); reference allele (A1); effect allele (A2); minor allele frequency (MAF); central retinal venular equivalent (CRVE); body mass index (BMI). r2 is the linkage disequil brium between the SNPs in the first column such that the first SNP relates to the second SNP and so on, in ascending order.

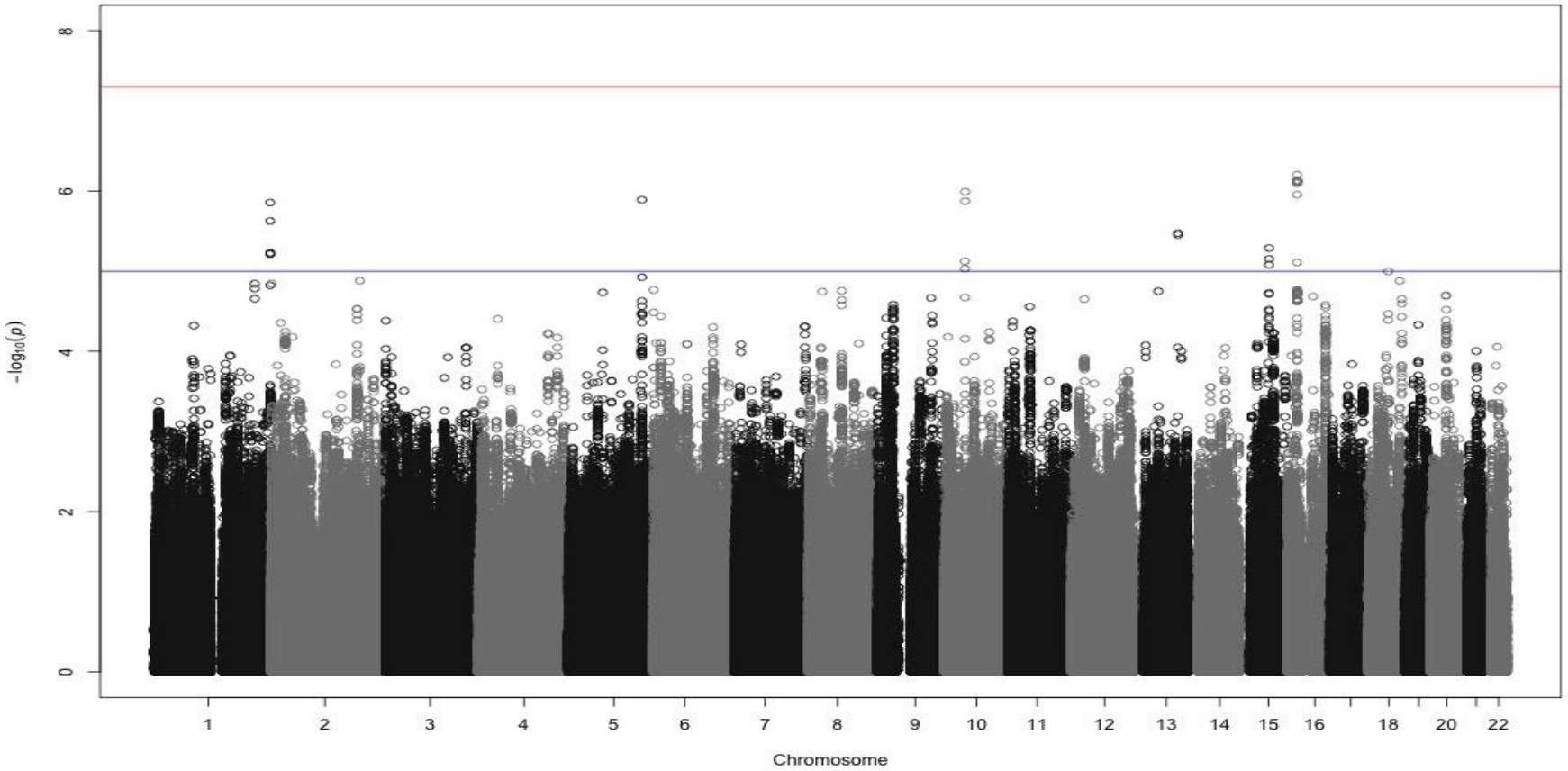

Figure 7.14. Manhattan plot of genome-wide association for venular tortuosity. The plot shows $-\log_{10} p$ values. The blue line corresponds to the p value threshold of 1.0×10^{-5} and the red line corresponds to the p value threshold of 5.0×10^{-8}.

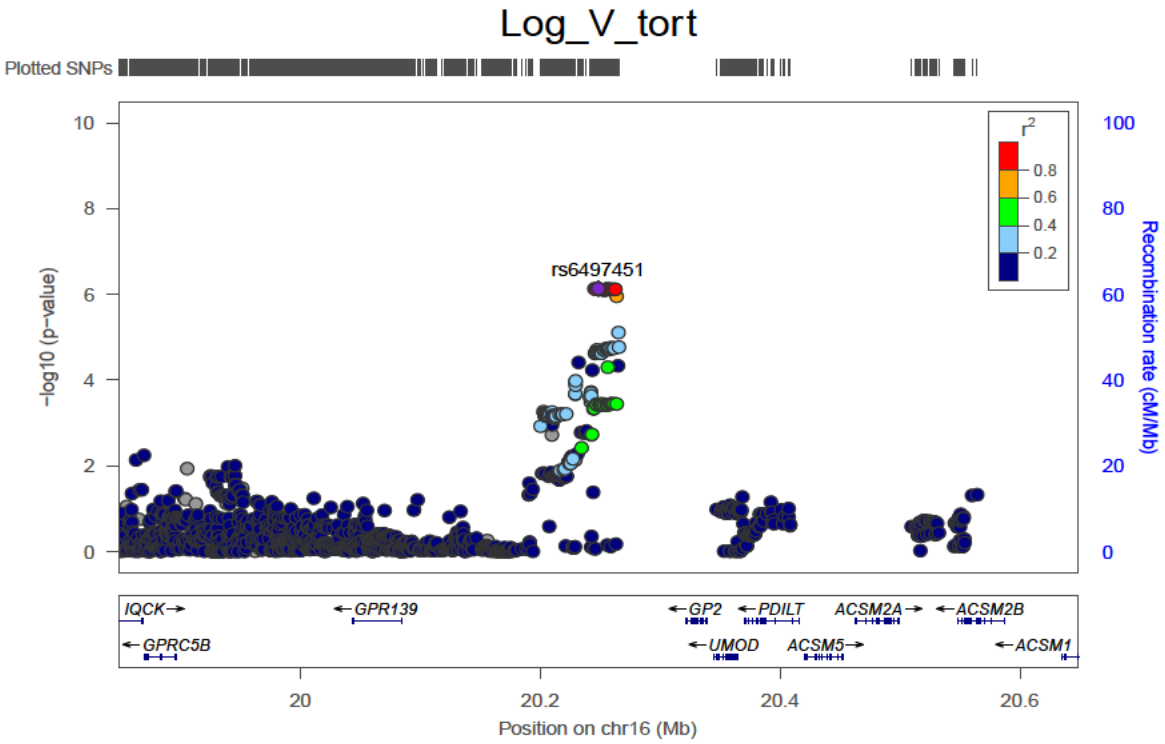

Figure 7.15. Regional plot of venular tortuosity. The colour coding of the LD between the SNP ranges from dark blue for r_2 = 0-0.2 to red r_2 = 0.8-1.

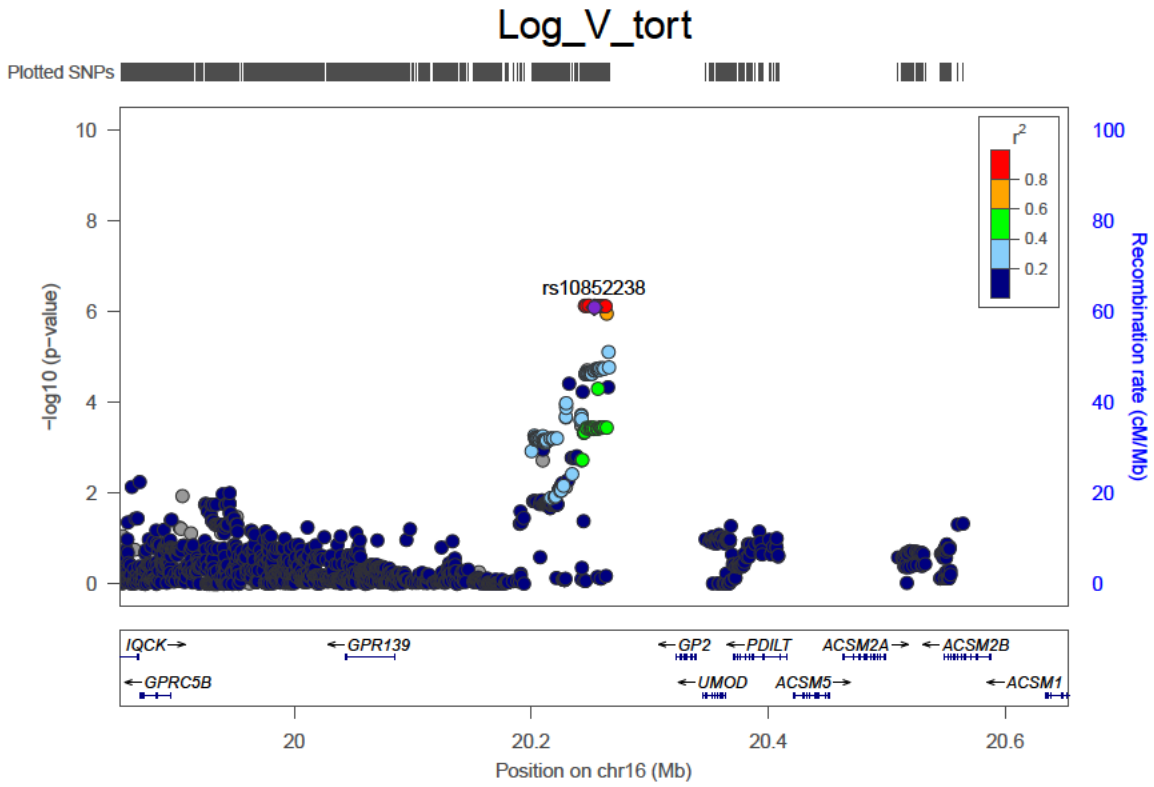

Figure 7.16. Regional plot of venular tortuosity. The colour coding of the LD between the SNP ranges from dark blue for r_2 =0-0.2 to red for r_2 = 0.8-1

7.2.8 GWAS of Minimum Venular Tortuosity

The results of the GWAS of minimum venular tortuosity are presented in this section. A summary of the most significant SNPs is presented in table 7.6 and the Manhattan plot is shown in figure 7.17. A quantile-quantile plot of revealed a genomic inflation factor of 0.99. The quantile-quantile plot is presented in the appendix 6.

Although, none of the SNPs reached genome-wide significance, five SNPs reached the suggestive threshold (table 7.6). The SNP rs34013641 (p = 8.53 x 10^{-7}) had the strongest significance level. The association of this variant was detected within *MYH11*, a gene which encodes a smooth muscle protein called myosin. The gene is located on chromosome 16p13.11 and has been associated with familial aortic aneurysms, an autosomal dominant disorder associated with an abnormally high occurrence of thoracic aortic aneurysms and aortic dissection (Keravnou et al, 2018). The regional association plot is shown in figure 7.18.

Analysis revealed that rs2021412 (p = 2.84 x 10^{-6}), rs56287009 (p = 3.28 x 10^{-6}), rs79706152 (p = 3.81 x 10^{-6}) and rs1432567 (p = 4.44 x 10^{-6}) had the strongest significance on chromosome 2. The regional plot is shown in figure 7.19. Variants are located near the *CCDC85A* gene. This gene has been associated with susceptibility of type 2 diabetes in a Japanese population at genome-wide significance (p = 6.97 x 10^{-10}), a finding that has been replicated in a multi-ethnic study (Imamura, et al 2016).

7.2.9 GWAS of Maximum Venular Tortuosity

None of the SNPs reached suggestive significance for maximum venular tortuosity. The Manhattan plot is shown in figure 7.20 and the quantile-quantile plot shown modest genomic inflation of 1.02 (Appendix 7).

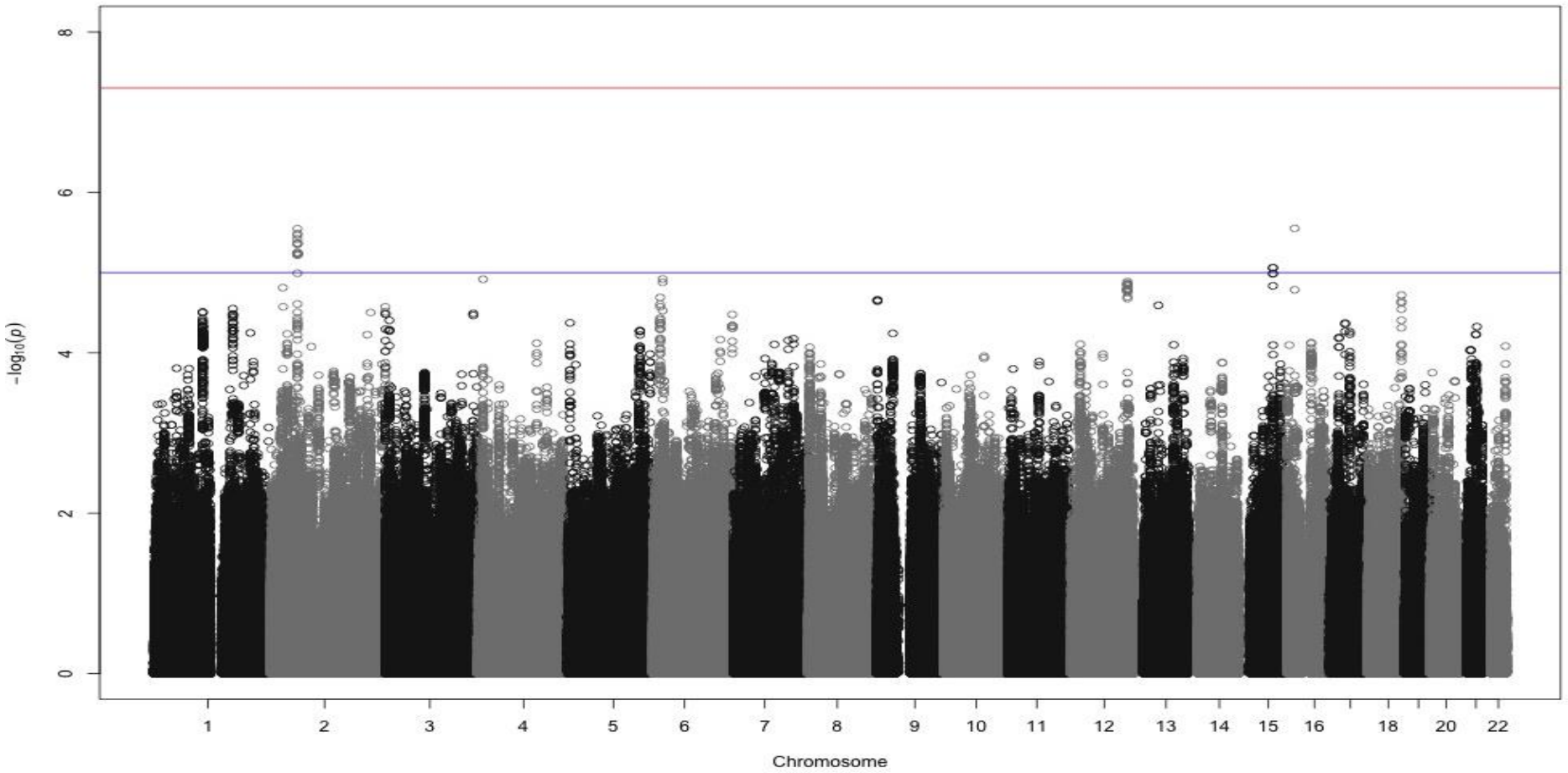

Figure 7.17. Manhattan plot of genome-wide association for minimum venular tortuosity. The plot shows -$\log_{10}$ p values. The blue line corresponds to the p value threshold of 1.0 x 10^{-5} and the red line corresponds to the p value threshold of 5.0 x 10^{-8}.

SNPs	chr	Position	Genic location	r_2	Distance	Gene(s) nearby	Associated traits	A1/A2	MAF	ß (SE)	*p*-value
rs79706152 (aka rs11683442)	2	56323650	Intergenic	0.83	86Kb	*CCDC85A*	Type 2 diabetes	C/T	0.36	-0.333 (0.072)	3.81E-06
rs2021412	2	56350662	Intergenic	0.83	60Kb	*CCDC85A*	Type 2 diabetes	G/A	0.37	-0.355 (0.075)	2.84E-06
rs1432567	2	56331228	Intergenic	0.86	79Kb	*CCDC85A*	Type 2 diabetes	G/A	0.36	-0.339 (0.073)	4.44E-06
rs56287009	2	56338148	Intergenic	0.86	72Kb	*CCDC85A*	Type 2 diabetes	G/T	0.35	-0.348 (0.074)	3.28E-06
rs34013641	16	15838328	Intronic	Unique	-	*MYH11*	Smooth muscle myosin heavy chain Aortic stiffness Aneurysms Pulse wave velocity Heart rate	C/G	0.08	0.766 (0.163)	2.81E-06

Table 7.6. Results of genome-wide association analysis of minimum venular tortuosity. Results are shown for p values ≤ 1.00×10^{-6} and MAF ≥ 0.05. Single nucleotide polymorphism (SNP); chromosome (chr); position (bp); (r2); reference allele (A1); effect allele (A2); minor allele frequency (MAF). r2 is the linkage disequil brium between the SNPs in the first column such that the first SNP relates to the second SNP and so on, in ascending order.

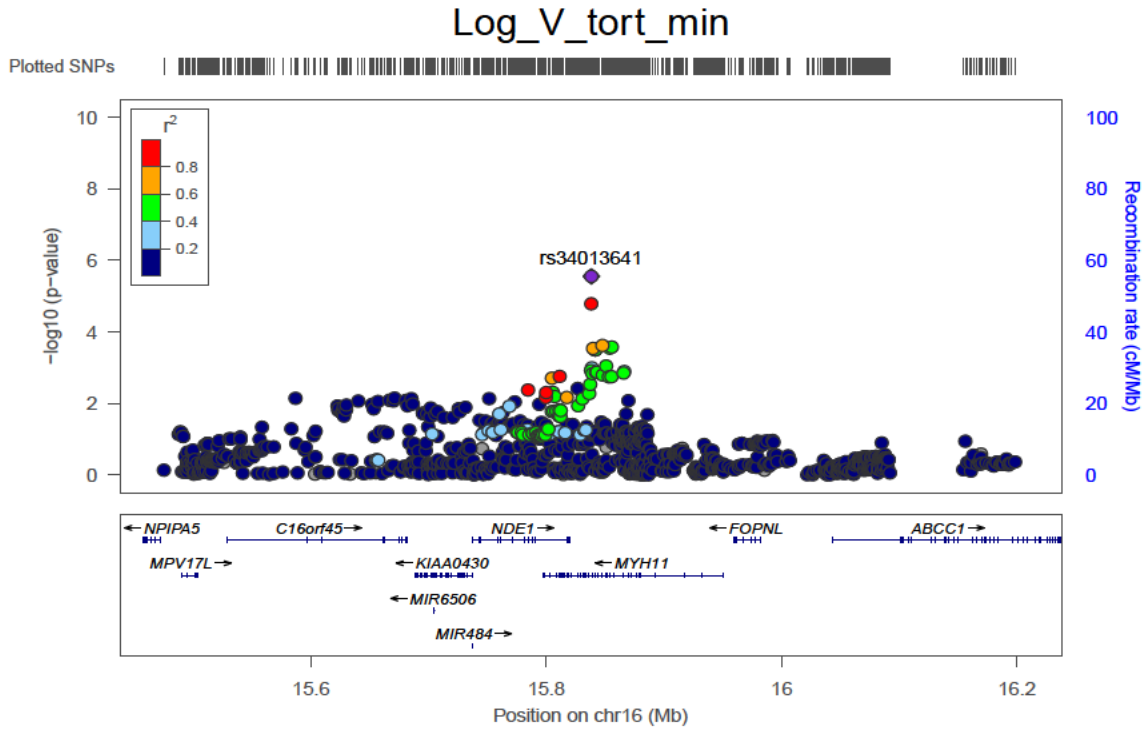

Figure 7.18. Regional plot for minimum venular tortuosity. The colour coding of the LD between the SNP ranges from dark blue for r_2 = 0-0.2 to red for r_2 = 0.8-1.

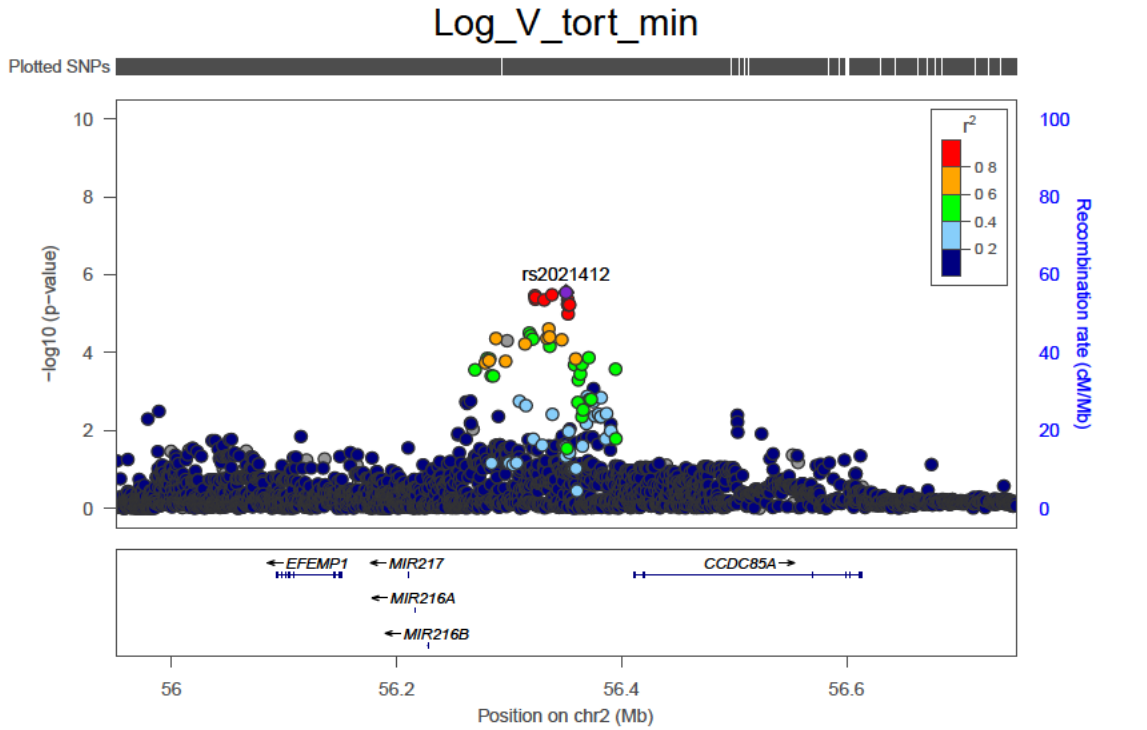

Figure 7.19. Regional plot for minimum venular tortuosity. The colour coding of the LD between the SNP ranges from dark blue for r_2 = 0-0.2 to red for r_2 = 0.8-1.

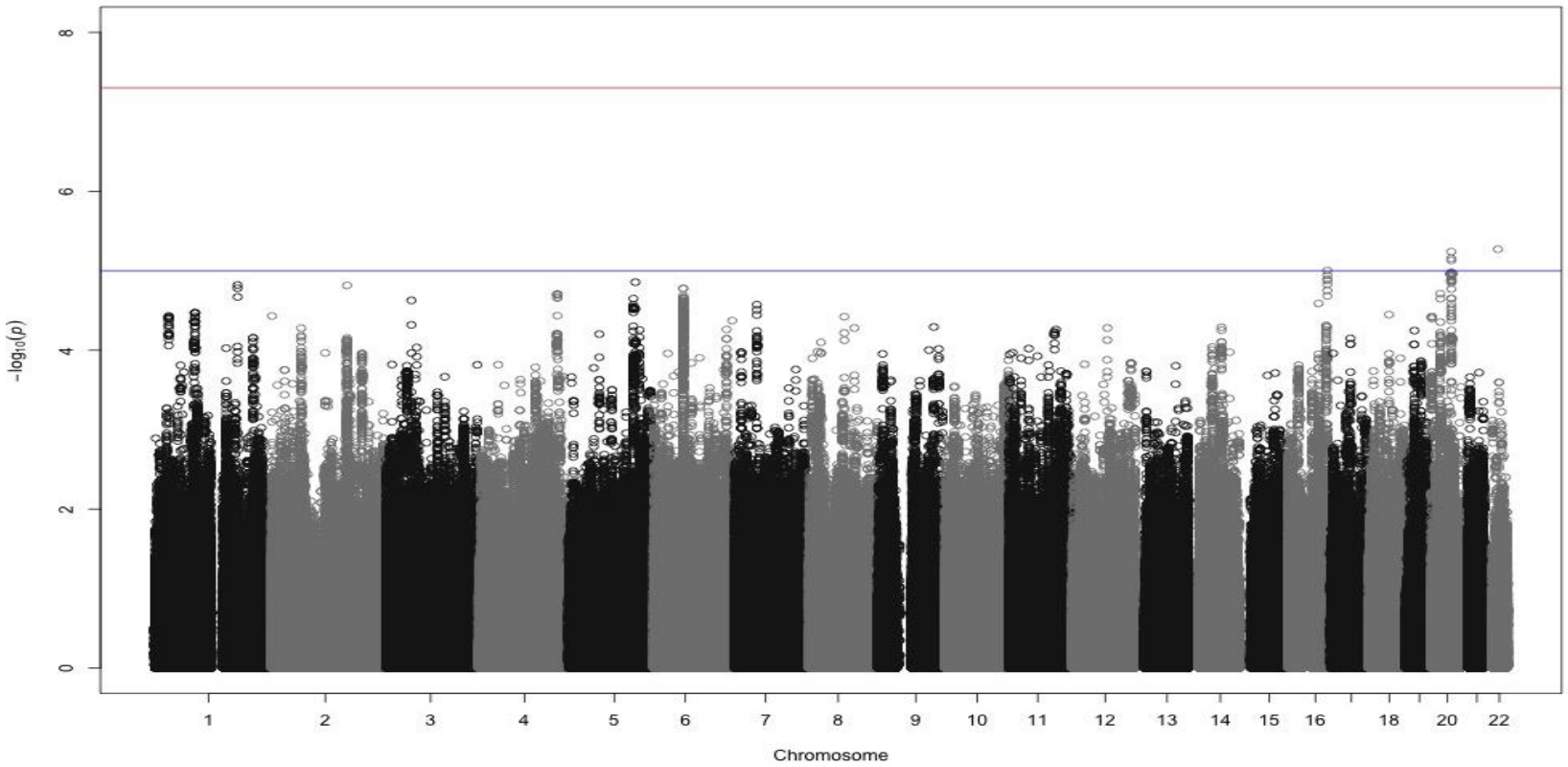

Figure 7.20. Manhattan plot of genome-wide association for maximum venular tortuosity. The plot shows -$\log_{10}$ p values. The blue line corresponds to the p value threshold of 1.0 x 10^{-5} and the red line corresponds to the p value threshold of 5.0 x 10^{-8}.

7.2.10 GWAS of Multifractal Dimensions

A summary of the most significant SNPs from the three genome wide association analyses performed for the multifractal dimensions traits (DO, D1 and D2) is shown in table 7.7. A total of three different variants showed significance at the suggestive threshold. Given the high correlation among the multifractal dimensions traits, it was not surprising that one variant was identified for all three traits and another variant was identified for two of the traits. The Manhattan plots for multifractal dimensions D0 and D1 are shown in figures 7.21 and 7.24 respectively. A modest genomic inflation factor of 1.01 was observed. Quantile-quantile plots are presented in the Appendix 6.

Two SNPs reached the suggestive threshold for multifractal dimension D0: rs10963694 ($p = 8.53 \times 10^{-7}$) and rs4977506 ($p = 4.95 \times 10^{-6}$). Association was detected within *ADAMTSL1*, a gene which encodes a protease and member of the *ADAMTS* family (a disintegrin and metalloproteinase with thrombospondin motif). This gene is located on chromosome 9p22.2. Regional association plots of these regions are shown in figures 7.22 and 7.23.

For multifractal dimension D1, two SNPs reached the suggestive threshold. Suggestive association was detected within *HNRPR.* The analysis revealed that rs9662596 ($p = 4.71 \times 10^{-6}$) had the strongest significance within this gene. This gene encodes nuclear ribonucleoproteins (hnRNPs), involved in binding to RNA polymerase II transcripts, and plays an important role in both transcript-specific packaging and alternative splicing of pre-mRNAs. The gene is located on chromosome 1p36.12. It has been reported that hnRNPR and beta-actin mRNA are localized in axons (Glinka et al*,* 2010). The second SNP identified ($p = 1.69 \times 10^{-6}$) was the variant identified for multifractal dimension D0, rs10963694 (figure 7.22). For multifractal dimension D2, two of the same SNPs identified for the other multifractal dimension traits were identified: rs9662596 ($p = 4.72 \times 10^{-6}$) and rs10963694 ($p = 1.69 \times 10^{-6}$).

Multifractal dimension D0											
SNPs	**chr**	**Position**	**Genic location**	**Distance**	**r_2**	**Gene(s) nearby**	**Associated traits**	**A1/A2**	**MAF**	**ß (SE)**	***p*-value**
rs10963694	9	18638692	Intronic	-	0.2	*ADAMTSL1*	Extracellular matrix, aging	A/G	0.42	-0.024 (0.005)	8.53E-07
rs4977506	9	18649769	Intronic	-	0.2	*ADAMTSL1*	Extracellular matrix, aging	C/G	0.36	-0.023 (0.005)	4.95E-06
Multifractal dimension D1											
SNPs	**chr**	**Position**	**Genic location**	**Distance**	**r_2**	**Gene(s)nearby**	**Associated traits**	**A1/A2**	**MAF**	**ß (SE)**	***p*-value**
rs9662596	1	23658958	Intronic	-	-	*HNRPR (aka hnRNP-R)*	axon growth	G/A	0.09	0.029 (0.006)	4.71E-06
rs10963694	9	18638692	Intronic	-	0.2	*ADAMTSL1*	Extracellular matrix, aging	A/G	0.42	-0.024 (0.005)	1.43E-06
Multifractal dimension D2											
SNPs	**chr**	**Position**	**Genic location**	**Distance**	**r_2**	**Gene(s) or nearby**	**Associated traits**	**A1/A2**	**MAF**	**ß (SE)**	***p*-value**
rs9662596	1	23658958	Intronic	-	-	*HNRPR (aka hnRNP-R)*	axon growth	G/A	0.09	0.029 (0.006)	4.72E-06
rs10963694	9	18638692	Intronic	-	0.2	*ADAMTSL1*	Extracellular matrix, aging	A/G	0.42	-0.024 (0.005)	1.69E-06

Table 7.7. Results of the genome-wide association analysis of multifractal dimensions D0, D1, D2. Results are shown for p values ≤ 1.00×10^{-6} and MAF ≥ 0.05. Single nucleotide polymorphism (SNP); chromosome (chr); position (bp); (r2); reference allele (A1); effect allele (A2); minor allele frequency (MAF). r2 is the linkage disequilibrium between the SNPs in the first column such that the first SNP relates to the second SNP and so on, in ascending order.

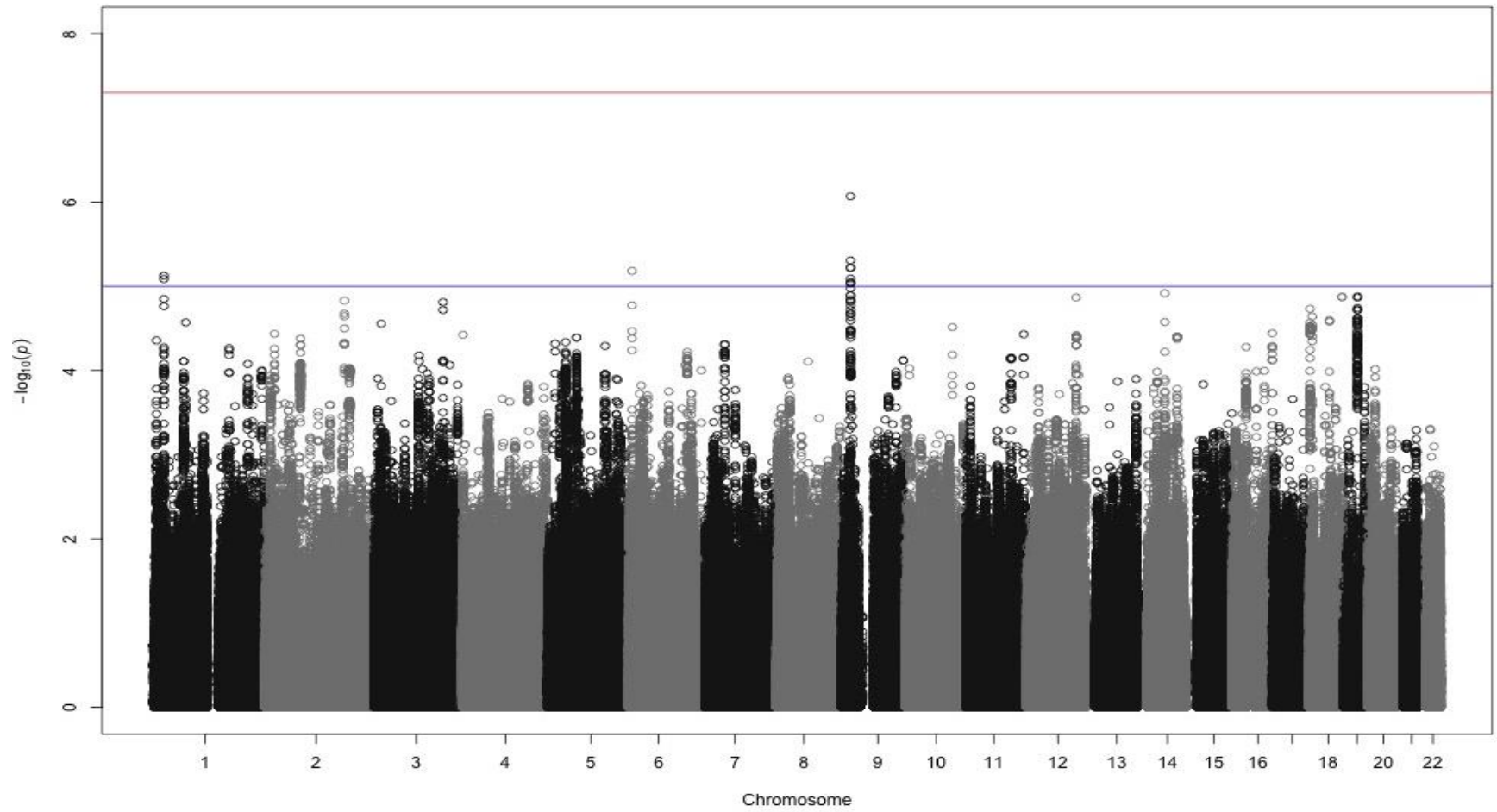

Figure 7.21. Manhattan plot of genome-wide association for Multifractal dimension D0 .The plot shows -$\log_{10}$ p values. The blue line corresponds to the suggestive threshold and the red line corresponds to significant GWAS threshold

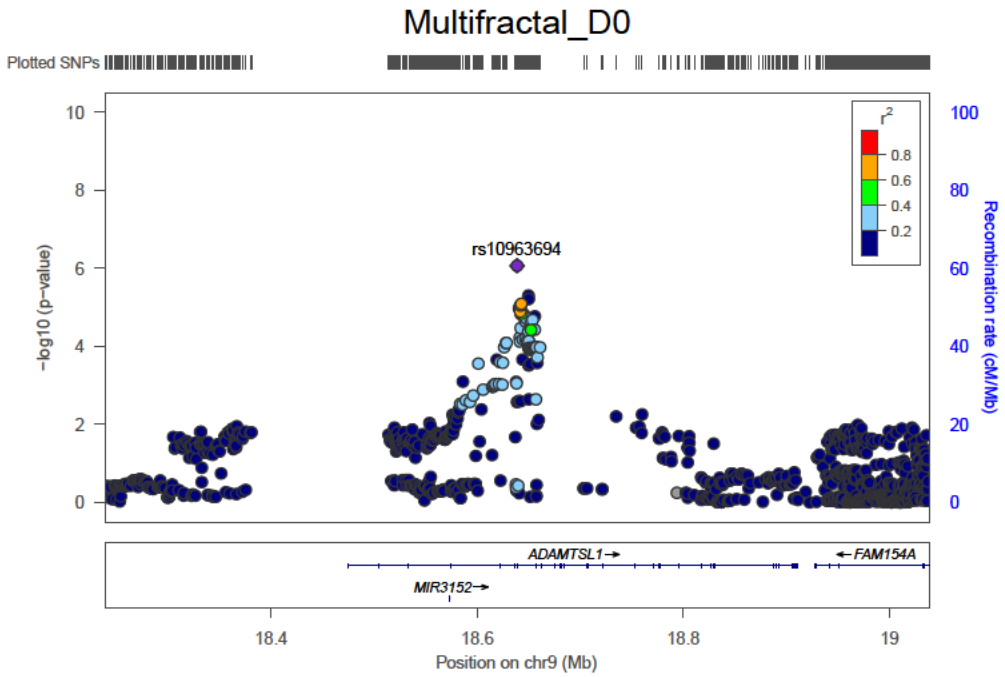

Figure 7.22. Regional plot for multifractal dimension D0. The colour coding of the LD between the SNP ranges from dark blue for r_2 = 0-0.2 to red for r_2 = 0.8-1.

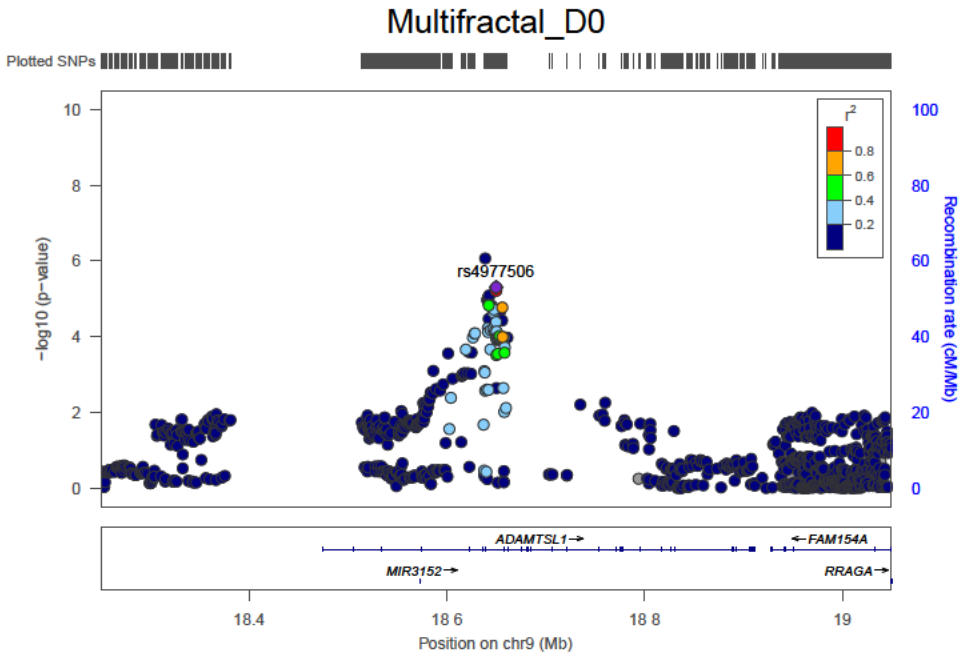

Figure 7.23. Regional plot for multifractal dimension D0. The colour coding of the LD between the SNP ranges from dark blue for r_2 = 0-0.2 to red for r_2 = 0.8-1.

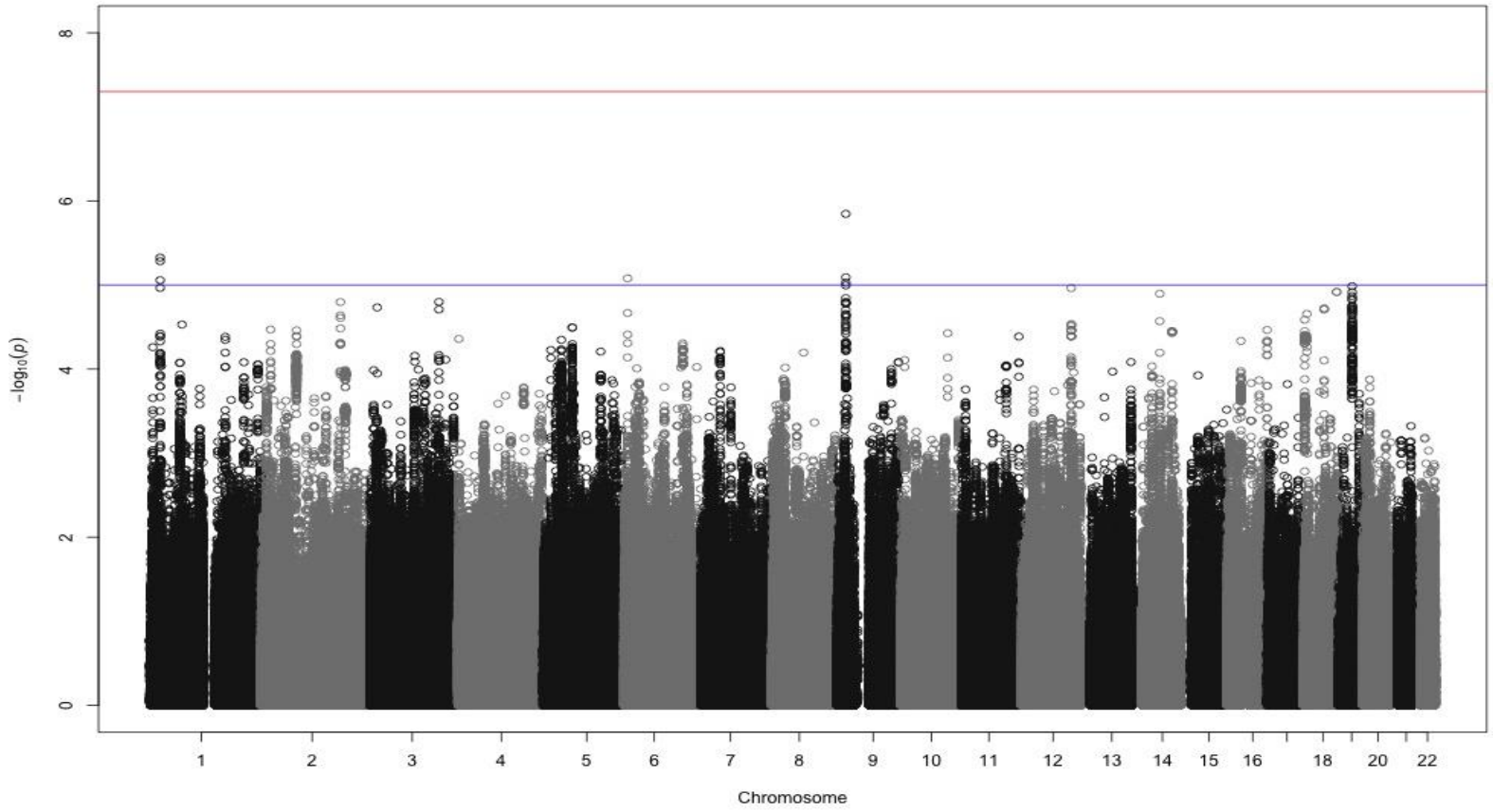

Figure 7.24. Manhattan plot of genome-wide association for multifractal dimension D1. The plot shows -$\log_{10}$ p values. The blue line corresponds to the suggestive threshold and the red line corresponds to significant GWAS threshold

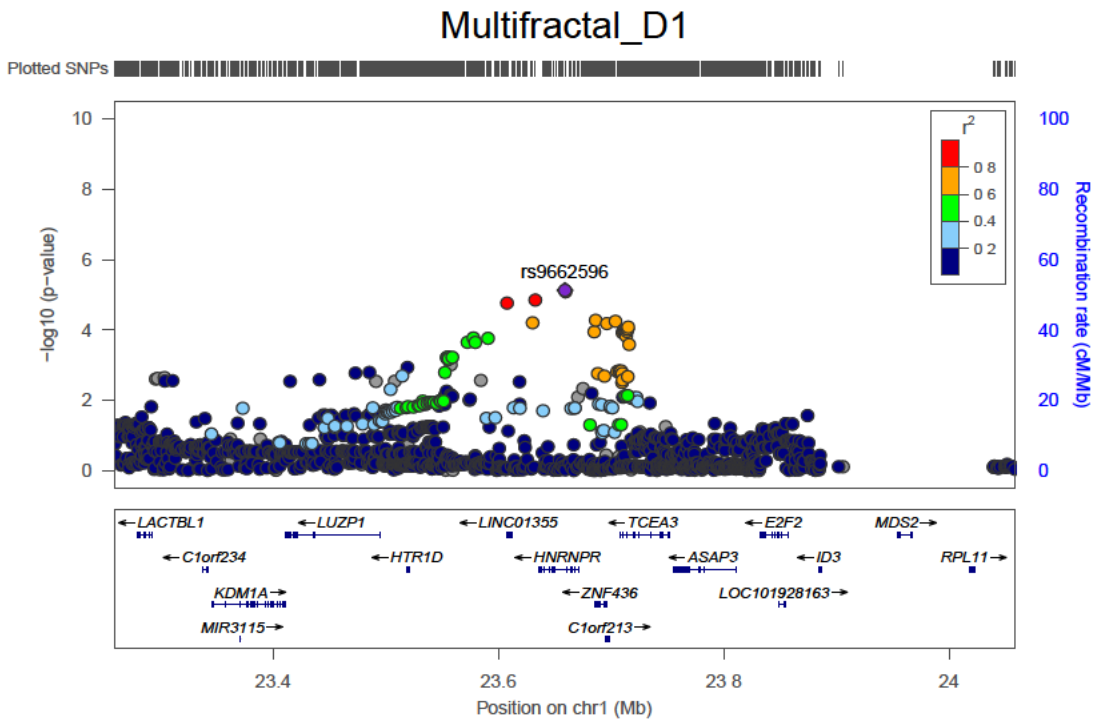

Figure 7.25. Regional plot for multifractal dimension D1. The colour coding of the LD between the SNP ranges from dark blue for r_2 = 0-0.2 to red for r_2 = 0.8-1.

7.3 Summary

Although no SNPs reached genome wide significance, some promising findings emerged from GWAS of the multiple retinal traits analysed. These included the minimum arteriolar tortuosity loci rs7991332 and rs2172724. These loci are located in the *COL4A2* gene. Another identified variant, rs7319323, is located in an intron of the neighbouring *COL4A1* gene. Previous studies cited in the literature show the relevance of these genes including an association with stroke and intracerebral haemorrhage. The two genes encode collagen protein chains, major components of the vascular basement membrane.

Another promising finding is the rs34013641 variant, associated with minimum venular tortuosity, which is located in the *MYH11* gene. This gene encodes smooth muscle myosin heavy chain protein, which is highly expressed in human arteries.

Finally, the multifractal dimension D0 loci rs10963694 and rs4977506, located on the *ADAMTSL1* gene, are also strong candidates in the pathophysiology of vascular disorders. This gene encodes a metalloproteinase, which appears to be relevant to extracellular matrix function or to cell-matrix interactions.

Chapter 8 Discussion

In this chapter, I summarise the key findings of this study, and compare these with the results published in the scientific literature. I discuss the strengths and limitations of the study, including an evaluation of the methods used in the data collection and statistical analyses. Finally, I outline recommendations for future research on the use of quantitative retinal traits for prediction of major cardiovascular events.

8.1 Key findings

8.1.1 Association of quantitative retinal traits with cardiovascular disease and incident events in diabetes

In the Edinburgh Type 2 Diabetes Study (ET2DS), a representative prospective study of men and women aged ≥65 years with type 2 diabetes living in the Lothian region of Scotland, a range of quantitative retinal traits showed statistically significant associations with a number of cardiometabolic risk factors and with cardiovascular disease measured as clinical events. Arteriovenous ratio (AVR) was inversely associated with total serum cholesterol. Both decreased arteriolar and venular widths (measured as CRAE and CRVE respectively) were associated with increased fasting plasma glucose. CRAE was associated with cardiovascular events independent of age and sex, though CRVE was associated only with diabetic retinopathy. Mean arteriolar tortuosity was inversely associated with age, whilst, it was associated with sex and diastolic blood pressure. Maximum arteriolar tortuosity was associated with total cholesterol. Mean venular tortuosity was associated with BMI, systolic blood pressure and with cardiovascular events, notably with stroke, where the association remained significant after adjustment for traditional cardiovascular risk factors.

Despite these cross-sectional results, only two quantitative retinal traits, mean arteriolar tortuosity and multifractal dimensions (D1, D2 and D3), were significantly associated with incident cerebrovascular events, and these findings were only related for stroke or recurrent stroke. However, the latter results for association with stroke remained significant after full adjustment for multiple known cardiovascular risk factors. Thus, retinal arteriolar tortuosity and multifractal dimensions D1, D2 and

D3 were not associated with coronary events or composite cardiovascular events in the ET2DS. Rather, this study showed that these retinal parameters were exclusively associated with cerebrovascular events. This may reflect the importance of considering the embryologic origin of the retinal vasculature and its possible effect in developing cardiovascular events. Conversely, there might be other coronary endophenotypes (e.g. silent ischaemia in women or presence of vessel disease present in coronary angiograms), which are associated with quantitative retinal traits. While these were not present in the cardiovascular endpoints of this study, previous evidence suggests an association between these traits and coronary events (Wang et al, 2018).

8.1.2 Vessel width traits (CRAE, CRVE and AVR) and cardiovascular events

This study showed that AVR was not associated with major cardiovascular events (e.g. ischaemic heart disease and stroke). In the previous literature, this retinal trait has been associated with acute myocardial infarction and risk of coronary heart disease (including MI fatalities) mainly in women (Wong et al, 2002). AVR represents a dimensionless parameter and its value depends on the measurement of diameters of arterioles and venules, raising a number of considerations. First, the retinal vessel classification depends on visual and geometric features, which discriminate arterioles and veins in semi-automated measurements. Generally, venules are wider and darker than arterioles and the central reflex is more recognizable (brighter) in arterioles. Importantly, arterioles and venules usually alternate near the optic disc and before branching off. Although, identification of the vessels was carried out carefully, selection of the vessel may be biased, as vessels in the outer regions of the image are dark because of the shading effect of the image. Therefore, misselection of arterioles and veins may lead to misclassification. The value of AVR has different components. For instance, narrower arterioles and wider venules may both lead to smaller values of AVR. Hence, a small AVR cannot differentiate specific changes in arteriolar and venular calibres.

Values of AVR could also explain the lack of association between CRAE and CRVE and cardiovascular events. The measurements of CRAE and CRVE have been

obtained differently across previous studies (Seidelmann et al, 2016; Wong et al, 2002). The algorithm for measurements used in VAMPIRE differs from that used in the other retinal softwares. McGrory and colleagues (2017) also found that agreement between retinal parameters including vessel width, tortuosity and fractal dimensions in VAMPIRE and SIVA platforms was poor.

Another reason for this finding could lie in the moment when the retinal photograph is taken. The cardiac cycle may affect the size of retinal vessels. Hao et al (2012) demonstrated that there was a significant variation in the diameter of individual retinal vessels over the cardiac cycle, and both arterioles and venules were affected by this. Although the vessels width summary (CRAE and CRVE) and tortuosity were relatively consistent across the cardiac cycle using SIVA software, the formula used in this platform differs from the algorithm used in VAMPIRE (Hao et al, 2012).

Additionally, camera factors and ocular factors can also have a bearing on the degree of magnification, and therefore, measurements from the fundal photography, as well as the degree of eccentricity of the measured object from the optical axis could alter the diameter measurement. Magnification of the fundal photographs should be known in order to make comparisons because this may differ according to the type of camera used. Biometric factors of the eye could affect ocular factors. These biometric factors include the axial length of the eye, anterior and posterior radii of curvature of the cornea and the lens, the corneal and lenticular thickness and anterior chamber depth (Patton et al, 2006). Correction for any or all such factors should be performed. It is unknown whether the previous studies have performed such a correction in their dataset, and these may alter the measurements of the retinal parameters.

8.1.3 Vascular tortuosity (arteriolar and venular) and cardiovascular events

This study found a significant association between mean arteriolar tortuosity and incident cardiovascular events (e.g. stroke). This finding is similar to the results reported by Saraf et al (2019) in relation to the familial vascular tortuosity syndrome. Retinal arteriolar tortuosity could be an indicator of vascular disease, as it is a

measurement that depends directly on the retinal vascular morphology (e.g. how, and how many times, the vessel bends). This retinal trait is a potential biomarker, which has previously shown association not only with cardiovascular complications (Sasongko et al, 2016; Sasongko et al, 2011) but also with genetic (and hence, biological) mutations in the vascular structural components such as collagen (Beyens et al, 2016). This retinal parameter showed the highest correlation between the right and left eye of all the retinal parameters examined in this study. These findings support this vascular parameter as a potentially informative retinal biomarker for exploring vascular complications.

As with the other retinal parameters analysed in this study, there are methodological considerations to be taken into account when quantifying retinal tortuosity. A recent study (Ramos et al, 2018) identified a limitation in the measurement of retinal vascular tortuosity, which was the lack of precise and standard guidance for tortuosity assessment regarding the image acquisition, measurement location and consequent calculation. Based on the approach implemented in the VAMPIRE platform, the quantification consists of a measure only depending on the vessel skeleton curvature. Ramos and colleagues (2018) also compared different algorithms, and the metrics that performed best were those, which combined the number of segments with constant convexity within a vessel with the evaluation of such segments. This means that the best results come from the methodologies, which integrate information about how many times a vessel changes its convexity. There are also limitations related to the availability of normative retinal data due to the absence of unified public datasets. This, along with the lack of standardised analyses regarding the computational algorithms hinder the validation of the available methods to measure retinal vessel tortuosity.

8.1.4 Multifractal dimensions and cardiovascular events

Another major finding of this study was the significant association between multifractal dimensions DO, D1 and D2 and incident stroke. Recent studies (McGrory et al, 2019; Wu et al, 2017; Kawasaki et al, 2011) have reported an association in the similar direction. Multifractal dimension is a parameter, which summarises the

complexity of the vascular tree. The main attraction of fractal geometry is based on the ability to describe the irregular or fragmented shape of natural features as well as other complex objects (e.g. the retinal vasculature) that traditional Eucledian geometry fails to analyse (Lopes et al, 2009). This retinal biomarker (with all its intrinsic limitations as a mathematical model) may be used as an objective and quantitative parameter for the evaluation of the retinal vasculature (Tālu et al, 2017). Like the other retinal parameters, the multifractal dimension significantly varies across different measurement methods. One consideration is the region of interest to analyse, and this should be standardised across platforms. In addition, vessel segmentation results in high variability in the methods incorporated, and it has been suggested that a threshold value for creating a high accuracy binary vessel segmentation map is required (Huang et al, 2016).

8.1.5 Association between quantitative retinal traits and GWAS data

In the imputed data from the ET2DS dataset, a number of SNPs were identified which surpassed the genome-wide suggestive significant threshold (*p* value < 1.0×10^{-6}) located in the genes *COL4A1, COL4A2, MYH11* and *ADAMTSL1*. Variants of these genes are involved in the physiopathology of vascular disease including thrombosis, cell aggregation, and atherosclerosis (Mejia-Renteria et al, 2018).

In this study, the variants rs7991332 and rs2172724 located in *COL4A2* and the variant rs7319323 of *COL4A1* gene were associated with minimum arteriolar tortuosity. Previous studies have reported a similar association between these genes and familial arterial tortuosity and stroke (Rannikmäe et al, 2015).

The role of the genetic variants identified in my GWAS warrant further consideration in relation to findings from previous research. The *COL4A1* gene encodes the alpha-1 subunit of collagen type IV, a component of basement membrane in the retinal vessels and the renal glomeruli. Different phenotypes have been linked to mutations of *COL4A1,* mainly in the brain and retinal structures. The main phenotype associated with this gene is stroke. Recent GWAS of white matter hyperintensity volumes and stroke (Traylor et al, 2016; Rannikmäe et al, 2015) reported a novel association of a variant in the *COL4A2* gene with these traits. Mutations in this gene

are closely related to the *COL4A1* gene. This particular phenotype suggests that the white matter changes seen on the brain magnetic resonance imaging scans of otherwise healthy elderly people reflect a similar disease process, the more severe forms of which underlie cerebral small vessel disease in patients with stroke. Studies in mice and humans have shown that mutations in both genes lead to basement membrane defects, which, as a consequence, weaken the blood vessels and alter vascular functions. Additionally, missense mutations in the intronic regions of this gene result in retention of mutant intracellular protein leading to a reticular endoplasmic dysfunction and stress (Rannikmäe et al, 2015).

Furthermore, this study also identified an association between the variant rs34013641 in gene *MYH11* and minimum venular tortuosity. This variant is located in the myosin 11 gene, which encodes myosin heavy chain family-protein. This protein has been found to be associated with multiple vascular disorders including heritable thoracic aortic disease, aortic stiffness, and aneurysms (Yamasaki et al, 2019; Keravnou et al, 2018). This protein is a cytoskeletal marker, encoded by this gene, and it plays an important role in the contraction of the smooth muscle cells of the vascular structure as well as in the development of atherosclerosis. Additionally, properties of the cytoskeleton include tissue remodelling, mechano-sensing and cell migration. All these actions are involved in the atherosclerotic process (Simmons et al, 2016). These proteins are also important markers of cytological tracing of cell type in the atherosclerotic plaque (Hansmeier et al, 2018).

Finally, the study also revealed an association between the loci rs10963694 and rs4977506 in *ADAMTSL1* gene with multifractal dimensions. Members of the ADAMTSL (a desintegrin and metalloproteinase with thrombospondin motifs-like protein) family are included in the abundant extracellular matrix proteins and are associated with the ADAMTS enzymes (proteases). The protein encoded, ADAMTSL-1, is suspected to be involved in extracellular matrix turnover. Generally, extracellular proteases are known to be involved in the breakdown of specific extracellular matrix elements, whereas intracellular proteases reorganise the cytoskeleton, and govern cell migration and differentiation. Both mechanisms are involved in the development of atherosclerosis. Interestingly, evidence has shown that these extracellular proteases play a critical role in de-establishing the fibrous

cap, leading to atherosclerotic plaque rupture (Hansmeier et al, 2018). This association adds more evidence of the multifactorial development of vascular diseases resulting in cerebrovascular disorders probably mediated by atherothrombotic processes. Gene defects in *ADAMTLS-1* raise the hypothesis that reduced integrity of the endothelial wall, together with inflammatory processes and defective vascular remodelling, plays an important role in the development of cerebral aneurysms (Arning et al, 2016). These processes could interact in the development of major cardiovascular outcomes such as stroke or cerebral aneurysms.

Overall, the most promising variants were located in genes, which encode three types of protein that may interfere in the causation of cardiovascular outcomes, mainly cerebrovascular disease. These genes are thus important in vascular function or involved in neuronal function.

In considering the results of the GWAS, it is also important to take into account the genetic heritability (h^2) of each retinal trait. The heritability estimates the degree of variation in a trait that is due to genetic variation between individuals in a specific population (Mayhew and Meyre, 2017). AVR has shown the lowest heritability in previous studies. In the Danish dataset of healthy twins, AVR heritability was 18% (Taarnhøj et al, 2006). While, in the Flemish analysis (Liu et al, 2013), after adjustment for traditional cardiovascular risk factors, AVR heritability was 27%; Kirin et al (2017) also reported a similar estimate of 27%. Conversely, in terms of CRAE and CRVE, genetic heritability estimates have shown some degree of variation. Twin studies have reported estimates of 70% and 83% (Taarnhøj et al, 2006) and 66% and 72% (Fahy et al, 2011), respectively. Studies in the general population have reported lower genetic heritability for CRAE and CRVE; 32% and 43% (Kirin et al, 2017) and 21% and 34% (Liu et al, 2013), respectively. Despite the variations in these findings, all discussed studies suggest that CRVE has the higher component of genetic heritability.

Only two studies have analysed the genetic heritability for retinal tortuosity. Taarnhøj et al (2008) showed a genetic heritability of 82% for retinal arteriolar tortuosity, while Kirin et al (2017) reported estimates of 55% and 21%, respectively. Importantly, in

the latter study, there was a high degree of genetic correlation (60%) between arteriolar and venular tortuosity. Heritability of multifractal dimension has not currently been analysed, but heritability of monofractal dimension (using the box counting method) was 79% in the Danish Twin Study (Vergmann et al, 2017) and only 22% in the general population in Orkney (Kirin et al, 2017).

Retinal arteriolar tortuosity appears to be a vascular trait with an important genetic component that could lead to vascular disease. Findings of this study thus lays important foundations for enhancing the knowledge of genetic risk factors underlying retinal vasculature and its possible association with vascular disease.

8.1.6 Possible pathophysiological mechanisms underlying associations of retinal traits with major cerebrovascular events

The association of arteriolar tortuosity with incident cerebrovascular events was one of the main findings of this study. One explanation for this association could lie in the fact that retinal vessels share common anatomical and physiological features with cerebral arterioles. Impaired microcirculation of the brain (cerebral small vessel disease), is increasingly recognised as a cause of cognitive decline and neurodegenerative disorders as well as contributing to stroke (McGrory et al, 2019; Rannikmäe et al, 2015).

Findings from this study on arteriolar retinal tortuosity, multifractal dimensions and genetic variants appear to be consistent with the biological mechanisms that are involved in the development of cerebrovascular disease. These mechanisms could also contribute to a series of degenerative changes in the cerebral vasculature such as fibrinoid degeneration, fibrous nodules, fibrohyalinoid thickening and calcification (Wu et al, 2017).

Arteriolar retinal tortuosity has been found in people with T2D (Sasongko et al, 2016). This finding had been associated with longer duration of diabetes and early stages of diabetic retinopathy. Possible mechanisms involved in this process include hyperglycaemia-mediated loss of auto regulatory function of the vessels (e.g. compromised function of endothelium), resulting in impaired compensatory

mechanism for hydrostatic pressure. This may result tin instability of the wall arterioles against longitudinal traction and transmural pressure causing tortuous vessels and dilation (Ciurica et al, 2019). Buckling instability is a possible mechanism that may lead to arteriolar tortuosity and also, the ratio of the media thickness to the adventitia thickness is shown to have a dramatic impact in arteriolar instability (Vandiver, 2015). Factors involved in these processes include the genetic defects in elastogenesis or collagen synthesis. In aging arteries, collagen degradation, deposition, and structural alteration may also occur.

Cerebral microvascular abnormalities could be caused by micro-atheroma, endothelial dysfunction or inflammation (Davis and Donnan, 2014). The endothelial cells of the cerebral vascular tissues play a role in the vasomotor control regulating cerebral blood flow, with the perfusion of the capillaries controlled by the regulation of the upstream arterioles (Mejía-Renteria, et al 2018).

Basement membranes adjoining the endothelium, comprise of key proteins (e.g. COL4A1 and COL4A2) which may then influence the structure of the retinal vessel and thereby the cerebral microvasculature. Additionally, the presence of impaired blood flow (e.g. turbulent) brought on by cardiovascular risk factors like hypertension, may induce activation of the endothelium. The activation of intracellular pathways and gene expression induces changes in the vessel tone (vasoconstriction), structural changes in the basement membrane, cytoskeleton and extracellular matrix, increased production of inflammatory cytokines, high oxidative stress and a leaky cell barrier. This process may lead to a “weak” vessel, which as consequence can modify the structural strength of the vessels, resulting in more tortuous arterioles and venules. These key proteins (ADAMTSL-1) may also play an important role in the development of atherosclerotic plaque and rupture.

8.2 Strengths and weaknesses of the research

8.2.1 Study population

The ET2DS is a well-phenotyped prospective cohort in which study participants were sampled and recruited directly from, and are therefore representative of, the Lothian region of Scotland (using the Lothian Diabetes register), as opposed to using the

subgroup of people with diabetes participating in a larger study, which is generally the case for other studies in this topic area. The Lothian region includes not only the city of Edinburgh but also smaller towns and rural communities in the surrounding area in East Scotland. While other cohort studies have usually recruited people from a single city or town, and often do not specify the type of population included. Furthermore, the ET2DS included people who managed their type 2 diabetes from a range of treatment methods, including from diet control to insulin treatment.

At baseline, participants in the ET2DS were largely similar with respect to demographic and clinical features compared to those who did not participate in the study (Price et al, 2008). There were slightly more men than women recruited into the study and people from the least deprived socio-economic status group were more likely to agree to participate than those from the most deprived socio-economic group. Nonetheless, these differences were small, and overall, the participants were largely representative and findings generalisable to the target population.

8.2.2 Accuracy and completeness of data collection

The ET2DS is a cohort thoroughly characterised phenotypically for a wide range of risk factors and biomarkers. Data were carefully collected by trained research staff according to strict protocols (standard operating procedures), ensuring that this process was consistent between research staff and over time, accurate, and with only a small amount of missing data. Strict quality control measures were used in the processing of the biomarkers and genotyping. This extensive phenotyping, quality control and accuracy of data collection are key strengths of the ET2DS cohort.

8.2.3 Prospective design of the ET2DS and follow up for cardiovascular events

The prospective design of the ET2DS is essential for longitudinal analyses to investigate the relationship of baseline cardiovascular risk factors with the development of subsequent cardiovascular events. Complete data on incident and recurrent cardiovascular events was required for my analyses of the association of quantitative retinal traits with cardiovascular risk. These incident events were

collected and recorded, following pre-defined protocols and using a systematic approach to reduce loss of follow-up and misdiagnosis of the clinical events at the four and eight-year stage of the study. ET2DS researchers used several sources to identify and confirm events. At the four-year follow-up, this included self-completion questionnaires, assessment of electrocardiograms and ISD data linkage. At the eight-year follow-up, a combination of procedures was used, including ISD data linkage combined with a review of clinical notes. The identification of events was as comprehensive as possible during the four and eight-years follow-up, however, events could be missed in participants who moved outside Scotland.

8.2.4 Method used to analyse retinal images

The software used in this study, **V**ascular **A**ssessment and **M**easurement **P**latform for **I**mages of the **RE**tina (VAMPIRE), is a semi-automatic software application developed by consortia of the University of Edinburgh and University of Dundee. This software quantifies some parameters of the retinal vasculature using images from the fundus camera taken in clinics. This free software is user-friendly; it can be easily installed and used on Windows platforms. Each software version presents improvements and updated algorithms for the analysis of the retinal quantitative traits. This software has been used in different datasets including UK Biobank (MacGillivray et al, 2015), the Lothian Birth Cohort 1936 (McGrory et al, 2019; McGrory et al, 2017) and ORCADES from the Orkney Islands in Scotland (Kirin et al, 2017). The use of this platform across multiple studies demonstrates its feasibility to measure the retinal vasculature in a cost-efficient way.

VAMPIRE uses a modified 2-D Gabor wavelet supervised classification algorithm for automatic vessel detection and locates centre lines through skeletonisation of the binary vessel map (McGrory et al, 2018). This enhances the detection of arterioles and venules. Optic disc automatic detection algorithm is also included in the analysis, whereas other software applications, such as SIVA (Singapore “I” Vessel Assessment), require the operator to assign and select the area of the optic disc. This may create bias due to inter-operator differences. Automatic detection of the

optic disc optimises the application to detect accurately either arterioles or venules and saves time in this process.

8.2.5 ET2DS genotyping and imputation

Genotyping of the ET2DS was performed used MetaboChip array. This array was developed using hundreds of loci for type 2 diabetes, coronary artery disease, myocardial infarction, cardiometabolic traits including, glucose, insulin levels, lipids levels, blood pressure and anthropometric traits such as body mass index (Voight et al, 2012). The MetaboChip genotyping array was designed to establish associations with these cardiometabolic loci, which included nearly 200 000 SNP markers. This assay offers a powerful and cost-effective approach to follow-up large-scale genotyping and for further genotype imputation.

The ability to use imputed data was a strength of my analysis of the ET2DS. Several GWAS have systematically evaluated the contributions of genetic factors to various complex diseases along with quantitative traits including blood pressure, human height and cholesterol levels. These contributions have revealed important factors involved in the pathophysiology of these traits, and are expected to enable the development of new therapeutic drugs. GWAS analyses have greatly changed human genetics in the last 10 years by providing a new, systematic method that can provide deeper insights into disease biology (Das et al, 2018). Low frequent variant genotypes that are not directly included in the GWAS array can be reconstructed by comparing each sample to a reference panel of sequenced genomes. This method, which is known as genotype imputation, involves estimating genotypes that have not been directly genotyped. 1000 Genotypes haplotypes panel offers a particularly large and dense reference panel that is commonly used as an imputation reference panel, particularly in GWAS studies. Imputation has thus helped to accelerate fine-mapping efforts, aid the combination of factors across meta-analyses, and increase the power of gene mapping analyses. Imputation was done in the ET2DS on cleaned genotypes in three phases - chunking, phasing and imputing - and the resulting final file contained approximately 4.5 million autosomal SNPs, which were then available for extended analysis for my thesis.

8.2.6 Design of the analyses

Special care was taken in developing the analysis plan to arrive at the most accurate and clinically informative results. Prospective analyses, as used in my study, which consider the time relationship between predictor (retinal vessel traits) and outcome (cardiovascular disease), can be more accurate than cross-sectional studies. This is because such analyses involve repeated observations of study participants over time and often represent the most comprehensive method as they use all available information of the population over the risk period (Pearce et al, 2012). Furthermore, the choice of the covariates in the models performed was made according to traditional cardiovascular risk factors, which have been identified in well-established cohorts such as the Framingham Study. Analyses were performed using different models in order to explore the independence of the association (if established) of quantitative retinal traits with the cardiovascular outcomes.

I performed the analyses carefully performed and placed special attention on the distribution of all quantitative retinal traits. Since, it is assumed that these traits are normally distributed; I adopted a stringent adherence to quality control and the statistical analyses. Violation of the assumption that the quantitative traits are normally distributed can severely affect the power and lead to type I error (Feingold, 2002). Thus, in this study, I tested harmonisation using parametric transformation to approximate to normality.

In this study, GWAS analysis was included to increase the understanding of major vascular complications associated with retinal parameters. Indeed, one key criterion to develop a GWAS is to acquire further informative results, which inform us about the pathophysiology of the retinal vasculature and cardiovascular events. Data generated from previous GWAS studies have been exploited for addressing many scientific questions other than SNP- trait associations (Visscher et al, 2017). GWAS have also been successfully implemented for better defining the relative role of genes and the environment in disease risk enabling preventative and personalised medicine (Visscher et al, 2017). For example, GWAS signals are known druggable targets and these potential variants may be used in further phase clinical trials, potentially saving huge costs for pharmaceutical production, which can be especial beneficial for public health systems.

Furthermore, GWAS of quantitative retinal traits were adjusted for sex and age, in this study. Recently, a large number of GWAS have been published for human traits adjusted for correlated traits. Adjustment for covariates in GWAS can have two purposes: first, to account for potential confounding factors that can bias SNP effect estimates and second, to improve statistical power by reducing residual variance. Adjustment for environmental or demographic factors such as age and sex may increase statistical power. This is because accounting for true risk factors decreases the residual variance of the outcome and hence increases the ratio of the true effect size of a predictor of interest over the total phenotypic variance resulting in better statistical power (Aschard et al, 2015).

8.3 Limitations

8.3.1 Generalisability

Although, the ET2DS is representative of the target population (older people with type 2 diabetes), care must be taken when generalising the results beyond that target population. Firstly, the participants recruited into the ET2DS are older adults aged between 60 and 75 years at baseline, so the results may differ from those of other studies, which recruited younger participants. Moreover, there is a potential impact of a healthy survivor bias, as people recruited at age 60 years or above might be biologically different to those who died when they were younger. Secondly, the majority of the population are north Europeans, reflecting the limited ethnic variability in this region of the UK. This limits generalisability of the results to multi-ethnic populations. Thirdly, people recruited into the ET2DS already had type 2 diabetes. This itself is a cardiovascular risk factor that may cover up other vascular risk factors, which are important in the development of cardiovascular complications. It is well known that the duration of type 2 diabetes, higher BMI and poor glycaemic control are risk factors for cardiovascular complications (Einarson et al, 2018). In fact, endothelial function and its regulation including vasodilation and vasoconstriction, may be impaired in hyperglycaemic people with type 2 diabetes, which results in a greater risk of developing major cardiovascular events (Loader et al, 2015). For instance, a recent study (Liu et al, 2018) using Mendelian randomization analysis

provided evidence to suggest that type 2 diabetes may be causally associated with cerebral small vessel disease (e.g. lacunar stroke) and fractional anisotropy.

8.3.2 Missing data

The loss of follow-up and missing outcome data is a major limitation of prospective cohort studies. Despite previous data cleaning, the baseline variables used for this thesis still included missing data for covariates for a few cases, prior to carrying out formal analysis. However, the number of missing data in the covariates used in this thesis was below 5% of the total number of the individuals included. Schafer (1999) emphasised that a missing rate of 5% or less is inconsequential. Generally, in regression models, only complete cases are analysed at each stage of the model. This in practice leads to more cases being part of the analysis in models adjusted for age and sex, than fully adjusted models, where a case with any of the covariates missing is excluded from the analysis. Therefore, each step in the regression models may not include the exact same cases.

Missing data with respect to multifractal dimensions from the retinal images was close to 5% of the total number of individuals in the ET2DS. While this loss of data might suggest a small risk of bias, Bennett (2001) asserts that statistical analysis is more likely to be biased when more than 10% of data are missing.

8.3.3 Analysis plan

There are some limitations of the statistical analysis used in this study. Individuals in the study reported taking lipid-lowering and antihypertensive medications; this may have altered the results of total cholesterol and blood pressure, which were included as covariates in the analysis. Including medication use in the definition of ‘hypertension’ or ‘hypercholestoreamia’ may be more reflective of a person’s increased lifetime risk of vascular damage due to these conditions, but this could be mitigated by the positive effects of the treatment.

Use of one-off measures of cholesterol and BP on the other hand could underestimate the effect of (treated) hypertension and hypercholesterolaemia. If aim is to assess prediction rather than knowing about aetiology, likely that both measures would need to be tested in developing best predictive models. Therefore, this may have introduced bias in the results.

In this study, I used eGFR as a covariate for renal function in the analysis models. Although, eGFR is a common biomarker of renal impairment and has been associated with cardiovascular prognosis and mortality (Fung et al, 2017), microalbuminuria is known to be the earliest clinical evidence of kidney disease in this population (Collins et al, 2010). Epidemiologic studies suggest that population patterns of chronic kidney disease among adults with type 2 diabetes, are not as uniform as those noted among adults with type 1 diabetes. Focusing solely on urine albumin excretion to screen for chronic kidney disease may miss a substantial number of cases in adults with type 2 diabetes, a more heterogeneous group of patients who are generally older and have more comorbid conditions at diagnosis compared with adults with type 1 diabetes (Kramer et al, 2018). Other etiologies for chronic kidney disease, which are not associated with increased urine albumin excretion, may be present at the time of diagnosis of type 2 diabetes and over the course of the disease, such as renal vascular disease and cholesterol emboli. Also, tubulointerstitial changes due to the presence of comorbid conditions, including long standing hypertension and senenscence of glomeruli due to aging may be present.

Moreover, studies have shown that stage 3 or higher chronic kidney disease stage (GFR <60 ml/min/1.73 m2) may occur in the absence of increased urine albumin excretion in a substantial proportion of adults with diabetes, and screening this population for elevated urine albumin excretion alone will miss a considerable number of chronic kidney disease cases (Alicic et al, 2017). Importantly, the use of angiotensin-converting enzyme inhibitors (ACEi) or angiotensin receptor blockers (ARBs) leads to decreased development microalbuminuria to macroalbuminuria and results in a reduced risk for CVD and mortality (Persson et al, 2016). These medications were taken by people of ET2DS; hence, microalbuminuria could have been mitigated by the positive effect of these medications.

Thus, taking into account these aforementioned limitations of microalbuminuria, I decided to include the biomarker of eGFR as a covariate of renal function in this population in my analysis models.

The power to discover new disease-associated genetic variants critically depends on the underlying genetic architecture, i.e., the number of risk loci and their frequencies and effect sizes. It has been stipulated that GWAS requires larger sample sizes to achieve an adequate statistical power as it evaluates thousands of SNPs. GWAS studies on quantitative traits in recent times, have included large sample sizes of more than 1 000 000 individuals (Wuttke et al, 2019). Testing a large number of SNP markers leads to a large number of multiple comparisons (multiple testing) and thus increased false positive rates (Hong and Park, 2012). Statistical methods, such as Bonferroni correction, are generally applied to avoid false positive (type I error) rates. However, its use to set the significance threshold might be too strict when considering the correlation among genetic variants. Increasing sample size may avoid these considerations and lead to adequate statistical power, which is essential to elucidate genetic associations.

In modern statistics, it is important to use tools when handling large-scale multiple testing datasets. Benjamini and Hochberg (1995) introduced the false discovery rate as a useful tool when multiple comparisons are carried out . This method is based on setting a limit on the false discovery rate, and this is generally preferable (Colquhoun, 2014). False discovery rate control is suggested as complementary to the use of point estimate and confidence intervals. It helps to evaluate the extent to which effect sizes are over-estimated, especially in underpower experiments. Following further recommendations, false discovery rate was examined in all significant models in the analysis, corroborating the findings of these analyses.

For my findings, a larger sample size would thus help demonstrate whether results still remain significant. Replication or meta-analysis including other datasets would be recommended to reproduce the original results and confirm true findings. This step was beyond the scope of this thesis. Nevertheless, it is important to consider that GWAS for quantitative retinal traits has been explored in few studies compared

to other human traits such as blood pressure or serum cholesterol, supporting the rationale for undertaking these exploratory analyses.

8.3.4 Method used to analyse retinal images

The method used to analyse retinal image may have introduced certain limitations including the analysis of only one image, a limited area of the retinal vasculature analysed, few traits obtained and non-established algorithms across different platforms.

First, for this analysis, I used only the best quality image from either the right or left eye. Despite moderate correlation of the retinal measurements between the two eyes (see methods chapter), variations may exist. High correlation ($r \geq 0.70$) is usually expected to consider the use of only one side. Measurements of both sides could have been done but this option was excluded due to the excessive work involved and time limitation for the purposes of this study.

Second, I only used the centrally located image in the analysis. However, for each participant, seven field images were taken for each eye at baseline. These images involved extensive retinal vasculature that may have offered an enriched assessment of the vasculature, as it includes other characteristics such as vessel length or multiple branching.

Third, VAMPIRE software measures only a limited number of retinal traits, and other traits may provide further insights into the association of the retinal vasculature with cardiovascular disease. Currently, other available software applications measure several additional traits of the retinal vasculature, including number of first branching arterioles and venules, branching coefficient for arteriole and venule, junctional exponent deviation for arterioles and venules and length-to-diameter ratio arteriole and venule (e.g. SIVA, Singapore ‘‘I’’ Vessel Assessment, National University of Singapore). Further research can include the use of such traits to examine the retinal vasculature and its links with cardiovascular disease.

Whilst multiple software applications have offered the opportunity to explore the role of the retinal microvasculature in the physiopathology of cardiovascular disorders,

the application of these retinal measurements in the clinical settings is yet to be fully established, partially due to methodological limitations. In the absence of ground truth measurements of the retinal vasculature, the accuracy (or the degree to which an instrument measures the true value of a variable) of such software applications remains to be determined (McGrory et al, 2018). Potential sources of variations among the software application include physiological characteristics of the eye, angle of imaging, image quality, type of camera used, algorithms, and intra-observer variability (Trucco et al, 2013). Method-comparison studies have been used to assess how measurements from different software applications agree, including agreement between SIVA and VAMPIRE software. McGrory et al (2018) reported intra-class correlation coefficients for vessel width, fractal dimensions and tortuosity indicated poor to limited agreement. The study also revealed proportional bias in the majority of measurements, and systematic bias in all measurements.

Since semi-automated retinal vasculature assessment appears to be software dependent, it is important that future studies work on standardisation and validation across software platforms. McGrory et al (2018) take this recommendation further by suggesting the formation of a consortia of retinal imaging clinicians and software developers to conduct such comparative analysis.

8.4 Conclusions and recommendations for future research

Coronary heart disease and cerebrovascular disease are two of the main causes of mortality in the UK and worldwide, hence, there is little doubt that research in both fields is urgently required to improve our understanding of these diseases and translate these insights into clinical solutions. Similarities between the retinal vasculature and other microcirculations suggest that exploration and examination of the retinal vasculature can be a vital avenue of research in this area. Despite increasing evidence, many aspects of the relationship between retinal vasculature and major cardiovascular events (e.g. stroke) remain poorly understood. The results from this study firstly point out the significant association between quantitative retinal traits and cerebrovascular events, and indicate that these traits, namely arteriolar tortuosity, venular tortuosity and multifractal dimensions can be used as potential

imaging traits which could provide important knowledge on the pathogenesis of cerebrovascular events.

While these results were found to be significant, external validation of the same, in larger datasets is required. In order to expand the generalisability of future results, such datasets should include younger individuals, multi-ethnic populations, and if sufficient number of cardiovascular events are captured, restrict analyses to people with no previous CVD. It would be also interesting to analyse prospectively the association of quantitative retinal traits with more specific cardiovascular phenotypes including the stroke subtypes (e.g. lacunar, cardioembolic, haemorrhagic), since there may be differences between these groups.

Another key recommendation for further research is the replication of the GWAS findings to ensure that the genetic associations observed represent credible associations and are not chance findings or an artefact due to uncontrolled biases (Hill, 1965). This forms part of reproducibility, which is a key step in the scientific method. Epidemiologically, the repeated observations of the association carried out by different teams, in different datasets, using different methodologies are taken as true evidence of the association. This is because the repeated observations add quantitative and qualitative evidence. While the former informs us that the association is not due to chance alone, the latter informs us that replication across different designs and populations is not due to uncontrolled bias affecting a single study (Kraft et al, 2009).

Two approaches can be used for replicating the GWAS findings. First, consortia of multiple GWAS have contributed to replicating associations of GWAS results and this approach would help confirm the results obtained from the quantitative retinal traits in this thesis. Increasingly, larger sample sizes will be needed to detect and reproduce the increasingly small effect sizes at common genetic variants that remain undetected in early analyses (Kraft et al, 2009). Second, further research should consider meta-analysis of multiple GWAS of quantitative retinal traits, and of note, in Scotland, GWAS of quantitative retinal traits has already been conducted in the ORCADES dataset (Kirin et al, 2017). An extended meta-analysis can also satisfy the requirement for replication in the context of discovery of novel genetic variants,

without the need to genotype yet more samples, as long as the combined evidence for association is robust and consistent.

Cardiovascular risk prediction is essential in identifying and managing people at risk for cardiovascular disorders. Phenotypic information from the retinal vasculature may provide prognostic information on risk of CVD and improve CVD risk stratification when incorporated into established risk models in people with T2D (Ho et al, 2017).

Artificial intelligence and machine learning may help to analyse retinal parameters in a cost-efficient and accurate way. Recent medical studies have used deep learning, a subtype of machine learning, to generate algorithms that diagnose diabetic complications such as diabetic retinopathy, from retinal images. The accuracy of the results of such studies are comparable to human experts (Poplin et al, 2018). This study also showed that application of deep learning to retinal fundus images alone helped to predict cardiovascular risk factors such as age, gender and systolic blood pressure. These findings demonstrate that the vascular retinal traits contain information on cardiovascular disease and that these traits could be measured with a high degree of precision using such techniques.

Validation of the findings from future studies will also help to determine whether the analysis of the quantitative retinal traits may be able to improve or replace some of the other cardiovascular risk biomarkers such as lipids profile, to produce a more precise cardiovascular risk score (Poplin et al, 2018). A combination of the approaches discussed above along with robust epidemiological methods using quantitative retinal parameters will thus enrich our understanding of the association between retinal microcirculation and major cardiovascular events.

Chapter 9 Bibliography

Abdul-Ghani, M., DeFronzo, R.A., Del Prato, S., Chilton, R., Singh, R., & Ryder, R. 2017. Cardiovascular Disease and Type 2 Diabetes: Has the Dawn of a New Era Arrived?. *Diabetes Care*, 40, 813–820.

Alicic, R.Z., Rooney, M.T., Tuttle, K.R. 2017. Diabetic Kidney Disease: Challenges, Progress and Possibilities. *Clin J Am Soc Nephrol*, 12, 2032-2045.

Arning, A., Jeibmann, A., Köhnemann, S., Brokinkel, B., Ewelt, C., Berger, K. et al. 2016. ADAMTS genes and the risk of cerebral aneurysm. *J Neurosurg*, 125, 269-274.

Aronow, W.S., & Shamliyan, T.A. 2018. Blood pressure targets for hypertension in patients with type 2 diabetes. *Ann Transl Med*, 6, 199.

Aschard, H., Vilhjálmsson, B. J., Joshi, A. D., Price, A. L., & Kraft, P. 2015. Adjusting for heritable covariates can bias effect estimates in genome-wide association studies. *Am J Hum Genet*, 96, 329–339.

Avgerinos, K.I., Spyrou, N., Mantzoros, C.S. & Dalamaga, M. 2019. Obesity and cancer risk: Emerging biological mechanisms and perspectives. *Metabolism*, 92, 121-35.

Azegrouz, H., Trucco, E., Dhillon, B., MacGillivray, T., & MacCormick, I.J. 2006. Thickness dependent tortuosity estimation for retinal blood vessels. Conf Proc IEEE *Eng Med Biol Soc*, 1, 4675-8.

Bakken, T. E., Roddey, J. C., Djurovic, S., Akshoomoff, N., Amaral, D. G., Bloss, C.et al. 2012. Association of common genetic variants in GPCPD1 with scaling of visual cortical surface area in humans. *Proc Natl Acad Sci USA*, 109, 3985–90.

Benjamini, Y., & Hochberg, J.1995. Controlling the False Discovery Rate: A Practical and Powerful Approach to Multiple Testing. *J R Stat Soc B*, 57, 289-300.

Bankhead, P., Scholfield, C.N., McGeown, J.G. & Curtis, T.M. 2012. Fast retinal vessel detection and measurement using wavelets and edge location refinement. *PLoS One*, 7, e32435.

Beagley, J., Guariguata, L., Weil, C. & Motala, A.A. 2014. Global estimates of undiagnosed diabetes in adults. *Diabetes Res Clin Pract*, 103,150-60.

Bennett, D.A. 2001. How can I deal with missing data in my study? *Aust N Z J Public Health*, 25, 464-9.

Bertoluci, M.C. & Rocha V.Z. 2017. Cardiovascular risk assessment in patients with diabetes. *Diabetol Metab Syndr*, 9:25.

Beyens, A., Albuisson, J., Boel, A., Al-Essa, M., Al-Manea, W., Bonnet, D. et al. 2018. Arterial tortuosity syndrome: 40 new families and literature review. *Genet Med*, 20,1236-45.

Bhatnagar, P., Wickramasinghe, K., Wilkins, E. & Townsend, N. 2016. Trends in the epidemiology of cardiovascular disease in the UK. *Heart*, 102, 1945-52.

Bots, S.H., Peters, S.A.E. & Woodward, M. 2017. Sex differences in coronary heart disease and stroke mortality: a global assessment of the effect of ageing between 1980 and 2010. *BMJ Glob Health*, 2, e000298.

British Heart Foundation Statistics. 2017 [Online] Available: https://www bhf org uk/what-we-do/our-research/heart-statistics [Accessed 10 October 2017]

Captur, G., Karperien, A.L., Hughes, A.D., Francis, D.P. & Moon, JC. 2017. The fractal heart - embracing mathematics in the cardiology clinic. *Nat Rev Cardiol*,14, 56-64.

Catelan, D., & Biggeri, A. 2010. Multiple testing in disease mapping and descriptive epidemiology. *Geospat Health*, 4, 219-229.

Causin, P., Guidoboni, G., Malgaroli, F., Sacco, R. & Harris, A. 2016. Blood flow mechanics and oxygen transport and delivery in the retinal microcirculation:

multiscale mathematical modeling and numerical simulation. *Biomech Model Mechanobiol*, 15, 525.

Cavalot, F., Pagliarino, A., Valle, M., Di Martino, L., Bonomo, K., Massucco, P. et al 2011. Postprandial blood glucose predicts cardiovascular events and all-cause mortality in type 2 diabetes in a 14-year follow-up: lessons from the San Luigi Gonzaga Diabetes Study. *Diabetes Care*, 34, 2237–2243.

Cavero-Redondo, I., Peleteiro, B., Álvarez-Bueno, C., Garrido-Miguel, M., Artero, E.G. & Martinez-Vizcaino, V. 2017. The effects of physical activity interventions on glycated haemoglobin A1c in non-diabetic populations: a protocol for a systematic review and meta-analysis. *BMJ Open*, 7, e015801.

Chatterjee, S., Khunti, K., & Davies, M.J. 2017. Type 2 diabetes. *Lancet*, 389, 2239-51.

Cheng, C.Y., Reich, D., Wong, T.Y, Klein, R., Klein, B.E, Patterson, N. et al. 2010. Admixture mapping scans identify a locus affecting retinal vascular caliber in hypertensive African Americans: the Atherosclerosis Risk in Communities (ARIC) study. *PLoS Genet*,15, e1000908.

Chesnutt, J.K. & Han, H.C. 2011. Tortuosity triggers platelet activation and thrombus formation in microvessels. *J Biomech Eng*, 133, 121004.

Cheung, C.Y., Zheng, Y., Hsu, W., Lee, M.L., Lau, Q.P., Mitchell, P. et al. 2011. Retinal vascular tortuosity, blood pressure, and cardiovascular risk factors. *Ophthalmology*, 118, 812-18.

Cheung, N., Liew, G., Lindley, R.I., Liu, E.Y., Wang, J.J., Hand, P. et al. 2010. Retinal fractals and acute lacunar stroke. *Ann Neurol*, 68, 107-11.

Cho, N.H, Shaw, J.E., Karuranga, S., Huang, Y., da Rocha Fernandes, J.D., Ohlrogge, A.W. & Malanda, B. 2018. IDF Diabetes Atlas: Global estimates of diabetes prevalence for 2017 and projections for 2045. *Diabetes Res Clin Pract*, 138, 271-81.

Christophersen, I.E., Rienstra, M., Roselli, C., Yin, X., Geelhoed, B. & Barnard J. et al. 2017. Large-scale analyses of common and rare variants identify 12 new loci associated with atrial fibrillation. *Nat Genet*, 49, 946-52.

Ciurică, S., Lopez-Sublet, M., Loeys, B.L., Radhouani, I., Natarajan, N., Vikkula, M. et al. 2019. Arterial tortuosity. *Hypertension*, 73, 951-60.

Collins, A.J., Foley, R.N., Herzog, C., Chavers, B.M., Gilbertson, D., Ishani, A. et al. 2010. Excerpts from the US Renal Data System 2009 Annual Data Report. *Am J Kidney Dis*, 55, S1-420, A6-7.

Colquhoun, D. 2014. An investigation of the false discovery rate and the misinterpretation of *p*-values. *R Soc Open Sci*, 19, 140216.

Costa, E.V., & Nogueira, R. de A. 2015. Multifractal dimension and lacunarity of yolk sac vasculature after exposure to magnetic field. *Microvasc Re*s, 99, 1-7.

Country, M.W. 2017. Retinal metabolism: A comparative look at energetics in the retina. *Brain Res*, 1672,50-57.

Das, S., Abecasis, G.R. & Browning, B.L. 2018. Genotype Imputation from Large Reference Panels. *Annu Rev Genomics Hum Genet*, 19, 73-96.

Davis, S., & Donnan, G.A. 2014. Time is Penumbra: imaging, selection and outcome. The Johann jacob wepfer award 2014. *Cerebrovasc Dis*, 38, 59-72.

De Boever, P., Louwies, T., Provost, E., Int Panis, L. & Nawrot, T.S. 2014. Fundus photography as a convenient tool to study microvascular responses to cardiovascular disease risk factors in epidemiological studies. *J Vis Exp*, 92, e51904.

Dobrin, P.B. 1988. Mechanics of normal and diseased blood vessels. *Ann Vasc Surg*, 2, 283-94.

Doubal, F.N, MacGillivray, T.J, Patton, N., Dhillon, B., Dennis, M.S. & Wardlaw, J.M. 2010. Fractal analysis of retinal vessels suggests that a distinct vasculopathy causes lacunar stroke. *Neurology*, 74,1102-7.

Doubal, F.N., Hokke, P.E. & Wardlaw, J.M. 2009. Retinal microvascular abnormalities and stroke: a systematic review. *J. Neurol. Neurosurg*. Psychiatry, 80,158-165.

Drobnjak, D., Munch, I. C., Glümer, C., Faerch, K., Kessel, L., Larsen, M. et al. 2016. Retinal Vessel Diameters and Their Relationship with Cardiovascular Risk and All-Cause Mortality in the Inter99 Eye Study: A 15-Year Follow-Up. *J Ophthalmol*, 2016, 6138659.

Early Treatment Diabetic Retinopathy Study Research Group. 1991. Grading diabetic retinopathy fromstereoscopic color fundus photographs- an extension of the modified Airlie House classification. ETDRS Report Number 10. *Ophthalmology*, 98, 786–806.

Eelen, G., de Zeeuw, P., Simons, M. & Carmeliet, P. 2015. Endothelial cell metabolism in normal and diseased vasculature. *Circ Res*, 116, 1231-44.

Ehret, G.B. 2010. Genome-wide association studies: Contribution of genomics to understanding blood pressure and essential hypertension. *Curr Hypertens Resp*, 12, 17-25.

Einarson, T.R., Acs, A., Ludwig, C. & Panton, U.H. 2018. Prevalence of cardiovascular disease in type 2 diabetes: a systematic literature review of scientific evidence from across the world in 2007-2017. *Cardiovasc Diabetol*, 17, 83.

Emdin, C.A., Rahimi, K., Neal, B., Callender, T., Perkovic, V., Patel, A. 2015. Blood Pressure Lowering in Type 2 Diabetes: A Systematic Review and Meta-analysis. *JAMA,* 313, 603–615.

Emerging Risk Factors Collaboration, Sarwar, N., Gao, P., Seshasai, S.R., Gobin, R., Kaptoge, S. et al. 2010. Diabetes mellitus, fasting blood glucose concentration, and risk of vascular disease: a collaborative meta-analysis of 102 prospective studies. *Lancet*, 375, 2215-22.

Fahy, S.J, Sun, C., Zhu, G., Healey, P.R, Spector, T.D, Martin NG. et al. 2011.The relationship between retinal arteriolar and venular calibers is genetically mediated,

and each is associated with risk of cardiovascular disease. *Invest Ophthalmol Vis Sci*, 52, 975-81.

Feingold, E. 2002. Regression-based quantitative-trait-locus mapping in the 21st century. *Am J Hum Genet*, 71, 217–222.

Flammer, J., Konieczka, K., Bruno, R.M., Virdis, A., Flammer, A.J. & Taddei, S. 2013. The eye and the heart. *Eur Heart J*, 34, 1270-8.

Fraz, M.M., Welikala, R.A., Rudnicka, A.R., Owen, C.G., Strachan, D.P. & Barman, S.A. 2015. QUARTZ: Quantitative analysis of retinal vessel topology and size an automated system for quantification of retinal vessels morphology. *Expert Syst Appl*, 42:7221-7234.

Fung, C. S., Wan, E. Y., Chan, A. K., & Lam, C. L. 2017. Association of estimated glomerular filtration rate and urine albumin-to-creatinine ratio with incidence of cardiovascular diseases and mortality in chinese patients with type 2 diabetes mellitus - a population-based retrospective cohort study. *BMC Nephrol*, 18, 47.

Glinka, M., Herrmann, T., Funk, N., Havlicek, S., Rossoll, W., Winkler, C., & Sendtner, M. 2010. The heterogeneous nuclear ribonucleoprotein-R is necessary for axonal beta-actin mRNA translocation in spinal motor neurons. *Hum Mol Genet*, 19, 1951-66.

Guo, V.Y., Chan, J.C, Chung, H., Ozaki, R., So, W., Luk, A. et al. 2016. Retinal information is independently associated with cardiovascular disease in patients with Type 2 diabetes. *Sci Rep*, 12, 19053.

Han, H.C, Chesnutt, J.K, Garcia, J.R., Liu, Q. & Wen, Q. 2013. Artery buckling: New phenotypes, models, and applications. *Ann Biomed Eng*, 41, 1399-410.

Han, H.C. 2012. Twisted blood vessels: symptoms, etiology and biomechanical mechanisms. *J Vasc Res*, 49,185-97.

Hansmeier, N., Buttigieg, J., Kumar, P., Pelle, S., Choi, K.Y., Kopriva, D. & Chao, T.C. 2018. Identification of Mature Atherosclerotic Plaque Proteome Signatures

Using Data-Independent Acquisition Mass Spectrometry. *J Proteome Res*, 17, 164-176.

Hao, H., Sasongko, M.B., Wong, T.Y., Che Azemin, M.Z., Aliahmad, B., Hodgson, L. et al. 2012. Does retinal vascular geometry vary with cardiac cycle? *Invest Ophthalmol Vis Sci*, 53, 5799-805.

Hartnett, M.E., Martiniuk, D., Byfield, G., Geisen, P., Zeng, G. & Bautch, V.L. 2008. Neutralizing VEGF decreases tortuosity and alters endothelial cell division orientation in arterioles and veins in a rat model of ROP: relevance to plus disease. *Invest Ophthalmol Vis Sci*, 49, 3107-14.

Heidrich, J., Wellmann, J., Heuschmann, P.U., Kraywinkel, K. & Keil U. 2007. Mortality and morbidity from coronary heart disease attributable to passive smoking. *Eur Heart J*, 28, 2498-502.

Higgins, J. P. T. & Green, S. 2011. Cochrane Handbook for Systematic Reviews of Interventions Version 5.1.0 [updated March 2011]. [Online]. Available: http://handbook-5-1.cochrane.org/

Hill, A.B.1965. The environment and disease: association or causation? *Proc R Soc Med*, 58, 295-300.

Hill, R.A., Tong, L., Yuan, P., Murikinati, S., Gupta, S., Grutzendler, J. 2015. Regional blood flow in the normal and ischemic brain is controlled by arteriolar smooth muscle cell contractility and not by capillary pericytes. *Neuron*, 87, 95-110.

Ho, H., Cheung, C.Y., Sabanayagam, C., Yip, W., Ikram, M.K., Ong, P.G., Mitchell, P., Chow, K.Y., Cheng, C.Y., Tai, E.S. & Wong, T.Y. 2017. Retinopathy signs improved prediction and reclassification of cardiovascular disease risk in diabetes: A prospective cohort study. *Sci Rep*, 7, 41492.

Holman, R.R., Paul, S.K., Bethel, M.A., Neil, H.A., Matthews, D.R. 2008. Long-term follow-up after tight control of blood pressure and type 2 diabetes. *N Engl J Med*, 359, 1565-1576.

Hong, E.P., & Park, J.W. 2012. Sample size and statistical power calculation in genetic association studies. *Genome Inform*, 10, 117-22.

Howie, B.N., Donnelly, P., & Marchini, J. 2009. A flexible and accurate genotype imputation method for the next generation of genome-wide association studies. *PLoS Genet*, 5:e1000529.

Hubbard, L.D., Brothers, R.J., King, W.N., Clegg, L.X., Klein, R., Cooper, L.S. et al. 1999. Methods for evaluation of retinal microvascular abnormalities associated with hypertension/sclerosis in the Atherosclerosis Risk in Communities Study. *Ophthalmology*, 106, 2269-80.

International Diabetes Federation 2017. IDF Diabetes Atlas: Eight Edition. Available: https://www.diabetesatlas.org/ [Accessed 23 February 2019].

Ikram, M.K., Sim, X., Jensen, R.A., Cotch, M.F., Hewitt, A.W., Ikram, M,A. et al. 2010. Four Novel Loci (19q13, 6q24, 12q24, and 5q14) Influence the Microcirculation In Vivo. *PLoS Genet*. 6, e1001184.

Ikram, M.K., de Jong, F.J., Bos, M.J., Vingerling, J.R., Hofman, A., Koudstaal, P.J. et al. 2006. Retinal vessel diameters and risk of stroke: the Rotterdam Study. *Neurology*, 66, 1339-43.

Ikram, M.K., de Jong, F.J., Vingerling, J.R., Witteman, J.C., Hofman, A., Breteler, M.M. & de Jong, P.T. 2004. Are retinal arteriolar or venular diameters associated with markers for cardiovascular disorders? The Rotterdam Study. *Invest Ophthalmol Vis Sci*, 45, 2129-34.

Ikram, M.K., Witteman, J.C, Vingerling, J.R, Breteler, M.M., Hofman, A. & de Jong, P.T. 2006. Retinal vessel diameters and risk of hypertension: the Rotterdam Study. *Hypertension*, 47, 189-94.

Imamura, M., Takahashi, A., Yamauchi, T., Hara, K., Yasuda, K., Grarup, N. et al. 2016. Genome-wide association studies in the Japanese population identify seven novel loci for type 2 diabetes. *Nat Commun*, 7, 10531.

Jensen, R.A, Sim, X., Smith, A.V, Li, X., Jakobsdóttir, J., Cheng, C.Y. et al. 2016. Novel genetic loci associated with retinal microvascular diameter. *Circ Cardiovasc Genet*, 9,45-54.

Kawasaki, R., Xie, J., Cheung, N., Lamoureux, E., Klein, R., Klein, B.E. et al. 2012. Retinal microvascular signs and risk of stroke: the Multi-Ethnic Study of Atherosclerosis (MESA). *Stroke*, 43, 3245-51.

Kawasaki, R., CheAzemin, M., Kumar, D.K., Tan, A.G., Liew, G., Wong, T.Y. et al. 2011. Fractal dimension of the retinal vasculature and risk of stroke: A nested case-control study. *Neurology*, 76, 1766-67.

Keravnou, A., Bashiardes, E., Michailidou, K., Soteriou, M., Moushi, A., & Cariolou, M. 2018. Novel variants in the ACTA2 and MYH11 genes in a Cypriot family with thoracic aortic aneurysms: a case report. *BMC Med Genet*, 19, 208.

Kirin, M., Nagy, R., MacGillivray, T.J., Polašek, O., Hayward, C., Rudan, I. et al. 2017. Determinants of retinal microvascular features and their relationships in two European populations. *J Hypertens*, 35, 1646-59.

Klein, A.R., Sharrett, B. E. Klein, L. E. Chambless, L. S. Cooper, L. D. Hubbard, G. Evans. 2000. Are retinal arteriolar abnormalities related to atherosclerosis? The Atherosclerosis Risk in Communities Study. *Arterioscler Thromb Vasc Biol*, 20, 1644–50.

Klein, B.E, Klein, R., McBride, P.E, Cruickshanks, K.J, Palta, M., Knudtson, M.D. et al. 2004. Cardiovascular disease, mortality, and retinal microvascular characteristics in type 1 diabetes: Wisconsin epidemiologic study of diabetic retinopathy. *Arch Intern Med*, 164, 1917-24.

Klein, R., Klein, B.E., Moss, S.E. & Wong, T.Y. 2007. Retinal vessel caliber and microvascular and macrovascular disease in type 2 diabetes: XXI: the Wisconsin Epidemiologic Study of Diabetic Retinopathy. *Ophthalmology*, 114, 1884-92.

Kleinloog, R., Verweij, B.H., van der Vlies, P., Deelen, P., Swertz, M.A., de Muynck, L. et al. 2016. RNA Sequencing Analysis of Intracranial Aneurysm Walls Reveals Involvement of Lysosomes and Immunoglobulins in Rupture. *Stroke*, 47, 1286-93.

Kochar, M. & Min, J.K. 2013. Physiologic assessment of coronary artery disease by cardiac computed tomography. *Korean Circ J*, 43, 435-42.

Kraft, P., Zeggini, E., & Ioannidis, J. P. 2009. Replication in genome-wide association studies. *Stat Sci*, 24, 561–573.

Kramer, H., Boucher, R.E., Leehey, D., Fried, L., Wei, G., Greene, T. et al. 2018. Increasing mortality in adults with Diabetes and low estimated glomerular filtration rate in the absence of albuminuria. *Diabetes Care*, 41, 775-81.

Kur, J., Newman, E.A. & Chan-Ling, T. 2012. Cellular and physiological mechanisms underlying blood flow regulation in the retina and choroid in health and disease. *Prog Retin Eye Res*, 31, 377-406.

Kwa, V. I.H., van der Sande, J. J., Stam, J., Tijmes, N. & Vrooland. J. L. 2002. Retinal arterial changes correlate with cerebral small-vessel disease. *Neurology*, 59, 1536-40.

Kwa, V.I. & Lopez, O.L. 2010. Fractal analysis of retinal vessels: peeping at the tree of life? *Neurology*, 74, 1088-9.

Lacey, B., Herrington, W.G., Preiss, D., Lewington, S. & Armitage, J. 2017. The role of emerging risk factors in cardiovascular outcomes. *Curr Atheroscler Rep*, 19, 28.

Lachman, S., Boekholdt, S.M., Luben, R.N., Sharp, S.J., Brage, S., Khaw, K.T. et al. 2018. Impact of physical activity on the risk of cardiovascular disease in middle-aged and older adults: EPIC Norfolk prospective population study. *Eur J Prev Cardiol*, 25, 200-208.

Lee, A.Y., Han, B., Lamm, S.D., Fierro, C.A. & Han, H.C. 2012. Effects of elastin degradation and surrounding matrix support on artery stability. *Am J Physiol Heart Circ Physiol*, 302, H873-84.

Lee, K.E., Klein, B.E.K., Klein, R., & Knudtson, M.D. 2004. Familial aggregation of retinal vessel caliber in the beaver dam eye study. *Invest Ophthalmol Vis Sci*, 45, 3929-33.

Leung, H., Wang, J.J., Rochtchina, E., Tan, A.G., Wong, T.Y., Hubbard, L.D. et al. 2003. Computer-assisted retinal vessel measurement in an older population: correlation between right and left eyes. *Clin Exp Ophthalmol*, 31, 326-30.

Lewontin, R., & Kojima, K. 1960. The Evolutionary Dynamics of Complex Polymorphisms. *Evolution*, 14, 458-472.

Liew, G., Mitchell, P., Rochtchina, E., Wong, T.Y., Hsu, W., Lee, M.L. et al. 2011. Fractal analysis of retinal microvasculature and coronary heart disease mortality, *Eur Heart J*, 32, 422–29.

Lim, L.S., Cheung, C.Y., Lin, X., Mitchell, P., Wong, T.Y., & Mei-Saw, S. 2011 Influence of refractive error and axial length on retinal vessel geometric characteristics. *Invest Ophthalmol Vis Sci*, 52, 669-78.

Lipsitz, L.A., & Goldberger, A.L. 1992. Loss of 'complexity' and aging. Potential applications of fractals and chaos theory to senescence. *JAMA*, 267, 1806-09.

Liu, Y.P, Kuznetsova, T., Thijs, L., Jin, Y., Schmitz, B., Brand, S.M. et al. 2011. Are retinal microvascular phenotypes associated with the 1675G/A polymorphism in the angiotensin II type-2 receptor gene? *Am J Hypertens*, 24, 1300-05.

Liu, J., Rutten-Jacobs, L., Liu, M., Markus, H. S., & Traylor, M. 2018. Causal impact of type 2 diabetes mellitus on cerebral small vessel disease: A mendelian randomization analysis. *Stroke*, 49, 1325–1331.

Liu, Y.P., Kuznetsova, T., Jin, Y., Thijs, L., Asayama, K., Gu, Y.M. et al. 2013. Heritability of the retinal microcirculation in Flemish families. *Am J Hypertens*, 26, 392-9.

Loader, J., Montero, D., Lorenzen, C., Watts, R., Méziat, C., Reboul, C. et al. 2015. Acute hyperglycemia impairs vascular function in healthy and cardiometabolic

diseased subjects: systematic review and meta-analysis. *Arterioscler Thromb Vasc Biol*, 35, 2060-72.

Locke, A. E., Kahali, B., Berndt, S. I., Justice, A. E., Pers, T. H., Day, F. R. et al. 2015. Genetic studies of body mass index yield new insights for obesity biology. *Nature*, 518, 197–206.

London. A., Benhar. I. & Schwartz. M. 2013. The retina as a window to the brain-from eye research to CNS disorders. *Nat Rev Neurol*, 9, 44-53.

Lopes, R. & Betrouni, N. 2009. Fractal and multifractal analysis: a review. *Med Image Anal*, 13, 634-49.

Lupaşcu, C.A., Tegolo, D. & Trucco, E. 2013. Accurate estimation of retinal vessel width using bagged decision trees and an extended multiresolution Hermite model. *Med Image Anal*, 17, 1164-80.

MacGillivray, T.J., Cameron, J.R., Zhang, Q., El-Medany, A., Mulholland, C., Sheng, Z., et al. 2015. Suitability of UK Biobank Retinal Images for Automatic Analysis of Morphometric Properties of the Vasculature. *PLoS ONE*, 10: e0127914.

MacGillivray, T.J., Trucco, E., Cameron, J.R., Dhillon, B., Houston, J.G. & van Beek, E.J. 2014. Retinal imaging as a source of biomarkers for diagnosis, characterization and prognosis of chronic illness or long-term conditions. *Br J Radiol*, 87, 20130832.

Marees, A.T., de Kluiver, H., Stringer, S., Vorspan, F., Curis, E., Marie-Claire, C., Derks, E.M. 2018. A tutorial on conducting genome-wide association studies: Quality control and statistical analysis. *Int J Methods Psychiatr Res*, 27, e1608.

Marioni, R.E., Strachan, M.W., Reynolds, R.M., Lowe, G.D., Mitchell, R.J., Fowkes, F.G. et al. 2010. Association between raised inflammatory markers and cognitive decline in elderly people with type 2 diabetes: the Edinburgh Type 2 Diabetes Study. *Diabetes*, 59, 710-3.

Martín-Timón, I., Sevillano-Collantes, C., Segura-Galindo, A., & Del Cañizo-Gómez, F. J. 2014. Type 2 diabetes and cardiovascular disease: Have all risk factors the same strength?. *World J Diabetes*, 5, 444–70.

Mayhew, A. J., & Meyre, D. 2017 . Assessing the Heritability of Complex Traits in Humans: Methodological Challenges and Opportunities. *Curr genomics*, 18, 332–340.

McGeechan, K., Liew G., Macaskill, P., Irwig, L., Klein, R., Klein, B.E. et al. 2009. Prediction of incident stroke events based on retinal vessel caliber: a systematic review and individual-participant meta-analysis. *Am J Epidemiol*, 170, 1323-32.

McGinnity, K. & Williams, M. 2019. Direct Ophthalmoscopy… Soon to be Forgotten? *Ulster Med J*, 88, 115-17.

McGowan, A., Silvestri, G., Moore, E., Silvestri, V., Patterson, C.C., Maxwell, A.P. & McKay, G.J. 2015. Evaluation of the retinal vasculature in hypertension and chronic kidney disease in an elderly population of irish nuns. *PLoS One*, 10, e0136434.

McGrory, S., Ballerini, L., Doubal, F. N., Staals, J., Allerhand, M., Valdes-Hernandez, M. et al. 2019. Retinal microvasculature and cerebral small vessel disease in the Lothian Birth Cohort 1936 and Mild Stroke Study. *Sci Rep*, 9, 6320.

McGrory, S., Taylor, A. M., Kirin, M., Corley, J., Pattie, A. et al. 2017. Retinal microvascular network geometry and cognitive abilities in community-dwelling older people: The Lothian Birth Cohort 1936 study. *Br J Ophthalmol*, 101, 993-98.

McGrory, S., Taylor, A.M., Pellegrini, E., Ballerini, L., Kirin, M., Doubal, F.N. et al. 2018. Towards standardization of quantitative retinal vascular parameters: comparison of SIVA and VAMPIRE measurements in the lothian birth cohort 1936. *Transl Vis Sci Technol*, 7, 12.

McKay, G.J., Paterson, E.N., Maxwell, A.P., Cardwell, C.C., Wang, R., Hogg, S. et al. 2018. Retinal microvascular parameters are not associated with reduced renal function in a study of individuals with type 2 diabetes. *Sci Rep*, 8, 3931.

McLachlan, S., Giambartolomei, C., White, J., Charoen, P., Wong, A., Finan, C. et al. 2016. Replication and characterization of association between abo snps and red blood cell traits by meta-analysis in Europeans. *PLoS One*, 11, e0156914.

Meeus, B., Nuytemans, K., Crosiers, D., Engelborghs, S., Peeters, K., Mattheijssens, M. et al. 2010. Comprehensive genetic and mutation analysis of familial dementia with Lewy bodies linked to 2q35-q36. *J Alzheimers Dis*, 20, 197-205.

Mejía-Rentería, H., Matias-Guiu, J.A., Lauri, F., Yus, M. & Escaned, J. 2018. Microcirculatory dysfunction in the heart and the brain. *Minerva Cardioangiol*, doi: 10.23736/S0026-4725.18.04701-1.

Miller, R. G., Prince, C. T., Klein, R. & Orchard, T. J. 2009. Retinal vessel diameter and the incidence of coronary artery disease in type 1 diabetes. *Am. J. Ophthalmol*, 147, 653-60.

Morling, J.R., Fallowfield, J.A., Williamson, R.M., Robertson, C.M., Glancy, S., Guha, I.N. et al. 2015 γ-Glutamyltransferase, but not markers of hepatic fibrosis, is associated with cardiovascular disease in older people with type 2 diabetes mellitus: The Edinburgh Type 2 Diabetes Study. *Diabetologia*, 58, 1484-93.

Morris, J.N. 1961. Epidemiology and cardiovascular disease of middle age. II. *Mod Concepts Cardiovasc Dis*, 30, 633-8.

Morrison, A.C., Felix, J.F., Cupples, L.A., Glazer, N.L., Loehr, L.R., Dehghan, A. et al. 2010. Genomic variation associated with mortality among adults of European and African ancestry with heart failure: the cohorts for heart and aging research in genomic epidemiology consortium. *Circ Cardiovasc Genet*, 3, 248-55.

Nagaoka, T., & Yoshida, A. 2013. Relationship between retinal blood flow and renal function in patients with type 2 diabetes and chronic kidney disease. *Diabetes care*, 36, 957–61.

National Institute for Health and Care Excellence (NICE). 2018 [Online]. Available: https://www.evidence.nhs.uk/search?q=nice+and+diabetic+retinopathy+and+guideline [Accessed 20 December 2019].

Nayor, M., Duncan, M.S., Musani, S.K., Xanthakis, V., LaValley, M.P., Larson, M.G., Fox, E.R. & Vasan, R.S. 2018. Incidence of cardiovascular disease in individuals

affected by recent changes to US blood pressure treatment guidelines. *J Hypertens*, 36, 436-43.

Ooi, Q.L., Tow, F.K., Deva, R., Alias, M.A., Kawasaki, R., Wong, T.Y. et al. 2011. The microvasculature in chronic kidney disease. *Clin J Am Soc Nephrol*, 6, 1872–78.

Ong, Y.T., De Silva, D.A., Cheung, C.Y., Chang, H.M., Chen, C.P., Wong, M.C. et al. 2013. Microvascular structure and network in the retina of patients with ischemic stroke. *Stroke*, 44, 2121-7.

Owen, C.G., Rudnicka, A.R., Welikala, R.A., Fraz, M.M., Barman, S.A., Luben, R. et al. 2019. Retinal vasculometry associations with cardiometabolic risk factors in the European prospective investigation of cancer-norfolk study. *Ophthalmology*, 126, 96-106.

Owens, A.P. III. & Mackman, N. 2010. Tissue factor and thrombosis: The clot starts here. *Thromb Haemost*, 104, 432-9.

Pakter, H.M., Fuchs, S.C., Maestri, M.K., Moreira, L.B., Dei Ricardi, L.M., Pamplona, V.F. et al. 2011. Computer-assisted methods to evaluate retinal vascular caliber: what are they measuring? *Invest Ophthalmol Vis Sci*, 52, 810-5.

Panwar, N., Huang, P., Lee, J., Keane, P.A., Chuan, T.S., Richhariya, A. et al. 2016. Fundus Photography in the 21st Century-A Review of Recent Technological Advances and Their Implications for Worldwide Healthcare. *Telemed J E Health*, 22, 198-208.

Parto, P. & Lavie, C.J. 2017. Obesity and CardiovascularDiseases. *Curr Probl Cardiol*, 42, 376-94.

Patton, N., Aslam, T.M., MacGillivray, T., Deary, I.J., Dhillon, B., Eikelboom, R.H. et al 2006. Retinal image analysis: concepts, applications and potential. *Prog Retin Eye Res*, 25, 99-127.

Pazoki, R., Dehghan, A., Evangelou, E., Warren, H., Gao, H., Caulfield, M. et al. 2018. Genetic predisposition to high blood pressure and lifestyle factors:

Associations with midlife blood pressure levels and cardiovascular events. *Circulation*, 137, 653-61.

Pearce, N. 2012. Classification of epidemiological study designs. *Int J Epidemiol*, 41, 393-7.

Perez-Rovira, A., MacGillivray, T., Trucco, E., Chin, K.S., Zutis, K. et al. 2011. VAMPIRE: Vessel assessment and measurement platform for images of the REtina. Conf Proc IEEE *Eng Med Biol Soc*, 3391-4.

Persson, F., Lindhardt, M., Rossing, P. & Parving, H.H. 2016. Prevention of microalbuminuria using early intervention with renin-angiotensin system inhibitors in patients with type 2 diabetes: A systematic review. *J. Renin Angiotensin Aldosterone Syst*, 17, 1470320316652047.

Phan, K., Mitchell, P., Liew, G., Plant, A. J., Wang, S.B., Thiagalingam, A. et al. 2018. Associations between retinal arteriolar and venular calibre with the prevalence of impaired fasting glucose and diabetes mellitus: A cross-sectional study. *PloS one*, 13, e0189627.

Phan, K., Mitchell, P., Liew, G., Plant, A.J., Wang, S.B., Xu, J. et al. 2016. Severity of coronary artery disease and retinal microvascular signs in patients with diagnosed versus undiagnosed diabetes: cross-sectional study. *J Thorac Dis*, 8, 1532–39.

Piché, M.E., Poirier, P., Lemieux, I. & Després, J.P. 2018. Overview of Epidemiology and Contribution of Obesity and Body Fat Distribution to Cardiovascular Disease: An Update. *Prog Cardiovasc Dis*, 61,103-113.

Pilling, L.C., Atkins, J.L., Duff, M.O., Beaumont, R.N., Jones, S.E., Tyrrell, J. et al. 2017. Red blood cell distribution width: Genetic evidence for aging pathways in 116,666 volunteers. *PLoS One*, 12, e0185083.

Poplin, R., Varadarajan, A.V., Blumer, K., Liu Y., McConnell, M.V., Corrado G.S. et al. 2018. Prediction of cardiovascular risk factors from retinal fundus photographs via deep learning. *Nat Biomed Eng*, 2, 158-164.

Potts, L.F., Cambon, A.C., Ross, O.A., Rademakers, R., Dickson, D.W., Uitti, R.J. et al. 2012. Polymorphic genes of detoxification and mitochondrial enzymes and risk for progressive supranuclear palsy: a case control study. *BMC Med Genet*, 13:16.

Pournaras, C.J., Rungger-Brändle, E., Riva, C.E., Hardarson, S.H. & Stefansson, E. 2008. Regulation of retinal blood flow in health and disease. *Prog Retin Eye Res*, 27, 284-330.

Price, J.F., Reynolds, R.M., Mitchell, R.J., Williamson, R.M., Fowkes, F.G., Deary, I.J. et al. 2008. The Edinburgh Type 2 Diabetes Study: study protocol. *BMC Endocr Disord*, 8, 18.

Pruim, R.J., Welch, R.P., Sanna, S., Teslovich, T.M., Chines, P.S., Gliedt, T.P., Boehnke, M., Abecasis, G.R., & Willer, C.J. 2010. LocusZoom: regional visualization of genome-wide association scan results. *Bioinformatics*, 26, 2336-7.

Ramos, L., Novo, J., Rouco, J., Romeo, S., Álvarez, M.D. & Ortega, M. 2018. Retinal vascular tortuosity assessment: inter-intra expert analysis and correlation with computational measurements. *BMC Med Res Methodol*, 18, 144.

Rannikmäe, K., Davies, G., Thomson, P.A., Bevan, S., Devan, W.J., Falcone, G.J. et al. 2015. Common variation in COL4A1/COL4A2 is associated with sporadic cerebral small vessel disease. *Neurology*, 84, 918-26.

Rannikmäe, K., Sivakumaran, V., Millar, H., Malik, R., Anderson, C.D., Chong, M. et al. 2011. Diabetes mellitus, fasting glucose, and risk of cause-specific death. *N Engl J Med*, 364, 829-41.

Ray, K.K., Seshasai, S.R., Wijesuriya, S., Sivakumaran, R., Nethercott, S., Preis, D. et al. 2009. Effect of intensive control of glucose on cardiovascular outcomes and death in patients with diabetes mellitus: a meta-analysis of randomised controlled trials. *Lancet*, 373, 1765-72.

Roth, G.A, Johnson, C., Abajobir, A., Abd-Allah, F., Abera, S.F., Abyu, G. et al. 2017. Global, regional, and national burden of cardiovascular diseases for 10 causes, 1990 to 2015. *J Am Coll Cardiol*, 70, 1-25.

Roy, M.S., Klein, R. & Janal, M.N. 2012. Relationship of retinal vessel caliber to cardiovascular disease and mortality in African Americans with type 1 diabetes mellitus. *Arch Ophthalmol*, 130, 561-7.

Saeed, A., Nambi, V., Sun, W., Virani, S.S., Taffet, G.E., Deswal, A. et al. 2018. Short-Term global cardiovascular disease risk prediction in older adults. *J Am Coll Cardiol*, 71, 2527-36.

Saraf, S.S., Tyring, A.J., Chen, C.L., Le, T.P., Kalina, R.E., Wang, R.K. et al. 2019. Familial retinal arteriolar tortuosity and quantification of vascular tortuosity using swept-source optical coherence tomography angiography. *Am J Ophthalmol Case Rep*, 14, 74-78.

Sasongko, M.B., Wong, T.Y., Nguyen, T.T., Cheung, C.Y., Shaw, J.E. & Wang, JJ. 2011. Retinal vascular tortuosity in persons with diabetes and diabetic retinopathy. *Diabetologia*, 54, 2409.

Sasongko, M.Y., Wong, T.Y., Nguyen, T.T., Cheung, C.Y., Shaw, J.E., Kawasaki, R. et al. 2016. Retinal Vessel Tortuosity and Its Relation to Traditional and Novel Vascular Risk Markers in Persons with Diabetes. *Curr Eye Res*, 41, 551-57.

Schafer, J.L. 1999. Multiple imputation: a primer. *Stat Methods Med Res*, 8, 3-15.

Seidelmann, S.B, Claggett, B., Bravo, P.E., Gupta, A., Farhad, H., Klein, B.E. et al. 2016. Retinal vessel calibers in predicting long-term cardiovascular outcomes: The Atherosclerosis Risk in Communities Study. *Circulation*, 134, 1328-38.

Selleck, M.J., Senthil, M. & Wall, N.R. 2017. Making Meaningful Clinical Use of Biomarkers. *Biomark insights*, *12*, 1177271917715236.

Selvam, S., Kumar, T. & Fruttiger, M. 2018. Retinal vasculature development in health and disease. *Prog Retin Eye Res*, 63, 1-19.

Senanayake, P.d., Drazba, J., Shadrach, K., Milsted, A., Rungger-Brandle, E., Nishiyama, K. et al. 2007. Angiotensin II and its receptor subtypes in the human retina. *Invest Ophthalmol Vis Sci*, 48, 3301-11.

Shah, T., Engmann, J., Dale, C., Shah, S., White, J., Giambartolomei, C. et al. 2013. Population genomics of cardiometabolic traits: design of the University College London-London School of Hygiene and Tropical Medicine-Edinburgh-Bristol (UCLEB) Consortium. *PLoS One*, 8, e71345.

Sherry, L.M., Wang, J.J., Rochtchina, E., Wong, TY., Klein, R., Hubbard, L.D. & Mitchell, P. 2002. Relationships between retinal arteriolar diameters, age and blood pressure in an older population: Findings from the Blue Mountains Eye Study. *Invest Ophthalmol Vis Sci*, 43, 4398.

Shin, S.Y., Fauman, E.B., Petersen, A.K., Krumsiek, J., Santos, R., Huang, J. et al. 2014. An atlas of genetic influences on human blood metabolites. *Nat Genet*, 46, 543-50.

Sim, X., Jensen, R.A., Ikram, M.K., Cotch, M.F., Li, X., MacGregor, S. et al. 2013. Genetic loci for retinal arteriolar microcirculation. *PLoS One*, 12, e65804.

Simmons, R.D., Kumar, S. & Jo, H. 2016. The role of endothelial mechanosensitive genes in atherosclerosis and omics approaches. *Arch Biochem Biophys*, 591,111-31.

Smith, W., Wang, J.J., Wong, T.Y., Rochtchina, E., Klein, R., Leeder, S.R. et al. 2004. Retinal arteriolar narrowing is associated with 5-year incident severe hypertension: the Blue Mountains Eye Study. *Hypertension*, 44, 442-7.

Stosić, T. & Stosić, B.D. 2006. Multifractal analysis of human retinal vessels. IEEE *Trans Med Imaging*, 25, 1101-7.

Sugano, E., Edwards, G., Saha, S., Wilmott, L.A., Grambergs, R.C., Mondal, K. et al. 2019. Overexpression of acid ceramidase (ASAH1) protects retinal cells (ARPE19) from oxidative stress. *J Lipid Res*, 60, 30-43.

Sun, C., Wang, J.J., Mackey, D.A. & Wong, T.Y. 2009. Retinal vascular caliber: systemic, environmental, and genetic associations. *Surv Ophthalmol*, 54, 74-95.

Sun, C., Zhu, G., Wong, T.Y., Hewitt, A.W., Ruddle, J.B., Hodgson, L. et al. 2009. Quantitative genetic analysis of the retinal vascular caliber: the Australian Twins Eye Study. *Hypertension*, 54, 788-95.

Taarnhøj, N.C., Larsen, M., Sander, B., Kyvik, K.O., Kessel, L., Hougaard, J.L. et al. 2006. Heritability of retinal vessel diameters and blood pressure: a twin study. *Invest Ophthalmol Vis Sci*, 47, 3539-44.

Taarnhøj, N.C., Munch, I.C., Sander, B., Kessel, L., Hougaard, J.L., Kyvik, K. et al. 2008. Straight versus tortuous retinal arteries in relation to blood pressure and genetics. *Br J Ophthalmol*, 92, 1055-60.

Ţălu, Ş., Stach, S., Călugăru, D.M., Lupaşcu, C.A. & Nicoară, S.D. 2017. Analysis of normal human retinal vascular network architecture using multifractal geometry. *Int J Ophthalmol*, 10, 434-38.

Thiese MS. 2014. Observational and interventional study design types; an overview. *Biochem Med*, 24, 199-210.

Traylor, M., Zhang, C.R., Adib-Samii, P., Devan, W.J., Parsons, O.E., Lanfranconi, S. et al. 2016. Genome-wide meta-analysis of cerebral white matter hyperintensities in patients with stroke. *Neurology*, 86, 146-53.

Trucco, E., Ruggeri, A., Karnowski, T., Giancardo, L., Chaum, E., Hubschman, J.P. et al. 2013. Validating retinal fundus image analysis algorithms: issues and a proposal. *Invest Ophthalmol Vis Sci*, 54, 3546-59.

van der Velde, M., Matsushita, K., Coresh, J., Astor, B.C., Woodward, M., Levey, A. et al. 2011. Lower estimated glomerular filtration rate and higher albuminuria are associated with all-cause and cardiovascular mortality. A collaborative meta-analysis of high-risk population cohorts. *Kidney Int*, 79, 1341-52.

Vandiver, R.M. 2015. Buckling instability in arteries. *J Theor Biol*, 371, 1-8.

van Zuydam, N.R, Ahlqvist, E., Sandholm, N., Deshmukh, H., Rayner, N.W., Abdalla, M. et al. 2018. A Genome-Wide Association Study of Diabetic Kidney Disease in Subjects With Type 2 Diabetes. *Diabetes*, 67, 1414-27.

Vanzetta, I., Hildesheim, R. & Grinvald, A. 2005. Compartment-resolved imaging of activity-dependent dynamics of cortical blood volume and oximetry. *J Neurosci*, 25, 2233-44.

Vergmann, A.S., Broe, R., Kessel, L., Hougaard, J.L., Möller, S., Kyvik, K.O. et al. 2017. Heritability of retinal vascular fractals: A Twin Study. *Invest Ophthalmol Vis Sci*, 58, 3997-4002.

Visscher, PM., Wray, NR., Zhang, Q., Sklar, P., McCarthy, M.I. et al. 2017.10 Years of GWAS Discovery: Biology, Function, and Translation. *Am J Hum Genet*, 101, 5-22.

Voight, B. F., Kang, H. M., Ding, J., Palmer, C. D., Sidore, C., Chines, P.S. et al. 2012. The metabochip, a custom genotyping array for genetic studies of metabolic, cardiovascular, and anthropometric traits. *PLoS genetics*, 8, e1002793.

Walford, G.A., Gustafsson, S., Rybin, D., Stančáková, A., Chen, H., Liu, C.T. et al. 2016. Genome-Wide Association Study of the Modified Stumvoll Insulin Sensitivity Index Identifies BCL2 and FAM19A2 as Novel Insulin Sensitivity Loci. *Diabetes*, 65,3200-11.

Wang, J. J., Liew, G., Wong, T. Y., Smith, W., Klein, R., Leeder, S. R. et al. 2006. Retinal vascular calibre and the risk of coronary heart disease-related death. *Heart*, 92, 1583-7.

Wang, J.J., Taylor, B., Wong, T.Y., Chua, B., Rochtchina, E., Klein, R. et al. 2006. Retinal vessel diameters and obesity: a population-based study in older persons. *Obesity*,14, 206-14.

Wang, S.B., Mitchell, P., Liew, G., Wong, T.Y., Phan, K., Thiagalingam, A. et al. 2018. A spectrum of retinal vasculature measures and coronary artery disease. *Atherosclerosis*, 268, 215-224.

Warren, H.R., Evangelou, E., Cabrera, C.P., Gao, H., Ren, M., Mifsud, B. et al. 2017. Genome-wide association analysis identifies novel blood pressure loci and offers biological insights into cardiovascular risk. *Nat Genet*, 49, 403-415.

Wheeler, E., Leong, A., Liu, C.T., Hivert, M.F., Strawbridge, R.J., Podmore, C. et al. 2017. Impact of common genetic determinants of Hemoglobin A1c on type 2 diabetes risk and diagnosis in ancestrally diverse populations: A transethnic genome-wide meta-analysis. *PLoS Med*, 14, e1002383.

Witt N., Wong T.Y., Hughes A.D., Chaturvedi N., Klein B.E., Evans R. et al. 2006. Abnormalities of retinal microvascular structure and risk of mortality from ischemic heart disease and stroke. *Hypertension*, 47, 975-81.

Wong, T.Y, Kamineni, A., Klein, R., Sharrett, A.R., Klein, B.E., Siscovick, D.S. et al. 2006. Quantitative retinal venular caliber and risk of cardiovascular disease in older persons: the cardiovascular health study. *Arch Intern Med*, 166, 2388-94.

Wong, T.Y., Islam, F.M.A., Klein, R., Klein, B.E.K., Cotch, M.F., Castro, C. et al. 2006. Retinal vascular caliber, cardiovascular risk factors, and inflammation: The Multi-Ethnic Study of Atherosclerosis (MESA). *Invest Ophthalmol Vis Sci*, 47, 2341-50.

Wong, T.Y., Klein, R., Klein, B.E.K., Tielsch, J.M., Hubbard, L. & Nieto, F.J. 2001.Retinal Microvascular Abnormalities and their Relationship with Hypertension, Cardiovascular Disease, and Mortality. *Surv Ophthalmol*, 46, 59-80.

Wong, T.Y., Klein, R., Nieto, F.J., Klein, B.E., Sharrett, A.R., Meuer, S.M. et al. 2003. Retinal microvascular abnormalities and 10-year cardiovascular mortality: a population-based case-control study. *Ophthalmology*, 110, 933-40.

Wong, T.Y., Klein, R., Sharrett, A.R., Duncan, B.B., Couper, D.J., Tielsch, J.M. et al. 2002. Retinal arteriolar narrowing and risk of coronary heart disease in men and women. The Atherosclerosis Risk in Communities Study. *JAMA*, 287, 1153-9.

Wong, T.Y., Klein, R., Sharrett, A.R., Manolio, T.A., Hubbard, L.D., Marino, E.K. et al. 2003. The prevalence and risk factors of retinal microvascular abnormalities in older persons: The Cardiovascular Health Study. *Ophthalmology*, 110, 658-66.

World Health Organization. 2018. The top 10 causes of death [Online].

World Health Organization. Available: http://www.who.int/en/news-room/fact-sheets/detail/the-top-10-causes-of-death [Accessed 23 July 2018].

World Health Organization. 2016. Global Report on Diabetes [Online]. Available: http://apps.who.int/iris/bitstream/10665/204871/1/9789241565257_eng.pdf?ua=1&ua=1. [Accessed 23 June 2018].

World Health Organization 2015a. Cardiovascular diseases (CVDs).

World Health Organization. 2015b. ICD-10 Version: 2015 [Online]. Available: http://apps who int/classifications/icd10/browse/2015/en [Accessed 23 November 2018].

World Health Organization. 2014. Diabetes Programme [Online]. World Health Organization, Avenue Appia 20, 1211 Geneva 27, Switzerland: World Health Organization. Available: http://www.who.int/diabetes/action_online/basics/en/ [Accessed September 12, 2018].

World Health Organization. 2011. Use of glycated haemoglobin (HbA1c) in the diagnosis of diabetes mellitus [Online]. Available: http://www.who.int/diabetes/publications/diagnosis_diabetes2011/en/.

Wu, H.Q., Wu, H., Shi, L.L, Yu, L.Y, Wang, L.Y., Chen, Y.L. et al. 2017. The association between retinal vasculature changes and stroke: a literature review and Meta-analysis. *Int J Ophthalmol*, 10,109-114.

Wuttke, M., Li, Y., Li, M., Sieber, K.B., Feitosa, M.F., Gorski, M. et al. 2019. A catalog of genetic loci associated with kidney function from analyses of a million individuals. *Nat Genet*, 51, 957-72.

Xing, C., Klein, B.E., Klein, R., Jun, G., Lee, K.E. & Iyengar, S.K. 2006. Genome-wide linkage study of retinal vessel diameters in the Beaver Dam Eye Study. *Hypertension*, 47, 797-802.

Yamasaki, M., Abe, K., Kosho, T., & Yamaguchi, T. 2019. Familial Aortic Dissection in a Young Adult Caused by MYH11 Gene Mutation. *Ann Thorac Surg*, 108, e49.

Yau, J.W., Xie, J., Kawasaki, R., Kramer, H., Shlipak, M., Klein, R., et al. 2011. Retinal arteriolar narrowing and subsequent development of CKD Stage 3: the Multi-Ethnic Study of Atherosclerosis (MESA). *Am J of Kidney*, 58, 39–46.

Yim-Lui, C.C., Wong, T.Y., Lamoureux, E.L., Sabanayagam, C., Li, J., Lee, J. et al. 2010. C-reactive protein and retinal microvascular caliber in a multiethnic Asian population. *Am J Epidemiol*, 171, 2 206-13.

Yip, W., Ong, P.G, Teo, B.W., Cheung, C.Y., Tai, E.S., Cheng, C.Y. et al. 2017. Retinal vascular imaging markers and incident chronic kidney disease: A prospective cohort study. *Sci Rep*, 7, 9374.

Zenteno, J.C., Crespí, J., Buentello-Volante, B., Buil, J.A., Bassaganyas, F., Vela-Segarra, J.I. et al. 2014. Next generation sequencing uncovers a missense mutation in COL4A1 as the cause of familial retinal arteriolar tortuosity. *Graefes Arch Clin Exp Ophthalmol*, 252, 1789-94.

Zhang, Q., Wu, K.H., He, J.Y., Zeng, Y., Greenbaum, J., Xia, X. et al. 2017. Novel Common Variants Associated with Obesity and Type 2 Diabetes Detected Using a cFDR Method. *Sci Rep*, 7, 16397.

Zheng, Y., Ley, S.H. & Hu, F.B. 2018. Global aetiology and epidemiology of type 2 diabetes mellitus and its complications. *Nat Rev Endocrinol*, 14, 88-98.

Zhu, P., Huang, F., Lin, F., Li, Q., Yuan, Y., Gao, Z. et al. 2014. The relationship of retinal vessel diameters and fractal dimensions with blood pressure and cardiovascular risk factors. *PLoS One*, 9, e106551.

Chapter 10 Appendices

10.1 Appendix 1: Search strategy

1. isch$emic heart disease.mp.
2. exp cardiovascular diseases/
3. exp myocardial ischemia/
4. exp arteriosclerosis/
5. acute coronary syndrome.mp.
6. exp angina pectoris/
7. exp coronary disease/
8. exp myocardial infarction/
9. coronary.tw.
10. exp coronary vessel anomalies/
11. coronary atherosclerosis.mp.
12. coronary angiography.mp.
13. exp heart diseases/
14. (heart attack or acs$ or heart isch?emi$ or CHD$ or coronary artery disease$).tw.
15. (retina* adj2 (microvascular or microvasculature or microcirculation) adj2 abnormal*).mp.
16. retina* microangiopath*.mp.
17. retina* vascul*.mp.
18. retina* microvascul*.mp.
19. retina* arter*.mp.
20. retina* vein*.mp.
21. retina* venul*.mp.
22. retina* vascu*.mp.
23. retina* arteriovenous.mp.
24. retina* tortuosity.mp.
25. retina* calib*.mp.
26. retina* vascular calib*.mp.
27. retinopath*.mp.

28. microaneurysm.mp.
29. retina* exudate*.mp.
30. retina* h$emorrhage*.mp.
31. retina* cotton wool.mp.
32. fractal analysis.mp.
33. multifractal.mp.
34. monofractal.mp.
35. retina* arteriol*.mp.
36. retina* microvessel*.mp.
37. (retina* arter* adj2 ratio).mp.
38. (retina* adj2 ratio).mp.
39. exp Retinal Vessels/
40. exp Fractals/
41. fractal dimension$.mp.
42. fractal analysis.mp.
43. exp mortality/
44. exp epidemiologic studies/
45. incidence.mp.
46. exp prognosis/
47. prognos$.tw.
48. predict$.mp.
49. course.tw.
50. (score or scoring or scored).tw.
51. observ$.mp.
52. risk:.mp.
53. between group:.tw.
54. exp photography/
55. photo$.tw.
56. image$.tw.
57. exp Ophthalmoscopy/
58. 1 or 2 or 3 or 4 or 5 or 6 or 7 or 8 or 9 or 10 or 11 or 12 or 13 or 14
59. 15 or 16 or 17 or 18 or 19 or 20 or 21 or 22 or 23 or 24 or 25 or 26 or 27 or 28 or 29 or 30 or 31 or 32 or 33 or 34 or 35 or 36 or 37 or 38 or 39 or 40 or 41 or 42

60. 43 or 44 or 45 or 46 or 47 or 48 or 49 or 50 or 51 or 52 or 53
61. 54 or 55 or 56 or 57
62. 58 and 59 and 60 and 61
63. "animals not humans"/
64. 62 not 63
65. limit 64 to "all adult(19 plus years)"

10.2 Appendix 2: Summary of the studies on general population

Title	Reference	Study Population	Study Type	Recruitment method	Number of people recruited	Duration of Follow-up (years)	Type of model	Retinal Vasculature Exam	End Points	Key findings
Are Retinal Arteriolar Abnormalities Related to Atherosclerosis?	Klein et al, 2000	Individuals from North Caroline, Mississippi, Minnesota and Maryland in the US. African American and European ethnicity	Cross-sectional	The Atherosclerosis in communities Study (ARIC)	8772	Cross-sectional analysis	Logistic	1- Focal Narrowing 2- Arteriovenous nicking 3 AVR One image. Digitised Knudtson-Parr-Hubbard formula	1-Carotid and popliteal plaques 2-Coronary heart disease 3- Biomarkers	No association with coronary events (end point) association with atherosclerosis (total cholesterol) and subclinical atherosclerosis (carotid plaque)
Risk Prediction of Coronary Heart Disease based on Retinal Vascular Caliber (From The Atherosclerosis Risk in Communities [ARIC] Study)	McGeechan et al, 2008	Individuals from North Caroline, Mississippi, Minnesota and Maryland in the US. African American and European ethnicity	Prospective	The Atherosclerosis in communities Study (ARIC)	9155	10	Cox	1-CRAE 2-CRVE 3-Retinopathy 4-Focal narrowing 5-Arteriovenous nicking One random eye. Digitised Knudtson-Parr-Hubbard formula	1-Incident CHD was defined as acute (definite or probable) myocardial infarction, fatal coronary heart disease, silent myocardial infarction, myocardial revascularization (e.g coronary angioplasty or coronary artery bypass graft surgery) in persons without pre-existing CHD at the time of retinal photography at the third admission	Both, lower CRAE: (HR 1.31, 95%CI, 1.10 to 1.56) and higher CRVE (HR 1.27, 95%CI 1.08 to 1.50) were associated with incident CHD in women.

Retinal Arteriolar Narrowing and Risk of Coronary Heart Disease in Men and Women: The Atherosclerosis Risk in Communities Study	Wong et al, 2002	Individuals from North Caroline, Mississippi, Minnesota and Maryland in the US. African American and European ethnicity. No previous CVD	Prospective	The Atherosclerosis in communities Study (ARIC)	9648	6	Cox	1) AVR 2)Hypertensive retinopathy One random eye. Digitised Knudtson-Parr-Hubbard formula	1- Incident CHD (As above)	In women, after adjustment for mean BP, diabetes, smoking, total cholesterol, HDL, waist-hip ratio, alcohol consumption and antihypertensive medication, AVR was associated with increased incident CHD [HR 1.40 (1.03-1.92)], p = 0.03.
Quantitative retinal venular caliber and risk of cardiovascular disease in older persons: the cardiovascular health study	Wong et al, 2006	Cohort of European and African Americans from Pennsylvania, California, North Carolina and Maryland	Prospective	The Cardiovascular Health Study (CHS)	1992 /115	5	Cox	1-CRAE 2-CRVE 3-AVR One random eye. Digitised Knudtson-Parr-Hubbard formula	1- Incident CHD (As above)	After full adjustment, higher CRVE was associated with incident CHD (HR, 3.0; 95% CI, 1.6 5.7, comparing largest with smallest venular calibre quartiles; p = 0.001) whereas lower CRAE was associated with incident CHD (HR, 2.0; 95% CI, 1.1-3.7, comparing largest with smallest arteriolar caliber quartiles; p = 0.03)
Retinal vascular calibre and the risk of coronary heart disease-related death	Wang et al, 2006	Cohort (predominantly Caucasian, participants from Blue Mountains New South Wales Australia	Prospective	The Blue Mountains Eye Study (Australia)	3340 /192	9	Cox	1-AVR 2-CRAE 3-CRVE One random eye. Digitised Knudtson-Parr-Hubbard formula with correction of magnification	1) Incident CHD mortality	In individuals aged 49-75 years, higher CRVE were associated with CHD death in men (HR 1.8, 95% CI 1.1-2.7) and women (HR 2.0, 95% CI 1.1-3.6) after adjustment for age, systolic blood pressure, diabetes and smoking. Moreover, after full adjustment with the above factors,

										women aged 49-75 years, smaller AVR and lower CRAE were associated with CHD death (HR 1.5, 95% CI 1.1-2.2) and (HR 1.9, 95% CI 1.0-3.5) respectively.
Retinal vessel diameter and cardiovascular mortality: pooled data analysis from two older populations	Wang et al, 2007	Individuals from Beaver Dam Wisconsin and Blue Mountain Region, West Sydney	Prospective	Beaver Dam Eye study and the Blue Mountain Eye Study (combination)	7494 /653	12	Cox	1-CRAE 2-CRVE One random eye Knudtson formula	1-Incident CHD mortality 2-Stroke mortality	When the measurements of CRAE and CRVE were categorised into quintiles, lowest CRAE quintile and highest CRVE quintile predicted increased CHD mortality (HR 1.34, 95% CI 1.11-1.62 and HR 1.24, 95% CI 1.02-1.52, respectively). These associations were strongest in persons aged 43-69 years (HR 1.70; 95% CI 1.27-2.28 and HR 1.41, 95% CI 1.06-1.89), respectively.
Associations between retinal microvascular structure and the severity and extent of coronary artery disease	Gopinath et al, 2014	Individuals were symptomatic patients presented in the hospital for assessment of suspected CAD	Cross-sectional	The Australian Heart Eye Study	1120	Cross-sectional	Logistic	1-CRAE 2-CRVE One eye (mainly right) Knudtson-Hubbard formula	Coronary angiograms 1-Vessel and segment score 2-Gensini score 3-Extent score	In a fully adjusted model, significantly narrower retinal arteriolar calibre lowest quartile of CRAE in women and highest quartile of CRVE in men were associated with increased odds of having at least one stenosis ≥50% in the epicardial coronary arteries (OR 2.22; 95% CI 1.09- 4.53 and OR 1.54; 95%

										CI 1.03- 2.29, respectively). Moreover, women in the lowest versus the highest tertile of CRAE had greater odds of having higher Extent scores (OR 2.99, 95% CI 1.45- 6.16).
Retinal Vessel Calibers in Predicting Long-Term Cardiovascular Outcomes	Seidelmann et al, 2016	Individuals from North Caroline, Mississippi, Minnesota and Maryland in the US. African American and European ethnicity. Free of CVD at baseline	Prospective	The Atherosclerosis in Communities Study (ARIC)	10470	16	Cox	1-CRAE 2-CRVE 3-AVR One random eye. Digitised Knudtson-Parr-Hubbard formula	1-Incident ischaemic stroke 2-Incident CHD 3-HF 4-Deaths	In women only, higher CRVE was associated with CHD (HR 1.10, 95% CI 1.00-1.20) whereas lower CRAE was associated with CHD (HR 1.13, 95% CI 1.03-1.24). These analyses were fully adjusted for traditional risk factors such as age, race, SBP, smoking, total cholesterol, HDL, diabetes and hypertensive medication.
Retinal microvascular abnormalities and 10-year cardiovascular mortality: a population-based case-control study	Wong et al, 2003	Individuals from Wisconsin. Population-based, nested, case-control study. Nearly 3 controls were matched for each case	Prospective	Beaver Dam Eye Study	413 cases and 1198 controls	10	Logistic	1-Retinopathy 2- Focal narrowing 3-Arteriouvenous nicking 4-AVR Both eyes Digitised Knudtson-Parr-Hubbard formula	1) Any CVD death 2)Coronary Heart Disease Death; 3) Stroke Death	In young people (< 74 years old), cardiovascular mortality was associated with lowest quintile of the retinal AVR, OR 1.9 (95% CI, 1.2, 2.9) in a fully adjusted model. Retinopathy was also associated with cardiovascular mortality OR 1.8 (95%CI, 1.2, 2.7) after full adjustment.

The prevalence and risk factors of retinal microvascular abnormalities in older persons	Wong et al, 2003	Elderly nondiabetic (healthy) persons aged 69 to 97	Cross-sectional	The Cardiovascular Health Study (CHS)	2050 /CHD(510) and MI (219)	Cross-sectional	Logistic	1- Retinopathy 2-Focal Arteriolar Narrowing 3-Arteriovenous nicking 4-Generalised arteriolar narrowing (AVR categorised as binary)	1-Coronary Heart Disease 2-MI 3-stroke 4-IMT (as subclinical atherosclerosis) 5-ankle arm index (as subclinical atherosclerosis) 6-subclinical cardiovascular disease (ECG abnormalities, echo- wall motion abnormality or low ejection fraction, increased carotid or internal carotid artery wall thickness, ankle-arm index, and positive responses to the Rose Questionnaire for angina or intermittent claudication	After controlling for age, gender, race, mean BP, and antihypertensive medication use, retinopathy was associated with prevalent coronary heart disease OR 1.7 (95% CI, (1.2, 2.6) and prevalent myocardial infarction OR, 1.7 (95% CI, 1.1-2.8). No associations were found with AVR.

Abnormalities of Retinal Microvascular Structure and Risk of Mortality From Ischemic Heart Disease and Stroke	Witt et al, 2006	Subjects 43-74 years old from Wisconsin	Nested Case-control	Beaver Dam Eye Study	528 controls and 154 cases	Nested (case-controls)	Logistic	1-Length-diamater ratio 2-Diameter 3-Length 4-Simple tortuosity 5-Curve tortuosity 6-Optimality ratio 7-Optimality deviation 8-Bifurcation angle Both eyes Digitised	1-Mortality of IHD 2-Mortality in stroke	Optimality ratio and deviation were significantly increased in IHD mortality cases, whereas arteriolar tortuosity (simple tortuosity and vessel curvature) were significantly reduced in IHD cases. There was a positive association between optimality deviation (abnormal bifurcation optimality) and IHD death (*p*=0.02) and a negative association between simple arteriolar tortuosity and IHD death (*p*=0.01) indicating that less tortuous arterioles were associated with increasing risk of death from IHD. Both of these effects persisted after full-adjustment.
A Prospective Cohort Study of Retinal Arteriolar Narrowing and Mortality	Wong et al, 2004	Subjects 43-84 years old from Wisconsin	Prospective	Beaver Dam Eye Study	4609	10	Cox	1-CRAE 2-CRVE 3-AVR right eye (3397) left (383), average of both eyes (829) Digitised	1-Any cause of mortality 2-Vascular mortality (heart disease, stroke, atherosclerosis, arterial disease) 3-Non-vascular disease mortality	No association was found between smaller AVR and any of the measured end points.

Relationship Between Retinal Arteriolar Narrowing and Myocardial Perfusion	Wang et al, 2008	Subjects men and women (45-84 years old) from Minnesota. Multi-ethnic.	Cross-sectional	The Multi-Ethnic Study of Atherosclerosis (MESA)	212	Cross-sectional	Linear	1-CRAE 2-CRVE Right eye (mainly) Hubbard and Knudtson formulas	1-CT scan Coronary calcification using Agatson Score. Analysis was performed for severity 2-Cardiac MRI perfusion (hyperemic and resting blood flow and perfusion flow with Adenosine)	Among subjects with no coronary artery calcification, smaller CRAE was associated with lower hyperaemic myocardial blow flow and perfusion reserve. These associations remained significant after adjusting for age, gender and ethnicity
Fractal analysis of retinal microvasculature and coronary heart disease mortality	Liew et al, 2011	Subjects ≥49 years old from South Wales Australia	Prospective	Blue Mountain Eye Study (New South Wales, Australia)	3303/468	14	Cox	1-Fractal Dimension (D_f) 2-CRAE 3-CRVE Both eyes Digitised Knudtson-Parr-Hubbard formula	1) Coronary heart disease mortality based on Australian national death index. There were 468 coronary heart disease deaths (14.2%)	The lowest and highest quartiles D_f (termed "suboptimal") were associated with CHD mortality in both unadjusted and fully adjusted models HR 1.51, (95% CI, 1.17 - 1.94) and HR 1.58 (95% CI, 1.19- 2.10, respectively). Among people aged ≤ 70 years, suboptimal D_f was associated with higher risk of CHD mortality HR 1.89, (95%CI, 1.25- 2.84) for the lowest quartile and HR 1.87 (95% CI 1.30- 2.69) for the highest quartile compared with the middle quartiles.

Are retinal microvascular caliber changes associated with severity of coronary artery disease in symptomatic cardiac patients?	Kreis et al, 2009	Subjects who underwent coronary angiography from Melbourne Australia (Austin Health Cardiology department)	Cross-sectional	98 symptomatic subjects who underwent coronary angiography	98	Cross-sectional	Logistic	1-CRAE 2-CRVE Digital retinal photographs Right eye Mainly analysed pre-procedure as Post-procedure images were used if the pre-procedure image was not readable.	Coronary angiograms 1-Leaman Score (severity of CAD, classified as : 0 score, >0 - 6.5 score, >6.5 - 10.5 score, >10.5) B) 2-Clinically significant CAD in LAD (<70% stenosis and ≥70% stenosis) 3-Diseased vessel score (0 diseased arteries, 1 diseased artery, 2 diseased arteries, 3 diseased arteries)	CRAE and CRVE were not significantly associated with increasing severity of CAD as assessed by Leaman scores, presence of clinically significant CAD, or the number of diseased vessels
Relation of Retinopathy to Coronary Artery Calcification: The Multi-Ethnic Study of Atherosclerosis	Wong et al, 2007	Subjects men and women (45-84 years old). Multi-ethnic. No cardiovascular disease at baseline from 6 US communities	Cross-sectional	The Multi-Ethnic Study of Atherosclerosis (MESA)	5971	Cross-sectional	Logistic	1-Retinopathy 2-Retinal arteriovenous nicking 3-Focal arteriolar narrowing 3-CRAE 4-CRVE Right eye (mainly) Hubbard and Knudtson formulas	CT scan for coronary calcification using Agatson score	After adjustment for age, gender, ethnicity, blood pressure, diabetes, lipid profile, smoking, and other risk factors, retinopathy was associated with having a moderate-to-severe CAC score (OR 1.43, 95% CI 1.18- 1.75). No associations were found with quantitative retinal traits and coronary calcification.

Retinal Microvasculature Is Associated With Long-Term Survival in the General Adult Dutch Population	Mutlu et al, 2016,	Europeans inhabitants from Rotterdam Netherlands	Prospective	The Rotterdam Study	5674	25	Cox	1-Retinal arteriolar calibre 2-Retinal venular calibre. One eye Parr and Hubbard formula. Correction for magnification performed	-Cardiovascular deaths = 1079 (19%) this included cardiac arrest (n=183), heart failure (n=230), stroke (n=234) and MI (n=183). 2-Non-cardiovascular deaths (n=2379; 41.9%) this included infectious diseases (n=56), cancer (n=910), dementia (n=348), pneumonia ((n=103), chronic respiratory disease (n=123), fracture (n=65) other causes (n=774)	Wider venules were associated with higher risk of all-cause mortality HR 1.07 (95% CI, 1.03–1.12) and non-cardiovascular mortality HR 1.08 (95% CI, 1.02–1.13) in models adjusted for age, sex, other retinal vessel, systolic and diastolic pressure, antihypertensive medication, BMI , total cholesterol, HDL, diabetes mellitus, CRP, carotid artery plaque score, and smoking. Narrower arterioles were associated with cardiovascular mortality HR 1.13 (95% CI, 1.01–1.26) in a model fully adjusted for the above covariates. Effect association were seen in individuals <70 years old.

10.3 Appendix 3: Criteria used to define prevalent cardiovascular events at baseline in the ET2DS

The following criteria were used to define a prevalent cardiovascular event:

Myocardial Infarction (MI): This was recorded if two of the first three of the following criteria were met, or if both the first and the last criteria were met.

(i) Self-report of a doctor diagnosis

(ii) Myocardial infarction according to the WHO chest pain questionnaire

(iii) Electrocardiographic evidence from Minnesota codes

(iv) Hospital discharge record with the code for MI (ICD-10 codes I21, I23, I252)

Angina: This was recorded if two of the first three of the following criteria were met, or if both the first and the last criteria were met.

(i) Self-report of a doctor diagnosis of angina pectoris or on regular medication for angina

(ii) Positive WHO chest pain questionnaire

(iii) Electrocardiographic evidence from Minnesota codes

(iv) Hospital discharge record with relevant codes (ICD10 codes I20 - I25)

Coronary intervention: The diagnosis of coronary intervention was made using the appropriate codes from the hospital discharge record (Office of

Population Censuses and Surveys, OPCS -4 codes K40-K44) (Office of Population Censuses and Surveys, 1993).

Stroke: This was recorded if two out of the three following criteria were met:

(i) Self- report of a doctor diagnosis of stroke

(ii) Hospital discharge record with appropriate code (ICD10 codes I20 -I25)

(iii) Confirmation in the clinical notes that event was not a transient ischaemic attack

Transient ischaemic attack (TIA): The diagnosis of TIA was recorded if two out of the three of the following criteria were present:

(i) Self-reported doctor diagnosis of “mini stroke” or “slight stroke”

(ii) Hospital discharge record with appropriate code (ICD10 G45, G659)

(iii) Confirmation from clinical notes review that event was a TIA

10.4 Appendix 4: Criteria used to define incident cardiovascular events during follow-up in the ET2DS

The following criteria were used to define incident or recurrent cardiovascular events between baseline and year four in the ET2DS.

Myocardial Infarction (MI): The diagnosis was recorded if two of the first three of the following criteria were met, or if both the first and the last criteria were met.

(i) Self-report of doctor diagnosis

(ii) New diagnosis of myocardial infarction according to the WHO chest pain questionnaire

(iii) New electrocardiographic evidence of coronary ischaemia

(iv) Hospital discharge record with the code for MI (ICD-10 for I21, I23, I252)

Angina: This was recorded if two of the first three of the following criteria were met, or if both the first and the last criteria were met.

(i) Self-report of new angina pectoris event or taking antianginal drugs after baseline

(ii) New diagnosis of angina pectoris according to WHO chest pain questionnaire

(iii) New evidence of electrocardiographic evidence of angina pectoris

(iv) Hospital discharge record with code for ischaemic heart disease (ICD10 codes I20 -I25)

Coronary intervention: OPCS-4 code for coronary intervention on hospital discharge record.

Fatal myocardial infarction: This was recorded according to primary or secondary ICD-10 code for MI on death certificate and with clinical and electrocardiographic criteria for non-fatal MI within 4 weeks of explained/sudden death.

Stroke: This was recorded if two out of the three following criteria were met:

(i) New self- report

(ii) Clinical notes from the hospital discharge with stroke codes (ICD10 codes I20 -I25) after baseline

(iii) Confirmation in the clinical notes that transient ischaemic attack (TIA) has not been diagnosed

Transient ischaemic attack (TIA): The diagnosis of TIA was recorded if two out of the three of the following criteria were present:

(i) New self-reported diagnosis of “mini stroke” or “slight stroke”

(ii) Clinical notes from hospital discharge with TIA codes (ICD10 G45, G659)

(iii) Confirmation with the clinical notes review with TIA after baseline.

Fatal stroke: This was recorded according to ICD-10 code for stroke on death certificate or clinical criteria for non-fatal stroke within 6 weeks of unexplained sudden death.

After 8 years from baseline, incident and recurrent cardiovascular events were identified by a further phase of record linkage. If there was uncertainty

as to whether criteria had been met, hospital notes were obtained and individual cases were discussed by researchers and senior clinicians to reach a consensus.

The following criteria were used to define incident or recurrent cardiovascular events between years 4 to 8 of follow-up. Unlike at baseline and year 4, data sources for the eight year follow-up were limited to ISD record linkage and clinical notes from the hospital.

Myocardial Infarction

ICD-10 code for MI (I21-I23) as primary diagnosis on discharge record, or

ICD-10 code for MI or previous MI (I252) as non-primary diagnosis according to clinical notes.

Angina

No evidence of angina at baseline or four years follow-up plus ICD-10 code for angina (I20) as diagnosis code on discharge record.

Coronary intervention

OPCS-4 code for coronary intervention (K40-K44, K49) on discharge record

Fatal ischaemic heart disease

Subjects who did not meet any criteria for MI and had an ICD-10 code for ischaemic heart disease (I209, I249, I258, I259) as primary cause of death.

Stroke

ICD-10 code for stroke (I61, I63-I64) as primary diagnosis on discharge record, or

ICD-10 code for stroke as secondary diagnosis confirmed in the clinical notes

Transient ischaemic stroke (TIA)

ICD-10 code for TIA (G45) as primary diagnosis on discharge record, or

Secondary ICD-10 code for TIA confirmed in the clinical notes

Fatal stroke

ICD-10 code for stroke (I61, I63, I64) as primary cause of death, or

Secondary ICD-10 code for stroke on death record confirmed with inspection of the clinical notes.

For my analyses, 4 year and 8 year follow-up incident cardiovascular events were combined,and events were defined as all cardiovascular events (first fatal or non-fatal MI, diagnosis of angina, fatal or non-fatal stroke, TIA, coronary intervention or fatal other ischaemic heart disease experience by a participant since baseline), coronary events (first fatal or non-fatal MI, diagnosis of angina, coronary intervention or fatal other ischaemic heart disease experienced by a participant since baseline) and cerebrovascular events (first fatal or non-fatal stroke or TIA experienced by a participant since baseline).

10.5 Appendix 5: Q-Q plots

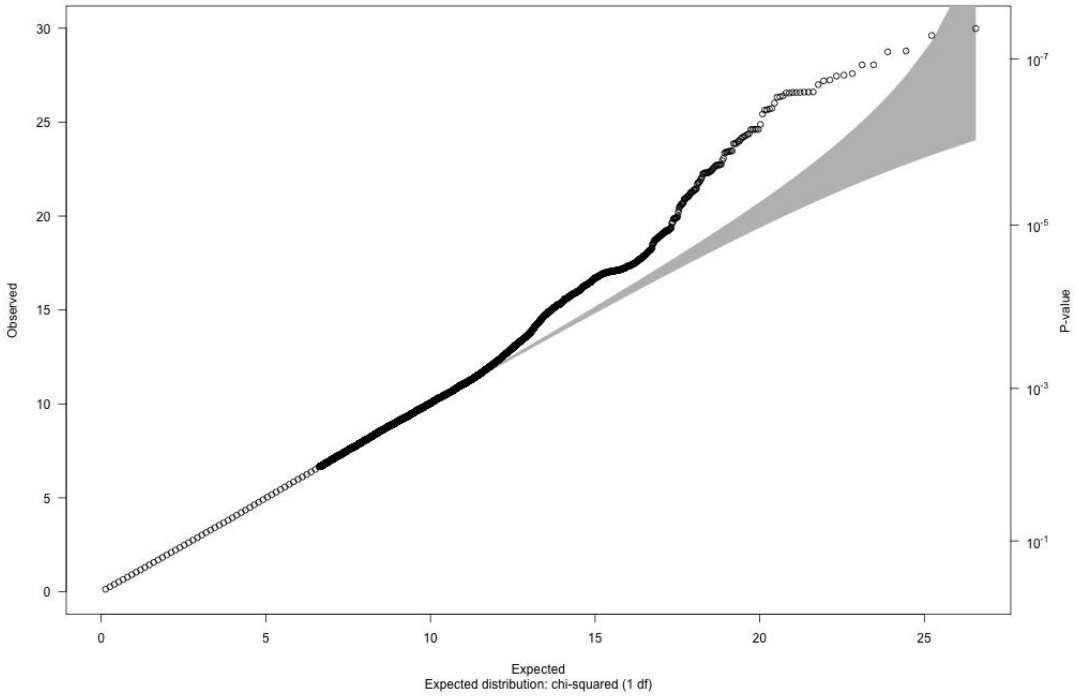

AVR Q-Q plot – Genomic inflation of 0.993

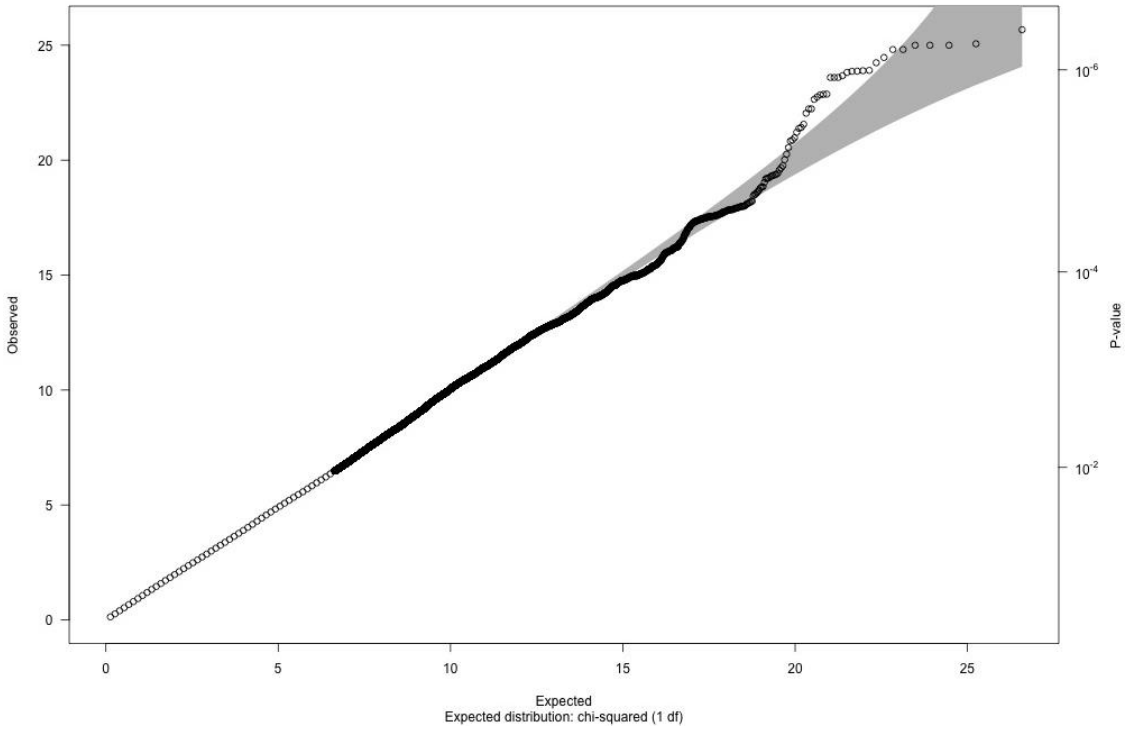

CRAE Q-Q plot – Genomic inflation of 0.999

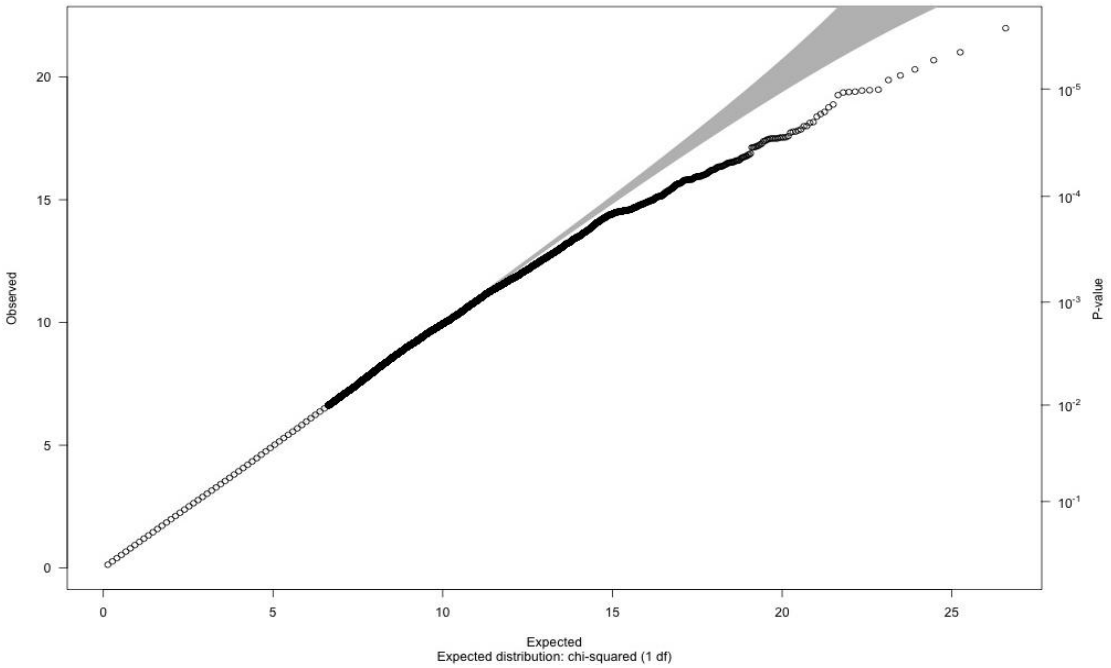

CRVE Q-Q plot – Genomic inflation of 1.002

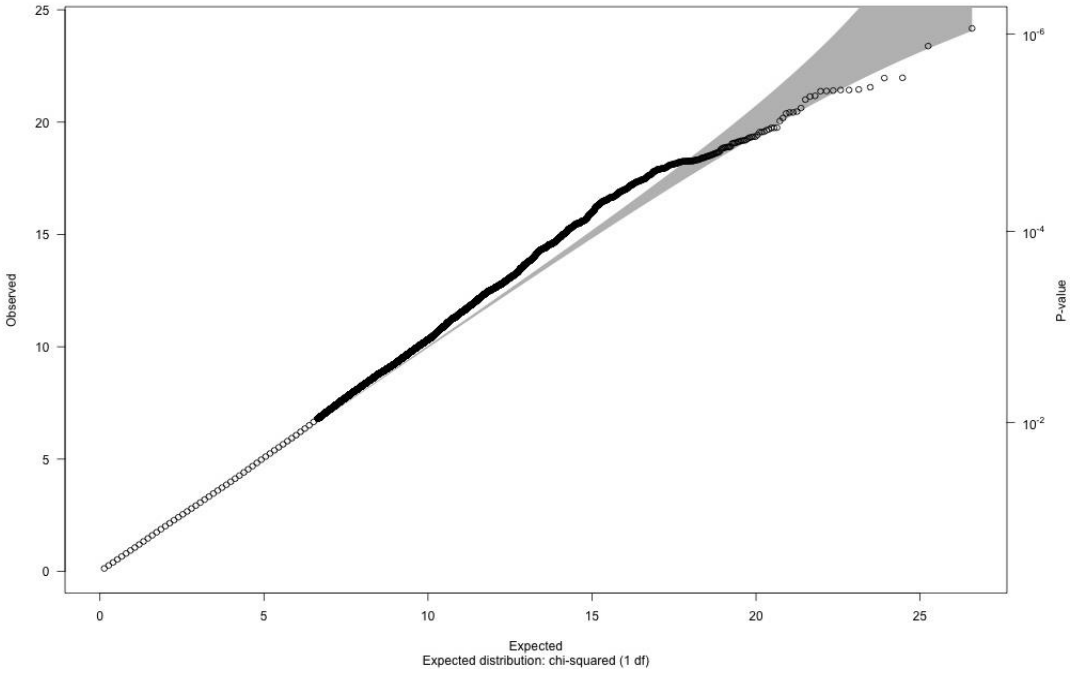

Arteriolar mean tortuosity Q-Q plot – Genomic inflation of 0.998

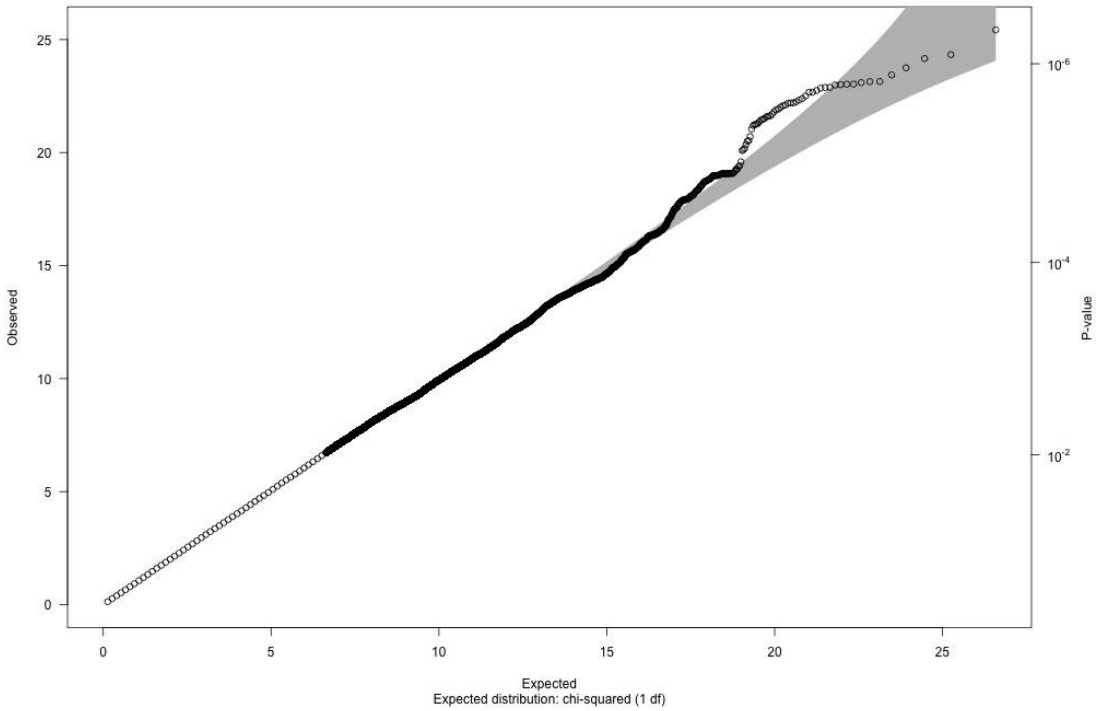

Arteriolar minimum tortusity Q-Q plot – Genomic inflation of 0.998

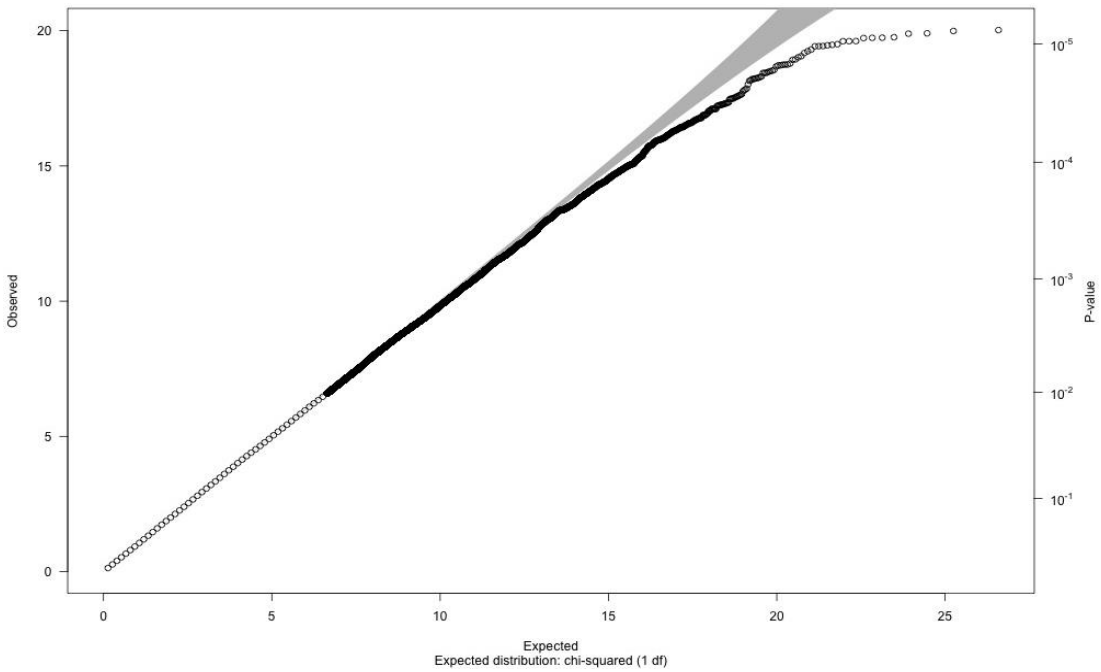

Arteriolar maximum tortuosity Q-Q plot – Genomic inflation of 1.004

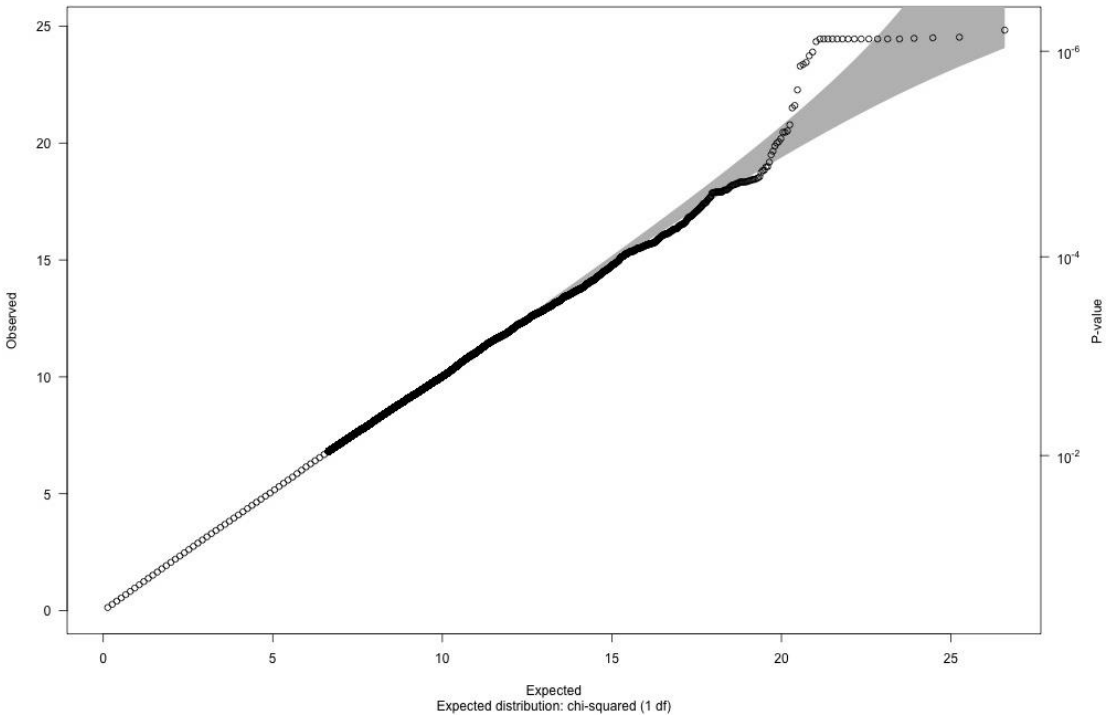

Venular mean tortuosity Q-Q plot – Genomic inflation of 1.016

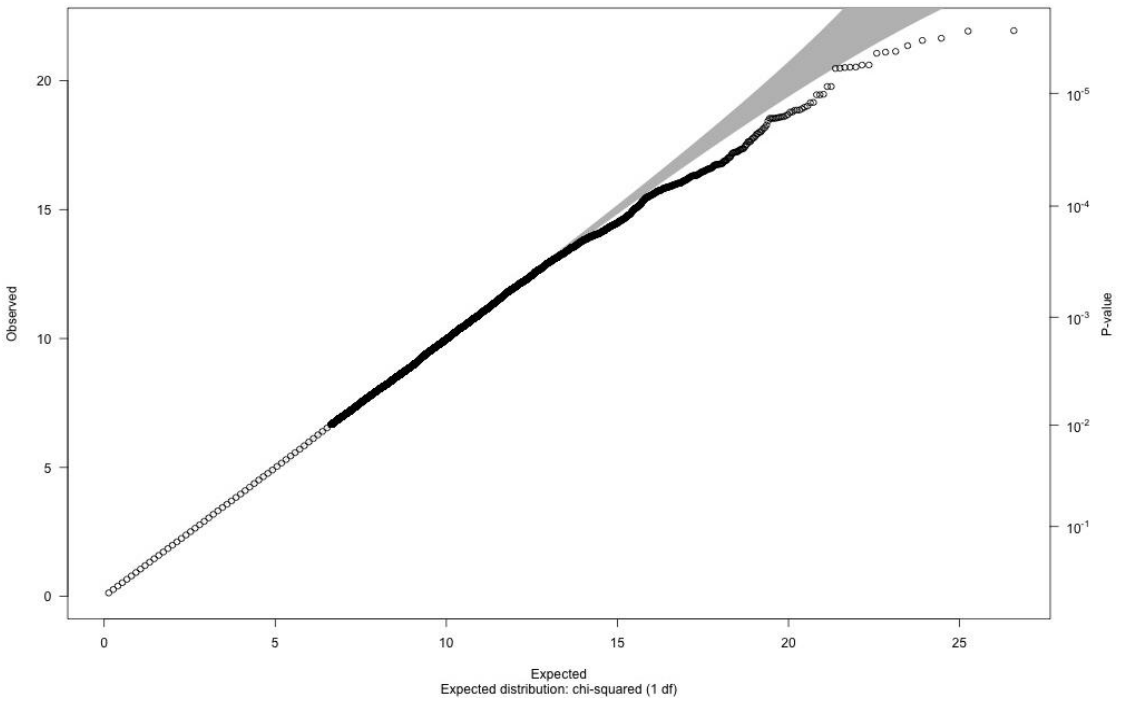

Venular minimum tortuosity Q-Q plot – Genomic inflation of 0.996

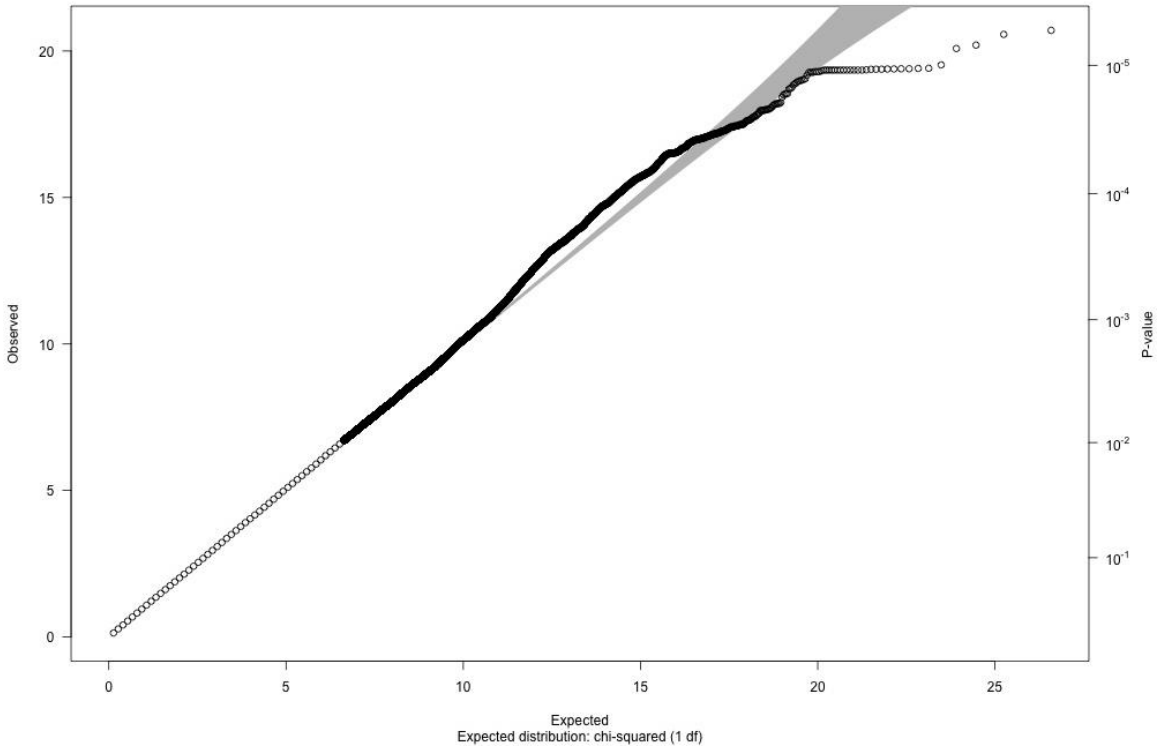

Venular maximum tortuosity Q-Q plot – Genomic inflation of 1.026

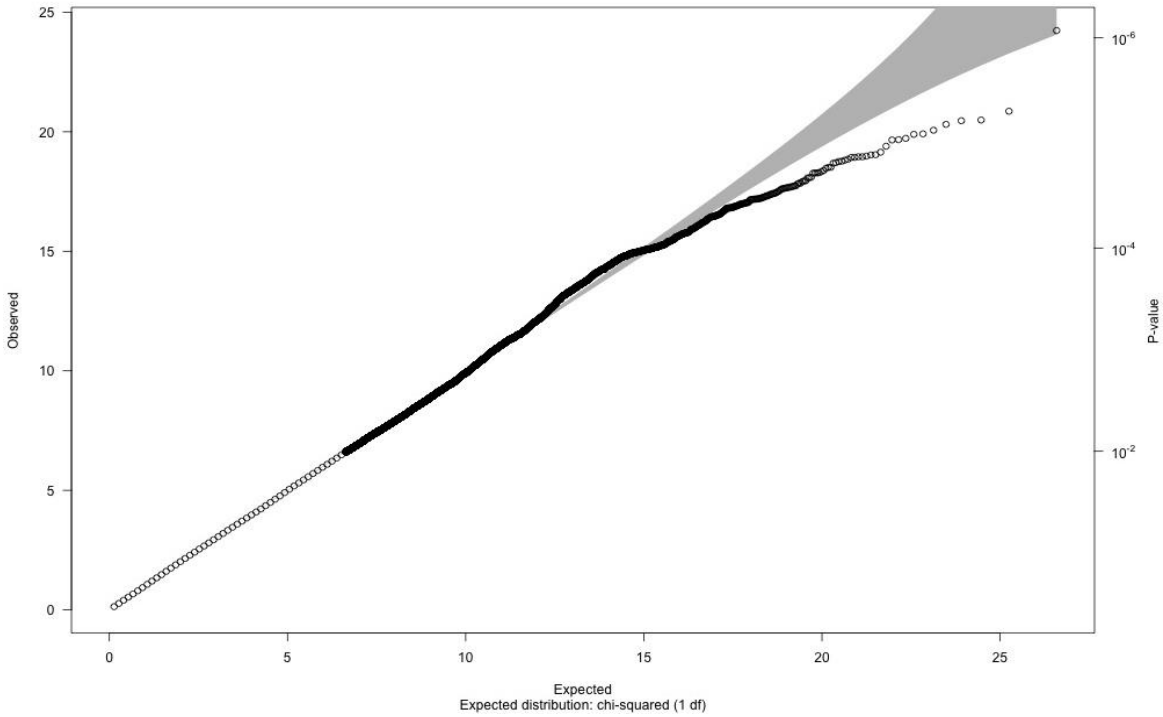

Multifractal dimensions D0 Q-Q plot – Genomic inflation of 1.01

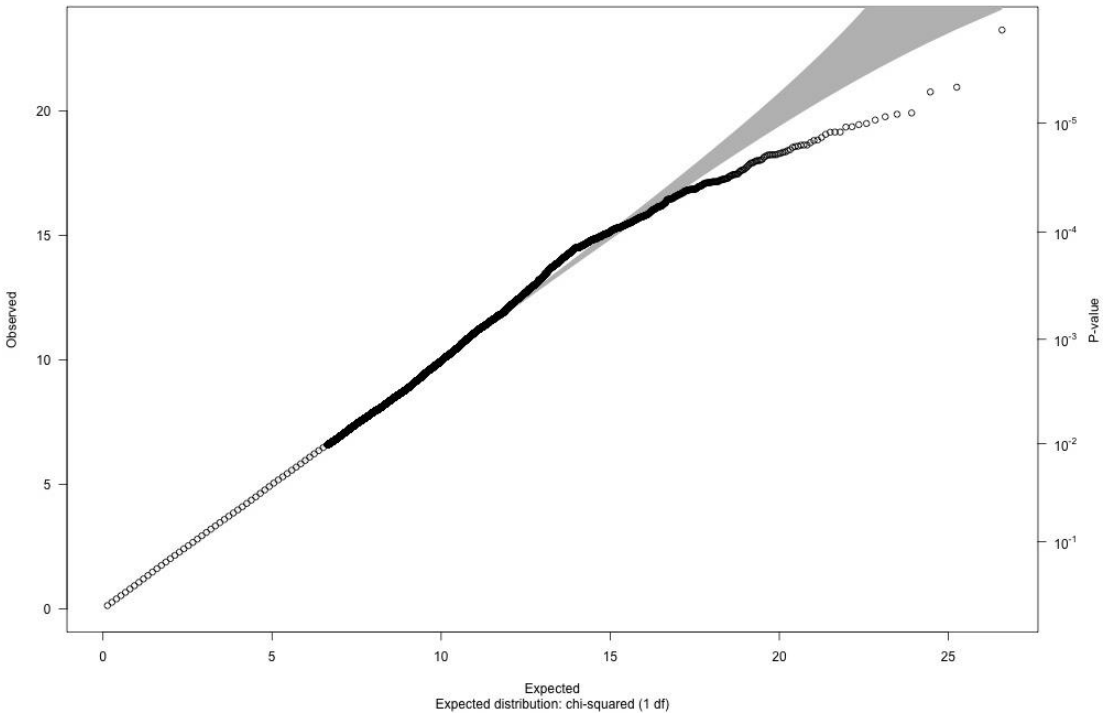

Multifractal dimensions D1 Q-Q plot – Genomic inflation of 1.011

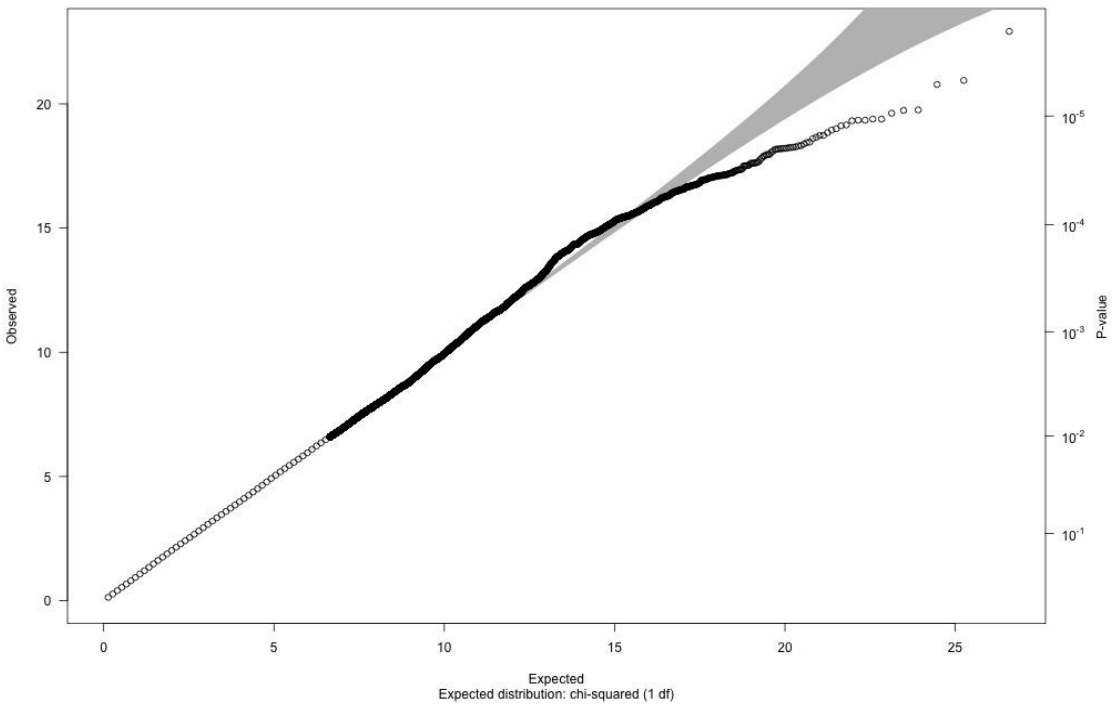

Multifractal dimensions D2 Q-Q plot – Genomic inflation of 1.011